University of Southampton

National Oceanography Centre Southampton

School of Ocean and Earth Sciences

Coral Reefs of the Indo-Pacific and Changes in Global Holocene Climate

by

Siwan Angharad Rees

Thesis for the degree of Doctor of Philosophy

August 2005

UNIVERSITY OF SOUTHAMPTON

ABSTRACT

SCHOOL OF OCEAN AND EARTH SCIENCES

Doctor of Philosophy

CORAL REEFS OF THE INDO-PACIFIC AND CHANGES IN GLOBAL HOLOCENE CLIMATE

By Siwan Angharad Rees

The key to understanding the future impact of the anthropogenic combustion of fossil fuels on the climate system, is to fully understand the complex feedback loops within the natural Earth system. One natural climate feedback that has been proposed is the Coral Reef Hypothesis whereby significant increases in coral reef growth may have contributed to the deglacial increase in atmospheric CO_2 observed in the ice core records. This thesis examines the role of coral reefs in the oceanic carbonate budget and global carbon cycle both spatially and temporally during the Holocene. Using the most comprehensive reef area estimate to date, a conservative estimate of cumulative $CaCO_3$ accumulation within coral reefs globally from 10 kyr BP to present is 7970 Gt. This estimate includes a temporal and spatial view of reef $CaCO_3$ accumulation during the Holocene and represents coral reefs alone, whereas previous budgets have included wider neritic carbonate facies. This mass of reefal $CaCO_3$ accumulation would have made approximately 2100 Gt CO_2 available for release to the atmosphere over the Holocene.

Radiocarbon dating of coral obtained from new drill cores from Rodrigues (Southwest Indian Ocean), Lizard Island and MacGillivray Reef (Northern Great Barrier Reef (NGBR)), helps to reveal the spatial and temporal pattern of Holocene $CaCO_3$ accumulation within these reefs and contributes to the dataset compiled to calculate the global mass balance of coral reef carbonate. The new data presented here demonstrates that the reefs at Rodrigues, like those at Reunion and Mauritius only reached a mature state (reached sea level) by 2 to 3 ka – thousands of years later than most of the reefs in the Australasian region. The windward margins at Lizard Island and MacGillivray Reef started growing ca 6.7 and 7.6 cal kyr BP respectively directly on an

assumed granite basement and reached sea level approximately 4 and 5.6 cal kyr BP respectively. The leeward margin at MacGillivray Reef was initiated by 8.2 cal kyr BP directly on a granite basement, only reaching sea level relatively recently between 260 and 80 cal yr BP. The absence of Pleistocene reefal deposits indicates the possibility that the shelf in this region may have subsided relative to modern day sea level by at least 15 m since the last interglacial (125 ka).

The role of the calcareous green alga *Halimeda* in the marine carbonate budget is still unknown both spatially and temporally for the Holocene. Here a quantification of the carbonate mass within the ribbon reefs and *Halimeda* bioherms on the outer shelf of the NGBR is presented. It is estimated that *Halimeda* bioherms contain at least as much (possibly 400 % more) $CaCO_3$ sediment than the adjacent ribbon reefs within the NGBR province.

Contents

List of Tables

List of Illustrations

List of Plates

List of Accompanying Material

DECLARATION OF AUTHORSHIP

I, Siwan Angharad Rees declare that the thesis entitled Coral Reefs of the Indo-Pacific and Changes in Global Holocene Climate and the work presented in it are my own. I confirm that:

This work was done wholly or mainly while in candidature for a research degree at this University;

- where any part of this thesis has previously been submitted for a degree or any other qualification at this University or any other institution, this has been clearly stated;
- where I have consulted the published work of others, this is always clearly attributed;
- where I have quoted from the work of others, the source is always given. With the exception of such quotations, this thesis is entirely my own work;
- I have acknowledged all main sources of help;
- where the thesis is based on work done by myself jointly with others, I have made clear exactly what was done by others and what I have contributed myself;
- parts of this work have been published as:

Chapter Three: Rees S. A., Opdyke, B. N., Wilson, P. A., L. K. Fifield and V. Levchenko (submitted manuscript) Holocene Evolution of the Granite based Lizard Island and MacGillivray Reef Systems, Northern Great Barrier Reef. *Coral Reefs.*

Chapter Four: Rees S. A., Opdyke, B. N., Wilson, P. A. and L. K. Fifield (2005) Coral Reef Sedimentation on Rodrigues and the Western Indian Ocean and its Impact on the Carbon Cycle. *Phil. Trans. R. Soc. Lond. A.* **363**, 101-120.

Chapter Five: Rees S. A., Opdyke, B. N. and P. A. Wilson (submitted manuscript) Quantifying the Global Coral Reef CO_2 Flux to the Atmosphere During the Holocene using a Dataset of Reef Carbonate Accumulation Rates. *Global Biogeochemical Cycles.*

Chapter Six: Rees S. A., Opdyke, B. N, Wilson, P. A. and T. Henstock (submitted manuscript) A Review of the Significance of *Halimeda* Bioherm Carbonate in the Global Budget revisited. *Coral Reefs*.

Signed:……

Date:……....

Supervisory Panel

I would like to thank my advisory panel:

Dr Paul A. Wilson
School of Ocean and Earth Sciences, National Oceanography Centre, Southampton, UK.

Dr Bradley N. Opdyke
Department Earth and Marine Sciences, Australian National University, Canberra, Australia.

Professor Philip P. Weaver
Challenger Division, National Oceanography Centre, Southampton, UK.

Professor Dorrik. A. Stow
School of Ocean and Earth Sciences, National Oceanography Centre, Southampton, UK.

Acknowledgements

I would like to thank those who helped me academically at NOCS:
Dr Paul Wilson, Professor Phil Weaver and Professor Dorrik Stow for support, advice and direction; Professor Peter Challenor for statistics discussions; Dr Tim Henstock for discussions and loan of high resolution seismic profiling equipment; John Davis for support, patience and for giving his holiday time to come to try to seismically profile the Lizard Island region in extreme heat, humidity, monsoon rain and winds!; Kate Davis for creating the figures for the Rodrigues paper at very short notice and for advice on creating figures during rest of my PhD.

I would also like to thank those who helped me academically at ANU:
Dr Brad Opdyke - for the idea for my project, constant support, enthusiasm and belief in my ability; Dr Keith Fifield and Dr Vladimir Levchenko for help with radiocarbon dating; Matt Stevens, Helen Bostock, Sarah Tynan and Nigel Caddy for help, support and donating muscle power with reef drilling.

I would also like to thank those institutions that gave me and my project financial and logistical assistance during the last 3 years; National Environment Research Council (NERC); National Oceanography Center, Southampton (NOCS); the Earth and Marine Science Department (EMS) and the Nuclear Physics Department, Australian National University; the Royal Geographic Society; The Royal Society; the *Shoals of Capricorn* Marine Research Program; the Rodrigues Research station and staff; the Lizard Island Research Station and staff (Dr Anne Hogget, Dr Lyle Vail, Marianne and Lance Pearce, Bob and Tania Lamb) for accommodating us and our bulky equipment!

Thanks also to my parents, family and friends, Amanda, Pete, Em, Em, Zac, Vic, JP, Jess, especially Matt Palmer and Marc Lucas for tea, biscuits and sanity at times of crisis!
Matt Stevens – if it weren't for you I would have probably never gotten past the first year, thank you for instilling enthusiasm about rocks and making my visits to Australia so much fun!

Thanks to my friends at ANU who made field work and visits to Canberra very enjoyable; Sarah and Ben, Helen, Nic, Mr and Mrs Stevens, Jen and all the other students and staff at ANU!

Definitions and Abbreviations

CRH	Coral Reef Hypothesis
CO_2	Carbon Dioxide
$CaCO_3$	Calcium Carbonate
$2HCO_3^-$	Hydrogen Carbonate/Bicarbonate
CO_3	Carbonate
CO_3^-	Carbonate Ion
GBR	Great Barrier Reef
NGBR	Northern Great Barrier Reef
CGBR	Central Great Barrier Reef
SGBR	Southern Great Barrier Reef
yr BP	years before present
kyr	thousands (1000) years
ka	thousands (1000) years ago
yr^{-1}	per year
M	meters
m kyr^{-1}	meters per thousand years
mol yr^{-1}	moles per year
Gt	Gigatonnes
kg $CaCO_3$ m^{-2} yr^{-1}	Kilograms of calcium carbonate per meter squared per year - rate of calcification
G	annual rate of net gain in carbonates (kg $CaCO_3$ m^{-2} yr^{-1})
°C	Degrees Celsius
±	Plus or Minus
Ψ	Greek Letter Psi - ratio of released CO_2 to $CaCO_3$
σ	Greek Letter Sigma
pCO_2	Partial Pressure of Carbon Dioxide
atm	Atmospheres
%	percent
×	multipication
º	Degree
LGM	Last Glacial Maximum
LAW	Leeward Accretionary Wedge
ppmv	parts per million by volume

ppmv yr^{-1}	parts per million by volume per year
WPO	Western Pacific Ocean
AC	Atlantic-Caribbean
WIO	Western Indian Ocean
EIO	Eastern Indian Ocean
EPO	East Pacific Ocean
MWP 1A	Melt-water pulse 1A
MWP 1B	Melt-water pulse 1B
g cm^{-3}	grams per centimetre cubed
Pg	Pica grams = Gigatonnes, = 10^{15}g
NERC	Natural Environment Research Council
SOC	Southampton Oceanography Center
ANU	Australian National University
IPCC	Intergovernmental Panel on Climate Change
AMS	Accelerator Mass Spectrometry

Chapter One

Introduction

Plate 1.1 Heart Reef, Great Barrier Reef, Australia (from www.ozmagic11.homestead.com/files/Reef-heart)

Chapter 1

Introduction

1.1 Introduction

Coral reefs are a significant component of the global carbon cycle, they represent an important resource to coastal nations, providing sources of food, natural coastal defenses, building material and revenue through tourism and the aquarium trade worth more than $375 billion per year to the global economy (Naim *et al.*, 2000; Bellwood and Hughes, 2001; Spalding *et al.*, 2001; Pandolfi *et al.*, 2005). The health and survival of reefs around the world are undoubtedly already under threat from point source pollution, terrestrial run-off, increased turbidity, destructive fishing practices and coral bleaching associated with increases in sea-surface temperatures (Naim *et al.*, 2000; Roberts *et al.*, 2002; McCulloch *et al.*, 2003; Cole, 2003; Sheppard, 2003). Projected anthropogenic increases in atmospheric carbon dioxide levels (CO_2 atm.) pose an additional threat to reef systems through acidification and warming of the surface tropical oceans (Gattuso *et al.*, 1999; Gattuso and Buddemeier, 2000). These effects are hypothesized to promote decreases in the aragonite saturation state of seawater which will reduce hermatypic coral calcification rates and may eventually lead to the destruction of the reef framework (Kleypas *et al.*, 1999; Langdon *et al.*, 2000; Anderson *et al.*, 2003).

1.2 Pleistocene Climate Change

The Earth's climate oscillates between glacial and interglacial periods on well-understood orbital timescales, but forcing mechanisms controlling climate change are the subject of much debate (Figure 1.1; Milankovitch, 1920; Pisias and Imbrie, 1986; Shackleton, 2000). Glacial-interglacial cycles have occurred with a periodicity of approximately 100 ka for about the last one million years. During glacials (for example, the Last Glacial Maximum, 18 kyr ago) average global surface temperatures and the partial pressure of atmospheric CO_2 (p CO_2) were approximately 10ºC and between 180 and 200 parts per million by volume (ppmv) respectively, whereas during interglacials (for example the Holocene, the last 10 kyr) these parameters averaged approximately 15ºC and 280 ppmv, respectively (Kump *et al.*, 1999; Sigman and Boyle, 2000; Marchitto *et al.*, 2005). Changes in the eccentricity, obliquity and precession of the Earth's orbit around the sun cause variation in the amount of solar insolation reaching

the Earth and thus the volume of ice sheets (Milankovitch, 1920). Thus, orbital variations can be thought of as the pacemaker of climatic changes on multimillenial timescales (Hayes *et al.*, 1976). However, the variations in solar insolation are not of sufficient magnitude to explain the full extent of the global temperature changes. Ice core records suggest that changes in atmospheric CO_2 concentration amplify changes in climate, although the cause of the CO_2 change is much debated (Barnola *et al.*, 1987; Broecker and Henderson, 1998; Shackleton, 2000).

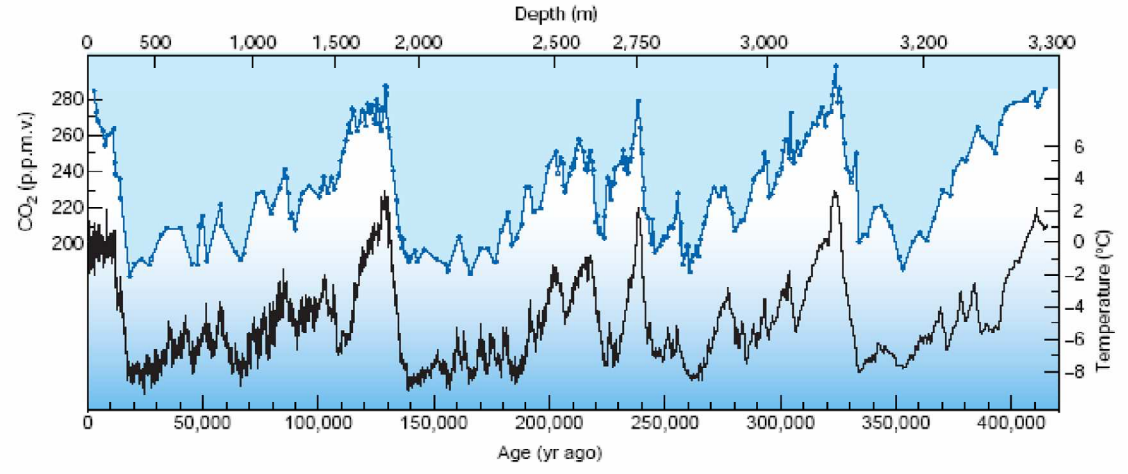

Figure 1.1 Vostok ice core record showing the correlation between atmospheric CO_2 and temperature oscillations though the glacial interglacial cycles during the last 425 kyr BP. Temperature and atmospheric CO_2 concentrations are high during interglacial periods but low during glacial periods (after Kump, 2002).

Following the Last Glacial Maximum (LGM) the Earth began to warm (between 15-10 kyr BP) and the large continental ice sheets began to melt causing global sea level to rise from approximately -135 m at 18 kyr BP to near the modern day level by approximately 6 kyr BP. Atmospheric CO_2 concentration began to increase from 180 to 280 ppmv between 19 and 10.5 kyr BP (Sowers and Bender, 1995). Holocene atmospheric CO_2 levels recorded in the Taylor Dome ice core show that atmospheric CO_2 increased from 270 ppmv at 10.5 kyr BP to the pre-industrial level of 290 ppmv by 100 yr BP (Indermuhle *et al.*, 1999). Atmospheric CO_2 concentration is controlled by a wide variety of processes operating at different timescales (Siegenthaler and Sarimento, 1993; Kleypas, 1997). Many hypotheses have been put forward to explain the changes in atmospheric CO_2 concentration over the glacial-interglacial cycle (Table 1.1).

Table 1.1 Summary of hypotheses put forward to account for the lower CO_2 content of the atmosphere during glacial times (modified from Broecker and Henderson, 1998)

Model	Problems	Advantages	References
$CaCO_3$ Compensation / Increase in the ratio of organic carbon to $CaCO_3$ in the material falling to the sea floor (Rain ratio hypothesis). Sediment Respiration Based. A decrease in the rain of $CaCO_3$ to the deep sea and therefore burial of $CaCO_3$ results in an imbalance between the input (from terrestrial weathering) and output (via burial) of $CaCO_3$. The ocean becomes more basic. To restore the balance CO_2 is drawn out of the atmosphere into the ocean, thereby lowering atmospheric CO_2.	Mass balance Requires too large a shift of the lysocline to be consistent with the sedimentary record.	System response time is right ($\approx$ 10 kyr). The hypothesis creates a CO_2 decrease of the right magnitude.	Archer and Maier-Reimer (1994); Sigman (1997); Sanyal *et al.* (1995);
Iron Hypothesis Southern Ocean Based. Increased input of iron (Fe) bearing silicate detritus into Southern Ocean increases productivity and draws down atmospheric CO_2.	Not seen in Southern Ocean paleo-productivity records and response time too quick, only accounts for < 40 ppm change in atmospheric CO_2.	Agrees with dust flux change and fits well with timing of dust demise in south which occurs immediately before the CO_2 change.	Martin (1990)
Polar Alkalinity Southern Ocean Based. Changes in CO_3^{2-} content of surface waters of Southern ocean may have had a disproportionately large impact on atmospheric CO_2. Deep ocean circulation during glaciations would have lead to CO_3^{2-} rich deep water surfacing in the Southern ocean the resulting increased productivity would have drawn down atmospheric CO_2.	Not seen in Southern Ocean paleo-productivity records and lacks mechanism for increased alkalinity.	Southern Ocean.	Broecker and Peng (1989)
Coral Reef Hypothesis / Shallow water $CaCO_3$ Shallow Ocean $CaCO_3$ Based. During glacial sea level is lower which restricts $CaCO_3$ burial to deep sea. Deep sea burial must increase to balance the influx of Ca^{2+} and CO_3^{2-} from weathering. An increase in deep sea $CaCO_3$ burial increase ocean pH (ocean becomes more basic). CO_2 would be drawn down to restore ocean pH.	Linked to sea level. Deep sea records to not record a change in the depth of lysocline of the right magnitude. Deep sea cores do not appear to record high enough $CaCO_3$ burial rates during glacial time.	Supported by paleotracers (Boron isotopes).	Berger (1982a;b); Opdyke and Walker (1992); Milliman (1993); Opdyke and Wilkinson (1993); Walker and Opdyke (1995); Ridgwell *et al.* (2003); Vescei and Berger (2004); Rees *et al.* (2005)
Increased Silica Supply Increased Silica supply (dust) promoting export of siliceous (Diatoms) rather than calcareous phytoplankton.	No evidence for large shift in lysocline depth in sedimentary record.	Evidence for high ocean pH in glacial.	Harrison (2000)

Table 1.1 Summary of hypotheses put forward to account for the lower CO_2 content of the atmosphere during glacial times continued.

Model	Problems	Advantages	References
Shelf Hypothesis Nutrient Based. Growth of terrestrial ice sheets resulted in higher weathering rates and an increase in river influx of nutrients (phosphate) to ocean and an increase in amount of organic compounds stored on the shelves during transgression. The increase in productivity would draw down atmospheric CO_2.	Linked to sea level Changes in cadmium content do not support and increase in phosphorus. Sediment $^{13}C/^{12}C$ record does not support this hypothesis. Requires too large amount of sediment deposition on shelves to be realistic.		Broecker (1982)
Vertical Redistribution Nutrient Based. Vertical redistribution of sediments and or alkalinity in global ocean.	$\Delta^{13}C$ change too late Change in CO_2 would be too rapid (100 yr) rather than that observed (8 kyr).	There is evidence for nutrient redistribution in the North Atlantic.	Boyle (1988); Keir (1991)
Southern Ocean Solubility Pump Southern Ocean Based. The solubility of CO_2 is increased with decreasing water temperature. Colder glacial Southern Ocean water would draw down more CO_2.	Effect on CO_2 not large enough Decrease in temperature-increase in freshwater in ice therefore sea water becomes more saline. The solubility of CO_2 is reduced as salinity increases.	Timing fits with *T* change.	Broecker and Henderson (1998)
Cooler Glacial North Atlantic Northern Atlantic Based. The solubility of CO_2 is increased with decreasing water temperature. Colder glacial North Atlantic water would draw down more CO_2.	Warming post dated the rise in CO_2. Decrease in temperature-increase in freshwater in ice therefore sea water becomes more saline. The solubility of CO_2 is reduced as salinity increases.		Keir (1993)

No one hypothesis can fully explain the magnitude of the observed changes in atmospheric CO_2 (of 80-90 ppmv) observed in the Antarctic ice cores (Neftel *et al.*, 1982; Sundiquist, 1993; Broecker and Henderson, 1998; Sigman and Boyle, 2000; Houghton *et al.*, 2001).

The present day oceans are a major sink for CO_2. The balance between the supply of $CaCO_3$ to the ocean from terrestrial weathering and the removal of $CaCO_3$ from the ocean into sediments (pelagic and neritic) controls both ocean pH and atmospheric CO_2 concentration (Archer and Maier-Reimer, 1994). Atmospheric CO_2 concentration is controlled by volcanism, terrestrial weathering and the formation of $CaCO_3$. Subducted carbonate rocks are thermally broken down and CO_2 is released to the atmosphere by volcanism. Over long time scales (millions of years) weathering of terrestrial silicate rocks removes CO_2 from the atmosphere and releases calcium and carbonate (bicarbonate) ions which are transported by rivers to the ocean.

On timescales shorter than 100 kyr the marine carbonate cycle has an important role in determining atmospheric CO_2. In the ocean calcifying planktonic foraminifera and corals remove carbonate ions from the water to make their $CaCO_3$ shells. $CaCO_3$ is removed from the ocean by alteration and burial of $CaCO_3$ in coral reefs and deep sea sediments. Terrestrial weathering and $CaCO_3$ formation (and burial) act as negative feedback on atmospheric CO_2 concentration. Recently the processes that control the marine $CaCO_3$ budget have become the focus of much scientific attention, specifically the role that the oceans might play in mitigating future anthropogenic CO_2 increase (Feely *et al.*, 2004).

This doctoral project focuses on the Coral Reef Hypothesis (CRH, Berger, 1982a; b; Keir and Berger, 1985; Opdyke and Walker, 1992), which suggests that significant increases in coral reef growth may have contributed to the deglacial increase in atmospheric CO_2 observed in the ice core records (Petit *et al.*, 1999; Indermuhle *et al.*, 1999).

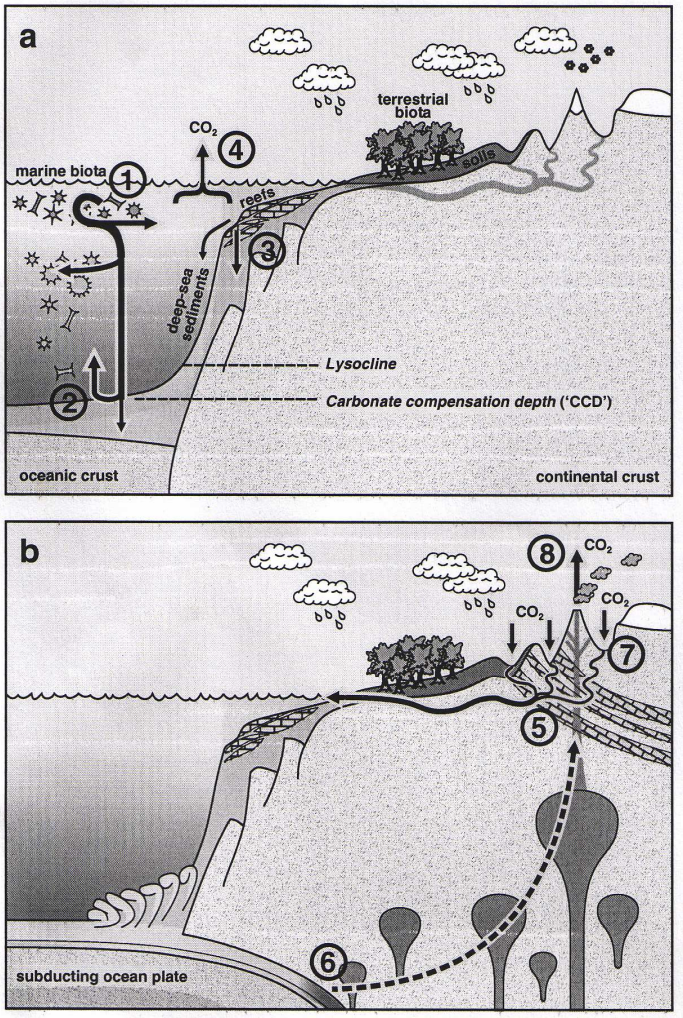

Figure 1.2 The global biogeochemical cycling of calcium carbonate (from Ridgwell and Zeebe, in press). (a) Modes of $CaCO_3$ transformation and recycling within the surficial system and loss to the geological reservoir (labelled '1' through '4'). 1 Precipitation of calcite by coccolithophores and foraminifera in the open ocean; $Ca^{2+} + 2HCO_3^- \rightarrow CaCO_3 + H_2O + CO_{2\,(aq)}$. 2 Carbonate reaching deep-sea sediments will dissolve during early diagenesis if the bottom water is under-saturated and/or the organic matter flux to the sediments is sufficiently high. 3 Precipitation of $CaCO_3$ by corals and shelly animals, with a significant fraction as the aragonite polymorph. Because modern surface waters are over-saturated relatively little of this carbonate that dissolves results in higher pCO_2 at the surface, driving a net transfer of CO_2 from the ocean to the atmosphere. (b) Modes of $CaCO_3$ transformation and recycling within the geologic reservoirs and return to the surficial system (labelled '5' through '8'). 5 $CaCO_3$ laid down in shallow seas as platform and reef carbonates and chalks can be uplifted and exposed to erosion through rifting and mountain-building episodes. $CaCO_3$ can then be directly recycled; $CO_2 + H_2O + CaCO_3 \rightarrow Ca^{2+} + 2HCO_3^-$. 6 Thermal breakdown of carbonates subducted in to the mantle or deeply buried. The decarbonation reaction involved is essentially the reverse of silicate weathering, and results I the creation of calcium silicates and release of CO_2; $CaCO_3 + SiO_2 \rightarrow CO_2 + CaSiO_3$. 7 Weathering of silicate rocks; $2CO_2 + H_2O + CaSiO_3 \rightarrow Ca^{2+} + SiO_2 + 2H_2CO_3^-$. 8 Emission to the atmosphere of CO_2 produced through decarbonation. This closes the carbon cycle on the very longest time-scales.

1.3 History of the Coral Reef Hypothesis:

1.3.1 An early attempt to explain increases in deglacial atmospheric CO_2

It was first suggested that an increase in the atmospheric carbon dioxide content could cause climate warming over a century ago (Arrhenius, 1896). Furthermore, carbon dioxide is a byproduct of calcification (Arrhenius, 1896),

Equation 1.1 Calcification

$$\mathbf{Ca^{2+}_{(aq)} + 2HCO_3^-{}_{(aq)} \rightarrow CaCO_{3\,(s)} + H_2O_{\,(aq)} + CO_{2\,(aq)}}$$

where HCO_3^- is bicarbonate, $CaCO_3$ is calcium carbonate, CO_2 is carbon dioxide. The Coral Reef Hypothesis is based on the fact that the precipitation of $CaCO_3$ in coral reef systems increases in the partial pressure of CO_2 in the surface waters which, in an open system, results in CO_2 out-gassing to the atmosphere (Berger, 1982a). Berger (1982a) originally proposed that the Coral Reef Hypothesis could have been responsible for the 180 to 350 ppm increase in atmospheric CO_2 between the LGM and 13 ka observed in the early ice core records (Delmas *et al.*, 1980). A simple box model of the Coral Reef Hypothesis yielded an atmospheric CO_2 change of the right magnitude, 3 atmospheric carbon masses (1 ACM = 6.2×10^{17} g C ≡ 300 ppm), at approximately 15 ka to fit the deglacial atmospheric CO_2 changes seen in the early ice cores (Figure 1.3; Berger, 1982a).

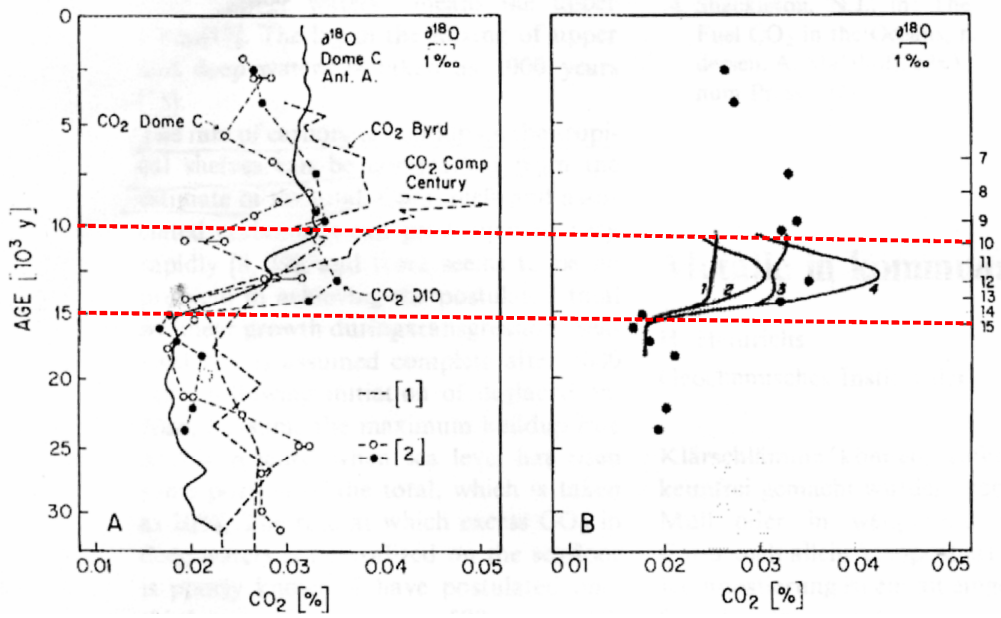

Figure 1.3 A Changes in atmospheric CO_2 content as seen early in ice core records The filled black circles are Dome 10 data from Delmas *et al.* (1980) which Berger's (1982a) model results are compared

to in Figure B. The ice core data were plotted using $\delta^{18}O$ curves as a means of correlation. The Camp Century results (Neftel *et al.*, 1982) although more recent at the time were considered to be less reliable. B shows attempts to model the CO_2 change using the Coral Reef Hypothesis (black lines; modified after Berger, 1982a).The filled circles represent the Dome 10 CO_2 record re-plotted for comparison with the model results represented by the black lines. The time scale in B is based on $\delta^{18}O$ correlation between the ice cores and marine box cores from the Pacific (Berger and Killingley, 1982). The four curves represent model runs with adjusted conditions, for example, coral reef growth, mixing rate and dissolution rates, the results show a reasonable fit to the type of CO_2 changes recorded in the ice cores (Berger, 1982a). The red lines highlight the time period where the model CO_2 increase corresponds to the changes in atmospheric CO_2 concentration recorded in the early ice cores.

Later in the same year Berger (1982b) constrained his simple box model with coral reef accumulation rate data, patterns of deep sea dissolution and lysocline depth changes during the transgression. Berger's (1982b) revised box model calculated that the coral reef mechanism released between 1 and 3 ACM during a 5 kyr period. This increase in atmospheric CO_2 concentration was much larger than the increase seen in the early ice core records (Dome C, Byrd, Camp Century) and would have resulted in too great a shoaling of the lysocline compared to deep sea core evidence. Berger (1982b) conceded that the Coral Reef Hypothesis did not fully or easily account for the ice core data and that other carbon sinks must therefore operate to absorb the excess coral reef CO_2 including build up of rain-forest or the soil carbon pool (Shackleton, 1977; Berger, 1977). Although the Coral Reef Hypothesis does represent a deglacial atmospheric CO_2 positive feedback mechanism (Figure 1.4) the initial cause (trigger) of de-glacial warming and sea level rise was probably due to a Milankovitch mechanism (Berger (1982b).

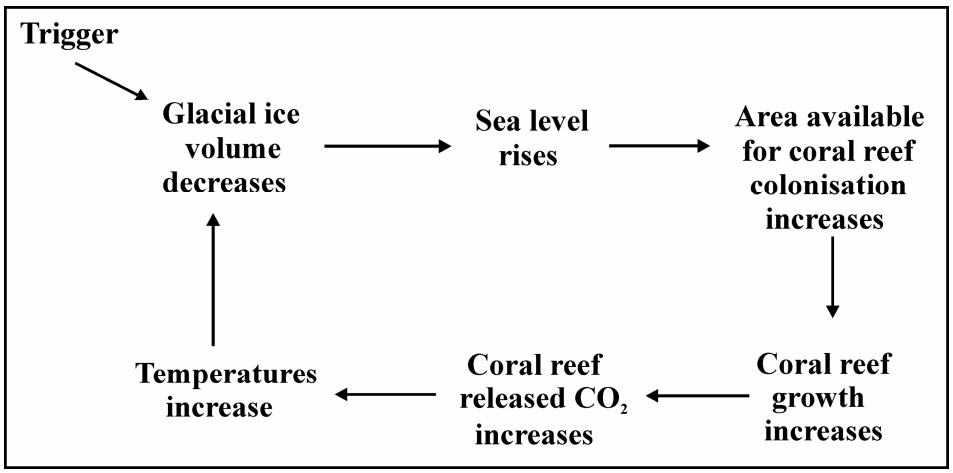

Figure 1.4 Coral Reef Hypothesis positive feedback mechanism. Some factor or combination of factors trigger the initiation of deglaciation causing glacial ice to melt and sea level to rise. Sea level rise

increases the space available for coral reef growth. As coral reefs grow into the newly available accommodation space, CO_2 is released as a byproduct of calcification. The reef-released CO_2 amplifies the deglacial atmospheric CO_2 increase and induces further warming, ice melt and continued sea-level rise.

1.3.2 Deep-Sea Dissolution

During glacials sea level is approximately 100 m lower than its present day level and the deep sea is the locus of carbonate deposition (Figure 1.5B). During interglacials vast areas of shallow shelf are flooded by sea level rise, increasing the area potentially available for reef growth by approximately 400 % (Kleypas, 1997). This rise in sea level shifts the locus of carbonate deposition from the deep sea to the shallow shelves (Figure 1.5A). The increase in coral reef calcification, caused by increased accommodation space, results in a lowering of the dissolved carbonate ion concentration in surface waters. The reduction in carbonate ion concentration is transmitted to the deep-sea and leads to enhanced dissolution of carbonate sediments below the lysocline (Figure 1.5A). This process can essentially be spilt into two parts, a build up of excess CO_2 resulting from coral reef calcification and the subsequent dissolution of deep sea carbonate. The transfer of this excess CO_2 or a reduction in the carbonate ion (in DIC) signal to the deep sea by the thermohaline circulation takes time (average mixing time of the ocean is approximately 1000 years (Sigman and Boyle, 2000)) hence there is a build up of the excess CO_2 in surface waters and the atmosphere.

Pelagic carbonate formation (by planktonic foraminifera and coccolithophores) does not result in the dissolution of deep-sea sediments because the carbonate shells formed by these planktonic organisms dissolve as they sink through the water column restoring the carbonate ion concentration (Figure 1.6). Pelagic recycling of foraminferal and coccolithophore $CaCO_3$ (through production and subsequent dissolution) occurs continuously throughout the glacial-interglacial cycle.

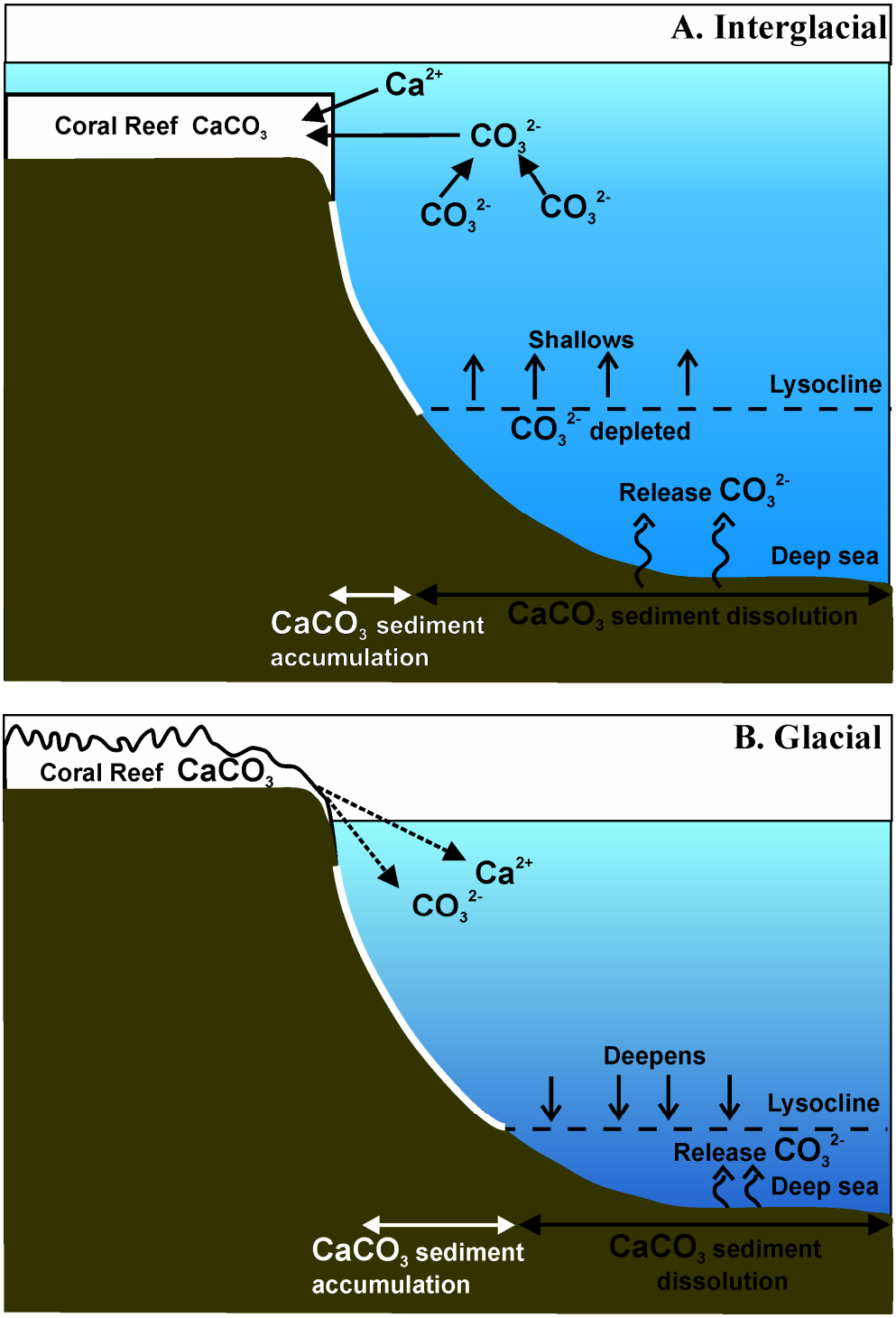

Figure 1.5 A. Cartoon of the interglacial ocean carbonate system. During interglacials the shift of carbonate deposition from the deep sea to coral reefs leads to a) a shoaling of the lysocline and b) an increase in the area of deep sea floor where dissolution of deep-sea carbonate sediments occurs to restore the oceanic carbonate ion concentration. B. Cartoon of the glacial ocean carbonate system. During glacial periods sea level is lower and area available for coral reef growth is significantly reduced. The ocean carbonate ion concentration is restored by riverine input and the erosion and dissolution of the now exposed reefs. The restoration of ocean carbonate causes the lysocline to deepen, reduces the area of the sea bed where deep sea carbonate sediments are dissolved and the deep sea becomes the dominant locus of carbonate deposition.

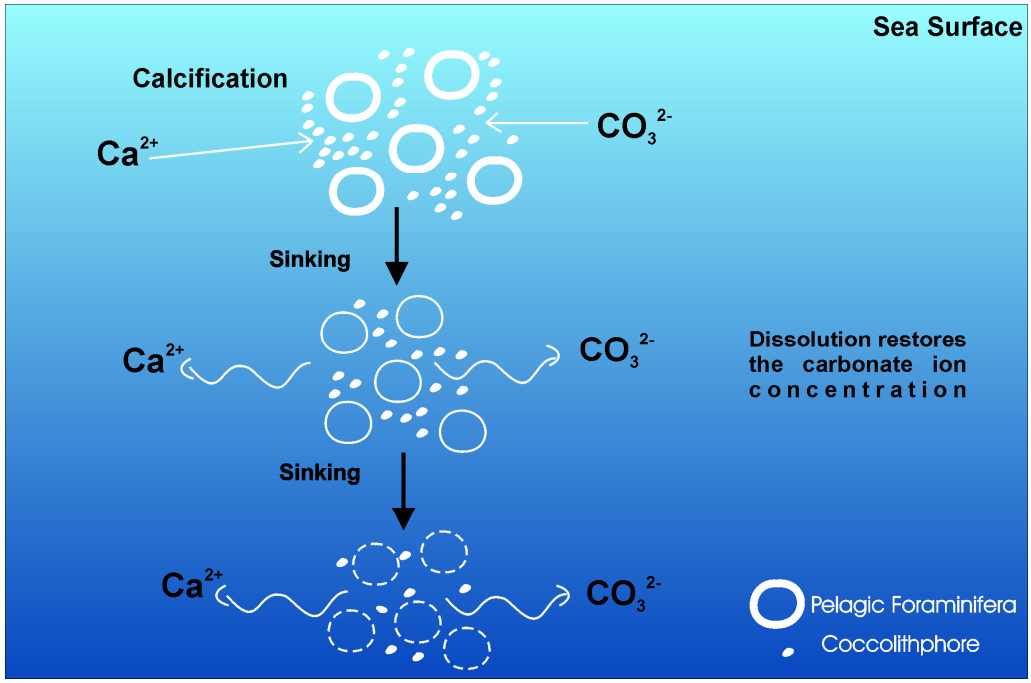

Figure 1.6 Pelagic foraminifera and coccolithophores deposit shells of calcium carbonate ($Ca^{2+} + 2HCO_3^- \rightarrow CaCO_3 + CO_2 + H_2O$), removing carbonate ($CO_3^{2-}$) and calcium ions ($Ca^{2+}$) from surface waters. After death these planktonic organisms sink. The carbonate shells rapidly dissolve as they sink through the water column restoring the carbonate ion concentration in surface waters.

Originally, basin to shelf transfer of $CaCO_3$, as invoked by the Coral Reef Hypothesis, was investigated as a possible mechanism to explain the late Holocene dissolution event well known from deep-sea carbonate in the equatorial Pacific. But results of a Coral Reef Hypothesis dissolution model suggested that although reef growth could have produced a deep-sea dissolution event of the same magnitude as that observed in the sedimentary record (approximately 8 g cm^{-2} $CaCO_3$), it would have not occurred at the correct time during the Holocene (Keir and Berger, 1985). If coral reef growth were responsible for the late Holocene dissolution in the deep-sea cores there would have been a substantial increase in reef growth in the late Holocene (3 ka) and a natural pulse of CO_2 recorded in the ice core records. Yet, no evidence had been found at that time for either. It was therefore concluded that the Coral Reef Hypothesis was a satisfactory explanation for post-transgression dissolution in general, but could not explain the additional late Holocene dissolution effect seen in the Pacific deep-sea sediment cores (Keir and Berger, 1985; Farrell and Prell, 1991).

1.3.3 Coral Reef Hypothesis Revisited

In light of improvements in the understanding of 1) the stoichometry of the calcification process and subsequent release of CO_2 to the atmosphere (Ware *et al.*, 1991)[1], ii) global $CaCO_3$ accumulation rates and (iii) the availability of new, high resolution ice core records. New box model experiments were designed to tackle the problem of Holocene $CaCO_3$ deposition (Opdyke and Walker, 1992). Results suggested that the CO_2 released by reef calcification might well correspond to the magnitude and timing of the atmospheric CO_2 change in the Vostok ice core (Figure 1.7).

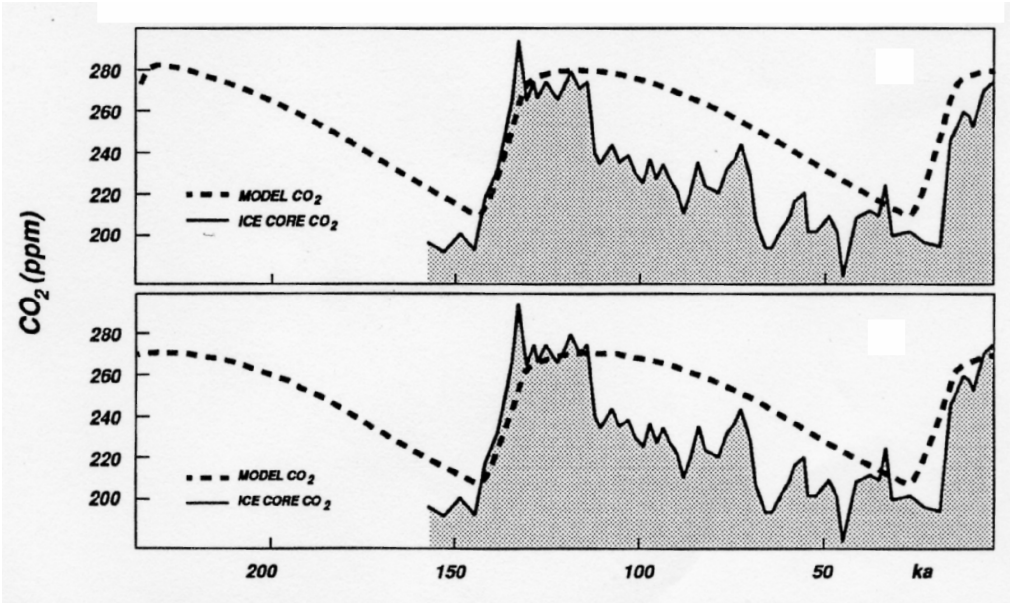

Figure 1.7 Calculated atmospheric CO_2 concentrations corresponding to changes in shelf carbonate deposition over the last 200 ka compared to the changes observed in the Vostok Ice core record (Opdyke and Walker, 1992). During glacial periods (25 and 150 ka) sea level was lower and the shallow shelves became sources of carbonate to the ocean. During interglacial periods (present and 125 ka) higher sea level shifted the locus of carbonate deposition to the shallow shelves. The timing and magnitude of the CO_2 released as a result of interglacial shallow water carbonate deposition is similar to the changes observed in the Vostok Ice core record. The top and bottom figures represent modelled atmospheric CO_2 changes using the dissolution constants of D=0.0002 g cm^{-2} yr^{-1} and D=0.0008 g cm^{-2} yr^{-1}.

These experiments were undertaken using an average Holocene $CaCO_3$ accretion rate of 1.6 m kyr^{-1} over a 5 kyr period that was calculated from 60 Holocene carbonate sequences (200 rate values). Results indicated that deglacial coral reef growth alone could account for the atmospheric CO_2 fluctuation seen in the ice core records and contribute to the pelagic $CaCO_3$ dissolution events observed in the equatorial Pacific

[1] The calcification reaction: $Ca^{2+} + 2HCO_3^- \rightarrow CaCO_3 + H_2O + CO_2$ states that for every mole of $CaCO_3$ precipitated one mole of CO_2 is released. However, in seawater the CO_2 produced is subject to the buffering effect of seawater (conversion to carbonate, see Equation 1.2, page 19) such that, in fact, only about 0.6 mol CO_2 is liberated per mole of $CaCO_3$ deposited (Ware *et al.*, 1991).

(Broecker *et al.*, 1991; Wu *et al.*, 1990). Opdyke and Walker (1992) concluded that the magnitude of the shallow water $CaCO_3$ flux had been underestimated by the previous modelling studies of de-glacial atmospheric CO_2 changes (Berger, 1982a; 1982b; Berger and Killingley, 1982; Berger and Keir, 1984; Keir and Berger, 1985).

Coupled simulations of the global carbon cycle, ocean chemistry, sediment dissolution and preservation were subsequently used to investigate how varying rates of neritic carbonate deposition affect the atmospheric CO_2 concentration and pelagic carbonate sedimentation (Walker and Opdyke, 1995). Results of these experiments indicated that the amount and timing of coral reef-released CO_2 was similar to that seen in the Vostok ice core record (Figure 1.8). Walker and Opdyke's (1995) model also yielded calcite saturation depth (CSD) change of several kilometres in response to changes in neritic $CaCO_3$. This result is not compatible with the equatorial Pacific sedimentary record, which shows changes in the CSD of less than a kilometre (Farrell and Prell, 1989; Sigman and Boyle, 2000). However, Walker and Opdyke's (1995) model reveals that rapid, brief changes in lysocline depth (~ 1000 years, > 5 km water depth), as a result of varying rates of neritic carbonate sedimentation, are rarely preserved in the deep sea sedimentary record (Walker and Opdyke, 1995). Walker and Opdyke (1995) concluded that variation in neritic carbonate sedimentation may have had a primary role in altering atmospheric CO_2 concentration during glacial-interglacial cycles.

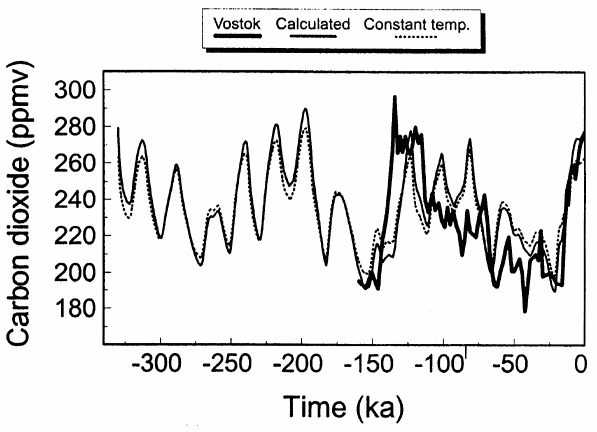

Figure 1.8 Modelled changes in atmospheric CO_2 concentration (thin line) in response to neritic carbonate deposition are similar to the changes observed in the Vostok ice core record (thick line; Barnola *et al.*, 1987; Walker and Opdyke, 1995). The modelled atmospheric CO_2 concentrations are shown for both constant and variable (calculated) seawater temperature. Poor correlations at substages 5c (105 – 90 ka) and 5a (85 – 75 ka) may result because sea level was 20 m lower than today and the model therefore overemphasizes the coral reef effect.

1.3.4 The Coral Reef Hypothesis: The Critique

In response to Opdyke and Walker's (1992) paper, Mylroie (1993) commented that de-glacial global warming could not have been initiated by the liberation of CO_2 from reef carbonate deposition because this mechanism is sea level-led. High-resolution ice core records suggest that increases in deglacial atmospheric CO_2 and temperature preceded glacio-eustatic sea level rise (Sowers *et al*., 1991).

Kayanne (1992) used accretion rates from eight reefs (Mariana Islands, Palau Islands, Great Barrier Reef, Florida Reef tract, Hanauma Bay and the Pacific and Caribbean coasts of Panama) along with Smith's (1978) global average reef production estimate of 0.072 Gt C yr^{-1} to parameterise Holocene coral reef growth in response to sea level rise. Using data from these few selected reefs, results from this parameterised study suggested that Holocene reef growth was initiated around 8 ka and that maximum reef growth occurred at a rate of 0.45 ACM yr^{-1} (Atmospheric Carbon Masses - ACM, 2 ACM = 1200 Gt C) between 6-5 ka (Figure 1.9). Kayanne (1992) concluded that the main phase of estimated reef growth did not match the period of atmospheric CO_2 increase recorded in the ice cores, providing further evidence to refute the notion of the Coral Reef Hypothesis as a mechanism capable of initiating deglaciation (Figure 1.9). This theme was also explored in a more recent review of the glacial-interglacial problem (Broecker and Henderson, 1998).

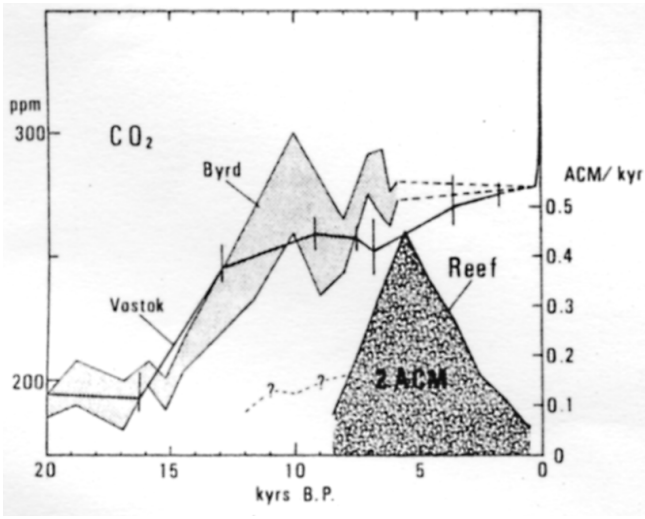

Figure 1.9 Rate of reef $CaCO_3$ deposition (ACM/kyr) and atmospheric CO_2 change (ppm) for the last 20 kyr compared to the Byrd (Neftel *et al.*, 1988) and Vostok (Barnola *et al.*, 1987) ice cores (Figure from Kayanne, 1992). Note that the main CO_2 increase observed in the ice core records (15 to 10 kyr BP) preceeds the main phase of reef growth (7 to 5 kyr BP). The total mass of reef $CaCO_3$ is 2 ACM (Atmospheric Carbon Masses - ACM, 2 ACM = 1200 Gt C). The shaded area under the Byrd ice core record shows the range of errors.

1.3.5 Modelled Reef Area and Production since the LGM

A diagnostic model (ReefHab) was constructed to predict areas suitable for coral reef growth during the last 21 kyr using measured environmental variables such as temperature, salinity, nutrients and light (Kleypas, 1997). This model estimates that reef area and carbonate production during the LGM was 20 % and 27 % of present day values respectively (Figure 1.10 A and B). ReefHab also predicts that reef area during deglaciation could have been more extensive than previously thought, contradicting Kayanne's (1992) assumption that reef area and production prior to 10 kyr BP is negligible. Kleypas (1997) used estimates of reef area and production during deglaciation to calculate coral reef released CO_2 to the atmosphere since the LGM. The model predicts that coral reef released CO_2 was in the same order of magnitude as the atmospheric CO_2 change seen in the Vostok ice core record (Figure 1.10, C), in agreement with Opdyke and Walker (1992).

1.3.6 High Resolution Benthic Foraminiferal Sr/Ca Records

Low sedimentation rates, blurring by chemical erosion and bioturbation obscure many of the deep-sea records previously used to identify dissolution events. Recently, ODP Site 1089 yielded a high-resolution record of the carbonate saturation state in the deep sea during the last 600 ka (Hodell *et al.*, 2001). This site provides a detailed record of the timing and response of the carbonate system that acted to reinforce the initial deglacial pCO_2 changes. If the basin-shelf fractionation (Milliman, 1974; 1993; Berger, 1982a; b; Keir and Berger, 1985; Opdyke and Walker, 1992) of marine $CaCO_3$ is responsible for episodes of deep sea carbonate dissolution, it is reasonable to expect a correlation between deep sea sediment's % $CaCO_3$ and benthic foraminiferal Sr/Ca ratio. The rationale behind this line of thought is that aragonite-rich shelf sediments have a higher Sr/Ca ratio than calcite-rich sediments (cocolithophores and foraminifera which accumulate on the deep sea floor). During interglacials sea level is high, Sr is incorporated into coral reefs on the shelves, the Sr/Ca ratio in the ocean is low and carbonate is dissolved in the deep sea.

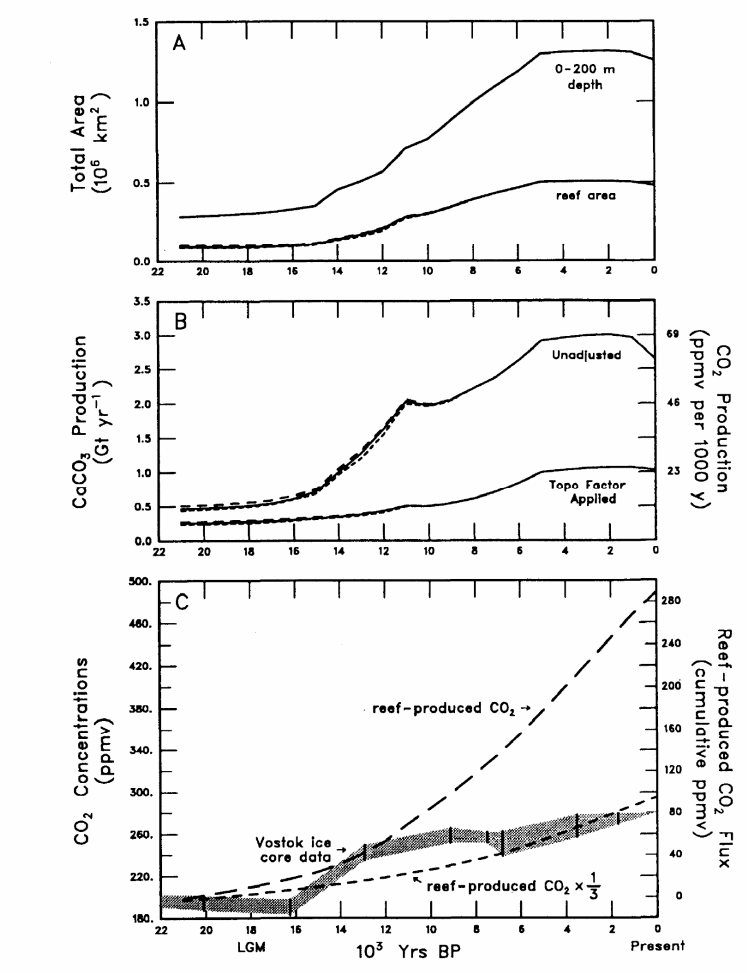

Figure 1.10 A Model estimates of changes in area available for coral reef growth since the Last Glacial Maximum. Dashed, solid and dotted lines indicate model sensitivity to sea surface temperature (SST); using CLIMAP SST, present day SST and CLIMAP × 2 values respectively. B Calculated changes in total reef $CaCO_3$ production since the LGM. The Topo factor applied refers to the model run incorporating a topography factor to attempt to localize reef growth to exposed portions of the continental shelves. Dashed, solid and dotted lines indicate model sensitivity to SST as in A. C Comparison of the ReefHab Model's cumulative flux of reef released CO_2 (using topography adjusted production values) compared to the Vostok ice core record (Kleypas, 1997). The reef-produced CO_2 ×1/3 represents the amount of CO_2 that might remain in the atmosphere if natural negative feedback processes (e.g. dissolution of carbonates at the carbonate compensation depth) act to reduce the atmospheric CO_2 concentration. The shaded area represents atmospheric CO_2 concentration recorded in the Vostok Ice Core (Barnola *et al.*, 1987). Dashed lines represent cumulative reef-released CO_2.

Conversely, during glacials, when sea level is lowered, subaerial exposure and erosion of coral reef aragonite on the shelves increases the ratio of Sr/Ca in the ocean. The % $CaCO_3$ in ODP core (Site 1089) and the Sr/Ca ratios from 6 different cores from various ocean basins (Martin *et al.*, 1999) show remarkable correlation for the last 250 kyr (Figure 1.11). The Site 1089 data also suggest that the lysocline depth changed by at

least 700 m. Although this depth change is not of sufficient magnitude to explain the entire glacial-interglacial atmospheric CO_2 signal, it is large enough to suggest that the Coral Reef Hypothesis may have had a significant effect on atmospheric CO_2 (Hodell *et al.*, 2001).

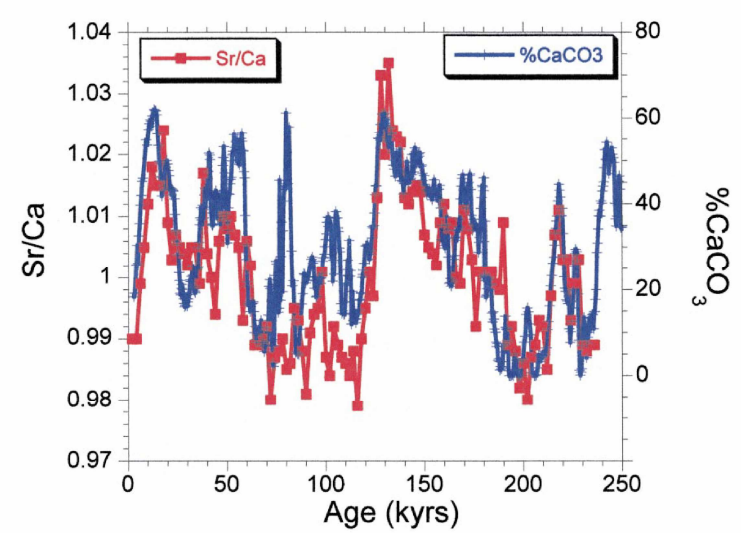

Figure 1.11 The highly correlated records of Wt % $CaCO_3$ (blue) versus foraminiferal Sr/Ca (red), at ODP Site 1089. These records are expected to be correlated if the locus of carbonate deposition changes in response to sea level rise (Hodell *et al.*, 2001).

1.3.7 Model of CRH and Terrestrial Vegetation Growth

Recently, a global atmosphere ocean sediment carbon cycle model, combining the effects of a Coral Reef Hypothesis mechanism and terrestrial vegetation re-growth generated an early Holocene deep sea carbonate preservation event consistent with proxy estimates and observations (Ridgwell *et al.*, 2003). It combines estimates of the change in reef area (Kleypas, 1997), reef accretion rates (Kayanne, 1992) and timing of reef growth (Montaggioni, 2000; Ryan *et al.*, 2001) since the LGM to quantify the contribution of reef released CO_2 to the atmosphere. Results suggest that a Coral Reef Hypothesis mechanism could have had a marked effect on atmospheric CO_2, causing an increase of 40 ppmv between 0-8 kyr BP. Ridgwell *et al.* (2003) commented that if the deposition rate, 1×10^{17} mol C, were halved the model results track the observed atmospheric CO_2 record well and may be contemporaneous with the 20 ppmv observed increase from 8 kyr BP to the industrial revolution. Because the predicted increase (using a deposition rate of 1×10^{17} mol C) is greater than that observed in the ice core records, Ridgwell *et al.* (2003) suggested that some secondary factor must dampen the coral reef released CO_2 signal, possibly the deglacial increase in the terrestrial

biosphere. These model results indicate that the expanding deglacial terrestrial biosphere could act as a negative feedback on ocean driven increases in CO_2 and drawn down atmospheric CO_2 by 33 ppmv. Ridgwell *et al.* (2003) proposed that the increase in the terrestrial biosphere between 15.4 – 13.8 kyr BP removed carbon from the ocean and caused a deep sea preservation event circa 15 kyr BP. The early Holocene increase in coral growth, in response to sea level rise, released CO_2 to the atmosphere and caused a decrease in the ocean carbonate concentration and deep sea carbonate dissolution. Ridgwell *et al.* (2003) concluded that changes in terrestrial carbon storage were able to offset the CO_2 released by coral reef calcification, thus by combining these two antagonistic mechanisms the model is able to reconcile both the deep sea sedimentary and ice core records (Berger, 1982b; Broecker *et al.*, 1993; 1999; 2001).

Recently, Vecsei and Berger (2003) and Vecsei (2004) re-evaluated the neritic carbonate budget using reef carbonate productivity estimates (calculated from the alkalinity anomaly technique) and suggested that the total accumulation of neritic carbonate since 14 kyr BP as approximately 4200×10^{15} g (4200 Gt). These studies estimate that accumulation of neritic carbonates peaked during the early Holocene and could have potentially released approximately 225 Gt C as CO_2, which they suggest was probably sequestered by the terrestrial biosphere.

1.4 Global Carbonate Budgets

At present the role of coral reefs in the global carbonate budget is poorly quantified and inadequately represented in models of the global carbon cycle (Figure 1.12). This is mainly a consequence of the rates and loci of $CaCO_3$ deposition being inadequately defined and the use of outdated or imprecise estimates of global reef area (Smith, 1978).

The export of carbon in plankton (foraminifera and coccolithophores) is relatively well defined (Figure 1.13; Milliman, 1993). Many carbonate budgets have combined the $CaCO_3$ fluxes of corals, ooids, carbonate muds and sands and shallow water carbonate embayments (Opdyke and Walker, 1992; Milliman, 1993), others combine the shallow water tropical carbonate fluxes (corals, ooids, carbonate mud and sand) together with the $CaCO_3$ flux from surface waters to the deep ocean (foraminifera and coccolithophores) (Houghton *et al.*, 2001).

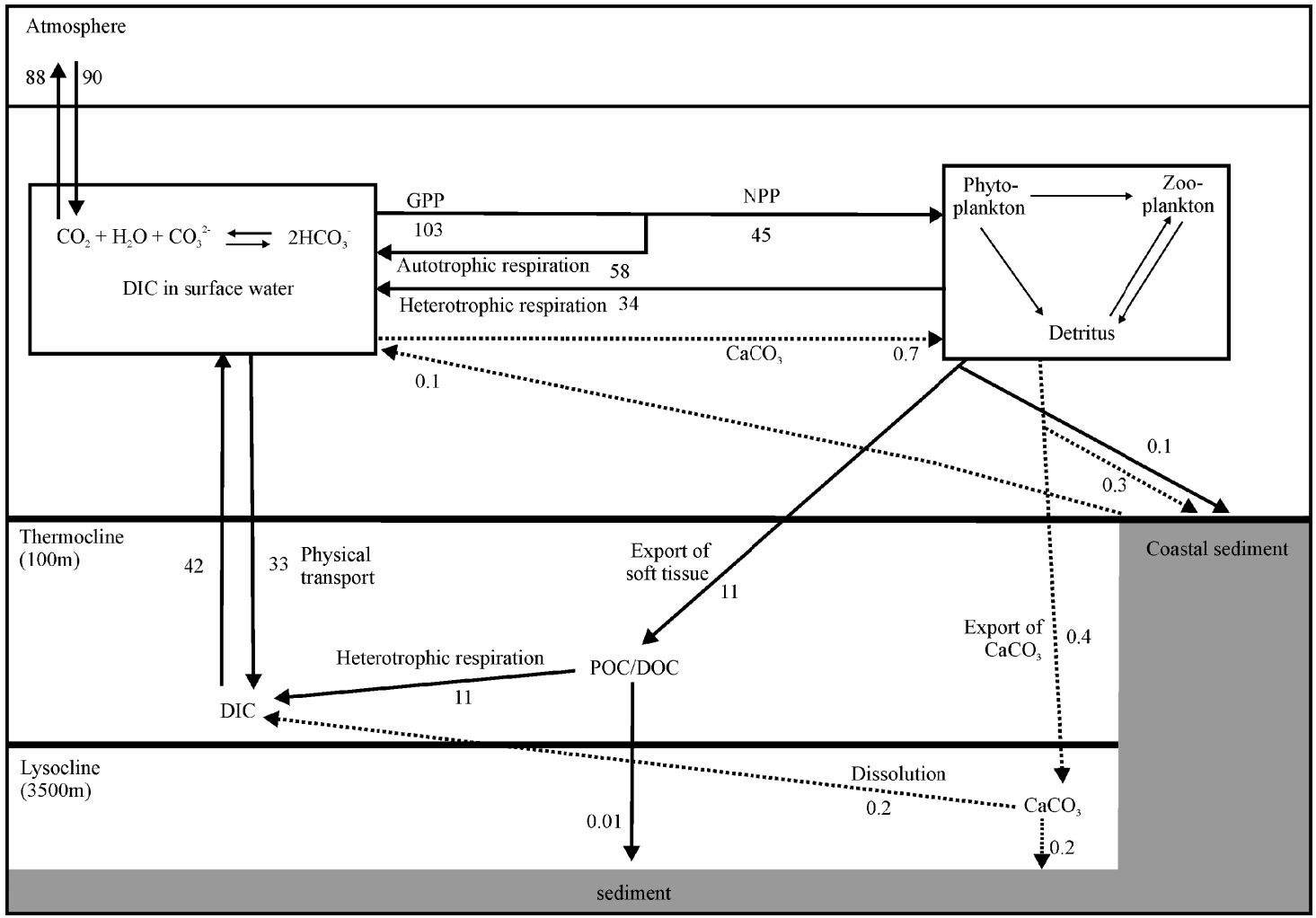

Figure 1.12 Ocean carbon cycle. Units of reservoirs – Pg C (Gt C), fluxes Pg C yr^{-1} (Gt C yr^{-1}) estimated for the 1980's (Houghton *et al.*, 2001, IPCC, Figure 3.1c). Arrows indicate natural fluxes, dashed lines indicate fluxes of carbon as $CaCO_3$. DIC represents dissolved inorganic carbon, CO_2, CO_3^{2-} and HCO_3^-. GPP represents gross primary production, NPP represents net primary production (that left after respiration). DOC is dissolved organic carbon, POC is particulate organic carbon. The $CaCO_3$ accumulated on the shelf, 0.3 Pg C yr^{-1} represents $CaCO_3$ produced plankton and detritus, 0.1 Pg C yr^{-1} returns to the pool of DIC by dissolution. The report does not indicate if the flux of 0.3 Pg C yr^{-1} of $CaCO_3$ to coastal sediments is due to corals or plankton.

In order to fully appreciate the role of ocean carbonate in the global carbon cycle it is most appropriate to split the various reservoirs of $CaCO_3$ so that they can be properly individually quantified. The new global reef area estimate of Spalding *et al.* (2001) and the increase in the quantity of reef drill core data available in the published literature allows evaluation of the role of coral reefs in the marine $CaCO_3$ budget.

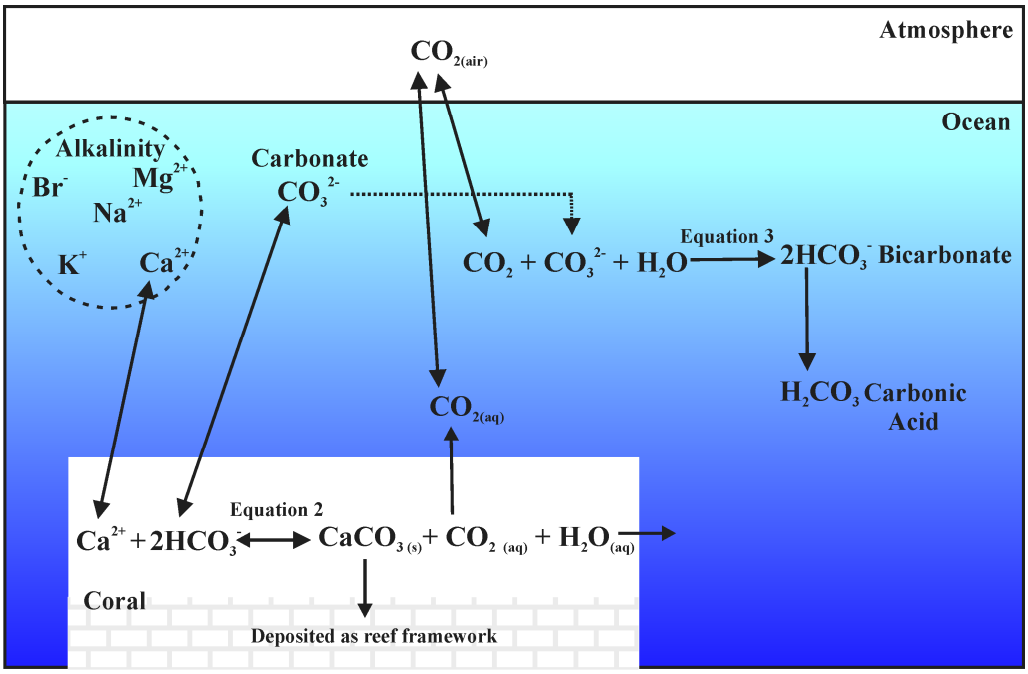

Figure 1.13 Role of coral reefs and CO_2 in the marine carbonate cycle. $CaCO_3$ is calcium carbonate, $2HCO_3^-$ is bicarbonate or hydrogen carbonate, CO_2 is carbon dioxide and CO_3^{2-} is carbonate ion.

Marine carbonate plays an important role with respect to the global carbon cycle and atmospheric CO_2 via the interaction of CO_{2atm} and DIC (dissolved inorganic carbon; CO_2, CO_3^{2-} and HCO_3^-) (Figures 1.12 and 1.13). When the atmospheric CO_2 concentration increases, CO_2 diffuses across the air-sea interface and reduces the concentration of carbonate ions by combining with them and water to form bicarbonate and eventually carbonic acid (Figure 1.13). Increased $CO_{2\ (atm)}$ also pushes equation 2 (Figure 1.13; calcification reaction) to the left resulting in dissolution of $CaCO_3$, which reduces the alkalinity and lowers the pH of seawater (formation of carbonic acid). The seawater becomes increasingly acidic, as the partial pressure of CO_2 increases its capacity to absorb more CO_2 from the atmosphere is reduced. Equally the formation of $CaCO_3$ (calcification) pushes the reactions in the opposite direction resulting in the production of CO_2 which combines with carbonate and water to form bicarbonate and carbonic acid, this lowers the surface water pH and increases the partial pressure of CO_2 so that CO_2 is released to the atmosphere.

The stoichometry of the calcification equation (Equation 1.2) holds true in freshwater such that one mole of CO_2 is released per mole of $CaCO_3$ deposited. However, in the marine environment, only ~0.6 mol CO_2 is released to the atmosphere per mole of $CaCO_3$ deposited because of the buffering effect of seawater (Wolast *et al.*, 1980; Ware *et al.*, 1991). In the marine environment the remaining 0.4 mol of the CO_2 formed is recombined with carbonate ions and water to form bicarbonate which remains in the water (hydrogen carbonate; Equation 1.2; Zeebe and Wolf-Gladrow, 2001).

Equation 1.2

Calcification

$$Ca^{2+}_{(aq)} + 2HCO_3^-{}_{(aq)} \longrightarrow CaCO_{3\,(s)} + H_2O_{(aq)} + CO_{2(aq)}$$

$$CO_{2(aq)} \longrightarrow CO_{2\,(atm)}$$

$$CO_{2(aq)} + CO_3^{2-}{}_{(aq)} + H_2O_{(aq)} \longrightarrow 2HCO_3^-{}_{(aq)}$$

[a] 0.6 mol available for release to the atmosphere.

[b] 0.4 mol recombines to form aqueous hydrogen carbonate (bicarbonate).

In Equation 1.2, HCO_3^- is bicarbonate or hydrogen carbonate, $CaCO_3$ is calcium carbonate, CO_2 is carbon dioxide and CO_3^{2-} is carbonate ion. The fate of the remaining 0.6 moles of CO_2 has been debated: CO_2 has been measured passing across the air sea interface to the atmosphere on several Pacific reefs (Gattuso *et al.*, 1993; 1999; Frankignoulle *et al.*, 1994). However, some studies have found the flux of CO_2 appears to be in the opposite direction, influx of CO_2 from the atmosphere into the sea (Kayanne *et al.*, 1995; Yamamuro *et al.*, 1995; Chrisholm and Barnes, 1998). These contradictory findings may have arisen because the studies inferring an influx of CO_2 were conducted on unhealthy, stressed fringing reefs exposed to high nutrient concentrations and turbidity which are not considered to be representative of the general picture of Holocene reef growth (Gattuso *et al.*, 1999). Determination of the CO_2 flux for reefs worldwide and over a variety of time scales has yet to be adequately quantified, however the current consensus is that healthy reefs are a source of CO_2 to the atmosphere (Barker *et al.*, 2003).

Increasing atmospheric CO_2 concentration pushes Equation 1.2 to the left which increases the dissociation of $CaCO_3$, and reduces the alkalinity and lowers the pH of seawater. Seawater acidification reduces calcification, which results in weaker coral skeletons which are more susceptible to disease and erosion. The reef framework may

be degraded and increasingly vulnerable to mechanical erosion and may become damaged.

1.5 Holocene Reef Evolution

Radiometrically dated reef drill cores, vibro and piston cores and seismic profiling investigations have revealed the evolution of many Holocene reefs worldwide. These studies have revealed a general pattern of Holocene reef growth in response to sea level rise (Figure 1.14 A-J; Montaggioni, 2005). As sea level rises, fresh space is created which can accommodate new coral growth. In order to remain in the photic zone (to maintain the photosynthetic process of their algal symbionts at a maximum), reef corals respond to sea-level rise by growing vertically upwards and ultimately producing the magnificent structures easily visible in tropical regions today.

Neumann and Macintyre (1985) proposed that coral reefs exhibit three types of growth in response to sea level rise, keep-up, catch-up or give-up. Keep-up reef growth tracks sea level rise rate by maintaining the reef surface at or near sea level. Catch-up reefs are initiated as shallow reefs, the depth of water covering them increases significantly because they cannot keep-up with the rate of sea level rise, after sea level has stabilised these reefs catch-up to sea level. Give-up reefs are relict reefs whose growth is so slow that it lags sea level rise by so much that they become unable to catch-up to sea level. Eventually give-up reefs are left in such great water depths that they cease to grow and are effectively drowned (Neumann and Macintyre, 1985). In the Indo-Pacific region, sea level broadly stabilized around 6 kyr BP whereas in the Caribbean modern sea level was reached within the last 3000 years (Thom and Roy, 1983; Bard *et al*. 1996; Blanchon, 2005). Once the reefs had reached this level (by either catch-up or keep-up growth (Neumann and Macintyre, 1985)) their growth was retarded by subareal exposure at the surface and they began to prograde laterally. Excess productivity (reef sediments) on the reef flat is transported to leeward forming lagoons and leeward accretionary wedges (LAW).

The rate of coral reef growth varied during the Holocene in response to sea level rise and other environmental factors including turbidity, substrate type, proximity to larval recruitment centres, light, salinity, nutrients and temperature (Lighty *et al.*, 1978; Kinsey, 1981; Hopley, 1982; Davies *et al.*, 1985; Neumann and MacIntyre, 1985; Bard *et al.*, 1990; Cortes *et al.*, 1994; Kleypas, 1997; Montaggioni and Faure, 1997; Gischler and Lomando, 2000; Montaggioni, 2005).

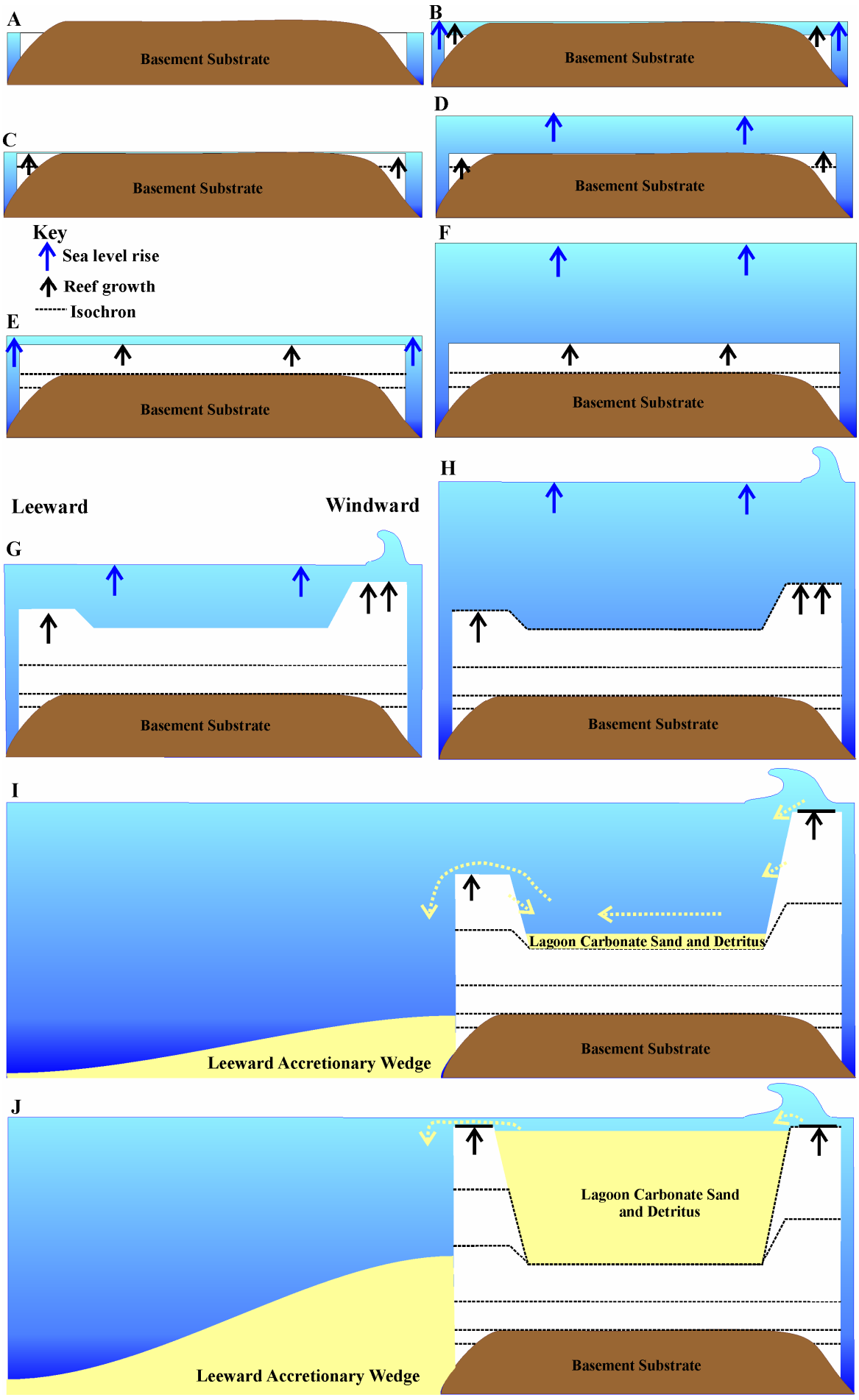
A
Basement Substrate
B
Basement Substrate
C
Basement Substrate
D
Basement Substrate
Key
Sea level rise
Reef growth
Isochron
E
Basement Substrate
F
Basement Substrate
Leeward
Windward
G
Basement Substrate
H
Basement Substrate
I
Lagoon Carbonate Sand and Detritus
Leeward Accretionary Wedge
Basement Substrate
J
Lagoon Carbonate Sand and Detritus
Leeward Accretionary Wedge
Basement Substrate

Figure 1.14 A-J. Cartoon sequence of Holocene (platform) reef growth in response to sea level rise. A-E sea level rise creates more accommodation space for coral growth. Initially the whole platform becomes covered with coral growth. G windward margin growth starts to accelerate, probably due to increased metabolic function resulting from more oxygen in the water from increased wave motion. This has an effect on both margins but is more pronounced on the windward margin, the lagoon corals lag behind and eventually become smothered by carbonate sediments transported from the reef margins, the reef starts to form a bucket shape. H-I the windward margin reaches sea level first and the excess sediments are moved to leeward (yellow dotted arrows) and to fill the lagoon and form the leeward accretionary wedge. J the windward and leeward margins are at sea level, the lagoon is almost full of carbonate sand and a large leeward accretionary wedge has formed.

Understanding the variety of reef shapes, sizes and growth histories is vital when constructing an accurate global coral reef $CaCO_3$ mass balance.

1.6 Rationale

The key to understanding the impact anthropogenic combustion of fossil fuels will have on the climate system, is to fully understand the complex feedback loops within the natural system including the Coral Reef Hypothesis (Berger, 1982a; b). Herein I examine the role of coral reefs in the global carbon cycle and oceanic carbonate budget and constrain the coral reef carbon fluxes into reef sediments and atmosphere both spatially and temporally during the Holocene. These new estimates of reef $CaCO_3$ accumulation during the Holocene and subsequent release of CO_2 calculated will be of interest to climate modellers trying to improve understanding of the various reservoirs and fluxes within the global carbon cycle. This project also examines the Holocene evolution of three reefs, Rodrigues fringing reef in the Southwest Indian Ocean, Lizard Island fringing reef and MacGillivray platform reef in the Northern Great Barrier Reef, using radiocarbon dated drill cores.

1.7 Aims and Objectives

The aims of this PhD thesis are to:

1. Quantify the global mass balance of $CaCO_3$ deposited by coral reef systems during the Holocene and to quantify the flux of CO_2 to the Holocene atmosphere resulting from carbonate deposition in reef systems.
2. Obtain accumulation rates and evolutionary history for previously unstudied reefs at three case study sites; Rodrigues (South West Indian

Ocean), Lizard Island and MacGillivray Reefs (Northern Great Barrier Reef).

3. Establish the mass of calcium carbonate sediments within the *Halimeda* bioherms of the Northern Great Barrier Reef and a carbonate budget for the outer shelf region of the Northern Province.

1.8 Structure of Thesis

The main body of this thesis (chapters three to six) comprises four papers, one published and three in review, submitted to peer refereed journals. Acknowledgement paragraphs at the end of chapters highlight the individual contributions, advice and expertise in field or laboratory and financial and logistic support. These science chapters have a common thread – they are all concerned with investigating Holocene coral reef evolution and the global carbonate budget. The chapters three and four investigate the Holocene evolution of three coral reefs using reef drill and radiocarbon dating, this information is then combined with data compiled from the published literature to create a global dataset of Holocene coral reef accretion rates to estimate the global Holocene reefal carbonate budget (chapter five). Chapter six investigates another poorly quantified neritic carbonate reservoir, *Halimeda* bioherms. Chapter seven pulls together data disseminated in the papers and summarises the conclusions and suggests topics for future research.

1.8.1 Chapter Two

Chapter two outlines the materials and methods used during the course of this project. These methods include coral reef drilling and radiometric dating methods. Other techniques discussed include seismic profiling and the measurement of modern day productivity on coral reefs.

1.8.2 Chapter Three

Chapter three comprises a paper which outlines the Holocene evolution of Lizard Island and MacGillivray Reefs (Northern Great Barrier Reef) which was investigated by drilling and radiocarbon dating of corals from cores taken from the reef flat of these reefs. This paper was co-authored by Dr Bradley Opdyke (ANU), Dr Paul Wilson (NOCS), Dr Keith Fifield and Dr Vladimir Levchenko (ANU) and submitted (02.11.04)

to Coral Reefs entitled 'Holocene Evolution of the Granite based Lizard Island and MacGillivray Reef Systems, Northern Great Barrier Reef'.

1.8.3 Chapter Four

Chapter four comprises a paper which outlines the Holocene evolution of Rodrigues fringing reef in the Southwestern Indian Ocean and a preliminary estimation of the contribution that Southwest Indian Ocean coral reefs could have made to the global Holocene calcium carbonate budget. This reef system was investigated by reef drilling, which was facilitated by the Shoals of Capricorn Programme, These shallow cores were radiocarbon dated and compared to other reefs in the region e.g. Mauritius and Reunion. This paper was co-authored by Dr Bradley Opdyke (ANU), Dr Paul Wilson (SOC), and Dr Keith Fifield (ANU) and was published in the Philosophical Transactions of the Royal Society of London, Series A, 363, 101-120 (2005) entitled 'Coral Reef Sedimentation on Rodrigues and the Western Indian Ocean and its Impact on the Carbon Cycle'.

1.8.4. Chapter Five

Chapter five comprises a re-evaluation of the contribution coral reef calcium carbonate deposition could have made to the global calcium carbonate budget and atmospheric carbon dioxide levels during the Holocene. This study was submitted to Global Biogeochemcial Cycles (06.08.05) entitled 'The Impact of Coral Reef $CaCO_3$ Accumulation on Holocene Atmospheric Carbon Dioxide Concentration' and is co-authored by Dr Bradley Opdyke (ANU) and Dr Paul Wilson (NOCS).

1.8.5. Chapter Six

Chapter six was written as a short communication investigating the relative masses of calcium carbonate contained within the coral reefs and *Halimeda* bioherms of the Northern Great Barrier Reef. The paper was submitted (25.08.05) to Coral Reefs entitled 'Coral Reef and *Halimeda* Bioherm $CaCO_3$ Accumulation on the Northern Great Barrier Reef Shelf During the Holocene' was co-authored by Dr Bradley Opdyke (ANU) and Dr Paul Wilson (NOCS) and Dr Tim Henstock (NOCS).

1.9 References

Andersson, A. J., Mackenzie, F. T. and L. M. Ver (2003) Solution of shallow-water carbonates: An insignificant buffer against rising atmospheric CO_2. *Geology,* **31**, 6, 513–516.

Archer, D. and E. Maier-Reimer (1994) Effect of deep-sea sedimentary calcite preservation on atmospheric CO_2 concentration. *Nature,* **367**, 260-263.

Arrhenius, S. (1896) On the influence of carbonic acid in the air upon the temperature of the ground. *Philos. Mag. J. Sci.*, **41**, 237-276.

Bard, E., Hamelin, B., Fairbanks, R. G. and A. Zindler (1990) Calibration of the ^{14}C timescale over the past 30,000 years using mass spectrometric U-Th ages from Barbados corals. *Nature,* **345**, 405-410.

Bard, E., Hamelin, B., Arnold, M., Montaggioni, L., Caboich, G., Faure, G. and F. Rougerie (1996) Deglacial sea level record from Tahiti corals and the timing of global melt water discharge. *Nature,* **382**, 241-244.

Barker, S., Higgins, J. A. and H. Elderfield (2003) The future of the carbon cycle: review, calcification response, ballast and feedback on atmospheric CO_2. *Phil. Trans. R. Soc. Lond. A,* **361**, 1977-1999.

Barnola, J. M., Raynaud, D., Korotkevic, Y. S. and C. Lorius (1987) Vostok ice core provides 160,000 years record of atmospheric CO_2. *Nature*, **329**, 408-414.

Bellwood, D. R. and T. P. Hughes (2001) Regional Scale Assembly Rules and Biodiversity of Coral Reefs. *Science*, **292**, 1532-1535.

Berger, W. H. (1977) Carbon dioxide excursions and the deep sea record: aspects of the problem. In N. R. Andersen and A. Malahoff (eds), *The Fate of Fossil Fuel CO_2 in the Oceans.* Plenum Press, New York, NY, pp 505-542.

Berger, W. H. (1982a) Increase of CO_2 in the atmosphere during deglaciation the coral reef hypothesis. *Naturwissenschaften*, **69**, 87-88.

Berger, W. H. (1982b) Deglacial CO_2 build-up: constraints on the coral reef model. *Pal. Pal. Pal.*, **40,** 235-253.

Berger, W. H. and J. S. Killingley (1982) Box cores from the equatorial Pacific: ^{14}C sedimentation rates and benthic mixing. *Mar. Geol.*, **45**, 93-125.

Berger, W. H. and R. S. Keir (1984) Glacial-Holocene changes in atmospheric CO_2 and the deep-sea record. In J. E. Hansen and T. Takahashi (eds), *Climate Processes and Climate Stability. Geophys. Monogr. Ser*., **29**, AGU, Washington DC, pp 337-351.

Blanchon, P. (2005) Comments on "Corrected western Atlantic sea-level curve for the last 11,000 years based on calibrated ^{14}C dates from *Acropora palmata* framework and intertidal mangrove peat" by Toscano and Macintyre [Coral Reefs (2003) 22: 257-270]. *Coral Reefs,* **24**, 183-186.

Boyle, E. A. (1988) The role of vertical chemical fractionation in controlling late Quaternary atmospheric carbon dioxide. *J. Geophys. Res.*, **93**, 701-715.

Broecker, W. S. (1982) Glacial to interglacial changes in ocean chemistry. *Prog. Oceanog.*, **11**, 151-197.

Broecker, W. S. and T-H. Peng (1989) The cause of the glacial to interglacial atmospheric CO_2 change: a polar alkalinity hypothesis. *Glob. Biogeochem. Cy.*, **3**, 215-239.

Broecker, W. S., Clark, E., McCorkle, D. C. and G. Bonani (1999) Evidence for a reduction in the carbonate ion content of the deep sea during the course of the Holocene. *Paleocean.,* **14**, 6, 744-752.

Broecker, W. S., Bonani, G., Chen, C., Clark, E., Ivy, S., Kais, M. and T-H. Peng (1993) A search for an early Holocene $CaCO_3$ preservation event. *Paleocean.*, **8**, 333-339.

Broecker, W. S. and G. M. Henderson (1998) The sequence of events surrounding termination II and their implications for the cause of glacial-interglacial CO_2 changes. *Paleocean*., **13**, 4, 352-364.

Broecker, W. S., Klas, M., Clark, E., Bonani, G., Ivy, S. and W. Wolfli (1991) The influence of $CaCO_3$ dissolution on core top radiocarbon ages for the deep-sea sediments. *Paleocean.*, **6**, 593-608.

Broecker, W. S., Lynch-Stirglitz, J., Clark, E., Hajdas, I. and G. Bonani (2001) What caused the atmosphere's CO_2 content to rise during the last 8000 years? *Geochem. Geophys. Geosystems.*, **2**, 2001GCOOO177, 2001.

Chrisholm, R. M. and D. J. Barnes (1998) Anomalies in coral reef community metabolism and their potential importance in the reef CO_2 source-sink debate. *Proc. Nat. Acad. Sci. USA.*, **95**, 6566-6569.

Cole, J. (2003) Global Change: Dishing the dirt on coral reefs. *Nature*, **421**, 705-706.

Cortes, J., Macintyre, I. G. and P. W. Glynn (1994) Holocene growth history of an Eastern Pacific fringing reef, Punta Islotes, Costa Rica. *Coral Reefs*, **13**, 65-73.

Davies, P. J., Marshall, J. F. and D. Hopley (1985) Relationships between reef growth and sea level in the Great Barrier Reef. *Proc. 5th Int. Coral Reef Congr. Tahiti*, **3**, 95-103.

Delmas, R. J., Ascencio, J. M. and M. Legrand (1980) Polar ice evidence that atmospheric CO_2 20,000 years BP was 50% of present. *Nature*, **284**, 155.

Farrell, J. W. and W. L. Prell (1989) Climate change and $CaCO_3$ preservation: an 800,000 year bathymetric reconstruction from the central equatorial Pacific ocean. *Paleocean.*, **4**, 447-466.

Farrell, J. W. and W. P. Prell (1991) Pacific $CaCO_3$ preservation and $\delta^{18}O$ since 4 Ma: Paleoceanic and paleoclimatic implications. *Paleocean*., **6**, 4, 485-498.

Feely, R. A., Sabine, C. L., Lee, K., Berelson, W., Kleypas, J., Fabry, V. J. and F. J. Millero (2004) Impact of Anthropogenic CO_2 on the $CaCO_3$ System in the Oceans. *Science*, **305**, 362-366.

Frankignoulle, M., Canon, C. and J. P. Gattuso (1994) Marine calcification as a source of CO_2: positive feedback of increasing atmospheric CO_2. *Limnol. Oceanogr.*, **39**, 2, 458-462.

Gattuso, J. P., M. Pichon, B. Delesalle, and M. Frankignoulle (1993) Community metabolism and air-sea CO_2 fluxes in a coral reef ecosystem (Moorea, French Polynesia). *Mar. Ecol. Prog. Ser*., **96**, 259-267.

Gattuso, J. P., Frankignoulle, M. and S. V. Smith (1999) Measurement of community metabolism and significance of coral reefs in the CO_2 source-sink debate. *Proc. National Acad. Sci. USA.*, **96**, 23, 13017-13022.

Gattuso, J. P. and R. W. Buddemeier (2000) Calcification and CO_2. *Nature*, **407**, 311-313.

Gischler, E. and A. J. Lomando (2000) Isolated carbonate platforms of Belize, Central America: sedimentary facies, late Quaternary history and controlling factors. In: E. Insalaco, Skelton, P. W. and T. J. Palmer (eds), *Carbonate Platform Systems: Components and Interactions*. *Geol. Soc. Special Pub*., **178**, The Geological Society, London, pp. 135–146.

Hays, J. D., Imbrie, J. and N. J. Shackleton (1976) Variations in the Earth's orbit: pacemaker of the ice ages. *Science*, **194**, 1121-1132.

Houghton, J. T., Ding, Y., Griggs, D. J., Noguer, M., van der Linden, P. J., Dai, X., Maskell, K. and C. A. Johnson (eds) (2001) *Climate Change 2001: the scientific basis. Contribution of Working Group I*

to the Third assessment Report of the International Panel on Climate Change. Cambridge University Press, Cambridge, United Kingdom and New York, USA, pp 881.

Hodell, D. A., Charles, C. D. and F. J. Sierro (2001) Late Pleistocene evolution of the oceans carbonate system. *Earth Planet. Sci. Lett.*, **192,** 109-124.

Hopley, D. (1982) *The geomorphology of the Great Barrier Reef: Quaternary development of coral reefs*, John Wiley, NY.

Indermuhle, A., Stocker, T. F., Joos, F., Ficher, H., Smith, H. J., Wahlen, M., Deck, B., Mastroianni, D., Tschumi, J., Blunier, T., Meyer, R. and B. Stauffer (1999) Holocene carbon cycle dynamics based on CO_2 trapped in ice at Taylor Dome, Antarctica. *Nature*, **398**, 121-126.

Kayanne, H. (1992) Deposition of $CaCO_3$ into Holocene reefs and its relation to sea level rise and atmospheric CO_2. *Proc. 7th Int. Coral Reef Symp. Guam*, **1**, 50-55.

Kayanne, H., Suzuki, A. and H. Saito (1995) Diurnal changes in the partial pressure of carbon dioxide in coral reef water. *Science*, **269**, 214-216.

Keir, R. S. (1991) The effect of vertical nutrient redistribution on surface ocean $\delta^{13}C$. *Glob. Biogeochem. Cy*., **5**, 351-358.

Keir, R. S. (1993) Cold surface ocean ventilation and its effect on atmospheric CO_2. *J. Geophys. Res.*, **98**, 849-856.

Keir, R. S. and W. H. Berger (1985) Late Holocene carbonate dissolution in the equatorial Pacific: reef growth or neoglaciation? In E. T. Sundiquist and W. S. Broecker (eds), *The carbon cycle and atmospheric CO_2 natural variations archean to present, Geophysics. Monograph. Ser*., **32**, 208-219.

Kinsey, D. W. (1981) The Pacific-Atlantic reef growth controversy. *Proc. 4th Int. Coral Reef Symp. Manilla*, **1**, 493-495.

Kleypas, J. A. (1997) Modelled estimates of global reef habitat and CO_2 production since the last glacial maximum. *Paleocean*., **12**, 533-545.

Kleypas, J. A., Buddemeier, R. W., Archer, D., Gattuso, J. P., Langdon, C. and B. N. Opdyke (1999) Geochemical consequences of increased atmospheric CO_2 on coral reefs. *Science*, **284**, 118-120.

Knox, F. and M. B. McElroy (1984) Changes in atmospheric CO_2: influence of the marine biota at high latitude. *J. Geophys. Res.*, **89**, 4629-4637.

Kump, L. R. (2002) Reducing uncertainty about carbon dioxide as a climate driver. *Nature*, **419**, 188-190

Kump, L. R., Kasting, J. F. and R. G. Crane (1999) *The Earth System.* Prentice Hall Inc. New Jersey, pp 351.

Langdon, C., Takahashi, T., Sweeney, C., Chipman, D., Goddard, J., Marubini, F., Aceves, H., Barnett, H. and M. J. Atkinson (2000) Effect of calcium carbonate saturation state on the calcification rate of an experimental coral reef. *Glob. Biogeochem. Cy.*, **14**, 639-654.

Lighty, R. G., MacIntyre, I. G. and R. Stuckenrath (1978) Submerged early Holocene barrier reef South-East Florida shelf. *Nature*, **276**, 59-60.

Marchitto, T. M., Lynch-Stieglitz, T. J. and S. R. Hemming (2005) Deep Pacific $CaCO_3$ compensation and glacial–interglacial atmospheric CO_2. *Earth Planet. Sci. Lett.*

Martin, P. A., Lea, D. W., Mashiotta, T. A., Papenfuss, T. and M. Sarnthenin (1999) Variation of foraminiferal Sr/Ca over quaternary glacial-interglacial cycles: evidence for changes in mean ocean Sr/Ca. *Geochem. Geophys. Geosyst*., **1**. Paper Number 1999GC000006.

McCulloch, M., Fallon, S., Wyndham, T., Hendy, E., Lough, J. and D. Barnes (2003) Coral record of increased sediment flux to the inner Great Barrier Reef since European Settlement. *Nature,* **421**, 727-730.

Milkankovitch, M. (1920) Theorie Mathematique des Phenomenes Thermiques produits par la Radiation Solaire. Gauthier – Villars Paris.

Milliman, J. D. (1974) Marine Carbonates. Recent sedimentary carbonates 1. Springer-Verlag. N.Y. pp 375.

Milliman, J. D. (1993) Production and accumulation of calcium carbonate in the ocean: budget of a nonsteady state. *Glob. Biogeochem. Cy.*, **7**, 927-957.

Montaggioni, L. F. (2000) Post glacial reef growth. *Earth Planet. Sci.*, **331,** 319-330.

Montaggioni, L. F. (2005) History of Indo-Pacific coral reef systems since the last glaciation: Development patterns and controlling factors. *Earth Sci. Revs.*, **71**, (1-2), 1-75.

Montaggioni, L. F. and G. Faure (1997) Response of reef coral communities to sea level rise: A Holocene model from Mauritius (Western Indian Ocean). *Sediment.*, **44**, 1053-1070.

Mylroie, J. E. (1993) Return of the Coral Reef Hypothesis: Basin to Shelf Partitioning of $CaCO_3$ and its Effect on Atmospheric CO_2 (Comment). *Geology*, **21**, 475.

Naim, O., Pascale, C. and V. Mangar (2000) The Mascarene Islands. Chapter 12. In T. R. McClanahan, Sheppard, C. R. C. and D. O. Obura (eds) *Coral Reefs of the Indian Ocean Their Ecology and Conservation.* Oxford University Press, NY.

Neftel, A., Oeschger, H., Schwander, J., Stauffer, B. and R. Zumbrunn (1982) Ice core sample measurements give atmospheric CO_2 content during the past 40,000 years. *Nature*, **295,** 220-233.

Neftel, A., Oeschger, H., Schwander, J. and B. Stauffer (1988) CO_2 record in the Byrd ice core 50,000-5,000 years BP. *Nature*, **331**, 609-611.

Neumann, A. C. and I. G. Macintyre (1985) Reef response to sea level rise: keep up, catch up or give up. *Proc. 5th Int. Coral Reef Congr. Tahiti*, **3**, 105-110.

Opdyke, B. N. and J. C. G. Walker (1992) Return of the coral reef hypothesis: Basin to shelf partitioning of $CaCO_3$ and effect on Holocene atmospheric CO_2. *Geology*, **20**, 733-736.

Opdyke, B. N. and B. H. Wilkinson (1993) Carbonate mineral saturation state and cratonic limestone accumulation. *Am. J. Sci.*, **293**, 217-234.

Pandolfi, J. M., Jackson, J. B. C., Baron, N., Bradbury, R. H., Guzman, H. M., Hughes, T. P., Kappel, C. V., Mitcheli, F., Ogden, J. C., Possingham, H. P. and E. Sala (2005) Are U.S. Coral Reefs on the Slippery Slope to Slime? *Science*, **307**, 1725-1726.

Pisias, N. G. and J. Imbrie (1986) Orbital geometry, CO_2 and Pleistocene climate. *Oceanus*, pp 43-49.

Petit, J. R., Jouzel, J., Raynaud, D., Barkov, N. I., Barnola, J. M., Basile, I., Bender, M., Chappellaz, J., Davis, M., Delaygue, G., Delmatte, M., Kotlyakov,V. M., Legrand, M., Lipenkov, V. U., Lorius, C., Pepon, L., Ritz, C., Saltzmane, E. and M. Stievenard (1999) Climate and atmospheric history of the past 420,000 years from the Vostock ice core, Antarctica. *Nature*, **399**, 429-435.

Roberts, C. M., McClean, C. J., Veron, J. E. N., Hawkins, J. P., Gerald, R. A., McAllister, D. E., Mittermeier, C. G., Schueler, F. W., Spalding, M., Wells, F., Vynne, C. and T. B. Werner (2002) Marine Biodiversity Hotspots and Conservation Priorities for Tropical Reefs. *Nature,* **295**, 1280-1284.

Ridgwell, A. J., Watson, A. J., Maslin, M. A. and J. O. Kaplan (2003) Implications of coral reef build-up for the late quaternary carbon cycle. *Paleocean.*, **18**, 4, 1083, doi:10.1029/2003PA000893.

Ridgwell, A. and R. E. Zeebe (in press) The role of the global carbonate cycle in the regulation and evolution of the Earth system. *Earth Planet. Sci. Lett.*

Ryan, D. A., Opdyke, B. N. and J. S. Jell (2001) Holocene sediments of Wistari Reef towards a global quantification of coral reef related neritic sedimentation in the Holocene. *Pal. Pal. Pal.,* **175,** 1-12.

Sarmiento, J. L. and R. Toggweiler (1984) A new model for the role of the oceans in determining atmospheric pCO_2. *Nature*, **308**, 621-624.

Shackleton, N. J. (1977) Carbon-13 in *Uvigerine*: tropical rain-forest history and the equatorial Pacific carbonate dissolution cycles. In N. R. Andersen and A. Malahoff (eds), *The Fate of Fossil Fuel CO_2 in the Oceans.* Plenum Press, NY, pp 401-427.

Shackleton, N. J. (2000) The 100,000-year ice age cycle identified and found to lag temperature, carbon dioxide and orbital eccentricity. *Science*, **289**, 1897-1902.

Sheppard, C. R. C. (2003) Predicted recurrences of mass coral mortality in the Indian Ocean. *Nature,* **425**, 294-297.

Siegenthaler, U. and T. Wenk (1984) Rapid atmospheric CO_2 variations and ocean circulation. *Nature,* **308**, 624-626.

Siegenthaler, U. and J. L. Sarimento (1993) Atmospheric carbon dioxide and the ocean, *Nature,* **365**, 119-125.

Sigman, D. M. (1997) *The role of biological production in Pleistocene atmospheric carbon dioxide variations and the nitrogen isotope dynamics of the Southern Ocean*, Unpublished PhD Thesis, Joint Program in Oceanogr., Mass. Inst. of Tech., Woods Hole Oceanogr. Inst., Woods Hole, Mass.

Sigman, D. M. and E. A. Boyle (2000) Glacial interglacial variations in atmospheric CO_2. *Nature*, **407**, 859-869.

Smith, S. V. (1978) Coral reef area and the contributions of reefs to the processes and resources of the world's oceans. *Nature*, **273**, 225-226.

Spalding, M. D., Ravilious, C. and E. P. Green (2001) *World Atlas of Coral Reefs*. Prepared at the UNEP World Conservation Monitoring Centre. University of California Press, Berkeley, USA.

Sowers, T., Bender, M., Raynaud, D., Kaotkevich Y. S. and J. Orchardo (1991) The $\delta^{18}O$ of atmospheric CO_2 from air inclusions in the Vostok ice core: timing of CO_2 and ice volume changes during the penultimate deglaciation. *Paleocean.*, **6**, 679-696.

Sowers, T. A. and M. Bender (1995) Climate records during the last deglaciation. *Science*, **269**, 210-214.

Sundiquist, E. T. (1993) The global carbon dioxide budget. *Science*, **259**, 934-941.

Thom, B. G. and P. S. Roy (1983) Sea-level change in New South Wales over the past 15,000 years. In D. Hopley (ed), *Australian Sea Levels in the Last 15,000 years: A Review*: Dept. Geography, James Cook University, Monograph Series, Occasional Paper No. 3 Townsville, Australia, pp 64-84.

Vecsei, A., and W. H. Berger (2003) Increase of atmospheric CO_2 during deglaciation: Constraints on the coral reef hypothesis from patterns of deposition, *Global Biogeochem. Cy.*, **18**, 1, GB1035 (DOI:10.1029/2003GB002147.

Vecsei, A. (2004) Holocene carbon fluxes from reef and peat accumulation: on the way to balancing the carbon cycle, *8th International Conference on Paleoceanography*, 5-10 September 2004, Biarritz, France, Program and Abstracts, 100, Bordeaux 1 University.

Ware, J. R., Smith, S. V. and M. L. Reaka – Kudla (1991) Coral reefs: sources or sinks of atmospheric CO_2. *Coral Reefs*, **11**, 127-130.

Walker, J. C. G. and B. N. Opdyke (1995) Influence of variable rates of neritic carbonate dissolution on atmospheric CO_2 and pelagic sediments. *Paleocean.*, **10**, 3, 415-427.

Wolast, R., Garrels, R. M. and F. T. Mackenzie (1980) Calcite-seawater reactions in ocean surface waters. *Am. J. Sci*., **280**, 831-848.

Wu, G., Herguera, J. C. and W. H. Berger (1990) Differential dissolution: modification of late Pleistocene oxygen isotope records in the Western Equatorial Pacific. *Paleocean*., **5**, 581-594.

Yamamuro, M., Kayanne, H. and M. Minagawa (1995) Carbon and nitrogen stable isotopes of primary producers in coral reef ecosystems. *Limnol. Oceanogr.*, **40**, 617–621.

Zeebe, R. E. and D. A. Wolf-Gladrow (2001) *CO_2 in Seawater: Equilibrium, Kinetics, Isotopes*. Elsevier Oceanography Series, 65, Amsterdam, pp 346.

Chapter Two

Materials and Methods

Plate 2.1 Reef Drilling on MacGillivray Reef (14°40’S, 145°30’E), Northern Great Barrier Reef, Australia.

Chapter 2

Materials and Methods

2.1 Introduction

Various methods have been employed to investigate the growth and $CaCO_3$ sediment mass balance of coral reefs including reef drilling, radiocarbon and U-Th dating, alkalinity measurements, core lithology and seismic profiling. The methods used in this PhD project included reef drilling and radiocarbon dating of corals cored at Rodrigues, Southwest Indian Ocean (Chapter 4), Lizard Island and MacGillivray reefs, Australian Great Barrier Reef (Chapter 3), the compilation of drill core data (thickness and radiometric ages) from reefs worldwide (Chapter 5) and utilization of seismic profiles of the Northern Great Barrier Reef in the published literature (Chapter 6).

2.2 Drilling Coral Reef Cores

The first reef drilling commenced between 1891-1898 on Funafuti Atoll. A Royal Society Expedition used coal mining equipment to drill down to 340 m in an effort to test Darwin's subsidence theory for the origin of Coral Reefs (Darwin, 1842; Bonney, 1904; Hopley and Davies, submitted for publication). Subsequent reef drilling on Southwest Pacific Atolls, to test atomic weapons during World War Two, lead to significant gains in knowledge of atoll structure and evolution (Revelle, 1654; Schlanger, 1963; Ladd, 1973). The first reef drilling within the Great Barrier Reef (GBR) province took place in 1926 on Michaelmas Cay and subsequently on Heron Island in 1937 down to 183 m and 223 m respectively (Hill, 1973). Indeed reef drilling has enabled the testing of various hypotheses of reef development (Darwin, 1842; Davies, 1973; Purdy, 1974). The first drilling operations used large heavy cumbersome drilling platforms and rigs. The expansion of reef drilling studies came with the invention of smaller light weight drilling rigs which can investigate a wider range of reef sites, are more economical and speed up the drilling process (Macintyre, 1975; 1978; Hopley, 1982; Davies *et al.,* 1977; Thom, 1978; Thom *et al.,* 1978; Shinn *et al.,* 1982; Hopley and Davies, submitted for publication). These modern drilling rigs lead to an explosion of reef drilling investigations world wide and resulted in the drilling of 161 holes into 48 reefs within the GBR alone since 1973. In the course of this project I have compiled a dataset of radiometrically dated coral cores from over 308 drill holes from

more than 133 reefs worldwide to calculate accretion rates and a global mass balance of coral $CaCO_3$ (Figure 2.1; Chapter 5).

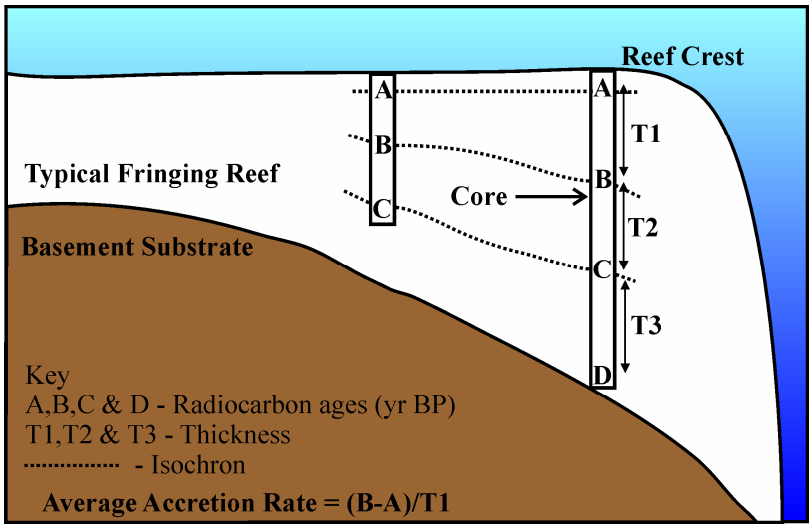

Figure 2.1 Cartoon illustrating the estimation of accretion rates from radiometric dating of coral drill cores for Chapter 5. The dotted lines linking surfaces of similar ages are called isochrons.

2.2.1 Reef Drilling at Rodrigues, Lizard Island and MacGillivray Reef

Reef drilling was undertaken to investigate the Holocene evolution of the fringing reefs of Rodrigues and Lizard Island and the platform reef of MacGillivray Reef. The drilling equipment was loaded onto a small aluminum dinghy driven to each drill location on a falling tide. The dinghy was anchored and crew waited until water depth would allow safe and efficient drilling ($\leq$ 0.5 m). Reef cores were obtained using a hydraulic rotary drill with diamond and tungsten drill heads (5 cm diametre for Rodrigues and 3.5 cm diametre for Lizard Island and MacGillivray Reef cores) powered by a petrol generator (Plates 2.1, 2.2 and 2.3).

Plate 2.2 Drilling into a thrown up coral head to access the reef margin below, near the leeward sand cay on MacGillirvay Reef (14˚39.916'S, 145˚29.310'E). Photo taken from support dingy harbouring generator and water pump.

The drill string was constructed of 1 and 1.5 m long rods and the whole system was flushed with seawater to aid drilling using a petrol generated water pump. Cored material was recovered by manually removing the entire drill stream from the core hole (Plate 2.3). Unlike many modern reef drill rigs (Braithwaite *et al*., 2000), the drilling equipment used at Rodrigues, Lizard Island and MacGillivray Reefs does not employ a scaffold and is therefore faster to deploy, operate and less expensive.

Plate 2.3 Reef drilling on Rodrigues showing drill string being manually removed from core hole to retrieve coral core.

Occasionally the drill would drop unhindered through voids in the reef, the approximate depth range of these voids was recorded. In some cases drilling was impeded or had to be abandoned because large volumes of sand made progress extremely slow or impossible. Drill hole Mac 1 was initially drilled during the first drilling field season to MacGillivray Reef in January 2003. This core site was revisited during the second field season in September 2003, during that time it had completely filled up with sand which first had to be pumped out using the water pump and hose (Plate 2.2). Unconsolidated material is not usually retained by reef drilling because water flushes the entire system to aid drill progress. It is therefore necessary to keep a log of drill bit behaviour, which, with experience, can be used to interpret the type of material the drill head encounters. Each piece of drilled core recovered was labeled to record orientation and position

within the section (reef sequence, Plate 2.4). Drilling was abandoned when progress was repeatedly impeded by sand or by some impenetrable surface, for example, granite basement. At both Lizard Island and MacGillivray Reef, drilling was interpreted to have reached granite basement based on drill bit refusal characteristics (Chapter 3).

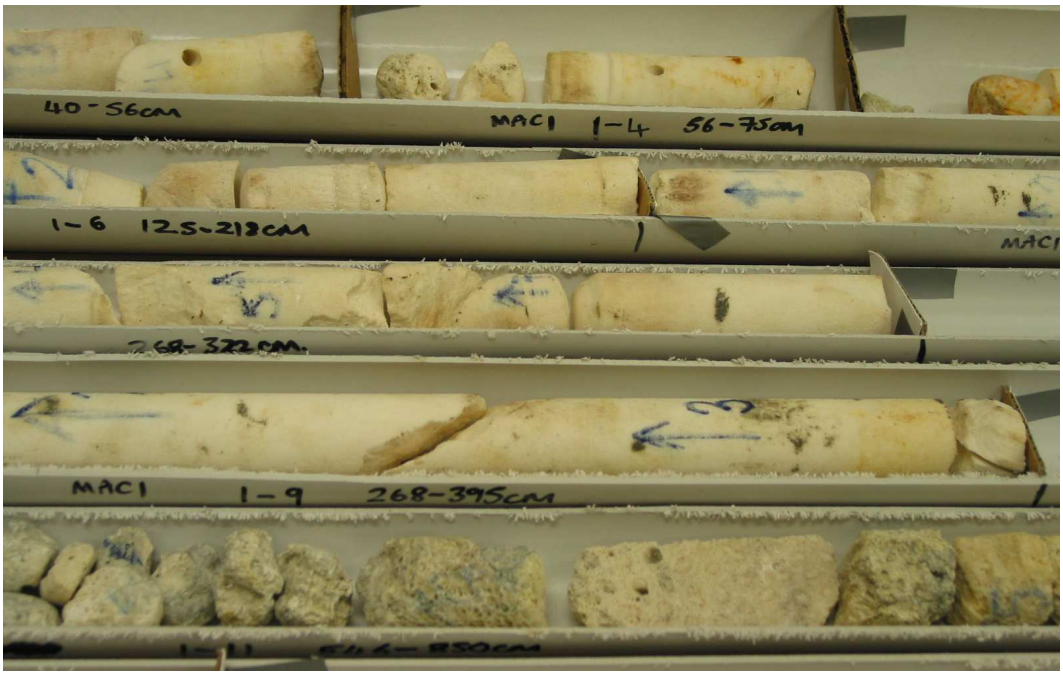

Plate 2.4 Drill core recovered from MacGillivray Reef leeward margin (Mac1). Cored material is labelled; for example, 1-9, number 1 refers to drill core name (e.g. Mac 1), number 9 refers to number of times the drill string was removed to extract coral core. The numbers and arrows labelling the coral indicate the sequence of coral pieces within each cored section. Increasing numbers indicate increasing depth from the top. Arrows indicate the orientation of the coral as it was retrieved from the core barrel. The orientation and order of the coral section retrieved assists in determining whether or not the coral was recovered in growth position, this is especially important for selecting material for radiometric dating and calculating accretion rates.

2.2.2 Thrown-up Coral Block

At MacGillivray Reef large thrown-up coral blocks were drilled through to reach the underlying reef because the water level here is too high during most of the tidal cycle to allow effective and safe drilling on the leeward margin. Drilling through thrown up coral blocks proved to be a very successful tactic allowing uninterrupted drilling for up to 5 hours at Mac 4 (Plate 2.5; Chapter 3) where a total of 8.5 m of core was recovered. It was important to log the contact between the thrown up coral block and the reef flat surface. This contact was actually quite obvious because (i) a large gap existed between the coral block and reef surface (0.5 m), (ii) encrusting foraminifera and detritus had built up at the contact area and (iii) the orientation of the corallites changed

markedly within the cored material. The recovered cores were cut longitudinally, logged, photographed, thin sections made and petrology carried out (Plate 2.4). Core logging involved recording detailed descriptions of flora and fauna to establish any changes in facies composition as the reef developed.

Plate 2.5. Large thrown up bombie (14˚38.95'S, 145˚29.25'E) on leeward margin of MacGillivray Reef and site of drill core Mac 4 at low tide.

2.2.3 Age Reversals

Occasionally age reversals appear in reef stratigraphies. There are various mechanisms which can lead to age reversals appearing in reef stratigraphy including;

1. The growth configuration of corals is not only vertical, as such a single slice through a coral colony might reveal older growth on top of younger growth.
2. Coral growth or deposition of younger material beneath overhangs.
3. Older fragments of corals being re-worked to a deeper but younger growth horizon for example from reef crest to reef slope.
4. Older coral fragments being re-worked to a younger growth horizon, for example, thrown-up coral blocks onto reef flats during storms and cyclones (Plate 2.5).

But the most common source of these reversals is incorrect interpretation of coral growth position (Kleypas, 1991; Graham, 1993). Meticulous recording of the position of each piece of coral material recovered by coring and examination of material in thin section is used to determine the orientation of cored coral material and aid the appropriate selection of cored material for radiometric dating (Chapters 3 and 4).

2.3 Age Determinations and Radiometric Dating

Radiometric dating allows determination of absolute chronologies making it possible to quantify the rate of development of landforms or patterns of sea level change and have lead to improvements in the understanding of the history of climate and ocean circulation. There are a variety of dating techniques (see Williams *et al*. (1998) and Woodroffe (2003) for summary) based on the following;

1. The rate of radioactive decay of a radioisotope e.g. Radiocarbon dating (^{14}C).
2. The relative balance of parent and daughter radioisotopes e.g. Uranium - series dating (U-Th).
3. The accumulation of electron traps e.g. luminescence (OSL – optically stimulated luminescence and TL-thermo luminescence) and electron spin resonance (ESR).

Radiometric dating, particularly the first two techniques above, are presently at a more advanced state of refinement than other methods and as such ages calculated by these methods are interpreted with greater confidence (Noller *et al.,* 2000). The decision as to which method is the most appropriate to apply must be made on the basis of the range of ages the dating method is able to measure accurately, the size of the sample available and the costs involved. Corals are mostly commonly dated by counting annual growth layers, radiocarbon dating or U-Th series dating. In this thesis radiocarbon (Accelerator Mass Spectrometry; AMS) dating of corals was used to establish the evolutionary nature of the Holocene reefs of Rodrigues (Southwest Indian Ocean, Chapter 4), Lizard Island and MacGillivray Reefs (Northern Great Barrier Reef, Chapter 3). To estimate the coral reef Holocene $CaCO_3$ mass balance a dataset of a variety of radiometric data of coral cores worldwide was compiled from the published literature (Chapter 5). This dataset was used to calculate accretion rates representative of the $CaCO_3$ deposition of coral reefs on spatial and temporal scale during the Holocene (Figure 2.1).

2.4 Radiocarbon Dating

2.4.1 Formation of Radiocarbon

Carbon exists as three isotopes, two are stable; carbon-12 (^{12}C; 98.9 %) and carbon-13 (^{13}C; 1.1 %) but carbon-14 (^{14}C; 1×10^{-10} %) is radioactive and decays with a half life of 5730 years ($t_{1/2}$=5730 years; Wagner, 1995; Woodroffe, 2003). Radiocarbon (^{14}C) is produced in the atmosphere through the interaction of cosmic ray neutrons (n)

with nitrogen atoms (^{14}N) which results in the emission of a proton (p) and creation of a ^{14}C atom ($^{14}N(n,p)^{14}C$; Equation 2.1). The ^{14}C is then oxidized to radioactive carbon dioxide ($^{14}CO_2$) which diffuses into the lower atmosphere and becomes distributed throughout the global carbon cycle (Equation 2.2).

Equation 2.1 $$\mathbf{n + {}^{14}N \rightarrow {}^{14}C + p}$$

Equation 2.2 $$\mathbf{{}^{14}C + O_2 \rightarrow {}^{14}CO_2}$$

Organisms, for example, corals, participating in the carbon cycle incorporate modern carbon, which has a $^{14}C/^{12}C$ ratio of about 10^{-12}, into their skeletons. At death they become separated from the carbon cycle and the ^{14}C begins to radioactively decay with a half life of 5730 years without being replenished and hence the ^{14}C content becomes reduced over time.

2.4.2 Basis of Radiocarbon Dating

The radiocarbon dating method was first proposed by Libby and co-workers (Anderson *et al.*, 1947; Libby, 1949). The half life ($t_{½}$) of a radioactive element is the amount of time taken for half of the radioactive atoms to undergo radioactive decay. Libby measured the half life ($t_{1/2}$) to be 5568 ± 30 years and this value is now known as the Libby half life (Stuiver and Polach, 1977). More recent measurements have refined this value and the presently accepted half-life of carbon is 5730 ± 40 years (Cambridge half-life) differs somewhat from Libby's value. However, it is accepted that the Libby half life be used to facilitate comparing ages calculated today with previously determined radiocarbon ages (Wagner, 1995). As ^{14}C decays back to ^{14}N it emits a beta particle (Equation 2.3).

Equation 2.3 $$\mathbf{{}^{14}C \rightarrow {}^{14}N + \beta}$$

After 10 half-lives, there is a very small amount of radioactive carbon remaining, as a consequence the dating limit of this technique is approximately 50 - 60 kyrs.

Because the ^{14}C concentration in the atmosphere is not constant, but varies in response to solar activity, changing geomagnetic field, and changes in galactic cosmic-ray flux, it is necessary to calibrate radiocarbon years in terms of calendar years. Trees

lay down one growth ring each year and the widths of these rings vary in response to growing conditions in a particular year. The patterns of these ring widths are the same for different trees growing at the same time. By comparing the patterns in living trees and in dead trees preserved in bogs, it has been possible to identify overlaps between logs and hence to associate each individual ring with the calendar year in which it was laid down. This "ring library" now extends from the present back to 12,400 years before present. Because each ring preserves the radiocarbon signature of the year in which it was laid down, it is possible, by measuring the radiocarbon age of individual rings (or more commonly decadal sequences of rings) to calibrate radiocarbon years in terms of calendar years (Wagner, 1995). Several species of tree have been used to create this library including, Bristlecone Pines (*Pinus aristata)* in the USA and waterlogged European Oaks (*Quercus sp)* in Ireland and Germany. It is possible to extend this calibration further back in time using other archives such as uranium series dated corals (Bard *et al.*, 1990; Stuiver *et al.*, 1993; Wagner, 1995). Note that ^{14}C concentrations (ages) sometimes correspond to more than one calendar age because the ^{14}C concentration of the atmosphere has varied through time. Computer programmes, for example, CALIB and Oxcal, are used to convert conventional radiocarbon ages in to calendar ages.

The conventional radiocarbon age BP of a sample is defined by Equation 2.4,

Equation 2.4 **$T = -8033 \ln(Asn/Aon)$**

where T is the conventional radiocarbon age, -8033 represents the mean life time of ^{14}C as measured by Libby (Stuiver and Polach, 1977), Aon represents the activity (counts per minute) of the modern standard (1880 wood corrected for decay to 1950 AD), Asn is the activity of the sample (counts per minute) and ln is the natural logarithm. Calculation of the conventional radiocarbon ages assumes the following

- a half-life of 5568 years (the Libby half-life)
- correction for sample isotopic fractionation ($\delta^{13}C$, delta^{13}C) to a normalized or base value of -25.0 per mille relative to the ratio of C12/C13 in the carbonate standard PDB
- the use of 1950 AD as 0 BP

The primary modern reference standard for radiocarbon dating is 95 % (after normalization to $\delta^{13}C$ =-25 ‰) of the count rate in 1950 of a batch of oxalic acid ($C_2H_2O_4$ / HOx1) from the US National Bureau of Standards. This material has $\delta^{13}C$ (^{13}C /^{12}C isotopic ratio) =-19.0 ‰ with respect to Pee Dee Belemnite (PDB). PDB refers to the Cretaceous belemnite formation at Peedee in South Carolina, USA and is the internationally accepted isotopic fractionation ($\delta^{13}C$) reference standard (Craig, 1957). The year 1950 is year 0 BP in radiocarbon dating and is deemed to be the 'present'. The ANU (Australian National University) Radiocarbon Lab introduced a secondary standard, ANU Sucrose, which has been related to the oxalic acid standard and has an activity of 150.8 % modern when normalized to $\delta^{13}C$ =-25 ‰ (Gupta and Polach, 1985).

There are two methods of measuring the ^{14}C content of a sample; conventional radiometry (Liquid Scintillation counting) which counts the radioisotope decay products (beta / β particles) and accelerator mass spectrometry (AMS) which measures the ^{14}C content directly by counting ^{14}C atoms.

2.4.3 Accelerator Mass Spectrometry (AMS)

AMS has several advantages over β counting including; applicability to smaller samples sizes (0.2-2 mg carbon compared to 2-10 g for β counting); AMS is 1000-10,000 times more sensitive than β counting; AMS extends the age range for detection from 40,000 years to approaching 55,000 years; AMS measurements are more rapid (less than an hour whereas β counting takes between 1-2 days, Gupta and Polach, 1985).

2.4.4 Corrections to Radiocarbon Ages

The following details must be taken into consideration when deriving radiocarbon ages and converting these into calendar years.

Blank Correction.

Each sample must be converted to graphite before being placed into the accelerator mass spectrometer. During creation of graphite, the sample may acquire a small amount of carbon contamination with its own ^{14}C signature (background). In order to correct for this, blanks are made in parallel with the real samples from material that contains no ^{14}C, for example, marble. The amount of ^{14}C measured in these blanks is then subtracted from the measured ^{14}C content of the real samples.

Isotopic Fractionation.

Isotopes of the same element behave the same chemically but have different mass numbers (number of neutrons and protons), for example ^{12}C, ^{13}C and ^{14}C. The difference in relative mass causes 'isotopic fractionation' where chemical reactions favour one isotope over another. For example, photosynthesis favours ^{12}C over the heavier ^{13}C and ^{14}C. As a result, the carbon in plants is isotopically lighter than the atmosphere. Conversely, inorganic carbon (DIC) in the oceans is generally enriched in ^{13}C relative to atmospheric carbon dioxide. The isotopic composition of a sample is expressed as delta ^{13}C ($\delta\ ^{13}C$) and is the difference in parts per thousand (per mil or ‰) between the ratio of ^{13}C to ^{12}C content of the sample and that of the international Pee Dee Belemnite (PDB) standard (Wagner, 1995). Samples of the same age but different $\delta\ ^{13}C$ values have different radiocarbon contents. If correction is not made for this fractionation a 1 ‰ difference in $\delta\ ^{13}C$ would correspond to a 16 year age difference. $\delta\ ^{13}C$ ranges for various materials normalized to the PDB standard can be found in Gupta and Polach (1985; page 114).

Marine Reservoir Effect.

As ^{14}C becomes distributed through the carbon cycle, the relatively slow exchange of ^{14}C between the atmosphere and layers of the ocean can lead to the ^{14}C content of the deep ocean being different from that of the atmosphere (Wagner, 1995). When deep water is excluded from exchange with the atmosphere its ^{14}C content declines. This apparent age is a result of a) the delay in exchange between atmospheric CO_2 and the marine carbonate system and b) the dilution of the ^{14}C content by mixing of surface and deep waters. As a result the conventional radiocarbon ages of marine samples may have an apparent age that is 400 years older than a terrestrial sample of same age. Marine radiocarbon ages can be converted to terrestrial radiocarbon ages by subtracting 400 years (Chapter 5). Oceanic mixing is controlled by local factors including coast shape; currents and winds and as such the apparent age of seawater varies across the globe (Stuiver and Braziunas, 1993). The delta R (ΔR) is the difference between the marine reservoir age of the local region and that of the global ocean average (400 years). ΔR is made up of two corrections, the shift in regional marine ^{14}C due to a) regional atmospheric ^{14}C age differences and b) oceanic mixing processes that vary the ^{14}C content from that of the global average (Stuiver *et al.*, 1986; Wagner, 1995). A global database of ΔR values (reservoir correction values) can be found at the Marine

Reservoir Correction Database (http://www.calib.org/marine, online at Queen's University, Belfast and the University of Washington). Computer programmes, for example, CALIB or Oxcal, correct conventional radiocarbon ages to calibrated calendar years and correct for the marine reservoir effect using ΔR values. I used ΔR= 135 ± 24 for Rodrigues (Southwest Indian Ocean; Chapter 4) and ΔR = 10 ± 7 for Lizard Island and MacGillivray Reef (Northern Great Barrier Reef; Chapter 3) to convert conventional ages into calibrated years using CALIB.

Conversion to Calendar Years (Calibrated Years).

Conventional radiocarbon ages are converted to calibrated radiocarbon ages (absolute time scale) using accepted calibration curves and programmes (CALIB and Oxcal). I used the CALIB 4.4 programme which was written by the Quaternary Isotope Lab, University of Washington and is maintained by Paula and Ron Reimer (Stuiver and Reimer, 1993). CALIB incorporates a correction for the marine reservoir effect mean global ocean of 400 years and regional factors using ΔR values from the online database (http://www.calib.org/marine).

Industrial or Suess Effect.

A large amount of 'dead' (not containing any ^{14}C) CO_2 released by the combustion of fossil fuels since the Industrial era began (1890) has diluted (reduced) the natural atmospheric ^{14}C concentration. Correction for this effect does not need to be made for radiocarbon ages (years BP) because the modern reference standard is 1880 wood extrapolated for decay to 1950 AD.

Bomb effect.

The atom bomb effect results from the production of a huge amount of ^{14}C ('artificial' or 'bomb') by nuclear weapons testing and was first recognized by de Vries (1958). The weapons testing lead to a doubling of the ^{14}C concentration of the atmosphere in the Northern Hemisphere by 1965 although this is now slowly diminishing as it becomes distributed through the global carbon cycle (Rafter and O'Brien, 1970). The Geochemical Ocean Section Study (GEOSEC) used the ^{14}C addition as a tracer of large-scale oceanic transport and mixing processes (Gupta and Polach, 1985).

2.4.5 Methods Used for Dating Coral Cores

Radiocarbon dating has been used to date Holocene reefs worldwide including the reefs investigated as part of this project (Rodrigues, Lizard Island and MacGillivray Reef). Drilled coral core sections were cut in half, thin sections made and examined under binocular microscope. Selected corals determined to have been in growth position by the orientation of their corallites and free from recrystalization (alteration) and contamination with internal cements or sediments were drilled using a dentist's drill under binocular microscope to extract samples for radiocarbon dating. This carbonate material was then dried in an oven for 24 hours before being prepared for ^{14}C dating. The detailed methodology and radiocarbon practices at ANU is given by Gupta and Polach (1985), an overview outline of the procedure is given here.

The calcium carbonate material was hydrolysed to CO_2 using hydrochloric acid and the evolved CO_2 passed through two dry dry ice/alcohol cooled traps within a vacuum system (Equation 2.5).

Equation 2.5 $$\mathbf{CaCO_3 + 2HCL \longrightarrow CO_2 + CaCl_2 + H_2O}$$

The CO_2 was then frozen in a break seal tube using a liquid nitrogen cold trap under vacuum. The CO_2 collected was reduced to graphite (graphitization) in the presence of hydrogen using iron (Fe) as a catalyst in a furnace at 600 ºC. The graphite powder samples were pressed into target holders and mounted into a target wheel along with standard targets. The target wheel was loaded into the Accelerator Mass Spectrometer (based on the ANU's 14UD pelletron accelerator) to detect the number and energy of ions. The measured $^{14}C/^{13}C$ ratio was corrected for isotopic fractionation and converted into a conventional radiocarbon age. This was subsequently converted to calibrated (calendar years) using the marine calibration in the CALIB 4.3 software programme (Chapters 3 and 4).

2.5 U-Th dating

Another method commonly used to date corals radiometrically is Uranium series dating (U-Th) which involves determining the relative balance of parent and daughter radioisotopes. Uranium exists as two naturally occurring radioactive isotopes, ^{238}U (99.3 %) and ^{235}U (0.7 %). These parent isotopes decay to daughter isotopes which are also radioactive and follow a decay chain until stable lead isotopes (^{206}Pb and ^{207}Pb) are

formed. Corals incorporate Uranium from seawater into their carbonate skeletons but exclude Thorium. Any Thorium present in the coral skeleton will be the result of radioactive decay of Uranium. The age of the coral can be determined by two methods.

1. Radiometry of alpha particles (alpha / α-spectrometry), detects the products of radioactive decay - alpha particles. This method has a detection range of several thousand years to 350 ka and requires at least 2 grams of sample (Wagner, 1995).
2. Thermal ionization mass spectrometry (TIMS), detects the radioactive isotopes directly with dating range between 10-550 kyr. TIMS dating has 5-10 times greater precision than α-spectrometry and only requires 0.5-3 grams of sample (Wagner, 1995).

U-Th dating has been used to correlate sea level variations with Milakovitch cycles and to extend the ^{14}C calibration curve, it can be applied to marine and freshwater carbonates, bones, teeth, peat and volcanic deposits (Bard *et al.*, 1990; Wagner, 1995). Although this method was not used in this project to date coral cores, ages determined by this method have been included in the Holocene coral reef accretion rate database in Chapter 5 (Bard *et al.*, 1990; 1996; Eisenhauer *et al.*, 1993; Edwards *et al.*, 1997).

2.5.1 Comparison of ^{14}C and U-Th Determined Ages

The Libby model is based on the assumption that the production of ^{14}C has been constant through time. De Vries (1958) subsequently discovered that ^{14}C production has varied spatially and temporally and as such ^{14}C ages should be considered on a relative radiometric and not absolute (calendar years) time scale. Comparison of ^{14}C and U-Th ages of corals from Barbados revealed that ^{14}C ages are systematically younger than calendar ages and that this offset increases into the past (Bard *et al.*, 1990; Figure 2.2).

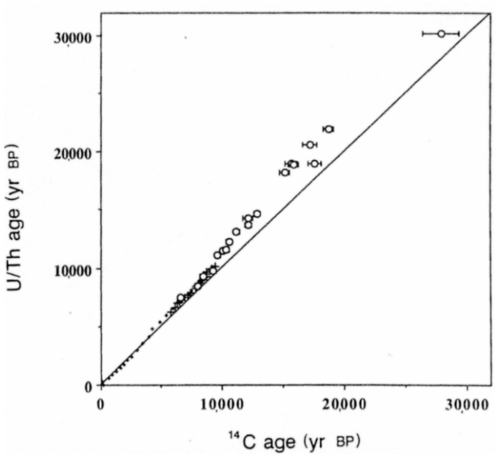

Figure 2.2 ^{14}C and U-Th ages from the same material, open symbols represent U-Th ages plotted against ^{14}C ages (Bard *et al.*, 1990).

In order to put all of the data collated in the global Holocene coral reef drill core database on a common time scale, it was more convenient for the purposes of this study (to avoid calibration of hundreds of dates) to convert dates that were on an absolute time scale to marine radiocarbon ages (Chapter 5). This was accomplished by converting calibrated and U-Th ages to marine radiocarbon ages using the graphs of Stuiver and Braziunas (1993). Marine radiocarbon ages which had been converted to terrestrial radiocarbon ages by subtracting 400 years to correct for the marine reservoir effect were back corrected to the original marine ages by adding 400 years.

Radiocarbon ages are reported as years 'before present' or BP, 'present' refers to the year 1950, the year modern chronometric dating methods were introduced (Wagner, 1995). Conversion of radiocarbon years (yrs BP) to calendar years (absolute time scale) is necessary if ages are to be precisely correlated with other dated processes, for example, ice cores. To assist subsequent researchers conventional radiocarbon ages should always be reported with the following information; the lab code and environmental corrections or calibrations made. If the conventional age is less than 200 years it is usually reported as modern. This convention was followed here in Chapters 3 and 4.

2.6 Seismic Profiling

Seismic profiling measures the two-way travel time (TWT) of seismic waves generated artificially at the surface and reflected back to a receiver (hydrophone). Seismic profiling is carried out by towing a sound source (acoustic energy) and receiver (hydrophone) behind a research vessel. The acoustic energy generated at the surface is reflected back to the surface when it encounters an interface between two surfaces of contrasting density and seismic velocity (acoustic impedance). The reflected signal is received by the hydrophone and is converted into a bipolar analog signal and then plotted onto paper (early data) or collected digitally (modern data; Figure 2.3). Seismic profiling provides a means of mapping rock sequences over vast areas, which are normally only accessible by time-consuming and expensive drilling operations, and has been employed extensively by the petroleum and mining industries.

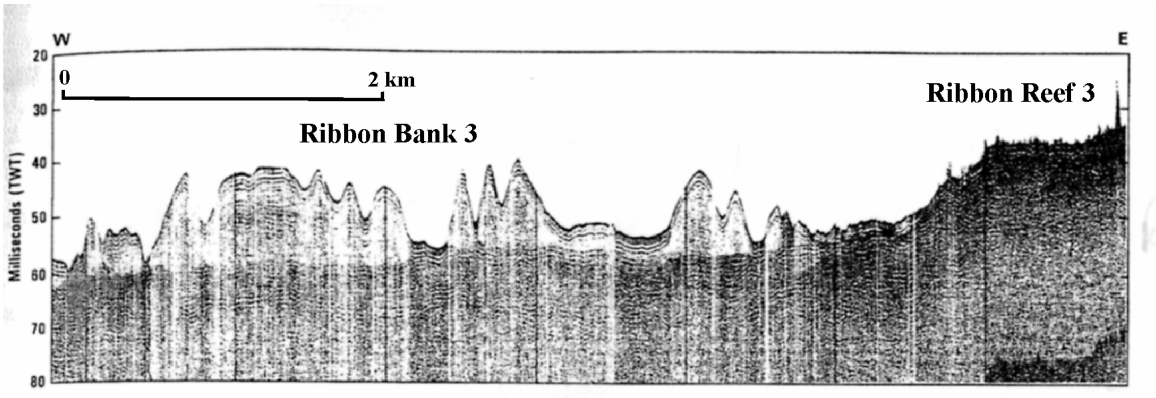

Figure 2.3 Seismic profile of the *Halimeda* bioherms of Ribbon Bank 3 adjacent to Ribbon Reef 3, directly east of Cooktown, Northern Great Barrier Reef (modified from Marshall and Davies, 1988). Vertical axis represents two way travel time (TWT) in milliseconds.

This project initially aimed to investigate the three dimensional structure of the Holocene reef system through a combination of reef drilling and high resolution seismic reflection profiling (sub-bottom profiling). Unfortunately, a seismic profiling expedition to the Lizard Island region, Northern Great Barrier Reef was unsuccessful because of a cyclone and equipment failure. However, seismic profiles and vibrocoring core logs obtained from the published literature and personal communication enabled the assessment of the volume of calcium carbonate within the *Halimeda* bioherms of the Northern Great Barrier Reef to be investigated (Figure 2.3; Chapter 6; Orme *et al.*, 1978; Orme, 1985; Davies and Marshall, 1985; Marshall and Davies, 1988; Orme and Salama, 1988; Wolanski *et al.*, 1988; John Jell, personal communication).

The seismic profiles were used to calculate the volume and mass of $CaCO_3$ within the *Halimeda* bioherms to compare with that of the adjacent Ribbon Reefs (estimated using drill cores and seismic profiles from studies herein and published literature (Chapters 3 and 6; Davies *et al.*, 1985; Rees *et al.*, submitted manuscript)) in two regions of the Northern Great Barrier Reef, Lizard Island and Cooktown (Chapter 6). The *Halimeda* bioherms appear acoustically soft (presumably a result of the scattering of acoustic energy by the *Halimeda* plants) with internal bedding also described as 'chaotic transparent seismic facies' (Roberts *et al.*, 1987; Hine *et al.*, 1988). To estimate the thickness of the bioherms a figure of 1500 m s^{-1} (centrally bracketing the seismic velocity of water) was assumed to represent the velocity of the acoustic pulse through the sediment in keeping with the methods of Orme *et al.* (1978), Orme (1985) and Orme and Salama (1988).

2.7 Estimating Coral Reef Calcification

There are several methods used to estimate the $CaCO_3$ productivity of coral reefs including biological, radioisotope, stratigraphic and alkalinity anomaly (Chapter 5; Smith and Kinsey, 1976; Vecsei, 2004a). A review of the methods is given by Vecsei (2004a). The stratigraphic or accumulation rate method has been used to calculate a global Holocene $CaCO_3$ mass balance (Chapter 5; Rees *et al.*, in preparation) and values estimated compared to those $CaCO_3$ budgets calculated using productivity values measured using the alkalinity anomaly technique.

2.7.1 Biological/census method

Biological/census method in which the standing crop of reef organisms (in terms of % cover or mass of $CaCO_3$ per unit area 'calcimass') is multiplied by their biological growth/turnover rate. This method gives an estimate of gross production or potential production but does not take into account losses through dissolution or erosion and transport (Smith and Kinsey, 1976; Smith, 1983).

2.7.2 Radioisotope method

Radioisotope method involves incubating the specimens in seawater labelled with either ^{45}Ca or ^{14}C. The skeleton is then dissolved with acid and the incorporated radioactivity is measured using a liquid scintillation counter (Chrisholm and Gattuso, 1991). This method has some disadvantages including the fact that it requires the specimen to be destroyed before its previous rate of calcification can be determined and there are problems associated with the interpretation of radioisotope incorporation data.

2.7.3 Stratigraphic/accumulation rate method

Stratigraphic/accumulation rate method involves using accretion rates estimated from radiometrically dated reef drill cores (Figure 2.1). This approach estimates 'net productivity', it takes into account the amount of $CaCO_3$ deposited and subsequent losses resulting from dissolution and erosion. It also reveals a record of productivity for the past (Chapter 5).

2.7.4 Alkalinity anomaly/ hydrochemistry/alkalinity depression method

The alkalinity anomaly/hydrochemistry/alkalinity depression method estimates 'net productivity' of present day coral reefs, this accounts for precipitation minus

dissolution in real time. This method does not account for $CaCO_3$ losses resulting from post-depositional erosion or dissolution, which may be between 20-25 % of the carbonate produced (Hubbard *et al.*, 1990; Milliman, 1993). To measure calcification, seawater samples are taken upstream and down-stream on a transect of known length. The alkalinity anomaly model is based on the stoichiometric relationship between total alkalinity and calcification; for every mole (100 g) of $CaCO_3$ precipitated (calcification) from a given volume of water, the total alkalinity (TA) is reduced by two molar equivalents and each volume of water remains in contact with a given area of the reef for some measurable length of time (Smith and Key, 1975; Smith, 1978b; Chrisholm and Gattuso, 1991). This model is based on the fact that neither photosynthesis nor respiration affect alkalinity (Chrisholm and Gattuso, 1991; Gattuso *et al.*, 1996). The $CaCO_3$ production rate equals the decrease in alkalinity (ΔTA in eq m^{-3}) multiplied by 50 g $CaCO_3$ eq^{-3}, multiplied by the water volume per unit area, divided by the period of time the water remains in the system (Smith 1978b). Units of productivity are given in kg $CaCO_3$ m^{-2} yr^{-1} or G. The total alkalinity is the capacity to neutralize hydrogen ions (H^+) in seawater and is measured by determining the pH of seawater samples using a pH electrode. A detailed description of the methods employed and calculations made in this technique is given by Smith and Kinsey (1978), Smith (1978b) and Kinsey (1978). This method is advantageous because it does not require direct examination, sampling or destruction of actual reef community; it does not include addition of reagents thus enabling repeated sampling over a protracted period of time and over a large area (Smith and Kinsey, 1978). However, it is limited because it can only be used at relatively shallow depths, logistics have restricted access and measurement of the fore-reef and wave zones, it does not account for post depositional losses (erosion/dissolution) and it is only representative of present day reef production (Vecsei, 2004a; Rees *et al.*, 2005).

Measurements of community metabolism using the alkalinity anomaly technique on coral reefs led to the characterization of three basic zones of productivity; the deep fore-reef, the reef flat and lagoon (Table 2.1; Smith and Kinsey, 1976; Kinsey, 1979). Coral reef productivity measurements have been extrapolated to represent reefs globally in an effort to calculate the global mass of neritic carbonate for the Holocene by several authors (Milliman, 1974; 1993; Smith, 1978a; Kinsey and Hopley, 1991; Milliman and Droxler, 1996; Inglesias-Rodriguez *et al.*, 2000; Vecsei and Berger, 2003; Vecsei, 2004a; b).

Table 2.1 Proposed Modes of Coral Reef Calcification (after Kinsey 1979; Kinsey, 1981)

Mode	Reef Environment	Calcification Rate / G (kg $CaCO_3$ m^{-2} yr^{-1})	Potential Vertical Accretion (IVGR) (mm yr^{-1})
1	100 % hard cor/algal substratum	10	>7
2	100 % sand and rubble	0.5	0.4
3	100 % algal pavement	4	3

Present day productivity measurements have also been converted to implied vertical growth rates (IVGR; Table 2.1). However, the validity of this translation is questionable because of the assumptions inherent in the calculation (Smith and Kinsey, 1976; Kinsey, 1981; Smith, 1983; Kinsey and Hopley, 1991). These assumptions include:

- The material is aragonite and has a density of 2.9 g cm^{-3}.
- The average porosity of the reef fabric is about 50 %, in reality porosity has been estimated to range from 0-90 % (Smith, 1983).
- The local gains or losses of reef materials precipitated are averaged out across the entire reef.

Implied vertical growth rates (IVGR) estimated from net productivity rates are often substantially lower than accumulation rates seen in the sedimentary record and may be in error by up to 50 % (Davies and Hopley, 1983; Davies, 1983; Smith, 1983). For example, modern day accumulation rates inferred by the alkalinity method are approximately 3 m kyr^{-1} compared to rates measured in reef cores of up to 8 m kyr^{-1} (Davies and Marshall, 1985; Davies, 1983). See Chapter 5 for further discussion.

2.7 References

Anderson, E. C., Libby, W. F., Weinhouse, S., Reid, A. F., Kirshenbaum, A. D. and A. V. Grosse (1947) Natural radiocarbon form cosmic radiation. *Phys. Rev.*, **72**, 931-936.

Bard, E., Hamelin, B., Fairbanks, R. G. and A. Zindler (1990) Calibration of the ^{14}C timescale over the past 30,000 years using mass spectrometric U-Th ages from Barbados corals. *Nature, **345***, 405-410.

Bard, E., Hamelin, B., Arnold, M., Montaggioni, L., Caboich, G., Faure, G. and F. Rougerie (1996) Deglacial sea level record from Tahiti corals and the timing of global melt water discharge. *Nature*, **382**, 241-244.

Bonney, T. G. (1904) *The Atoll of Funafuti: Borings into a coral reef and the results being the report of the coral reef committee of the Royal Society London.* The Royal Society, London, pp 428.

Braithwaite, C. J. R., Montaggioni, L. F., Camoin, G. F., Dalmasso, H., Dullo, W. C. and A. Mangini (2000) Origins and development of Holocene coral reefs: a revisited model based on reef boreholes in the Seychelles, Indian Ocean. *Int. J. Earth Sci.*, **89**, 431–445.

Chrisholm, J. R. M. and J. P. Gattuso (1991) Validation of the Alkalinity Anomaly Technique for Investigating Calcification and Photosynthesis in Coral Reef Communities. *Limnol. Ocean.*, **36**, 6, 1232-1239.

Craig, H. (1957) Isotopic standards for carbon and oxygen and correction factors for mass spectrometric analysis of carbon dioxide. *Geo. Cosmo. Acta*., **12**, 133-140.

Darwin, C. R. (1842) *The structure and distribution of coral reefs.* Smith, Elder and Co., London, pp 214.

Davies, P. J. (1973) Subsurface solution unconformities at Heron Island, Great Barrier Reef. *Proc 2nd Int. Coral Reef Symp*, **2**, 573-578.

Davies, P. J. (1983) Reef Growth. In D. J. Barnes (ed), *Perspectives on Coral Reefs.* Aust. Inst. Mar. Sci. Brian Clouston Publishing, Manuke, ACT, Australia, pp 69-106.

Davies, P. J., Marshall, J. F., Thom, B. G., Harvey, N., Short, A. D. and K. Martin (1977) Reef development Great Barrier Reef. *Proc. 3rd Int. Coral Reef Symp. Miami*, **2**, 332-337.

Davies, P. J. and D. Hopley (1983) Growth facies and growth rates of Holocene reef in the Great Barrier Reef, *B. M. R. J. Aust. Geol. Geophys.*, **8**, 237-251.

Davies, P. J. and J. F. Marshall (1985) *Halimeda* bioherms - low energy reefs, northern Great Barrier Reef. *Proc. 5th Int. Coral Reef Congr. Tahiti*, **5**, 1-7.

Davies, P. J., Marshall, J. F. and D. Hopley (1985) Relationships between reef growth and sea level in the Great Barrier Reef, *Proc. 5th Int. Coral Reef Congr. Tahiti, 3*, 95-103.

De Vries, H. (1958) Variation of the concentration of radiocarbon with time and location on earth. *Kon Ned Akad Wetensch Proc. Ser. B*, **61**, 267-281.

Edwards, R. L., Cheng, H., Murrell, M. T. and S. J. Goldstein (1997) Protactinium-231 dating of carbonates by thermal ionization mass spectrometry: implications for Quaternary climate change. *Science*, **276**, 782-786.

Eisenhauer, A., Wasserburg, G. J., Chen, J. H., Bonani, G., Collins, L. B., Zhu, Z. R. and K. H. Wyrwoll (1993) Holocene sea-level determinations relative to the Australian continent: U/Th (TIMS) and 14C (AMS) dating of coral cores from the Abrolhos Islands. *Earth Planet. Sci. Lett.*, **114**, 529-247.

Gattuso, J. P., Pichon, M., Delesalle, B., Canon, C. and M. Frankignouelle (1996) Carbon fluxes in coral reefs. I. Lagrangian measurement of community metabolism and resulting air-sea CO_2 disequilibrium. *Mar. Ecol. Prog. Ser.*, **145**, 109-121.

Gupta, S. K. and H. A. Polach (1985) *Radiocarbon dating practices at ANU.* An ANU Laboratory Publication. The Australian National University, Canberra, Australia, pp 169.

Graham, T. L. (1993) *Geomorphological Response of Continental Shelf and Coastal Environments to the Holocene Transgression – Central Great Barrier Reef.* Unpubl. Ph.D. Thesis, James Cook University.

Hill, D. (1973) An introduction to the Great Barrier Reef. *Proc. 2nd Int. Coral Reef Symp.*, **2**, 723-731.

Hine, A. C., Hillock, P., Harris, M. W., Mullins, H. T., Belknap, D. F. and W. C. Jaap (1988) *Halimeda* bioherms along an open seaway: Miskito Channel, Nicaraguan Rise, SW Caribbean Sea. *Coral Reefs*, **6**, 173-178.

Hopley, D. (1982) *The geomorphology of the Great Barrier Reef: Quaternary development of coral reef.* John Wiley, NY.

Hopley, D. and P. J. Davies (submitted for publication) Shallow drilling on the Great Barrier Reef and adjacent islands.

Hubbard, D. K., Miller, A. I. and D. Scaturo (1990) Production and cycling of $CaCO_3$ in a shelf edge reef system (St Croix, US Virgin Islands): applications to the nature of reef systems in the fossil record. *J. Sediment. Petrol.*, **60**, 3, 335-360.

Inglesias-Rodriguez, M. D., Armstrong, R., Feely, R., Hood, R., Kleypas, J. A., Milliman, J. D., Sabine, C. and J. Sarmiento (2000) Progress made in study of ocean's calcium carbonate budget. *Eos*, **83**, 34, 365 – 375.

Kleypas, J. A. (1991) Use of AVHRR data to assess environmental controls on reef development in the southern Great Barrier Reef, Australia. *Proc. 8th Thematic Conf. Geol. Remote Sensing*, pp. 265-276.

Kinsey, D. W. (1978) Productivity and calcification estimates using slackwater periods and field enclosures. In D. R. Stoddart and R. E. Johannes (eds), *Coral Reefs: Research Methods*. UNESCO, Paris, pp 439-468.

Kinsey, D. W. (1979) *Carbon turnover and accumulation by coral reefs.* Unpublished PhD Thesis University of Hawaii, 248.

Kinsey, D. W. (1981) The Pacific-Atlantic reef growth controversy. *Proc. 4th Int. Coral Reef Symp. Manila*, **1**, 493 – 495.

Kinsey, D. W. and D. Hopley (1991) The significance of coral reefs as global carbon sinks – response to greenhouse. *Pal. Pal. Pal.* (Global and Planetary change section), **89**, 363 – 377.

Ladd, H. S. (1973) Bikini and Eniwetok Atolls, Marshall Islands. In O. A. Jones and R. Endean (eds), *Biology and Geology of Coral Reefs*. Geology, **1**, Academic Press, New York, pp 93-112.

Libby, W. F., Anderson, E. C. and J. R. Arnold (1949) Age determination by radiocarbon content, world-wide assay. *Science*, **109**, 227-228.

Macintyre, I. G. (1975) A diver-operated hydraulic drill for coring submerged strates. *Atoll. Res. Bull.*, **185**, 21-26.

Macintyre, I. G. (1978) A hand-operated submersible drill for coring reef substrata. In D. R. Stoddart and R. E. Johannes (eds), *Coral Reefs: Research Methods*, UNESCO, Paris, pp 75-80.

Marshall, J. F. and P. J. Davies (1988) *Halimeda* Bioherms of the Northern Great Barrier Reef. *Coral Reefs*, *6*, 139-148.

Milliman, J. D. (1993) Production and accumulation of calcium carbonate in the ocean: budget of a non-steady state. *Glob. Biogeochem. Cy.*, ***7***, 927 – 957.

Milliman, J. D. (1974) *Marine Carbonate, Recent sedimentary carbonates*, 1, Springer-Verlag, N.Y.

Milliman, J. D. and A. W. Droxler (1996) Neritic and pelagic carbonate sedimentation in the marine environment: ignorance is not bliss, *Geol. Rundsch.*, **85**, 495 – 511

Noller, J. S., Sowers, J. M. and W. R. Lettis (eds) (2000) *Quaternary Geochronology: Methods and Application*. American Geophysical Union, Washington, DC, pp 582.

Orme, G. R. (1985) The sedimentological importance of *Halimeda* in the development of back reef lithofacies, Northern Great Barrier Reef (Australia). *Proc. 5th Int. Coral Reef Symp.*, **5,** 31-37.

Orme, G. R., Flood, P. G. and G. E. G. Sargent (1978) Sedimentation trends in the lee of outer (ribbon) reefs, Northern region of the Great Barrier Reef Province. *Phil. Trans. R. Soc. Lond.* A, **291**, 85-99.

Orme, G. R. and M. S. Salama (1988) Form and seismic stratigraphy of *Halimeda* banks in part of the Northern Great Barrier Reef Province. *Coral Reefs,* **6**, 131-137.

Purdy, E. G. (1974) Reef configurations: cause and effect. In L. F. Laporte (ed) *Reefs in Time and Space*. Society of Economic Palaeontologists and Mineralogists, Special Publication, 18, Tulsa, OK, pp 9-76.

Rafter, T. A. and B. J. O'Brien (1970) Exchange rates between the atmosphere and the ocean as variations and absolute chronology. Almquist and Wiksell, Stockholm, pp 355-378.

Rees, S. A., Opdyke, B. N. and P. A. Wilson (in prep) The Impact of Coral Reef $CaCO_3$ Accumulation on Holocene Atmospheric Carbon Dioxide Concentration.

Rees, S. A., B. N. Opdyke, P. A. Wilson, and L. K. Fifield (2005) Coral Reef sedimentation on Rodrigues and the Western Indian Ocean and its impact on the carbon cycle. *Phil. Trans. R. Soc. Lond. A,* **363**, 101-120.

Rees, S. A., Opdyke, B. N., Wilson, P. A., Fifield, L. K. and V. Levchenko (submitted manuscript) Holocene Evolution of the Granite based Lizard Island and MacGillivray Reef Systems, Northern Great Barrier Reef.

Revelle, R. (1654) Forward in Geology of Bikini and nearby Atolls. U. S. Geol. Surv. Prof. Pap., 260-A., i-vii.

Roberts, H. H., Phipps, C. V. and L. Effendi (1987) Morphology of large *Halimeda* bioherms, eastern Java Sea (Indonesia): a side scan sonar study. *Geo-marine Lett.*, **7**, 7-14.

Schlanger, S. O. (1963) Subsurface geology of Eniwetok Atoll. U.S. Geol. Surv. Prof. Pap., 260-BB, 991-1066.

Shinn, E. A., Hudson, J. H., Halley, R. B., Lidz, B., Robbin, D. M. and I. G. Macintyre (1982) Geology and sediment accumulation rates at Carrie Bow Cay, Belize. In K. Rutzler and I. G. Macintyre (eds), *The Atlantic Barrier Reef Ecosystem at Carrie Bow Cay, Belize I: Structure and Communities.* Smithsonian Contributions to Marine Science, Washington, D. C., pp 63-75.

Smith, S. V. (1978)a Coral reef area and the contributions of reefs to the processes and resources of the world's oceans. *Nature*, **273**, 225-226.

Smith, S. V. (1978)b Alkalinity depletion to estimate the calcification of coral reefs in flowing waters. In D. R. Stoddart, and R. E. Johannes (eds), *Coral Reefs: Research Methods*. UNESCO, Paris, pp 397-404.

Smith, S. V. (1983) Coral Reef Calcification. In D. J. Barnes (ed) *Perspectives on Coral Reefs.* Aust. Inst. Mar. Sci., Brian Clouston Publishing, Manuka, ACT, Australia, pp 240-247.

Smith, S. V. and G. S. Key (1975) Carbon dioxide and metabolism in marine environments. *Limnol. Oceanogr.,* **20**, 493-495.

Smith, S. V. and D. W. Kinsey (1976) Calcium carbonate production, coral reef growth and sea level change. *Science,* **194**, 937-939.

Smith, S. V. and D. W. Kinsey (1978) Calcification organic carbon metabolism as indicated by carbon dioxide. In D. R. Stoddart and R. E. Johannes (eds), *Coral Reefs: Research Methods*. UNESCO, Paris, pp 469-484.

Stuiver, M. and H. A. Polach (1977) Discussion Reporting of 14-C data. *Radiocarbon,* **19**, 355-363.

Stuiver, M., Pearson, G. W. and T. F. Braziunas (1986) Radiocarbon age calibration of marine samples back to 9000 cal yr BP. In M. Stuiver, and R. S. Kra (eds), Proc. 12th Int. ^{14}C Conf. *Radiocarbon*, **28**, (2B), 980-1021.

Stuiver, M. and T. F. Braziunas (1993) Modeling atmospheric ^{14}C influences and ^{14}C ages of marine samples to 10,000 BC. *Radiocarbon*, **35**, 1, 137-189.

Stuiver, M., Long, A. and R. S. Kra (1993) Calibration 1993. *Radiocarbon*, **35**.

Stuiver, M. and P. J. Reimer (1993) Extended ^{14}C data base and revised CALIB 3.0 ^{14}C age calibration programme. *Radiocarbon*, **35,** (1), 215-31.

Thom, B. G. (1978) Coastal sand depostition in southeast Australia during the Holocene. In J. L. Davies and M. A. F. Williams (eds), *Landforms Evolution in Australiasia*. Australian National University Press, Canberra, pp 197-214.

Thom, B. G., Orme, G. R. and H. A. Polach (1978) Drilling investigation of Bewick Island. *Phil. Trans. R. Soc. Lond. A*, **291**, 37-54.

Vecsei, A. (2004)a, A new Estimate of global reefal carbonate production including the fore-reefs. *Global Planet. Change*, **43**, 1-18

Vecsei, A. (2004)b, Holocene carbon fluxes from reef and peat accumulation: on the way to balancing the carbon cycle. *8th International Conference on Paleoceanography*, 5-10 September 2004, Biarritz, France, Program and Abstracts, 100, Bordeaux 1 University.

Vecsei, A. and W. H. Berger (2003) Increase of atmospheric CO_2 during deglaciation: Constraints on the coral reef hypothesis from patterns of deposition, *Global Biogeochem. Cy.*, **18**, 1, GB1035 (DOI:10.1029/2003GB002147).

Wagner, G. A. (1995) *Age determination of young rocks and artifacts. Physical and Chemical clocks in quaternary geology and archaeology*. Springer, NY, pp 466.

Williams, M., Dunkerely, D., De Deckker, P., Kershaw, P. and J. Chappell (1998) *Quaternary Environments*. Arnold, London, pp 329.

Wolanski, E., Drew, E., Abel, K. and J. O'Brien (1988) Tidal jets, nutrient upwelling and their influence on the productivity of the alga *Halimeda* in the ribbon reefs, GBR. *Est. Coast. Shelf Sci.*, **26**, 169-201.

Woodroffe, C. D. (2003) *Coasts, Form, Process and Evolution*. Cambridge University Press, Cambridge, UK, pp 84-89.

Chapter Three

Holocene Evolution of the Granite based Lizard Island and MacGillivray Reef Systems, Northern Great Barrier Reef.

Plate 3.1 Lizard Island with MacGillivray Reef in the background, Northern Great Barrier Reef, Australia (14°38.9'S, 145°29'E).

Chapter 3

Holocene Evolution of the Granite based Lizard Island and MacGillivray Reef Systems, Northern Great Barrier Reef.

Reference: Rees S. A., Opdyke, B. N., Wilson, P. A., L. K. Fifield and V. Levchenko (manuscript submitted 02.11.04) Holocene Evolution of the Granite based Lizard Island and MacGillivray Reef Systems, Northern Great Barrier Reef. *Coral Reefs.*

3.1 Abstract

Radiocarbon dating of seven drill cores from both the windward Lizard Island fringing reef and the windward and leeward margins of MacGillivray platform reef, Northern Great Barrier Reef (NGBR) Province, reveal the Holocene evolutionary nature of these two mid shelf coral reefs. The windward margin at Lizard Island started growing approx 6.7 cal kyr BP directly on an assumed granite basement and reached present day sea level approximately 4 cal kyr BP. Growth of the windward margin at MacGillivray Reef was initiated by 7.6 cal kyr BP and reached present day sea level by approximately 5.6 cal kyr BP. The leeward margin at MacGillivray was initiated by 8.2 cal kyr BP directly on a granite basement, only reaching sea level relatively recently between 260 and 80 cal yr BP. None of our cores penetrated the Holocene-Pleistocene unconformity. The absence of Pleistocene reefal deposits, even at 15 m depth in the cores from MacGillivray Reef, indicates the possibility that the shelf in this region may have subsided relative to modern day sea level by at least 15 m since the last interglacial (125 ka).

3.2 Introduction

The Great Barrier Reef (GBR), a high energy epicontinental shelf edge reef system, is the largest reef system in the world covering an area of approximately 49 000 km^2 and comprises nearly 3000 individual reefs (Davies and Marshall, 1980; Spalding *et al.,* 2001). The foundations of the GBR were initiated around 600 ka ago in the mid-Pleistocene and consist of a mixture of carbonate and terrigenous sediment accumulated during a succession of flooding and emergence of the continental shelf (International Consortium for Great Barrier Reef Drilling, 2001; Dunbar and Dickens, 2003).

Lizard Island and MacGillivray reef are located in the northern Great Barrier Reef province approximately 270 km north of Cairns (Figure 3.1). This region is characterised by an almost continuous line of shelf edge ribbon reefs enclosing a narrow (<50 km wide) shallow continental shelf; water depth rarely exceeds 40 m (Orme and Flood, 1977; 1980; Kinsey, 1979; Flood, 1984). No major rivers discharge into this part of the GBR shelf (Flood, 1984). This area is anomalous in the GBR due to a north-south trending line of granite continental/high islands (Lizard Island; North Direction Island and South Direction Island; Figure 3.1) which are surrounded by fringing reefs and it is one of a small number of areas where fringing reefs can be found growing adjacent to the mainland coast (Johnson and Carter, 1978; Orme *et al.*, 1978; Partain and Hopley, 1989). Numerous shoals, platform reefs and *Halimeda* bioherms are also found in the region (Orme *et al.*, 1978; Hopley, 1982; Orme, 1985; Marshall and Davies, 1988; Graham, 1993).

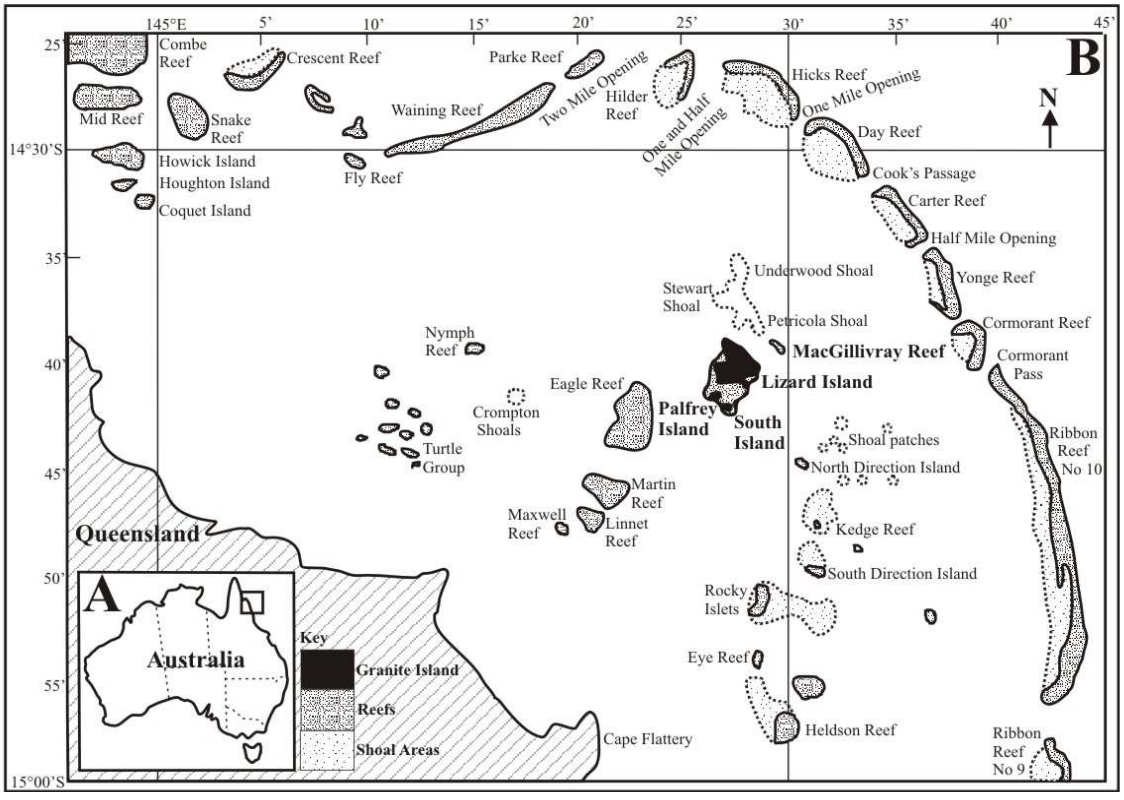

Figure 3.1A Map of the Australian continent showing location of NGBR region (modified after Heap *et al.*, 2001); B Locations of the Lizard Island Group and MacGillivray Reef within the NGBR Province (modified after Admiralty chart 373).

In 1973 the Royal Society and the Universities of Queensland participated in an expedition to the GBR which included seismic and side scan sonar surveys, shallow reef drilling (Bewick and Stapleton Islands) and surface sediment sampling within the area

between the mid-shelf continental islands and the shelf-edge ribbon reefs (Orme and Flood, 1977; Mclean and Stoddart, 1978; Orme *et al.,* 1978; Stoddart *et al.,* 1978; Thom *et al.,* 1978). Drilling investigations at two of the Howick Island group platform reefs, Bewick and Stapleton, approximately 50 km north of Lizard Island, reveal that the depth to the Holocene-Pleistocene unconformity is 7 m below the reef flat and 14.6 m below the beach surface respectively, with the oldest Holocene corals in the Bewick core returning radiocarbon dates of 6.39 to 6.92 kyr BP (Stoddart *et al.,* 1978; Thom *et al.,* 1978).

Seismic investigations in the region have revealed an almost continuous seismic reflector, believed to represent the Holocene-Pleistocene unconformity, across the whole shelf at a depth of 40 m below present sea level (m bsl) on the outer shelf rising to 25 m below present sea level on the inner shelf (Orme *et al.,* 1978; Orme, 1983; 1985; Orme and Salama, 1988). One of the major findings of these investigations was the discovery of extensive *Halimeda* bioherms behind the ribbon reefs, these can be up to 6 km wide, 100 km long and can reach thicknesses of 18 m at a depth of 25 m below present sea level (Orme *et al.,* 1978; Orme, 1983; Flood and Orme, 1988; Marshall and Davies, 1988; Orme and Salama, 1988). Radiocarbon dating of the surface immediately below these bioherms reveals that they were formed entirely during the Holocene (radiocarbon age of a peat sample 10 ± 0.2 kyr BP; Orme, 1985) and were initiated some 1.5 kyr before the nearby ribbon reefs (Orme, 1985; Davies *et al.,* 1985; Marshall and Davies, 1988). The mechanism of their formation is still debated. It is most likely, however, that they were able to form as a consequence of jets of up-welled nutrient-rich oceanic water intruding onto the outer shelf through the narrow passages between the karst remnants of Pleistocene ribbon reefs and forming eddies in the relative shelter behind the ribbons (Drew and Abel, 1985; Marshall and Davies, 1988). Vibrocoring has revealed that the bioherms are composed of mainly *Halimeda*; with forams, molluscs and bryozoans also present and the carbonate content averaging approximately 75 % (Davies and Marshall, 1985; Marshall and Davies, 1988). The existence of large $CaCO_3$ *Halimeda* bioherms is important in global carbonate budget studies because they may have produced $CaCO_3$ several of orders magnitude greater than the neighbouring ribbon reefs during the Holocene (Flood, 1984).

Immediately north-west of Lizard Island (the leeward side, Watson's Bay area; Figure 3.2), away from the influence of the Lizard Island fringing reefs, quartz sediments derived from granite islands are abundant (Orme *et al.,* 1978; Flood, 1984). It

has been noted that in the NGBR province, reef-derived carbonate sediments form leeward accretionary wedges which extend for only 1 to 3 km from the reefs (Maxwell and Swinchatt, 1970; Frankel, 1974).

Drilling and seismic surveys across the outer ribbon reefs (Carter and Yonge Reefs, 15 km east of Lizard Island) revealed that these reefs reached modern sea level approximately 5.4 kyr BP and 5.19 kyr BP respectively, that modern sea level was reached on the outer ribbon reefs by approximately 5.5 kyr BP and that the Holocene-Pleistocene unconformity occurs at approximately 19.3 m below reef flat at Yonge Reef and 19 m below reef flat on the leeward edge of Carter Reef (Figure 3.1B; Harvey, 1977; Hopley, 1977; 1994; Harvey and Hopley, 1981a; Hopley and Davies, submitted for publication). However, seismic profiles also reveal discontinuity surfaces at about 10 m below the reef flat on the windward margins of Carter, Nymph and Three Isle reefs (Harvey, 1977; Orme *et al.*, 1978). Other reefs drilled to the south of the region include Long Reef, Boulder Reef, Williamson Reef, Ribbon Reef 5, East Hope Reef, Michaelmas Cay (Hopley, 1977; Davies *et al.*, 1985; International Consortium for Great Barrier Reef Drilling, 2001).

Radiocarbon dating of recovered Holocene material from these reefs indicates that reef growth was initiated between 8.38 and 6.32 kyr BP on Pleistocene foundations at depths ranging from 15 to 17 m below the reef flat and reached modern sea level between 6.7 and 5.94 kyr BP indicating that modern sea level was established in this region by 6.5 kyr BP (Thom and Chappell, 1975; Mclean and Stoddart, 1978; Stoddart *et al.*, 1978; Chappell *et al.*, 1983). Debate over the possible existence of higher mid-Holocene sea levels on the GBR was resolved when Chappell *et al.* (1983) used radiocarbon ages of emerged coral micro-atolls and beach ridges to show that higher (+ 1 m) relative mid-Holocene sea levels had occurred on the inner shelf zone in the region.

In 1975 a team of researchers took part in the "Lizard Island metabolic exchanges on reefs" (LIMER) expedition which investigated calcification, water currents, the sulphur cycle, nitrogen metabolism, and primary and secondary production within the Lizard Island reef system (LIMER, 1975). Calcification budget studies for the modern day reefs at Lizard Island using the alkalinity anomaly method (Smith and Kinsey, 1976; Kinsey, 1979) revealed that calcium carbonate production on the windward reef flat, central – leeward reef flat and lagoon to be 3.8, 3.7 and 1 kg $CaCO_3m^{-2}yr^{-1}$ respectively (LIMER, 1975; Smith and Kinsey, 1976; Kinsey, 1979). These values are

consistent with global observations on coral reefs (Kinsey, 1979). These studies concluded that most of the $CaCO_3$ produced does not remain *in situ* but is transported in a leeward direction. It bypasses the lagoon, and is deposited on the western side of the inter-island reef mass forming a leeward extension of the system or leeward accretionary wedge (LIMER, 1975).

In an attempt to rationalise the coral reef CO_2 source-sink debate (Kayanne *et al.*, 1995; Gattuso *et al.*, 1996; 1999), Chrisholm and Barnes (1998), using measurements of O_2 and pH of sea water, calculated lower calcification rates (1.9-2.1 kg $CaCO_3$ m^{-2} yr^{-1}) than the ones revealed by the LIMER expedition for the windward reef flat at Lizard Island. These lower values may have been observed because of high rainfall (low salinity) and extreme low tides during the field visit (Gattuso *et al.*, 1999). The reef was also recovering from a recent Crown of Thorns plague and high sea water temperatures (30°C) during the previous months that had resulted in a very low level of live coral cover (0 to 10 %; Chrisholm and Barnes, 1998). The methods used in this study were brought into question by Gattuso *et al.* (1999).

The geomorphology of the reefs within the GBR varies considerably due to differences in the topography (relief) of the underlying substrate and environmental conditions during the Holocene (Coventry *et al.*, 1980). There have been numerous drilling investigations of the Holocene reefs of the Southern and Central GBR. By comparison, there have been few studies of the NGBR reefs. The aim of this investigation is to place new constraints on the nature of the Holocene evolution of the NGBR reefs.

3.3 Regional Setting

The Lizard Island group (14°38.9'S, 145°29'E) and MacGillivray Reef (14°40'S, 145°30'E) are located within the lagoon of the NGBR approximately 27 km from the Queensland Coastline and 15 km from the main outer ribbon reefs (Figure 3.1; Flood, 1984). The Lizard Island group is composed of three Late Permian granite (high/continental) islands, Lizard, Palfrey and South Island (Figure 3.2; Reitner and Neuweiler, 1995) which currently rise approximately 395 m above present sea level. The majority of the fringing reef has developed in the South East as a triangle of inter-island reefs covering an area of approximately 2 km^2 (Kinsey, 1979) and enclosing a deep (10 m) fully tidal lagoon (Blue Lagoon).

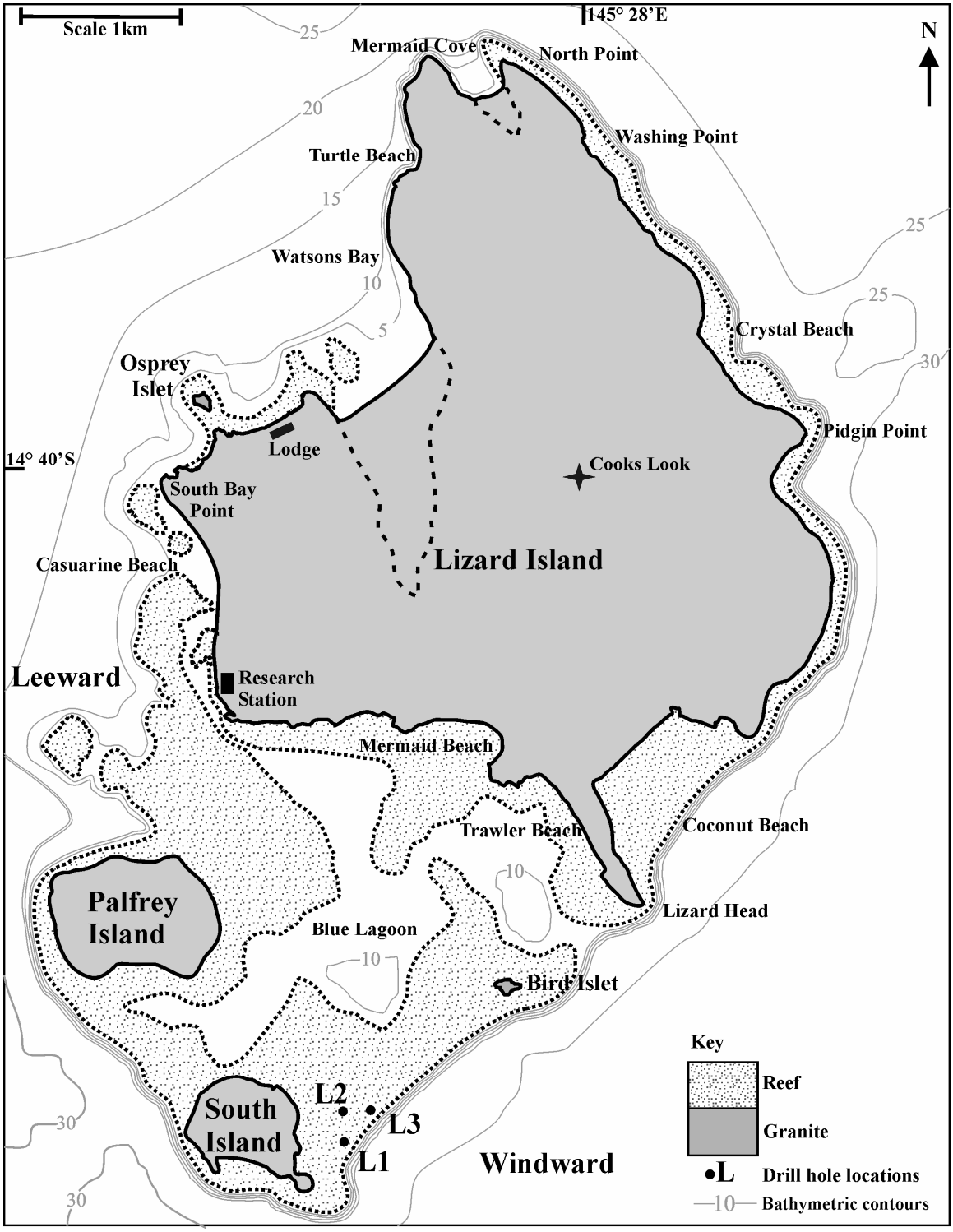

Figure 3.2. Diagram of Lizard Island reef system, showing locations of windward drill holes (modified after Flood, 1984).

The windward margin reef flat comprises a consolidated coral algal zone of small coral heads and loose rubble (Kinsey, 1979). The windward reef at Lizard Island exhibits very limited lateral development compared to the leeward margin (Scoffin *et al.,* 1978; Coventry *et al.,* 1980). The sheltered leeward margin at Lizard Island is not clearly defined by a reef edge or classic reef zonation. It consists of a gentle slope dominated

by sand and massive *Porites* coral heads. On the east, northeast and western coastlines the reefs are narrow (less than 50 m wide) and steeply sloping, rising from water depths of approximately 20 m (Figure 3.2; Flood and Orme, 1988). There is a fourth much smaller granite island, Bird Islet, three quarters of the way between South Island and Lizard Island along the windward reef flat. Between Bird Islet and Lizard Head there is a deep channel which allows almost complete tidal flushing of the lagoon (Flood and Orme, 1988). Beach rock, found on the leeward facing beaches within the range of modern day tides, comprises quartz grains (derived from the granite islands), coral and *Tridacna* fragments and rubble cemented in a carbonate matrix. Modern diagenetically unaltered aragonite micro-ooids with quartz and carbonate grain nuclei have been described by Davies and Martin (1976) and may constitute up to 10 % of the inter-island channel sands between Lizard and Palfrey Island.

MacGillivray Reef (formerly known as Shadwell Reef) is a small oval platform reef (0.9 km long and 0.35 km wide) oriented southeast to northwest with a shallow lagoon (<3 m deep; Figure 3.3).

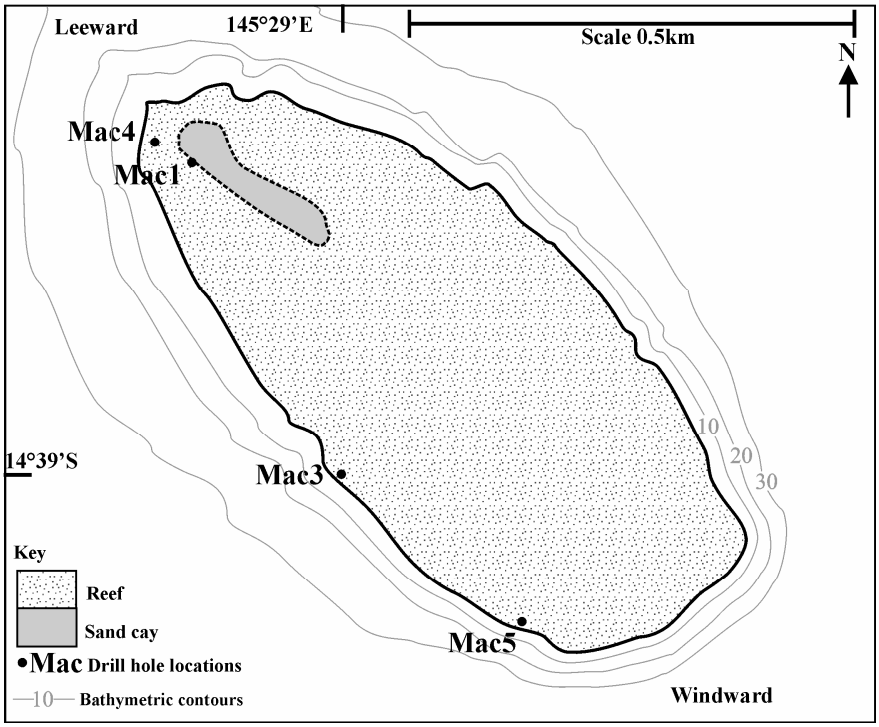

Figure 3.3. Diagram of MacGillivray reef system, showing locations of windward and leeward drill holes.

An oval non-vegetated sand cay approximately 1.5 m high (of variable dimensions; 20 m long and 3 to 4 m wide in 2003 and 2004) is located at the reef's western leeward end. It is composed of coral shingle, rubble and sand surrounded by a large number of

reef blocks (Hopley, 1982). The windward reef margins are steeply sloping and drop into about 5 m depth of water, are dominated by massive and tabulate coral forms and exhibit spur and groove morphology, gullies, caves and overhangs (Figure 3.3; Heyward *et al.*, 1997). The leeward margin is gently sloping and is dominated by branching *Acropora* species.

The annual air temperature in the region ranges from 20 to 34°C; mean sea surface temperature is 27°C. The south-east trade winds predominate (March to September) and usually range from 15 to 30 knots and generate swells up to 3 m for much of the year (Orme and Flood, 1980). The southeast trade winds have a dominant influence on the direction of the water currents flowing through the Lizard Island fringing reef system, the currents predominantly flow in a north westerly direction independent of tidal state. Cyclones occasionally occur from November to April. Cyclones create northward along-shelf currents and bring large amounts of fresh water and terrestrial sediment to the GBR lagoon (Larcombe *et al.*, 1995). Cyclone winds create large waves which mainly affect the outer ribbon reefs and have been known to move large coral heads from depth onto reef flats, for example, those on the top of MacGillivray reef. Tides are semidiurnal, ranging between 2.6 m (springs) and 0.3 m (neaps).

3.4 Materials and Methods

During two field expeditions to the NGBR in January and September 2003, three drill cores were obtained from Lizard Island and five cores were obtained from MacGillivray Reef using a portable hydraulic drilling rig with a 3.5 cm diameter core barrel and diamond drill head with a core catcher (Figures 3.2 and 3.3). The drilling equipment was loaded onto a small aluminum dinghy driven to each drill location on a falling tide. The boat was anchored and crew waited until water depth (0.5 m deep) would allow safe and efficient drilling before deploying the drilling rig. Unlike many modern reef drill rigs, the drilling equipment did not employ a scaffold and was therefore faster to deploy, operate and less expensive. Cored material was recovered every 0.1 to 0.2 m during drilling at Lizard Island and every 0.5 to 1 m during drilling at MacGillivray Reef. All of the Lizard cores were extracted from the windward margin because the leeward margin was too deep to access and did not form a conventional (well consolidated shallow) reef flat margin (Figure 3.2). The maximum depth reached was 4.5 m in core L1, where we assume we encountered the granite basement because i) the drill could not be advanced further and ii) of the close proximity of the drill hole

locations to the granite island, South Island (Figure 3.4). Cores L2 and L3 were abandoned after encountering thick sand layers. Recovery in the Lizard Island cores ranged from 13 to 24 %.

Two windward and two leeward cores were recovered from MacGillivray Reef during the spring low tides when practically the whole reef surface emerges (Figure 3.3). Two of the cores were initiated through thrown up coral blocks on the leeward margin which allowed a longer drilling window during the tidal range (Figure 3.5). In fact, the coral block through which core Mac 4 was drilled was so large (approximate dimensions 2 m^3) that we were able to drill with our feet dry during 70 % of the spring tidal range. Using thrown up coral blocks like this one as a platform for drilling may allow access to margins exposed to rougher sea conditions (e.g. outer ribbon reefs) and deeper water locations. Cores Mac 3 and 5 were abandoned due to the rising tide and equipment failure respectively; Mac 4 was abandoned after encountering a thick sand layer. It is assumed that core Mac 1 encountered a granite basement as several attempts to advance the drill further were unsuccessful. The maximum depth reached was 11 m and 15 m on the windward and leeward margins respectively; recovery ranged from 12-50 %.

The cores were logged and photographed, and thin sections were made and petrographically examined. Corals that were determined to be *in situ* (by the orientation of their corallites) and free from internal cement and detritus by microscope examination were selected for radiocarbon dating. Radiocarbon dating of the tops of cores Mac 1 and 4, (which were initiated through thrown up coral blocks, Figure 3.5), was achieved by selecting corals at depths level with the surrounding reef flat, as such the ages are not of the thrown up coral blocks. We also dated the thrown up coral block through which Mac 1 was initiated, this returned a modern date (the radiocarbon age of 200 ± 190 yr).

Accelerator Mass Spectrometry (AMS) radiocarbon dating was performed at the Department of Nuclear Physics, Australian National University, Canberra. The dates were corrected for isotopic fractionation and the marine reservoir effect (North East Australia $\Delta R = 10 \pm 7$) and converted to calendar years using the CALIB 4.4 software programme (Table 3.1; Stuvier and Reimer, 1993). Errors are at 1σ.

3.5 Results

3.5.1 Lizard Island Reef

The Lizard cores reveal five facies types; a massive coral framestone facies (*in situ* coral heads); a massive coral bindstone facies (*in situ* massive coral heads encrusted and bound by coralline algae); a branching coral framestone facies (*in situ* branching corals); a branching coral bindstone facies (*in situ* and reworked branching coral bound together by coralline algae) and a sand facies (carbonate sand with blue grey carbonate mud occurring near the base of core L1). The massive coral bindstone facies dominated core L1 whereas the massive coral framestone facies dominated cores L2 and L3. Cavities are abundant in all cores making up almost 85 % of L2.

The radiocarbon age indicates that reef growth on the windward margin at Lizard Island was initiated by approximately 6.7 cal kyr BP at a depth of 4.5 m below the reef flat (Figure 3.4, Table 3.1). Radiocarbon dates from the top of the windward margin cores confirm that the small corals in the cores were indeed living recently (Table 3.1, Figure 3.4). Rates of vertical accretion for Lizard windward margin range from 0.5 to 0.7 m kyr^{-1} (Figure 3.4).

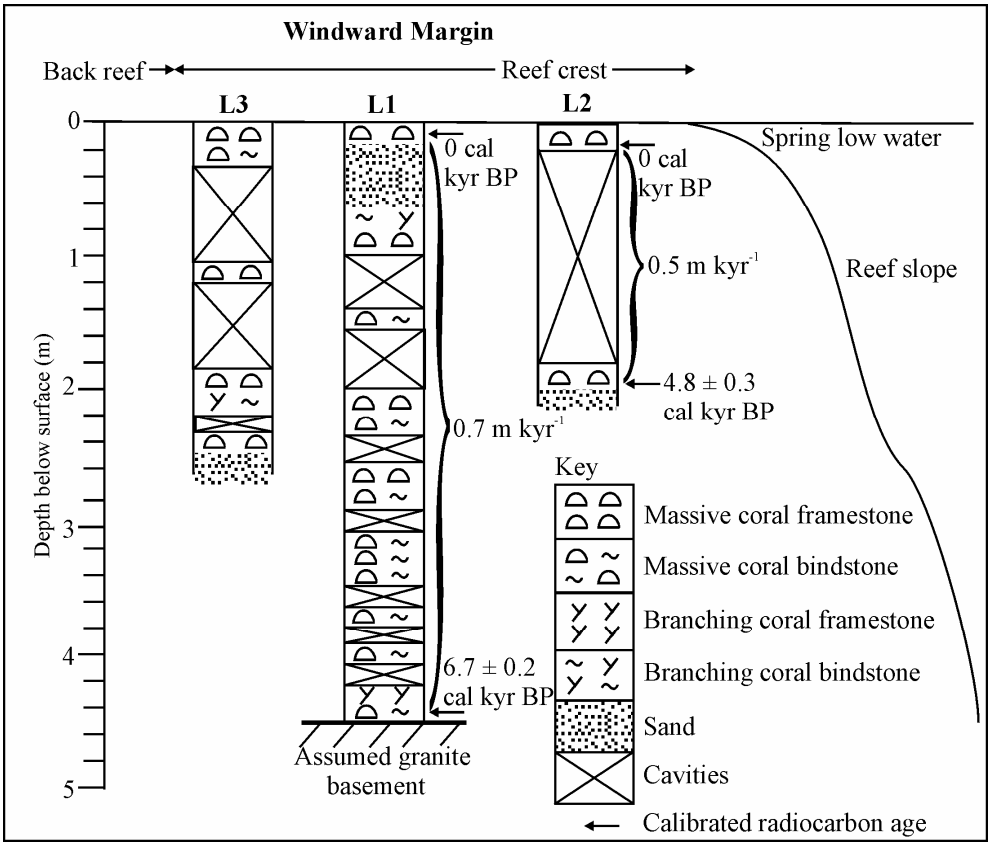

Figure 3.4. Core logs from Lizard Island windward fringing reef.

3.5.2 MacGillivray Reef

There are five facies present in the cores from MacGillivray Reef, four of which are also present in the Lizard cores; the massive coral framestone facies; the massive coral bindstone facies; the branching coral bindstone facies and the sand facies. A branching coral and sand facies is also present in the MacGillivray Reef cores which consists of reworked or *in situ* branching coral rubble embedded in blue grey carbonate sand and mud matrix (Figure 3.5). The windward core Mac 5 was dominated by the massive coral framestone facies (which consisted of smallish coral heads approximately 5 to 20 cm in length) and the branching coral and sand facies with a layer of coralline algae at the top of the core. Windward core Mac 3 was dominated by the branching coral bindstone facies interspersed by the branching coral and sand facies; this core also had a coralline algae layer at the top. The leeward core Mac1, located on the southwest fringe of the sand cay, was dominated by the massive coral framestone facies (essentially the core advanced through four large, approximately 1 to 2.5 m in length, *Porites* head corals in sequence) with the branching coral and sand facies being encountered at the base of the core between 12.5 and 14.5 m below the reef flat. A large sand-free cavity (approximately 1.5 m in length) was encountered between 5.7 and 7.2 m below the reef flat. Mac 4 comprised branching coral and sand facies (although the volume of sand was less than in the windward cores) and the massive coral framestone facies with the branching coral bindstone facies at the top of the core (Figure 3.5). The cored reef sequences at MacGillivray range from 3.2 to 15 m. None of the cores penetrated the Holocene-Pleistocene unconformity, however.

Radiocarbon dating indicates that the windward margin at MacGillivray Reef approached within 2 m of present day sea level by approximately 5.6 cal kyr BP (Figures 3.5 and 3.6, Table 3.1). Although the two radiocarbon ages at the top of windward core Mac 5 are statistically indistinguishable we assume that they represent an age reversal. The age reversal is probably the result of older material (that of radiocarbon age 5.73 ± 0.2 cal kyr BP at 0.7 m below the reef flat) being broken off from the reef front or slope, transported and deposited on the reef flat above younger material (5.58 ± 0.2 cal kyr BP at 2 m below the reef flat). We assumed that the younger material (5.58 ± 0.2 cal kyr BP) represents in place coral growth because it was taken from a fairly large *Porites* massive coral and it is unusual for younger material to fall a great distance down through the reef structure.

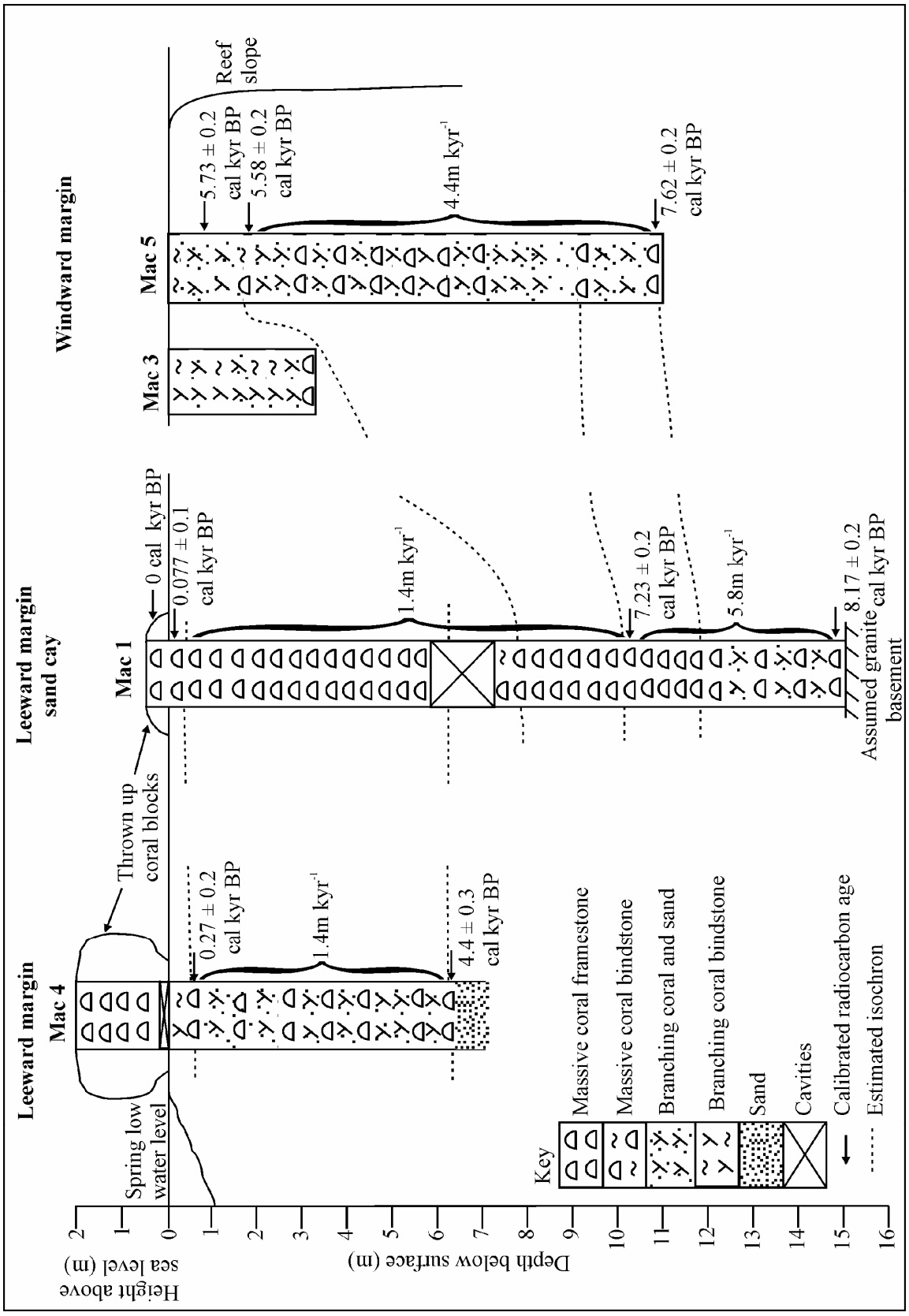

Figure 3.5. Core logs from MacGillivray platform reef

The younger radiocarbon age was therefore used to calculate the accretion rate for the windward margin. Dates of 267 ± 219 cal yr BP (Mac 4, 0.5 m below the reef flat) and 77 ± 145 cal yr BP (Mac 1, top of core) indicate that the leeward margin approached sea level much more recently. The radiocarbon date at the base of core Mac 1 indicates that reef growth was initiated approximately 8.2 cal kyr BP at a depth of 15 m below the reef flat on a basement which is assumed to be granite (Figure 3.5, Table 3.1).

Table 3.1. AMS Radiocarbon dating results. Radiocarbon ages are corrected for isotopic fractionation. Conversion to calendar ages was carried out using the marine calibration in the CALIB 4.4 programme (Stuvier and Reimer, 1993) assuming a marine reservoir offset $\Delta R = 10 \pm 7$ a. Errors are 1σ. † This sample came from the thrown up coral block through which core Mac 1 was initiated.

Lab Code	Reef	Core No.	Margin	Depth below surface (m)	Conventional radiocarbon age (kyr BP)	Calibrated age (cal kyr BP)
ANUA25523	Lizard	L1	Windward	0.1	-0.653 ± 0.181	-
ANUA25524	Lizard	L1	Windward	4.5	6.289 ± 0.202	6.722 +0.249/-0.236
ANUA25525	Lizard	L3	Windward	0.3	-0.469 ± 0.184	-
ANUA25526	Lizard	L3	Windward	2.35	4.637 ± 0.202	4.830 +0.368/-0.293
ANUA25520	MacGillivray	Mac1	Leeward	+0.2†	0.201 ± 0.193	-
ANUA26224	MacGillivray	Mac1	Leeward	0	0.487 ± 0.178	0.077 +0.212/-0.212
ANUA25521	MacGillivray	Mac1	Leeward	9.5	6.700 ± 0.227	7.228 +0.183/-0.252
ANUA26225	MacGillivray	Mac1	Leeward	15	7.736 ± 0.207	8.170 +0.209/-0.214
ANUA26228	MacGillivray	Mac4	Leeward	0.5	0.619 ± 0.175	0.267 +0.171/-0.267
ANUA26627	MacGillivray	Mac4	Leeward	6.2	4.296 ± 0.189	4.403 +0.239/-0.266
ANUA26229	MacGillivray	Mac5	Windward	0.7	5.390 ± 0.181	5730 +193/-157
ANUA26230	MacGillivray	Mac5	Windward	2	5.234 ± 0.188	5.583 +0.174/-0.173
ANUA26231	MacGillivray	Mac5	Windward	11	7.172 ± 0.202	7.618 +0.197/-0.168

The deepest date at Mac 5 is 7.62 ± 0.2 cal kyr BP at approximately 11 m below the reef flat, whereas the deepest date in the leeward core Mac 4 is 4.4 ± 0.3 cal kyr BP at a depth of 6.2 m below the reef flat. We also dated the thrown up coral block through which Mac 1 was initiated. This returned a modern date (the radiocarbon age of 200 ± 190 yr BP indicates some contribution from bomb radiocarbon), and hence we conclude that this block was broken off a living coral and thrown up on to the reef flat (Figure 3.5, Table 3.1).

Average rates of vertical accretion range from 1.4 m $kyr^{-1}$to 5.8 m kyr^{-1} in the leeward cores (Figure 3.5). The rate of vertical accretion in the top 10 m of the two leeward cores (Mac 1 and 4) were the same; 1.4 m kyr^{-1}. A higher rate vertical accretion of 5.8 m kyr^{-1} was encountered between 10 and 15 m below the reef flat in Mac 1. The rate of vertical accretion in windward core Mac 5 was 4.4 m kyr^{-1} between 2 and 11 m below the reef flat.

3.6 Discussion

A radiocarbon date indicates that the fringing reef at Lizard Island started growing directly on an assumed granite basement approximately 6.7 cal kyr BP at approximately 4.5 m below the reef flat surface (Table 3.1). This finding is consistent with the view that many modern reefs are only thin veneers (Thom and Orme, 1976; Davies *et al.,* 1977; Hopley, 1977; Orme *et al.,* 1978). Comparison with the sea level curves for North East Australia (L1, Figure 3.6; Thom and Chappell, 1975; Thom and Roy, 1983; 1985; Larcombe *et al.,* 1995), suggests that reef initiation followed rapidly after flooding of the granite basement, within about 500 years. The modern radiocarbon dates for the top of L1 and L3 suggest that the reef reached present day sea level only recently (Table 3.1). However, these dates are anomalously young compared to data from other reefs in the region (Mclean and Stoddart, 1978; Chappell *et al.,* 1983) which is probably due to the coral material being at the top of the cores and therefore representing recent coral growth and not the time when the windward margin as a whole reached sea level. The date of 4.8 cal kyr BP (L3) at 2.35 m below the reef flat is probably more representative of when the Lizard Island windward margin began to approach modern day sea level, as it is more consistent with the regional trend (Chappell *et al.,* 1983; Hopley, 1977). It is widely accepted that in the GBR region sea level stabilised at its present level approximately 6.5 - 6 kyr BP, the radiocarbon dates for the windward margin are consistent with sea level reaching its present level by 6 kyr BP (Figures 3.4 and 3.6; Table 3.1; Thom and Chappell, 1975; Thom and Roy, 1985). The radiocarbon dates obtained in the present work suggest that the fringing reefs at Lizard Island displayed the catch-up growth strategy of Neumann and Macintyre (1985; Figure 3.6). The presence of massive coral and algae throughout the cores indicates that this margin was and still is exposed to a relatively high energy environment. The radiocarbon date at the base of drill core L1 reveals that this reef developed entirely in water depths of less than 5 m (Figure 3.6). The windward cores are dominated by massive corals and coralline

algae; a similar coral assemblage was discovered in drill cores of Carter ribbon reef (Hopley, 1997). The presence of coralline algae in the windward cores from Lizard Island and Carter reefs is indicative of a high-energy environment (Adey, 1986).

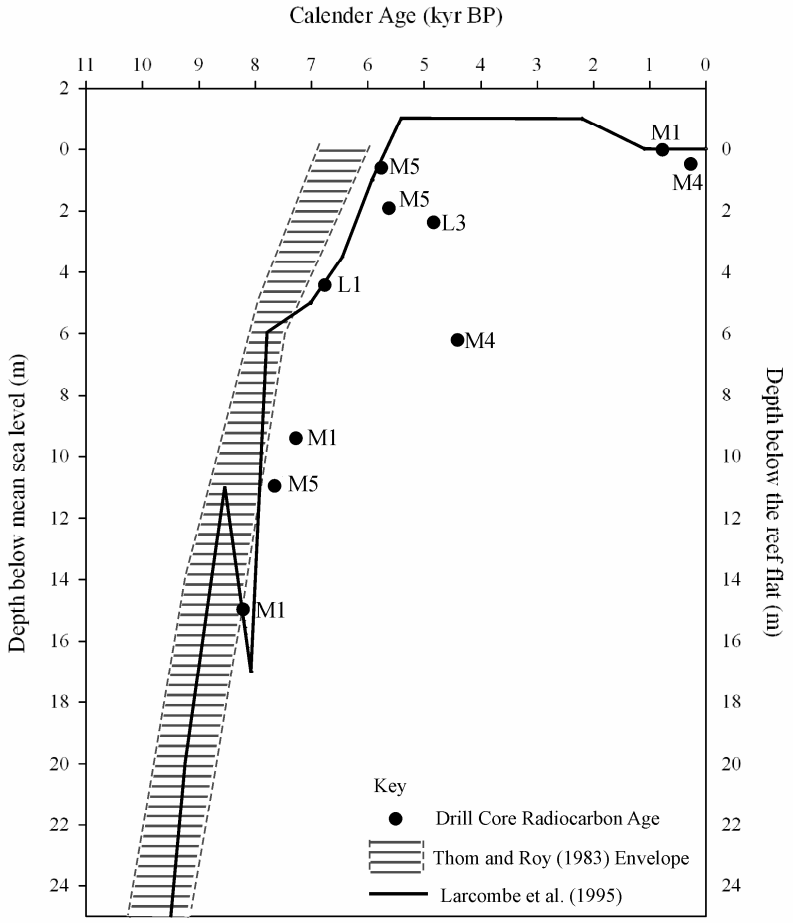

Figure 3.6. Relative sea level curve and envelope for north east Australia modified from Larcombe *et al.* (1995) and Thom and Roy (1983) for comparison with our radiocarbon ages for Lizard Island and MacGillivray Reefs (Table 3.1). It is important to note that these curves are approximations of sea level rise during the Holocene. The envelope of Thom and Roy's (1983) is a revision of Thom and Chappell's (1975) earlier sea level curve for southeast Australia; the curve shown represents the relative sea level envelope for eastern Australia. Larcombe *et al.*'s (1995) relative sea level curve for the Central Great Barrier Reef (CGBR), between Hayman Island and Cape Tribulation, was established using 364 radiocarbon dates from across the shelf. Although Larcombe *et al.*'s (1995) curve used an extensive database of 364 radiocarbon dates it has been critised because it employed radiocarbon dates of a variety of material including peat, mangrove mud, wood, organic C fraction from soil, mangrove root, coral, foraminifera, bivalve shells, shell hash and carbonate sand, taken from across the shelf in the central GBR. In both cases we have converted the conventional radiocarbon ages reported by Thom and Roy (1983) and Lacombe *et al.* (1995) to calendar years for comparison with our data in Table 1. Elevations were corrected to Australian Height Datum (AHD). Our data, represented by filled circles, are plotted in terms of depth below the present day reef flat (left hand axis). The labels L1 and L3 refer to Lizard Island

windward margin cores, while for MacGillivray Reef, M5 is a windward core and M1 and M4 are leeward cores.

Results from previous drilling investigations have suggested that the majority of reefs fringing continental islands in the GBR have grown on unconsolidated sediments overlying the rocky foundations and growth was only initiated once the rapid phase of sea level rise had been completed (Hopley *et al.,* 1983). Evidence from our drill cores at Lizard are not consistent with this observation because we assume the windward margin at Lizard Island grew directly on a granite basement although colonisation only began after sea level had stabilised in the region (Figures 3.4 and 3.6).

Rates of vertical accretion at Lizard range from 0.5 to 0.7 m kyr^{-1}, although a somewhat higher value of 1.1 m kyr^{-1} is implied if the date of 4.8 cal kyr BP (at 2.35 m below the reef flat in L2) is taken to be representative of when the windward margin at Lizard Island approached modern day sea level (Figure 3.4). These rates are at the lower end of the range for typical GBR fringing reef, which extends from 1 to 4 m kyr^{-1} (Davies and Hopley, 1983). This may be due to the dominance of slow growing massive corals and coralline algae under the higher hydrodynamic energy conditions that this exposed and relatively shallow margin would have encountered during the mid to late Holocene. Although we assume that the windward margin grew directly on a granite basement, no traces of quartz grains or other granite material were found in the thin sections from the base of L1. We assume that the drill holes encountered a granite basement at 4.5 m below the reef flat (L1) because it is obvious to a driller when the drill head encounters a transition between a soft rock, like carbonate and a hard rock, like granite. We assume that the basement is granite because of the close proximity of the core sites to the granite South Island (Figure 3.2). None of the cores penetrated the Holocene-Pleistocene unconformity; this does not however, exclude the possibility that there may be karst remnants of Pleistocene reef in deeper locations, for example, on the reef slope and in the lagoon.

Once the reef reached within 2.5 m of present-day sea level it would have been increasingly subject to wave action and vertical extension would have been limited by sub-areal exposure. This would have resulted in retardation of vertical growth rates. The excess carbonate produced would have been transported leeward into the lagoon instead of being incorporated *in situ* within the reef framework. Indeed the LIMER (1975) expedition discovered that the dominant water flow was to leeward and suggested that this was also the direction of flow of reef-derived material. They concluded, however,

that most of this sediment was not accumulating in the lagoon but being transported further leeward to the slope behind the leeward reef (LIMER, 1975). This may explain why the lagoon is relatively deep (10 m). It is reasonable to assume that the morphology of the present lagoon may be related to the topography of an eroded paleo river channel of the underlying granite basement, which was subsequently accentuated by Holocene reef growth. This could explain the meandering morphology and deep depth (10 m) of the lagoon (Figure 3.2). It has been shown that the morphology of Holocene reefal formations often reflects Pleistocene topography (for example, in Belize (Purdy, 1974)).

Radiocarbon dating suggests that MacGillivray platform reef developed on a topographic high, which is assumed to be granite, at a depth of 15 m below the reef flat approximately 8.2 cal kyr BP (Mac 1; Figure 3.5). This period of initiation is consistent with the regional Holocene sea level curves for North East Australia (Figure 3.6; Thom and Roy, 1983; Larcombe *et al.,* 1995) which indicate that sea level was approximately 12 m lower than today at 8 cal kyr BP and that reef initiation did not lag sea level rise. This timing is consistent with (i) evidence of reef initiation from other regions of the GBR (Davies and Hopley, 1983; Davies *et al.,* 1985) between 8 and 9 kyr BP and (ii) the global reef initiation event between 7 and 8 kyr BP (Davies *et al.,* 1985; Davies and Montaggioni, 1985; Montaggioni, 1988). The radiocarbon date of 7.6 cal kyr BP at a depth of 11 m below the reef flat in core Mac 5 is also in agreement with the local sea level curves (Figure 3.6). We assume that the windward margin at MacGillivray Reef (M5) displayed keep-up growth strategy of Neumann and MacIntyre (1985) because the reef crest maintained a surface near to sea level throughout its growth (Figure 3.6). The radiocarbon date of 4.4 cal kyr BP (at 6.2 m below the reef flat) reveals that leeward margin reef growth lagged sea level rise by at least 2.5 kyr and was covered by at least 6 m of water at that time (M4; Figure 3.6). It is not possible to suggest with absolute certainty that the leeward core Mac 1 (M1) caught up with sea level rise because of the lack of radiocarbon dates between 7.23 and 0.077 cal kyr BP, although the radiocarbon date of 7.23 cal kyr BP at 9.5 m below the reef flat indicates that reef growth lagged sea level rise by approximately 500 years (Figure 3.6). Therefore, we assume that the leeward margin at MacGillivray Reef displayed catch-up growth (M1, M4; Figure 3.6).

Comparison of the radiocarbon dates at the bases of both the windward and leeward cores (8.2 cal kyr BP at 15 m below the reef flat, Mac 1; 7.6 cal kyr BP at 11m below the reef flat, Mac 5) indicates that reef growth across the platform may have initially been uniform (Figure 3.5). This agrees with Ryan *et al.*'s (2001) suggestion that

early Holocene reef growth on planar foundations may have been prolific across entire platforms. Later, during the mid-Holocene, the reef margins would have out grown the middle of the reef platform creating a bowl shape which forms a lagoon (Figure 3.5). Accretion of the windward margin kept-up with sea level rise at a rate of 4.4 m kyr^{-1} to reach modern day sea level at approximately 5.6 cal kyr BP (Figure 3.5). The leeward margin lagged behind the windward margin by about 5.3 kyr, only reaching present day sea level in the last 300 years, at an accretion rate of 1.4 m kyr^{-1} (Figure 3.5). The observation that the windward margin approached the present-day sea level before the leeward at MacGillivray Reef is consistent with global observations of reef development (Davies *et al.,* 1985) and is believed to be associated with higher wave energy on the windward margin. Once the windward margin had reached present day sea level any subsequent calcium carbonate production would be eroded and transported to leeward. The 5 kyr history of subsequent accumulation of carbonate detritus is evidenced by the almost completely full lagoon and leeward sand cay at MacGillivray Reef.

The radiocarbon dates in Figure 3.5 indicate that growth in leeward core Mac 1 was initially rapid at a rate of 5.8 m kyr^{-1}, probably due to the presence of fast growing branching corals. After 7.2 cal kyr BP, however, accretion on this margin slowed dramatically to 1.4 m kyr^{-1}, probably as a consequence of a facies succession from branching to massive coral colonies in response to conditions of increasing hydrodynamic energy. This is consistent with observations of reef growth in the Pacific and Caribbean which commonly exhibit a facies succession from branching corals in the lower half of a core to coral head facies in the upper section (Davies and Hopley, 1983; Cortes *et al.,* 1994; Caboich *et al.,* 1995).

The windward core Mac 5 exhibited very low porosity. All cavities were filled with the branching coral and sand facies, which contain large volumes of blue grey carbonate mud and sand. There are a succession of coral forms from branching to massive in the top section of the core (Figure 3.5). These characteristics probably result from the exposure of the windward margin to high energy conditions. Indeed the radiocarbon dates (Mac 5) suggest that the lower section of the windward margin was covered by only about two metres of water according to the sea level curves (Figure 3.6) and therefore within the depth range that is influenced by breaking waves.

None of the cores at MacGillivray penetrated the Holocene-Pleistocene carbonate unconformity. Other coring programmes and seismic profiling in the GBR has shown

that this surface lies at depths between 3.9 and 24 m below the reef flat. At Bewick Island, for example, it is at 7 m below the reef flat; at Stapleton Island, 14.6 m below the beach surface; at Carter Reef, 10.2 to 19.3 m below the reef flat; at Yonge Reef, 19 m below the reef flat and Potter Reef, 25.2 m below the reef flat (Harvey, 1977; Thom *et al.*, 1978; Harvey and Hopley, 1981b; Graham, 1993).

The date of 267 ± 219 cal yr BP for the surface of the leeward core Mac 4 indicates that the coral block which presently sits proud of the reef flat must have been thrown up or moved into its present position relatively recently. The date of 77 ± 145 cal yr BP for the reef flat surface of core Mac 1 indicates that the coral block situated on top has only been in place in the last 100 years.

3.6.1 Subsidence

The absence of Pleistocene deposits in the cores from Lizard and MacGillivray reefs suggests that the underlying substrate of these reefs may have tectonically subsided by at least 15 m since the last interglacial with respect to the coast. We assume, because we did not recover any Pleistocene material, that none of the cores from either Lizard Island or MacGillivray, encountered Pleistocene limestone, even at a depth of 15 m below the reef flat at MacGillivray Reef (Figure 3.5). This suggests the possibility that at MacGillivray Reef the top of the granite topographic high was exposed during the last interglacial sea level high stand (125 kyr BP), which was believed to be close to or up to 5 m above the present day sea level on the GBR (Flood, 1984; Graham, 1993). Hence we infer that the area may have tectonically subsided by at least 15 m between 125 and 10 kyr BP.

Graham (1993) suggested that the Holocene foundations of Potter Reef must have subsided by at least 27.5 m during the last 122 ka (subsidence rate of 0.23 mm yr^{-1}) to account for the depth to the Holocene-Pleistocene unconformity on this reef. Drilling on ribbon reefs (Carter and Yonge) east of MacGillivray Reef reveal depths to the Holocene-Pleistocene unconformity at approximately 19 m below reef flat, revealing a potential subsidence rate of 0.19 to 0.2 mm yr^{-1} (Harvey and Hopley, 1981a; Hopley, 1994; Hopley and Davies, submitted for publication). It has also been suggested that there is gradual subsidence of the GBR shelf on the order of 0.05 to 0.1 mm yr^{-1} (Davies, 1983; Flood, 1983). Although these rates suggest subsidence of only 12.5 m since 125 kyr BP. Deep drilling at Ribbon Reef 5, on the outer shelf near Cairns,

suggests subsidence at a rate of 0.19 to 0.2 mm yr^{-1} since 600 ka (International Consortium for Great Barrier Reef Drilling, 2001).

Our inferred subsidence rate is based on the assumption that no Pleistocene reef grew on top of the granite high at MacGillivray Reef because it was not submerged. It is possible that a Pleistocene reef did grow on top of a topographic high at the base of Mac 1 that was subsequently eroded during the Pleistocene regressions. Davies (1983) and Hopley (1982) postulated that the top 12 to 29 m of Pleistocene carbonate within the GBR may have been eroded during lower sea levels over the last 100, 000 years based on estimates of rates of sub-aerial erosion of Pleistocene carbonate at Aldabra Atoll (Trudgill, 1983). If these rates are correct, it could mean that any Pleistocene reef limestone at the base of Mac 1 could have been completely eroded, effectively erased from the sedimentary record.

Alternatively, Marshall (2004) suggests that suggested erosion/subsidence rates are unrealistically high for a stable continental margin like the GBR and proposes that the last interglacial reef did not achieve modern day sea level, let alone 5 m above it. However, both Stoddart *et al.* (1978) and Murray-Wallace and Belperio (1991) noted that the 'absence of outcropping Pleistocene reefs within the province leads to the inference that subsidence rather than stability has dominated reef development in the area'. This followed from Chappell (1974) and Hopley's (1977) debate about what could have caused the greater subsidence of the outer ribbon reef substrate compared to the substrate under the inner shelf reefs. The greater depth of the Holocene-Pleistocene unconformity under the outer shelf reefs could explain why the outer shelf reefs reached sea level after the inner shelf reefs. Discussions revolved around possibility that the cause of this subsidence was hydroisostatic warping of the shelf in response to the increased water mass on the shelf during the Holocene transgression, general slow tectonic subsidence near the Halifax Basin or a combination of the two (Chappell, 1974; Hopley, 1977, Hopley and Harvey, 1981). Hydroisostatic tilting of the shelf creates short-term vertical movements and involves vertical movements of the land in both directions depending on whether sea level is rising or falling. Over long-term glacial-interglacial cycles the vertical movement is negligible. Tectonic subsidence occurs continuously over long time scales (~ 120 kyr) and in the same direction (Chappell, 1987). The radiocarbon dates from MacGillivray Reef suggests long-term tectonic subsidence of the shelf of at least 15 m over the last 125 kyr (Hopley, 1977; Hopley and Harvey, 1981).

Our drill core data from MacGillivray Reef, together with other drill core and seismic profiling observations that the Holocene-Pleistocene unconformity occurs at a depth of 19.3 m and 19.1 m below the reef flat at Carter and Yonge reefs respectively suggest that there is indeed a reduction in the rate of subsidence nearer the land in this area (Harvey, 1977; Hopley, 1994; Hopley and Davies, submitted for publication). The rate of subsidence at MacGillivray Reef suggested by our drill core data of at least 0.12 mm yr^{-1} is in agreement with the rates determined from the two deep drill cores taken off Cairns (Boulder Reef and Ribbon Reef 5) and drilling at Yonge, Carter and Potter Reefs of 0.19 to 0.2 mm yr^{-1} (Graham, 1993; Hopley, 1994; International Consortium for Great Barrier Reef Drilling, 2001; Hopley and Davies, submitted for publication) but higher than the rates determined by Flood (1983) and Davies (1983). We infer that there is variation in subsidence within the GBR province as a whole with a possible NS trend, with higher rates of subsidence occurring in the North (Hopley, 1982; Davies and Hopley, 1983; Graham, 1993).

3.7 Conclusions

The windward reef at Lizard Island was initiated directly on a granite basement approximately 6.7 cal kyr BP at a depth of 4.5 m below the reef flat. The windward margin at Lizard Island approached modern day sea level approximately 4 cal kyr BP. The leeward reef at MacGillivray was also initiated directly on a granite basement approximately 8.2 cal kyr BP at a depth of 15 m below the reef flat and approached sea level only within the last 500 years (260 to 80 cal yr BP). The windward margin was initiated by 7.6 cal kyr BP and approached modern day sea level approximately 5.6 cal kyr BP. Rates of vertical accretion ranged from 1.4 to 5.8 m kyr^{-1} at MacGillivray and 0.5 to 1 m kyr^{-1} at Lizard Island. Higher rates of accretion were associated with the early stages of reef growth between 8.1 and 5.6 cal kyr BP. When the reefs approached within 2 m of modern day sea level the rates of vertical accretion slowed to 1.4 m kyr^{-1}. None of the cores penetrated the Holocene-Pleistocene unconformity. The absence of Pleistocene reefal deposits in the MacGillivray cores suggests that the shelf may have subsided by at least 15 m since the last interglacial. A lot more drilling, vibro-coring and seismic profiling is needed (specifically in the northern and far northern GBR province) to explain the models of reef evolution we develop here.

3.8 References

Adey, W. H. (1986) Coralline algae as indicators of sea level. In O. V. D. Plassche (ed), *Sea Level Research a Manual for the Collection and Evaluation of Data*. Galliard LTD, UK.

Caboich, G., Montaggioni, L. F. and G. Faure (1995) Holocene initiation and development of New Caledonian fringing reefs, S.W. Pacific. *Coral Reefs,* **14**, 131-140.

Chappell, J. (1974) Geology of Coral Terraces, Huon Peninsula, Papua New Guinea: A Study of Quaternary Tectonic Movements and Sea Level Changes. *Geol. Soc. Am. Bull.,* **85**, 553-570.

Chappell, J. (1987) Late quaternary sea-level changes in the Australian region. In M. J. Tooley and I. Shennan (eds), *Sea Level Changes.* Basil-Blackwell, Oxford, pp 296-331.

Chappell, J., Chivas, A., Wallensky, E., Polach, H. A. and P. Aharon (1983) Holocene paleo-environmental changes, Central to North Great Barrier Reef inner zone. *Jn. Aust. Geol. Geophys.,* **8**, 223-235.

Chrisholm, R. M. and D. J. Barnes (1998) Anomalies in coral reef community metabolism and their potential importance in the reef CO_2 source-sink debate. *Proc. Nat. Acad. Sci. USA.,* **95**, 6566-6569.

Cortes, J., MacIntyre, I. G. and P. W. Glynn (1994) Holocene growth history of an Eastern Pacific fringing reef, Punta Islotes, Costa Rica. *Coral Reefs,* **13**, 65-73.

Coventry, R. J., Hopley, D., Campbell, J., Douglas, I., Harvey, N., Kershaw, A. P., Oliver, J., Phipps, C. V. G. and K. Pye (1980) The Quaternary of Northeastern Australia. In R. A. Henderson and P. J. Stephenson (eds), *The Geology and Geophysics of Northeastern Australia.* Geological Society of Australia, Queensland Division, Brisbane, pp 375-419.

Davies, P. J. and K. Martin (1976) Radial aragonite ooids, Lizard Island Great Barrier Reef, Queensland Australia. *Geology,* **4**, 120-122.

Davies, P. J., Marshall, J. F., Thom, B. G., Harvey, N., Short, A. D. and K. Martin (1977) Reef development Great Barrier Reef. *Proc. 3rd Int. Coral Reef Symp. Miami,* **2**, 332-337.

Davies, P. J. and J. F. Marshall (1980) A model of epi-continental reef growth. *Nature,* **287**, 37-38.

Davies, P. J. and D. Hopley (1983) Growth facies and growth rates of Holocene reef in the Great Barrier Reef. *B.M.R. J. Aust. Geol. Geophys.,* **8**, 237-251.

Davies, P. J. (1983) Reef Growth. In D. J. Barnes (ed), *Perspectives on Coral Reefs.* Aust. Inst. Mar. Sci. Brian Clouston Publishing, Manuke, ACT, Australia, pp 69-106.

Davies, P. J. and J. F. Marshall (1985) *Halimeda* bioherms - low energy reefs, northern Great Barrier Reef. *Proc. 5th Int. Coral Reef Congr. Tahiti,* **5**, 1-7.

Davies, P. J., Marshall, J. F. and D. Hopley (1985) Relationships between reef Growth and sea level in the Great Barrier Reef. *Proc. 5th Int. Coral Reef Congr. Tahiti,* **3**, 95-103.

Davies, P. J. and L. F. Montaggioni (1985) Reef growth and sea level change: the environmental signature. *Proc. 5th Int. Coral Reef Congr. Tahiti,* **3**, 477 – 511.

Drew, E. A. and K. M. Abel (1985) Biology, sedimentology and geography of the vast inter-reefal *Halimeda* meadows within the Great Barrier Reef Province. *Proc. 5th Int. Coral Reef Congr. Tahiti,* **5**, 15-20.

Dunbar, G. B. and G. R. Dickens (2003) Massive siliciclastic discharge to slopes of the Great Barrier Reef Platform during sea-level transgression: constraints from sediment cores between 15°S and 16°S latitude and possible explanations. *Sed. Geol.,* **162**, 141-158.

Flood, P. G. (1983) Coated grains from the Great Barrier Reef. In T. Peryt (ed), *Coated Grains*. Springer-Verlag, Berlin, pp 561-565.

Flood, P. G. (1984) *A geological guide to the northern Great Barrier Reef*. Australasian Sedimentologists Group Field Guide Series, No. 1, Sydney, Geological Society of Australia.

Flood, P. G. and G. R. Orme (1988) Mixed siliciclastic/carbonatesediments of the northern Great Barrier Reef province Australia. In L. J. Doyle and H. H. Roberts (eds), *Carbonate–Clastic Transitions*. Developments in Sedimentology, 42, Elsevier, Amsterdam, pp. 175–205.

Frankel, E. (1974) Recent sedimentation in the Princess Charlotte Bay area, Great Barrier Reef province. *Proc. 2nd Int. Coral Reef Symp., Brisbane*, 355-369.

Gattuso, J. P., Frankignouelle, M., Smith, S. V., Ware, J. R., Wolast, R., Buddemeier, R. W. and H. Kayanne (1996) Coral Reefs and Carbon Dioxide. *Science*, **271**, 5253, 1298-1300.

Gattuso, J. P., Frankignouelle, M. and S. V. Smith (1999) Measurement of community metabolism and significance of the coral reef CO_2 source-sink debate. *PNAS*, **96**, 13017-13022.

Graham, T. L. (1993) *Geomorphological Response of Continental Shelf and Coastal Environments to the Holocene Transgression – Central Great Barrier Reef*. Unpublished PhD Thesis, James Cook University.

Harvey, N. (1977) The identification of subsurface disconformities of the Great Barrier Reef, Australia between 14°S and 17°S, using shallow seismic refraction techniques. *Proc. 3rd Int. Coral Reef Symp. Miami*, 45-51.

Harvey, N. and D. Hopley (1981)a Radiocarbon ages and morphology of reef tops in the Great Barrier Reef between 14º39'S and 20º45'S: Indicators of shelf neotectonics? *Proc. 4th Int. Coral Reef Symp. Manila*, **1**, 523-530.

Harvey, N. and D. Hopley (1981)b The relationship between modern reef morphology and a pre-Holocene substrate in the Great Barrier Reef Province. *Proc. 4th Int. Coral Reef Symp. Manila*, **1**, 549-554.

Heap, A. D., Dickens, G. R. and L. K. Stewart (2001) Late Holocene clastic and carbonate sediment in Nara Inlet on the middle shelf, central Great Barrier Reef platform, Australia. *Mar. Geol.*, **176**, 39–54

Heyward, A., Pinceratto, E. and L. D. Smith (1997) *Big Bank Shoals of the Timor Sea: an environmental resource atlas*. Australian Institute of Marine Science & BHP Petroleum, pp 115.

Hopley, D. (1977) The age of the Outer Ribbon Reef Surface, Great Barrier Reef, Australia: implications for hydrostatic models. *Proc. 3rd Int. Coral Reef Symp.*, **2**, 23-28.

Hopley, D. (1982) *The geomorphology of the Great Barrier Reef: Quaternary development of coral reefs*. John Wiley, NY.

Hopley, D. (1994) Continental shelf reef systems. In R. W. G. Carter and C. D. Woodroffe (eds), *Coastal Evolution: Late Quaternary shoreline morphodynamics*. Cambridge University Press, Cambridge, pp 303-340.

Hopley, D. (1997) *Coral reefs and global climate change*. Report commissioned by the WWF, Washington DC, pp 46.

Hopley, D. and N. Harvey (1981) Radiocarbon ages and morphology of reef tops in the Great Barrier Reef between 14º39'S and 20º45'S: Implications of shelf neotectonics? Proc. 4th Int. Coral Reef Symp. Manila, 1, 523-530.

Hopley, D., Solcombe, A. M., Muir, F. and C. Grant (1983) Nearshore fringing reefs in north Queensland. *Coral Reefs*, **1**, 151 – 160.

Hopley, D. and P. J. Davies (submitted for publication) Shallow drilling on the Great Barrier Reef and adjacent islands.

International Consortium for Great Barrier Reef Drilling (2001) New constraints on the origin of the Australian Great Barrier Reef: results from an international project of deep coring. *Geology*, **29**, 483–486.

Johnson, D. P. and R. M. Carter (1978) Sedimentary framework of mainland fringing reef development, Cape Tribulation Area. *Great Barrier Reef Marine Park Authority Technical Memorandum* GBRMPA-TM-14, 4-17.

Kayanne, H., Suzuki, A. and H. Saito (1995) Diurnal changes in the partial pressure of carbon dioxide in coral reef water. *Science*, **269**, 5221, 214-216.

Kinsey, D. W. (1979) *Carbon turnover and accumulation by coral reefs.* Unpublished PhD Thesis University of Hawaii, pp 248.

Kump, L. R., Kasting, J. F. and R. G. Crane (1999) *The earth system.* Prentice Hall Inc., New Jersey, pp 351.

Larcombe, P., Carter, R. M., Dye, J., Gagan, I. M. K. and D. P. Johnson (1995) New evidence for episodic post-glacial sea-level rise, central Great Barrier Reef, Australia. *Mar. Geol.*, **127**, 1-44.

LIMER (Barnes, D. J., Caperon, J., Cox, T. J., Crossland, C. J., Davies, P. J., Devereux, M., Hamner, W. M., Jitts, H. R., Kinsey, D. W., Knauer, G. A., Lundgren, J. A., Olafson, R., Skyring, G. W., Smith, D. F., Webb, K. L. and W. J. Wiebe) (1975) LIMER Expedition 1975 Metabolic processes of coral reef communities at Lizard Island, Queensland. *Search*, **7,** 11-12, 463-468.

Marshall, J. F. (2004) Was the Great Barrier Reef that "Great" during the Last Interglacial? *8th Int. Conf. Paleocean.*, 5-10 September 2004, Biarritz, France, Program and Abstracts, 94, Bordeaux 1 University.

Marshall, J. F. and P. J. Davies (1988) *Halimeda* bioherms of the Northern Great Barrier Reef. *Coral Reefs*, **6**, 139-148.

Maxwell, W. G. H. and J. P. Swinchatt (1970) Great Barrier Reef: regional variation in a terrigenous-carbonate province. *Geol. Soc. Am. Bull.*, **81**, 691–724.

Mclean, R. F. and D. R. Stoddart (1978) Reef island sediments of the northern Great Barrier Reef. *Phil. Trans. R. Soc. Lond. A*, **291**, 101-117.

Montaggioni, L. F. (1988) Holocene reef growth history in mid-plate high volcanic islands. *Proc. 6th Int. Coral Reef Symp. Australia***, 3**, 455-461.

Murray-Wallace, C. V. and A. P. Belperio (1991) The last interglacial shoreline in Australia: a review. *Quat. Sci. Revs.*, **10**, 441-46l.

Neumann, A. C. and I. G. MacIntyre (1985) Reef response to sea level rise: keep up, catch up or give up. *Proc. 5th Int. Coral Reef Congr. Tahiti*, **3**, 105 – 110.

Orme, G. R. and P. G. Flood (1977) The geological history of the Great Barrier Reef: a reappraisal of some aspects in the light of new evidence. *Proc. 3rd Int. Coral Reef Symp.*, 37-43.

Orme, G. R., Flood, P. G. and G. E. G. Sargent (1978) Sedimentation trends in the lee of outer (ribbon) reefs, Northern region of the Great Barrier Reef Province. *Phil. Trans. R. Soc. Lond. A*, **291**, 85-99.

Orme, G. R. and P. G. Flood (1980) Sedimentation in the Great Barrier Reef Province, Adjacent Bays and Estuaries. In R. A. Henderson and P. J. Stephenson (eds), *The geology and geophysics of Northeastern Australia*. Geological Society of Australia Inc, Queensland Division, pp 419-434.

Orme, G. R. (1983) Shallow structure and lithofacies of the northern Great Barrier Reef, In J. T. Baker, R. M. Carter, P. W. Sammarco and K. P. Stark (eds), *Proc. Great Barrier Reef Conf. JCU Press, Townsville*, pp 135-142.

Orme, G. R. (1985) The sedimentological importance of *Halimeda* in the development of back reef lithofacies, northern Great Barrier Reef (Australia). *Proc. 5th Coral Reef Symp.*, **5**, 31-37.

Orme, G. R. and M. S. Salama (1988) Form and seismic stratigraphy of *Halimeda* banks in part of the northern Great Barrier Reef Province. *Coral Reefs*, **6**, 131-137.

Partain, B. R. and D. Hopley (1989) Morphology and Development of the Cape Tribulation Fringing Reefs, Great Barrier Reef, Australia. *GBRMPA Tech. Mem*., T.M21, pp 45.

Purdy, E. G. (1974) Reef configurations: cause and effect. In L. F. Laporte (ed), *Reefs in Time and Space*. Society of Economic Paleontologists and Mineralogists Special Publication, 18, pp. 9-76.

Reitner, J. and F. Neuweiler (1995) Mud mounds: a polygenetic spectrum of fine-grained carbonate buildups. *Facies***, 32**, 1-70, 1-16.

Ryan, D. A., Opdyke, B. N. and J. S. Jell (2001) Holocene sediments of Wistari Reef towards a global quantification of coral reef related neritic sedimentation in the Holocene. *Pal. Pal. Pal.,* **175**, 1-12.

Scoffin, T. P., Stoddart, D. R., Mclean, R. F. and P. J. Flood (1978) The recent development of the reefs in the northern province of the Great Barrier Reef. *Phil. Trans. R. Soc. Lond. B***, 284**, 129-139.

Smith, S. V. and D. W. Kinsey (1976) Calcium carbonate production, coral reef growth and sea level change. *Science*, **194**, 937-939.

Spalding, M. D., Ravilious, C. and E. P. Green (2001) *World Atlas of Coral Reefs*. Prepared at the UNEP World Conservation Monitoring Centre. University of California Press, Berkeley, USA.

Stoddart, D. R., McLean, R. F., Scoffin, T. P., Thom, B. G. and D. Hopley (1978) Evolution of reefs and islands, northern Great Barrier Reef: synthesis and interpretation. *Phil. Trans. R. Soc. Lond. B*, **284**, 149-159.

Stuiver, M. and P. J. Reimer (1993) Extended ^{14}C data base and revised CALIB 3.0 ^{14}C age calibration programme. *Radiocarbon*, **35,** 1, 215-31.

Thom, B. G. and J. Chappell (1975) Holocene sea-levels relative to Australia. *Search,* **6,** 90-93.

Thom, B. G. and G. R. Orme (1976) Shallow structure of reefs from coring. In D. R. Stoddart and M. Yonge (Convenors), *The northern Great Barrier Reef a meeting for discussion*, Abstr **4**. The Royal Society (London).

Thom, B. G., Orme, G. R. and H. A. Polach (1978) Drilling investigation of Bewick Island. *Phil. Trans. R. Soc. Lond. A***, 291**, 37-54.

Thom, B. G. and P. S. Roy (1983) Sea-level change in New South Wales over the past 15,000 years. In D. Hopley (ed), *Australian Sea Levels in the Last 15,000 years: A Review*. Dept. Geography, James Cook University, Monograph Series, Occasional Paper No. 3, Townsville, Australia, pp 64-84.

Thom, B. G. and P. S Roy (1985) Relative sea levels and coastal sedimentation in South East Australia in the Holocene. *Jn. Sed. Petrol.*, **55**, 2, 257-264.

Trudgill, S. T. (1983) Measurement of rates of erosion of reefs and reef limestones. In D. J. Barnes (ed), *Perspectives on Coral Reefs.* Aust. Inst. Mar. Sci. Brian Clouston Publishing, Manuke, ACT, Australia, pp 256-262.

3.9 Acknowledgements

This research has been supported by the National Environment Research Council (NERC); Royal Society; Lizard Island Research Station and Staff; Australian Museum; Great Barrier Reef Marine Park Authority; Australian National University Earth and Marine Sciences Department and the Australian National University Nuclear Physics Department. We would especially like to thank Matthew Stevens, Nigel Craddy and Sarah Tynan (ANU) for muscle power during drilling. This work was carried out under the GBRMPA Permit No G03/5027.1.

Chapter Four

Coral Reef Sedimentation on Rodrigues and the Western Indian Ocean and its Impact on the Carbon Cycle

Plate 4.1 Rodrigues Island, Southwestern Indian Ocean (http://seawifs.gsfc.nasa.gov/cgi/landsat.pl)

Chapter 4

Coral Reef Sedimentation on Rodrigues and the Western Indian Ocean and its Impact on the Carbon Cycle

Reference: Rees S.A., Opdyke, B.N., Wilson, P.A. and L.K. Fifield (2005) Coral Reef Sedimentation on Rodrigues and the Western Indian Ocean and its Impact on the Carbon Cycle. *Phil. Trans. R. Soc. Lond. A.*, **363**, 101-120.

4.1 Abstract

Coral reefs in the Southwest Indian Ocean cover an area of approximately 18,530 km^2 compared to a global reef area of nearly 300,000 km^2. These regions are important as fishing grounds, tourist attractions and as a significant component of the global carbon cycle. The mass of calcium carbonate stored within Holocene neritic sediments is a number that we are only now beginning to quantify with any confidence, in stark contrast to the mass and sedimentation rates associated with pelagic calcium carbonate, which have been relatively well defined for decades.

We report new data that demonstrate that the reefs at Rodrigues, like those at Reunion and Mauritius only reached a mature state (reached sea level) by 2 to 3 ka– thousands of years later than most of the reefs in the Australasian region. Yet, field observations show that the large lagoon at Rodrigues is already completely full of carbonate detritus (typical lagoon depth < 1 m at low spring tide). The presence of aeolian dunes at Rodrigues indicates periodic exposure of past lagoons throughout the Pleistocene. The absence of elevated Pleistocene reef deposits on the island indicates that the island has not been uplifted. Most Holocene reefs are between 15 and 20 m in thickness and those in the Southwest Indian Ocean appear to be consistent with this observation. We support the view that the CO_2 flux associated with coral reef growth acts as a climate change amplifier during deglaciation, adding CO_2 to a warming world. Southwest Indian Ocean reefs could have added 7-10 % to this global flux during the Holocene.

4.2 Introduction

Coral reefs represent an important resource to coastal nations providing sources of food, building material and revenue through tourism and the aquarium trade (Naim *et al.*, 2000; Spalding *et al.*, 2001). They also provide natural coastal defenses and are regions of high biodiversity (Bellwood and Hughes, 2001). The health and survival of reefs around the world are undoubtedly already under threat from point-source pollution, terrestrial run-off, increased turbidity, destructive fishing practices and coral bleaching associated with increases in sea surface temperatures (Naim *et al.*, 2000; Roberts *et al.*, 2002; McCulloch *et al.*, 2003; Cole, 2003; Sheppard, 2003). In addition, projected anthropogenic increases in atmospheric carbon dioxide levels (CO_2 atm) pose threats to reef systems through acidification and warming of the surface tropical oceans (Gattuso *et al.*, 1999; Gattuso and Buddemeier, 2000). These effects are hypothesized to promote decreases in the aragonite saturation state of seawater and hermatypic coral calcification rates (Kleypas *et al.*, 1999; Langdon *et al.*, 2000). Since the discovery that oceans are a major sink for atmospheric CO_2, the processes that control the marine $CaCO_3$ budget have become the focus of much scientific attention, specifically the role that the oceans might play in mitigating future anthropogenic CO_2 increases. The main reservoir of CO_2 in the oceans is biogenic carbonate sediments (e.g. coral reefs and pelagic foraminiferal-nannofossil ooze).

Herein a coral reef is defined as the calcium carbonate sediment (rock, sands and muds) generated by coral and coralline algae calcification which remains as solid $CaCO_3$ and is not dissolved. Corals and coralline algae produce a calcium carbonate skeleton by calcification (Equation 4.1),

Equation 4.1 Calcification

$$\mathbf{Ca^{2+} + 2HCO_3^- = CaCO_3 + CO_2 + H_2O}$$

where $2HCO_3^-$ is bicarbonate, $CaCO_3$ is calcium carbonate, CO_2 is carbon dioxide. It can be seen from Equation 4.1 that CO_2 is released as a byproduct of calcification. The stoichiometry of Equation 4.1 holds true in freshwater such that one mole of CO_2 is released per mole of $CaCO_3$ deposited, however in the marine environment, only ~0.6 mol CO_2 is released to the atmosphere per mole of $CaCO_3$ deposited because of the buffering effect of seawater (Wolast *et al.*, 1980; Ware *et al.*, 1991). In the marine environment the remaining 0.4 mol of the CO_2 formed is recombined with carbonate

ions and water to form bicarbonate which remains in the water (hydrogen carbonate; Equation 4.2; Zeebe and Wolf-Gladrow, 2001),

Equation 4.2

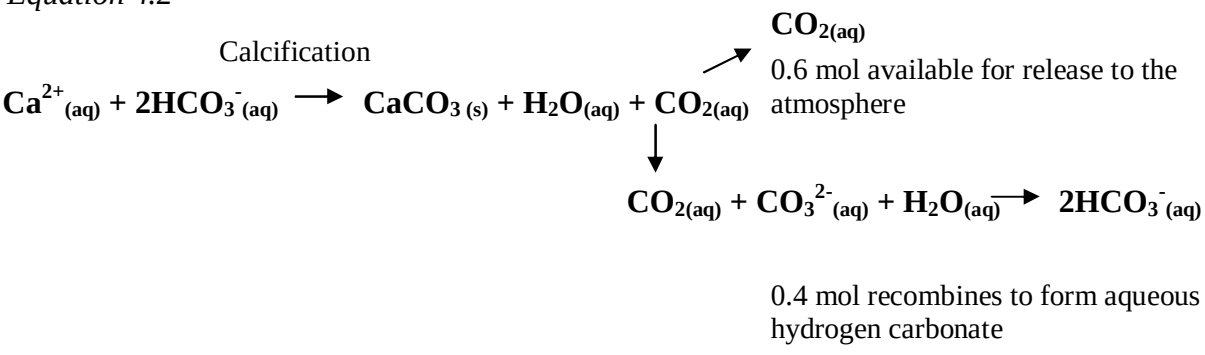

where $2HCO_3^-$ is bicarbonate, $CaCO_3$ is calcium, CO_2 is carbon dioxide and CO_3^{2-} is carbonate ion.

The fate of the remaining 0.6 mol of CO_2 is under debate; CO_2 has been measured passing across the air sea interface in the field on a few Pacific reefs (Gattuso *et al.*, 1993; 1999; Frankignoulle *et al.*, 1994). Determination of this flux for reefs worldwide and over a variety of time scales has yet to be adequately quantified, however the current consensus is that reefs are a source of CO_2 to the atmosphere (Barker *et al.*, 2003).

The present flux of coral reef CO_2 to the atmosphere is relatively small 0.02 – 0.08 Gt C as CO_2 yr^{-1} (Ware *et al.*, 1991), however reef growth and flux of CO_2 to the atmosphere may be important on geological time scales (Berger, 1982a; 2004b; Opdyke and Walker, 1992). The response of reef growth to sea level rise may have played an important role in the global carbon cycle on glacial interglacial timescales through the basin to shelf partitioning of the global $CaCO_3$ reservoir (Milliman, 1974; 1993; Berger, 1982a; 1982b; Keir and Berger, 1984; Opdyke and Walker, 1992; Opdyke, 2000). As sea level rose and flooded the continental shelves during deglaciation, large shallow areas became available for colonisation by coral reefs. Results from predictive global habitat model experiments suggest that the area potentially available for coral reef colonization expanded by about 400 % between the last glacial maximum (LGM) and today (Kleypas, 1997). In order to remain in the photic zone (to maintain the photosynthetic process of their algal symbionts at a maximum) reef corals respond to sea level rise by growing vertically upwards and ultimately producing the magnificent

structures easily visible in tropical regions today. The interglacial increase in reef carbonate sedimentation as a consequence of increased accommodation space created by sea level rise should therefore have released a substantial quantity of CO_2 to the atmosphere. This reef-released CO_2 should act as a positive feedback mechanism to amplify deglacial atmospheric CO_2 increase and induce further warming, ice melt and continued sea level rise. This is the basis of the Coral Reef Hypothesis (CRH, Berger, 1982a; Berger, 1982b; Keir and Berger, 1984; Opdyke and Walker, 1992). Quantifying the Holocene reef response to deglacial sea level rise is crucial if we are to a) fully understand the global carbon cycle and predict possible future CO_2 scenarios and b) predict possible future responses of reefs to anthropogenically induced sea level rise, temperature rise and oceanic saturation states.

Presently the mass of the shallow water carbonate reservoir is not well constrained (Opdyke, 2000) and the predictive IPCC (Houghton *et al.*, 2001) global carbon cycle models do not contain a coral reef component. Estimates of Holocene $CaCO_3$ accumulation have been obscured by inaccurate estimates of global reef area and dubious extrapolation of present day production values into the Holocene (Chave *et al.*, 1972; Milliman, 1974; 1993; Smith, 1978; Schlanger, 1981; Keir and Berger, 1984; Kinsey and Hopley, 1991; Opdyke and Walker, 1992; Iglesias-Rodriguez *et al.*, 2000). Calculation of the mass balance of global reef carbonate has been complicated by use of different datasets, different assumptions regarding manipulation of the data and inclusion of non-reef areas (Milliman, 1993). In light of improvements in our understanding of the stoichiometry of the calcification process and subsequent release of CO_2 to the atmosphere (Ware *et al.*, 1991; Gattuso *et al.*, 1993; 1999; Frankignoulle *et al.*, 1994; Barker *et al.*, 2003), an increase in the number of Holocene drill cores and quality of the reef area estimate (Spalding *et al.*, 2001) it now necessary to re-evaluate the contribution of reefs to Holocene atmospheric CO_2 concentration.

This chapter aims to i) investigate the evolution of the Rodrigues reef system; ii) quantify the mass balance of reefal carbonate in the Southwest Indian Ocean using accretion rates calculated from geological data; and iii) estimate the contribution of Southwest Indian Ocean reefs to the global mass balance of reef carbonate accumulated during the Holocene and possible subsequent release of CO_2 to the atmosphere, using geological data from reef sequences taken both from the published literature and the most comprehensive reef area estimate to date.

4.3 Regional Environment

4.3.1 The Southwest Indian Ocean.

Early studies of the reefal formations in the Indian Ocean include those of Darwin (1842), Sewell (1935) and Gardiner (1936). More recently geological investigations have focused on Mayotte (Figure 4.1; Guilcher *et al.*, 1965; Colonna *et al.*, 1996; Camoin *et al.*, 1997; Dullo *et al.*, 1998), Madagascar (Guilcher, 1956; 1958; Battistini, 1964; Camoin *et al.*, 2004), the Mascarene Islands (Pichon, 1967; Faure and Montaggioni, 1970; Montaggioni, 1970; Montaggioni, 1988; Montaggioni and Faure, 1997; Camoin *et al.*, 1997; Camoin *et al.*, 2004), the Seychelles (Braithwaite *et al.*, 2000; Camoin *et al.*, 2004), the Maldives (Stoddart, 1966; Davies *et al.*, 1971) and Aldabra Atoll (Stoddart and Yonge, 1971).

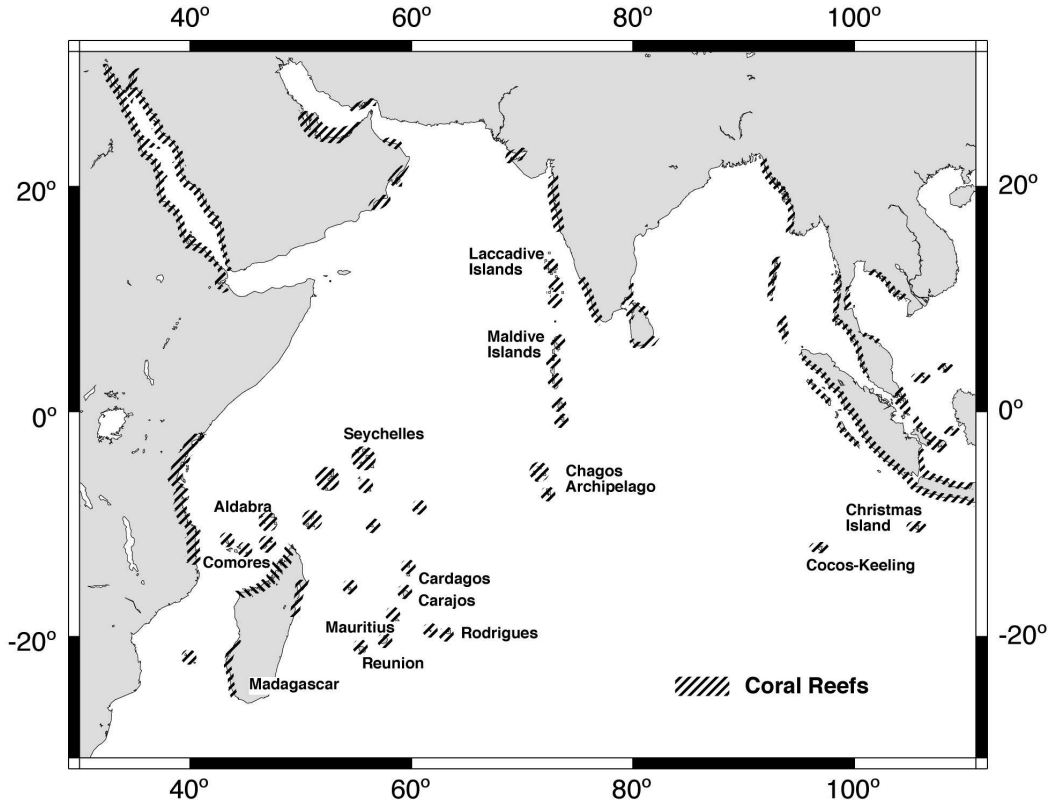

Figure 4.1 Locations of coral reefs in the Indian Ocean (modified after Stoddart (1973); drafted by Kate Davis).

The main sites of reef development in the Western Indian Ocean are the Chagos-Laccadive ridge, the Mascarene Plateau followed by the Chagos, Maldive and Laccadive archipelagos (Stoddart, 1973). Seismic profiling studies in the region have

revealed reef carbonate thicknesses of up to 1.7 km for the Chagos Bank, 1 km for Saya de Malha and under 1 km for Amirantes and the Seychelles (Francis and Shor, 1966; Davies and Francis, 1964; Shor and Pollard, 1963; Mathews and Davies, 1966), similar to some Pacific atolls (Stoddart, 1973). These thick limestone accumulations that form atolls and submerged bank chains cap older volcanic structures mainly in the north of the Western Indian Ocean (Sheppard, 2000). The barrier and fringing reefs further south surround younger volcanoes for example, Mauritius and Reunion, the bulk of reef carbonate accumulated in Pleistocene and Holocene times.

In detail, the pattern of Holocene reef growth in a given region is sensitive to a number of factors (e.g. substrate type, substrate morphology, turbidity, terrestrial run off and availability of larval recruitment centres). Ultimately, however, growth is controlled by the creation of accommodation space through the combined effects of hydroisostacy and eustasy on regional sea level rise. The islands of the Southwest Indian Ocean are considered reliable sites for reconstructing eustatic sea level change because of their relative tectonic stability during the Holocene and distance from former ice-sheets (negligible post-glacial hydrostatic rebound; Peltier, 1991; Lambeck, 1993; Camoin *et al.,* 1997; Camoin *et al.,* 2004). Sea level rise in the Southwest Indian Ocean during Holocene transgression has been investigated using reef drill cores at Reunion (La Saline), Mauritius (Pointe aux Sables), Mayotte (Pamandzi Islet), Madagascar (Grand Récif, Toliara) and the Seychelles (Anse aux Pins, Mahé) (Camoin *et al.* 1997; Camoin *et al.,* 2004) and a submersible to study the fore slopes of Mayotte (Colonna *et al.,* 1996; Dullo *et al.,* 1998). Sea level in the Western Indian Ocean was approximately 110-115 m below its present level between 18 – 17 kyr BP (Camoin *et al.,* 2004). The foreslopes of Mayotte record a rapid sea level rise corresponding to meltwater pulse MWP 1A at around 13.5 kyr BP similar to that identified by Fairbanks (1989) in Barbados and Bard *et al.* (1996) in Tahiti. However, Camoin *et al.* (2004) did not find sufficient evidence to support the occurrence of a second meltwater pulse, MWP 1B. Sea level curves constructed using drill core data from Mauritius, Reunion, Mayotte, Seychelles and Toliara indicates that, between 10 and 7.5 kyr BP, sea level was rising at approximately 6 mm yr^{-1}, after which the rate decreased to 1 – 1.5 mm yr^{-1} until it stabilised at its present level around 3 to 2.5 ka (Camoin *et al.,* 1997; Camoin *et al.,* 2004). Thus, the Holocene sea level curve constructed using drill cores from Mauritius, Reunion and Mayotte shows a continuous rise in sea level indicating that these small oceanic islands subsided with the ocean floor as it became depressed by the increased

volume of the water resulting from ice sheet melt (Nakada and Lambeck, 1991; Lambeck, 1993; Camoin *et al.*, 2004).

Elevated reefs have been described from the African East Coast, the Red Sea, Christmas Island, Madagascar, the granitic Seychelles and the southern Seychelles (Aldabra, Assumption, Astove, Cosmoledo, St Pierre), the Mascarenes, Mozambique Channel, Southern shores of the Persian Gulf, West India, Sri Lanka, Western Australia and Indonesia (Stoddart, 1973; 1984; Pirazzoli, 1991; Eisenhauer *et al.*, 1993; Camoin *et al.*, 2004). Camoin *et al.*, (1997) suggested that evidence for Holocene emergence was missing from most Southwest Indian Ocean islands, although evidence for Holocene sea level high stands has been found elsewhere in the Indian Ocean on Madagascar, Farquhar Atoll and the Cocos-Keeling Islands (Woodroffe *et al.*, 1990; Camoin *et al.*, 2004). Camoin *et al.* (2004) attributed this regional variability to differences in the response of the underlying substrate to the increase in water volume in the ocean basin. As such the smaller islands (for example, Reunion and Mauritius) subsided with the depression of the ocean basin as a result of the increase in water volume caused by the melting of polar ice, hence there is no evidence of higher sea levels on these islands. Whereas the larger micro-continents (for example, Madagascar) and the continental coasts (for example, Kenya and Mozambique) did not subside with the ocean basin and as such recorded the redistribution of the melt-water with a late Holocene high stand recorded by coral growth.

4.3.2 Rodrigues

Rodrigues is located at latitude 19°43’S and longitude 63°25’ E in the Southwest Indian Ocean and features the best developed reefs in the Mascarenes (Figure 4.2; Montaggioni and Faure, 1980). Early reports on the geology of Rodrigues gave brief descriptions of the basalts and the general morphology of limestone deposits (Higgin, 1849; Balfour, 1879; Snell and Tams, 1920; Lacroix, 1923). McDougall *et al.* (1965) were the first to examine in detail the volcanic nature of the island and the raised limestone deposits reported by Balfour (1879). The island (~18.3 km long and 6.5 km wide) is surrounded by an almost continuous reef rim approximately 90 km long and constitutes a reef area of approximately 200 km^2. The width of the reef flat ranges from 50 m in the north east to 2 km in the south west and encloses a shallow (0.5 m to 4 m at low water springs) lagoon, which measures from 50 m to 8 km wide (Figure 4.2).

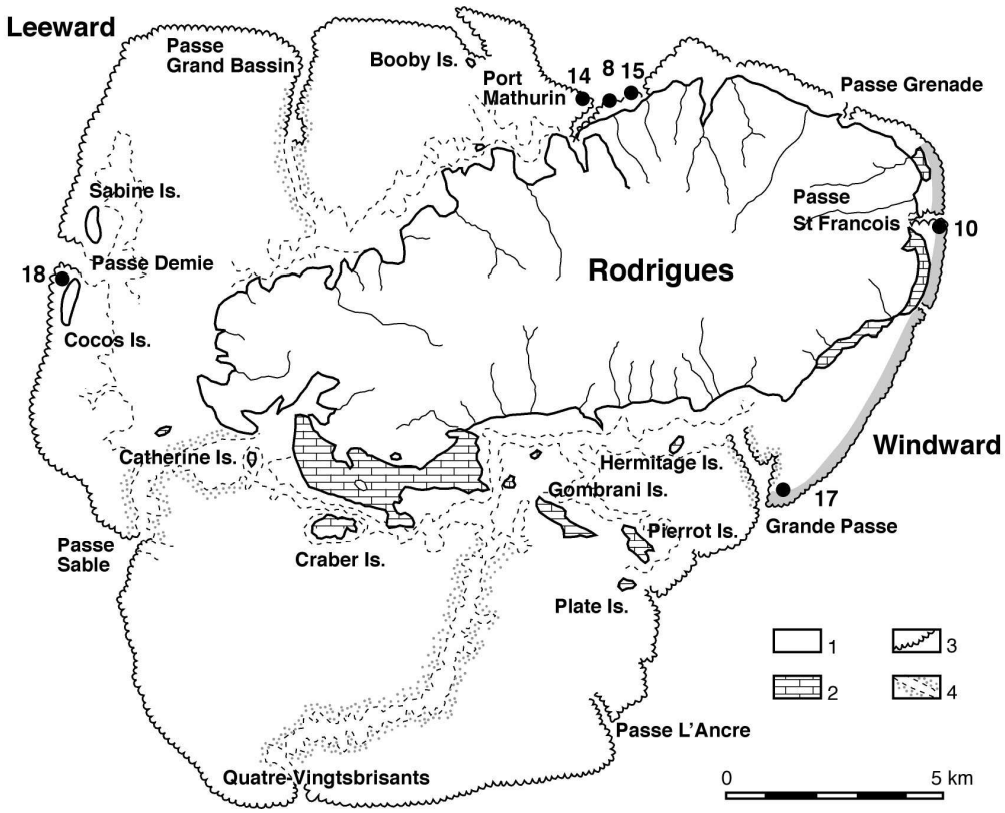

Figure 4.2 Map of Rodrigues showing locations of windward (10 and 17) and leeward (8,14,15 and 18) drill holes (black dots) and prominent algal ridge (grey shading). Key: 1-Basalt (most of the island), 2-aeolian dunes (mainly on Southern and Eastern coasts), 3- modern reef flat, 4-lagoon channels (modified after Faure (1974); drafted by Kate Davis).

The island rises from an elliptical submarine platform approximately 30 x 50 km across at the 100 m water depth contour (McDougall *et al.*, 1965; Upton *et al.*, 1967). The submarine platform is thought to have been formed by lava flows in the early Pliocene that gave rise to a complex shield volcano which was subsequently truncated by marine erosion to give the form of a guyot (McDougall *et al.*, 1965; Upton *et al.*, 1967; Montaggioni, 1974). It has been suggested that this truncated platform could have been covered by an extensive coral bank (Gardiner, 1936; Upton *et al.*, 1967). Rejuvenation of basaltic lava flows built a small volcano to the east of the centre of the submarine plateau between 1.5 – 1.3 Ma (McDougall *et al.*, 1965). The island presently reaches a maximum height of 396 m at Mt Limon. The origin of the Rodrigues ridge upon which Rodrigues Island is located is still debated (Mckenzie and Sclater, 1971; Morgan, 1978; Bonneville *et al.*, 1988), however it is agreed that Rodrigues does not have a common origin with the other Mascarene Islands because it does not lie on the track of the hotspot that created Mauritius and Reunion.

Faure (1974) suggested that the channels which form discontinuities in the reef rim (for example, Port Mauthurian Channel and Port Sud Est) can be separated into three morphologically distinct types; passes; outfalls and outer creeks; and reef channels, inner creeks and reef pools. These discontinuities formed by the erosion of river valleys during the Pleistocene regressions gave rise to topographic highs and lows, which subsequently became accentuated by Holocene reef growth. Faure (1974) also noted the abundance of alcyonarians on the reef flats and outer slopes of the reef and a reduction in erect branching corals within the reef channels and concluded that these result from high turbidity and increased hydrodynamic energy respectively. Montaggioni (1974) reported spur and groove morphology (25 to 30 metres below sea level) on the outer slopes of high-energy windward coasts but noted its absence on leeward sheltered coasts. Naim *et al.* (2000) describes depressions of between 15-45 m diameter with depths of 6-10 m within the wide southern reef flat. The reef flat is compact at the outer edge and is comprised of mainly algal-coral flagstone and the outer slope forms a steep wall down to approximately 10-25 m depth where it meets a skeletal sandy floor around most of the island (Faure, 1974; Montaggioni, 1974).

Within Rodrigues lagoon there are several small islands to the south and west of the main island (Hermitage, Crab and Booby) which, like the main island, are of volcanic origin. The action of the south east trade winds, currents and swell has led to the formation of several sand cays and banks (Cocoa, Sandy, Combrani and Pierrot) within the lagoon which only rise slightly above the lagoon surface (Upton *et al.*, 1967). There is no evidence of raised reef deposits on Rodrigues and, like other islands in the Southwest Indian Ocean, a pattern of general and unceasing subsidence during the Holocene is assumed (McDougall *et al.*, 1965; Upton *et al.*, 1967; Montaggioni, 1974). Early reports suggested the presence of coralline limestone up to 150 m above present sea level on Rodrigues (Snell and Tams, 1920; Balfour, 1879). However, other investigations have revealed this to be a cross bedded limestone consisting of well rounded bioclasts such as foraminifera, gastropod and echinoderm fragments of probable Pleistocene age (McDougall *et al.*, 1965). This aeolian deposit is formed on the basalt basement along the south and east coasts of the island (Figure 4.1 and Plate 4.2) and is as much as 20 m thick in places. It was probably formed during the Pleistocene regressions (between 80-40 ka and 30-20 ka) by the South-East trade winds blowing carbonate sand generated by erosion of Pliestocene reef from the lagoon onto the island (Montaggioni, 1974). Gardiner (1936) suggested that even today Holocene

lagoon sediments are being transported in this way during spring low tides. The aeolian limestone was only observed to occur up to 62 m above sea level by McDougall *et al.*, (1965) and has undergone considerable erosion inland culminating in a series of caves and shallow holes. Today the aeolian limestone provides building material for the island population.

Plate 4.2 Photograph of the Aeolian dunes at Rodrigues which the locals use as building material.

The South-East trade winds usually occur between June and October with speeds of 7-10 km hr^{-1}, producing swells of up to 2 m amplitude (Naim *et al.*, 2000). During the rest of the year winds are generally lighter and produce swells less than 0.5 m amplitude. Rodrigues lies within the tropical cyclone belt and is occasionally subject to cyclones from the NNE with winds of 180-250 km hr^{-1} generating swells of up to 6 m height. Islands in the Southwest Indian Ocean are also subject to long wavelength austral swells from the south (Stoddart, 1973; Naim *et al.*, 2000). Tides are semidiurnal; the spring tide range being approximately 1.2 m (Farrow and Brander, 1971).

4.4 Materials and Methods

In 2001 a field expedition to Rodrigues as part of the *Shoals of Capricorn* programme recovered five drill cores using a portable hydraulic drilling rig with 7 cm diametre tungsten and diamond tip drilling heads (Figure 4.2). The portable drilling system was designed to take cores right on the margin of the reef front, in areas that are accessible only at low tide. The drilling gear and engines were towed out to the drill sites on the falling tides and drilling only took place during low tides. In fact, at windward locations drilling was only possible during spring low tides. In the north east (core 10) the coring was initiated within 3 m of the deep drop into St Francois passage, in what is now a head coral facies, within the typical surf zone. Core 15 in the north was also taken within metres of the drop off into the passage in the same facies. In the south

east, core 17 was taken on the windward side of the broad algal ridge, within the surf zone, about 15 metres from the reef front. In all, two cores were recovered from the windward margin (cores 10 and 17), with a maximum depth of penetration of 4 m. Four cores were recovered from the leeward margin (8, 14, 15, 18) where the maximum depth penetration attained was 4.2 m. Recovery ranged from 23 to 63 %. The drill cores were photographed and logged. Thin sections were made and examined petrographically. Radiocarbon dating was performed on selected corals from the base of each core interpreted to have grown *in situ* and to be free from intraskeletal contamination. Accelerator Mass Spectrometry (AMS) was undertaken at the department of Nuclear Physics, the Australian National University. The dates were corrected for isotopic fractionation, the marine reservoir effect (Indian Ocean $\Delta R = 153 \pm 24$) and converted to calendar years using the CALIB 4.4 programme (Stuiver and Reimer, 1993). Errors are reported to 1σ.

4.5 Results

The radiometric dating results suggest that Rodrigues reefs approached sea level between 3.1 ± 0.3 cal kyr BP and 1.3 ± 0.2 cal kyr BP (Table 4.1). In fact, the windward margin apparently grew to within 2.5 m of present day sea level by approximately 2.7 ± 0.2 cal kyr BP (core 17). The leeward margin approached modern day sea level more recently between 1.3 ± 0.2 cal kyr BP (core 18, 2.2 m depth) and 2.4 ± 0.3 cal kyr BP (core 14, 1.1 m depth). Rates of vertical accretion for the top 4 m of the cores range from 0.46 – 1.96 m ky $^{-1}$ (Table 4.1).

Table 4.1 AMS Radiocarbon dating results and accretion rates. Ages corrected for isotopic fractionation and the marine reservoir effect ($\Delta R = 135 \pm 24$) using the CALIB 4.4 Software programme (Stuvier and Reimer, 1993). Accretion rates were calculated assuming a zero age at the top of the core. DBS, depth below surface; CA, conventional radiocarbon age; ECA, environmentally corrected ages; AAR, average accretion rate.

Lab code	Core no.	Margin	DBS (m)	CRA (kyr BP)	ECA (cal kyr BP)	AAR (m kyr^{-1})
ANUA2225	8	Leeward	1.4	2.565±0.184	2.062±0.228	0.68
ANUA2226	10	Windward	3.7	3.371±0.182	3.052±0.258	1.2
ANUA2227	14	Leeward	1.1	2.856±0.182	2.366±0.260	0.46
ANUA2228	15	Leeward	4.2	2.642±0.184	2.147±0.210	1.96
ANUA2229	17	Windward	2.5	3.056±0.182	2.714±0.218	0.92
ANUA22210	18	Leeward	2.2	1.758±0.179	1.332±0.182	1.7

The cored reef sequence ranges from 2 to 4.2 m thick and did not penetrate the Holocene-Pleistocene unconformity (Figure 4.3).

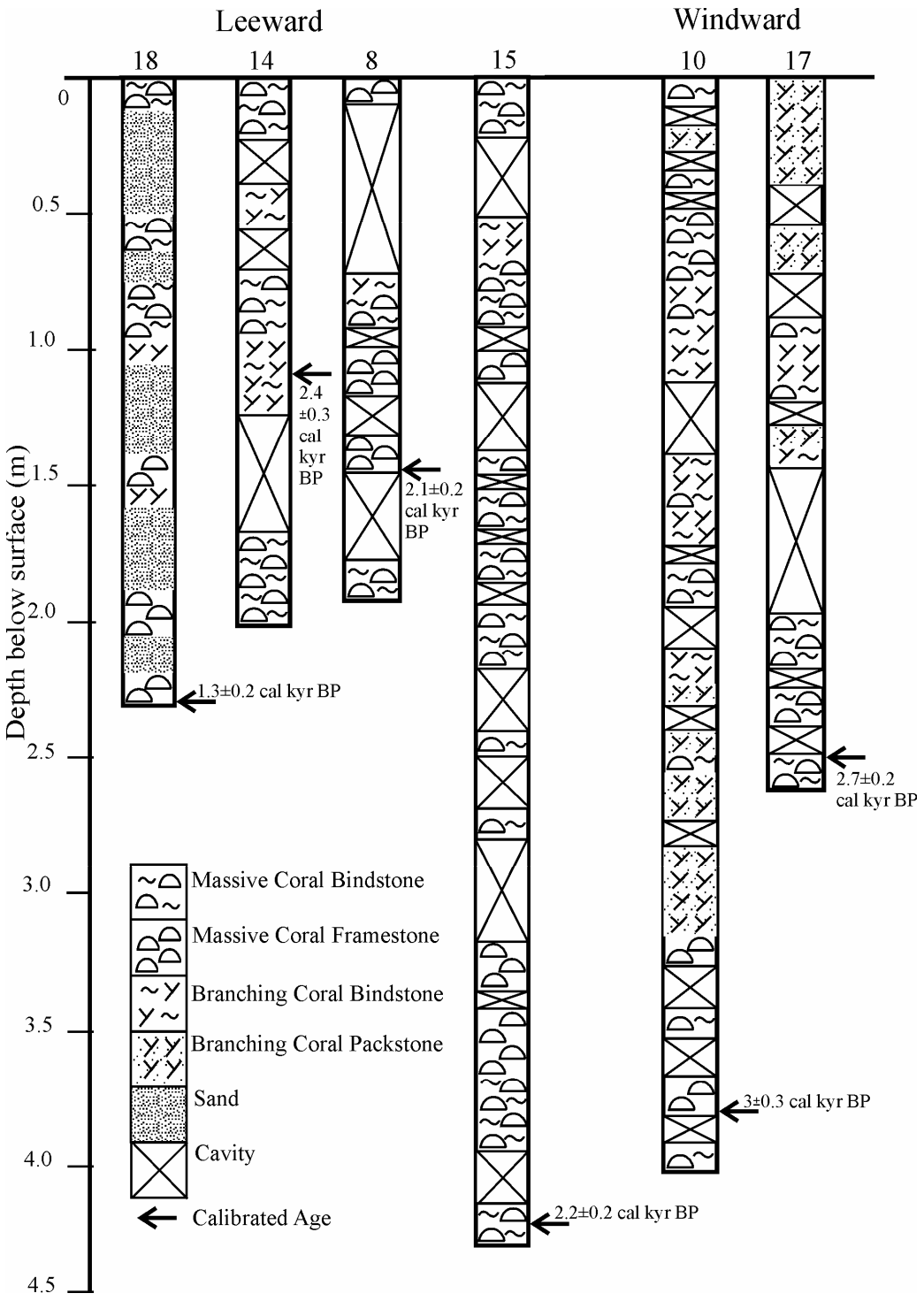

Figure 4.3. Core logs for Rodrigues windward (10 and 17) and leeward (8, 14, 15 and 18) drill holes.

The cores from Rodrigues reveal four facies types; a coral-algal bind-stone of branching coral rubble and *in situ* massive corals heavily encrusted and bound together by coralline algae; a frame-stone of larger *in situ* massive coral heads with occasional

red algal crusts, and a pack-stone facies comprising reworked branching coral rubble encrusted with coralline algae and packed together in a solid mass of poorly lithified (grey brown) sediments and a rubble facies of loose reworked branching coral rubble. The bind-stone and frame-stone facies are found in all of the cores whereas the pack-stone facies is only present in those taken from the windward margin. The cores from windward margins are dominated by branching coral whereas those from leeward margins contain significantly more coral heads. The windward cores are composed of coral-algal bind-stone and branching coral pack-stone facies with small volumes of branching coral rubble, the cores are virtually sand free. Significant percentages of coralline algae were found in core 17 at 2.7 m depth and core 10 at 3.2 m depth. The leeward margin cores (8, 14, and 15) were composed of mainly coral-algal bind-stone, massive coral frame-stone and small volumes of branching rubble and sand. Core 18, considered the true leeward core contained frame-stone and bind-stone facies but was dominated by sand.

4.6 Discussion

The radiometric dating results indicate that the Rodrigues windward margin approached within two metres of present day sea level approximately 3 cal kyr BP whereas growth along the leeward margin lagged by about 1.5 cal kyr, only reaching modern day sea level approximately 1.3 cal kyr BP. These dates are consistent with the growth stabilisation event recorded on other Southwest Indian Ocean reefs of around 3 ka (Camoin *et al.*, 1997; Braithwaite *et al.*, 2000; Camoin *et al.*, 2004) and the sea level curves constructed for the region by Camoin *et al.* (1997), Colonna *et al.* (1996) and Camoin *et al.* (2004). Furthermore, it appears that the approach to modern day sea level of reefs in the Southwest Indian Ocean lagged behind those of the Pacific Atolls and the Great Barrier Reef, which typically reach sea level between 6 and 4 kyr BP. This lag may be a reflection of sea level behaviour in the different ocean basins. Sea level rise is believed to have stabilised around 5.5 to 5 kyr BP in the Pacific and 6 kyr BP in the Great Barrier Reef (Hopley, 1982) whereas in the Southwest Indian Ocean sea level stabilised only relatively recently (~3-2.5 kyr BP, Camoin *et al.*, 2004). The observation that the windward margin approached present day sea level before the leeward at Rodrigues is consistent with global observations of reef development (Davies *et al.*, 1985) and is believed to be associated with higher wave energy on the windward margin. The abundance of fast-growing *Acropora* corals out-competing the slower

growing massive corals in this region also contributes to faster accumulation rates on windward margins. Since reaching present sea level the Rodrigues reef margins have probably prograded laterally particularly on the leeward margin and much of calcium carbonate produced by the reef today is transported to the shallow lagoon, which is now nearly full of sediment (it is possible to wade considerable distances at low tide).

Rates of vertical reef growth within the top 4 m of the Rodrigues cores range from 0.46 to 1.96 m kyr $^{-1}$ (Table 4.1). These slow rates of accretion are similar to those observed from drill cores from other Southwest Indian Ocean reefs of 0.4 to 1.1 m kyr $^{-1}$ (Montaggioni, 1988; Montaggioni and Faure, 1997; Camoin *et al.,* 1997; Braithwaite *et al.,* 2000). These slow rates are probably related to the reef margins being exposed to increasing hydrodynamic energy conditions as they approached modern day sea level, which led to an increasing abundance of wave-resistant but slow growing coralline algae (Davies and Hopley, 1983; Adey, 1986).

The facies distribution observed in the Rodrigues drill cores is related to high hydrodynamic energy as reefs approached modern-day sea level (Figure 4.3) within the last 3 kyr BP, the climax or growth stabilisation stage. The windward cores (10 and 17) contain predominantly branching coral bound by thick layers of coralline algae and poorly lithified sediments (coral-algal bind-stone and pack-stone). The predominance of slow growing coral-algal bind-stone facies of low porosity within the top 4 m of cores 10 and 17 suggests a high-energy environment. The facies distribution for the top 4 m of Rodrigues cores is similar to that reported from Mauritius, Mayotte, Reunion and the Seychelles although the degree of encrustation by coralline algae is much higher in the windward Rodrigues cores (Montaggioni and Faure, 1997; Camoin *et al.,* 1997; Braithwaite *et al.,* 2000). Camoin *et al.,* (1997) commented that the facies distribution in the Southwest Indian Ocean reefs contrasts with that of Caribbean and Pacific reefs in that the branching coral facies predominates over the coral head facies throughout the Holocene. Caribbean and Pacific reefs commonly exhibit a succession from branching to massive coral head facies in the upper section of reefs in response to higher energy conditions near the surface (Davies and Hopley, 1983; Cortes *et al.,* 1994; Caboich *et al.,* 1995). All cores from Rodrigues contain massive coral heads in the upper 4 m, suggesting a similar facies succession to that found in the Indo-Pacific and Caribbean. The lack of coral head facies and coralline algae in the cores from the Mauritius, Reunion and Mayotte may reflect the fact that these cores were drilled in moderately exposed sites and up to 250 m behind the reef front whereas the Rodrigues windward

cores were taken from an extremely exposed coast close to the reef edge (Camoin *et al.,* 2004).

Some authors have suggested that algal ridges are absent from Southwest Indian Ocean reefs, possibly related to lower energy conditions during the Holocene (Camoin *et al.,* 1997) or because seasonal shifts in the wind direction prevent these reefs from receiving the constant surf necessary to construct these high-energy features (Stoddart, 1973; Milliman, 1974; Camoin *et al.,* 1997; Naim *et al.,* 2000). However, a relatively large algal ridge is prominent on Rodrigues on the windward margin between St Francois Channel and Grande Passe which is one of the most spectacularly well developed algal ridges in the world. This ridge is most pronounced where the reef is the narrowest, in the central section of the eastern coast. The algal ridge then becomes broader and less pronounced in the south east, where the reef trend leaves the coast of the island and moves south towards Grande Passe passage; core 17 was drilled within this facies (Figure 4.2). The morphology of the algal ridge at Rodrigues is intriguing because it appears as a very smooth ridge running parallel to the shore and reef front, with an elevation of approximately 1 m above the present reef flat. It is located approximately 7 m behind the present reef slope drop off which may be a consequence of the reef growing laterally seaward since reaching sea level. The reef probably grew up to present sea level and the locus of maximum wave energy force created the present algal ridge. Algal ridge structures have also been reported from the St Brandon Shoals, Mahé in the granitic Seychelles and Chagos seaward reef flats (Sheppard, 2000; Jennings *et al.,* 2000; Stoddart, 1973; Rajkumar and Parulekar, 2001). The presence or absence of algal ridges in the Western Indian Ocean is probably related to variations with respect to the consistency of the south east trade winds within the region. The reefs of Rodrigues, St Brandon Shoals and the Seychelles are under the influence of the south east trade winds for on average 3 to 4 months a year whereas reefs further west (Mauritius and Reunion) are only influenced by the south east trade winds for less than one month a year (Stoddart, 1973).

The presence of large aeolian dunes on the southern and eastern coasts of the island suggests relatively arid conditions prevailed as sea level fell and lagoonal sands were exposed and mobilised. The width of the reef flat at Rodrigues ranges from less than 50 m in the east to 2 km in the south, compared to reef flat widths of Mauritius and Reunion of 25 m and 150 m respectively (Camoin *et al.,* 1997; Montaggioni, 1988). Rodrigues has similar reef flat width to that of Mayotte where Pleistocene reef deposits

have been recovered at 21.5 m below surface (Guilcher *et al.,* 1965; Camoin *et al.,* 1997). Indeed both Balfour (1879) and Davis (1928) commented that the present reef flat is too large to have been formed during the Holocene alone and suggest that present reef may cap a succession of reef generations. The drill cores at Rodrigues did not penetrate any Pleistocene deposits but we assume that the Holocene-Pleistocene unconformity occurs around 20 m depth on the basis of what is known from Mayotte, Mauritius and Reunion (Montaggioni, 1988; Camoin *et al.,* 1997; Montaggioni and Faure, 1997). The regional sea level curve indicates that sea level was approximately 22 ± 3 m below present sea level at 9.1 kyr BP (Camoin *et al.,* 2004) and drill core data indicate that the initiation of reef growth at Mauritius and Reunion on the volcanic basement was slow. However reef initiation at Mayotte began suddenly and quickly on the karstified Pleistocene surface. This difference in initiation style and rate is possibly due to substrate type. Corals readily colonise karst surfaces and as such it might be expected that the initiation of the Holocene reef at Rodrigues would show the same pattern as that for Mayotte. If we assume Rodrigues windward reef growth was initiated at approximately 9.5 kyr BP and accreted 20 m of carbonate sediment by 3 ± 0.3 kyr BP (3.7 m depth), the reef would have accreted at an average rate of 2.2 m kyr $^{-1}$. This value is broadly consistent with average Holocene rates of reef accretion for Reunion (1.75 m kyr $^{-1}$), Mauritius and Mayotte (2 m kyr $^{-1}$) (Camoin *et al.,* 1997) and the Seychelles (0.97-1.6 m kyr $^{-1}$; Braithwaite *et al.,* 2000). This rate was probably achieved by fast-growing *Acropora* corals, which were replaced by an algal dominated facies (with vertical accretion rates of less than 2 m kyr $^{-1}$) as the reef approached modern sea level.

There is no evidence of raised beach deposits, emerged coral or elevated intertidal notches in the aeolianites at Rodrigues, implying that the island was not subject to higher sea level stands during the Holocene. The lack of elevated Holocene reef deposits on mid-oceanic islands in the Southwest Indian Ocean suggests that they were not influenced by hydroisostatic effects to the same extent as the continental margins (e.g. Africa) and microcontinents (Madagascar) during the most recent transgression (Camoin *et al.,* 1997). The submarine plateau at Rodrigues is approximately 30 km wide and 55 km long at the 100 m contour (McDougall *et al.,* 1965) and as such it is possible that coral veneers could have colonised the slopes of the platform around 18.4 kyr BP and possibly formed significant accumulations between 18.2 – 16.5 kyr BP. This large platform is undoubtly the site of accumulation of large volumes of carbonate sediment

(in the form of a leeward accretionary wedge) shed by reefs presently at sea level (Davies, 1983).

4.7 Quantification of SW Indian Ocean Reef $CaCO_3$ Sediment

Many of the published marine $CaCO_3$ budgets use coral reef production values (estimated by alkalinity method) to calculate coral reef $CaCO_3$ accumulation and subsequent CO_2 release (Chave *et al.*, 1972; Milliman, 1974; 1993; Smith, 1978; Kinsey and Hopley, 1991; Iglesias-Rodriguez *et al.*, 2000). However converting present day production values into accretion rates and using them to represent reef accretion in the late to mid-Holocene is subject to large errors. Extrapolating present day values of coral reef production to calculate a marine $CaCO_3$ budget over a full glacial-interglacial cycle is subject to gross inaccuracies because the loci and rates of neritic $CaCO_3$ sedimentation has varied greatly during the recent deglaciation (Kinsey, 1981; Davies *et al.*, 1985; MacIntyre, 1988; Montaggioni, 2000). Other $CaCO_3$ budgets include non-reef and low productivity (lagoon) areas e.g. ooid shoals and carbonate dominated embayments, which have obscured the coral reef contribution (Milliman, 1974; 1993; Smith, 1978; Opdyke and Walker, 1992). A more accurate way to estimate global coral reef $CaCO_3$ accumulation is to measure changes in well-dated coral reef sequences (Schlanger, 1981; Opdyke and Walker, 1992). Accumulation rates are a conservative estimate of past coral reef accumulation and CO_2 liberation because they only represent retained $CaCO_3$ (Kleypas, 1997) whereas use of production values fails to account for less productive areas and potential erosive loss (Smith and Kinsey, 1976; Smith, 1978; Hubbard *et al.*, 1990; Milliman, 1993).

Using a collection of reef cores from the published literature, and the new data from Rodrigues reported herein, it is possible to estimate the average accretion rate and average duration of accretion for Southwest Indian Ocean reefs. We calculate that Southwest Indian Ocean reefs were accreting at an average rate of 2.88 m kyr^{-1} for an average duration of 5032 years. This rate calculated for the Southwest Indian Ocean is higher than the average rate of sedimentation for reefs, ooid shoals and carbonate embayments estimated by Opdyke and Walker (1992) of 1.6 m kyr^{-1} normalised to 5 kyr.

Reefs in the Indian Ocean cover an area of approximately 32,000 km^2 of which mid oceanic fringing reefs and atolls in the Western Indian Ocean account for approximately 18,530 km^2 (Spalding *et al.*, 2001). Unfortunately, we could not find any

data pertaining to the Holocene growth history of reefs on the African continent, Red Sea and Arabian Seas. This may be due to their poor development or inaccessibility (Stoddart, 1973).

The rate of sea level change during the last deglaciation has varied across the globe because of geoid and tectonic deformations (Lambeck and Chappell, 2001). It would be inaccurate to assume all the reefs in the Southwest Indian Ocean responded to Holocene sea level rise in the same way, therefore we only calculated the mass of $CaCO_3$ using a reef area estimate associated with oceanic island reefs where accretion rate data was available. This should give a good indication of the mass of Holocene $CaCO_3$ accumulated by reefs within the Western Indian Ocean because the oceanic island and atoll chains (the Mascarenes, the Chagos, the Maldives and Laccadives) are the main sites of extensive reef development in the Western Indian Ocean (Stoddart, 1973).

The average Holocene accretion rate for Western Indian ocean reefs was combined with the most up to date and comprehensive reef area estimate for oceanic islands in this region of 18,530 km^2 (Spalding *et al.,* 2001) to calculate a mass of $CaCO_3$ accumulated within the Western Indian Ocean during the Holocene (Equation 4.3).

Equation 4.3 **M = CAD * AAR * RA * D * APRS**

M is $CaCO_3$ mass balance, CAD is corrected average duration, AAR is average accretion rate (m ky^{-1}), RA is reef area (km^2), D is density of $CaCO_3$ (g cm^3), APRS is average porosity reef sediments. The average density of reef rock $CaCO_3$ is 2.9 g cm^3, with an average porosity for reefal sediments of 50 % (Hopley, 1982).

In order to put the average accretion rate into a Holocene perspective, it is necessary to apply a correction factor to account for the fact that although reefs in the Western Indian Ocean were actually growing from approximately 9 ka to 0 ka (Camoin *et al.,* 1997; Montaggioni and Faure, 1997; Braithwaite *et al.,* 2000), there was a peak in reef growth when the majority of reef $CaCO_3$ was laid down. The calculated duration of accretion at any one point on the platform is only 5 kyr. This requires a rate calculated over a smaller duration (corrected average duration) e.g. 5000/9000 = 0.6, this indicates that any given platform surface was accumulating at the average accretion rate calculated from the dataset for approximately 60 % of the time. For the other 40 % of the time of actual growth between 9 ka and 0 ka the reefs were probably growing at a

much slower rate during the initiation and catch up to sea level stages of reef development. The mass of $CaCO_3$ accumulated by ocean islands in the Western Indian Ocean is estimated to be approximately 217 Gt $CaCO_3$ over 5,032 years during the Holocene, corresponding to a flux of $CaCO_3$ into reef sediments of 4.3 x 10^{11} mol yr^{-1}. This flux is small in comparison to the global carbonate fluxes estimated by previous authors using a variety of methods and including non-reef environments (Table 4.2).

Table 4.2. Previous global flux estimates of $CaCO_3$ into reefs by various authors.

Author	Year	Global flux of $CaCO_3$ into reefs (10^{13} mol yr^{-1})
This study (Western Indian Ocean only)		**0.043**
Opdyke	2000	1.7
Milliman	1993	0.5
Opdyke and Walker	1992	1.4-1.9
Kinsey and Hopley	1991	1.1
Schlanger	1981	0.8
Smith	1978	0.6
Hay and Southam	1977	1.3

Assuming that 0.6 mol CO_2 is released per mole of $CaCO_3$ laid down in the marine environment (Wolast *et al.*, 1980; Ware *et al.*, 1991) it is estimated that approximately 2.6 x 10^{11} mol yr^{-1} CO_2 was released by Western Indian Ocean reef calcification over 5,032 years. At present, quantification of the proportion of this CO_2 that passed across the air sea interface in the tropical shallow marine environment to result in an increase in Holocene atmospheric CO_2 concentration has yet to be measured (Gattuso *et al.*, 1993; 1999; Frankignoulle *et al.*, 1994; Barker *et al.*, 2003). If we assume that all 0.6 mol of CO_2 available for release were transferred to the atmosphere, Western Indian Ocean reefs could have contributed at least 57 Gt CO_2 (0.003 Gt C as CO_2 per year) to the atmosphere during the peak in their growth (9-4 kyr). It is important to note that this value is conservative. Firstly, it does not include drowned reefs and those reefs which are yet to reach sea level. Submerged limestone banks in the Western Indian Ocean cover an area of approximately 140, 000 km^2 (Stoddart, 1973). These drowned banks and atolls presently lie at water depths of between 8-20 m, and hence could have been sites of significant reef growth during the early Holocene in keeping with ReefHab model results which predict that global reef area during deglaciation would have been much more extensive than previously thought (Kleypas,

1997). The discovery of reefs older than 10 kyr (submerged, drowned and uplifted) adds to a growing body of evidence to say that coral reefs may have played a significant role in contributing to atmospheric CO_2 prior to 10 ka. Firstly corals may be more thermo-tolerant than previously thought and thus could have flourished during the deglaciation before being outpaced by rapid melt-water pulses of sea level rise which occurred at approximately 11 ka and 14 ka (Montaggioni, 2000). Secondly, the estimate does not include contributions from reefs fringing the African continent and the Red and Arabian Seas. Thirdly, early and late Holocene reef accretion is omitted because the estimates only include contributions over the 5 kyr period of peak accretion. For example, present day reef flats produce on average 4 kg $CaCO_3$ m^2 yr^{-1} (Smith and Kinsey, 1976) of which only 25 % is transported offshore, the rest accumulates as sediments within lagoon systems (Hubbard *et al.*, 1990). Previous mass balance calculations have not included data from the Western Indian Ocean although it covers approximately 11 % of the global reef area today (Milliman, 1974; 1993; Kayanne, 1992). It has recently been suggested that lagoonal and leeward accretionary wedge accumulations of carbonate sediment reflect higher $CaCO_3$ production during the Holocene than that presently estimated by extrapolating present day production values into the past (Ryan *et al.*, 2001). Using accumulation rates from reef drill cores is conservative because they record only sediments retained by reef framework. However, the large accumulations of sediments in lagoons and leeward accretionary wedges suggest that $CaCO_3$ production must have been much higher than that seen today and that recorded by drill cores. These accumulations may effectively have doubled the reef area for accretion in the early Holocene (Ryan *et al.*, 2001). Nevertheless, it is important to emphasize that even the geologically significant CO_2 release estimates associated with even these extended areas are dwarfed by the rates of current anthropogenic release of CO_2 of 6.3 ± 0.4 Gt C as CO_2 yr^{-1} (Houghton *et al.*, 2001; Western Indian Ocean Reefs released approximately 0.003 Gt C as CO_2 yr^{-1}).

4.8 Conclusions

The Rodrigues windward margin approached present day sea level at approximately 3 kyr BP, with the leeward margin reaching sea level at about 1.5 kyr BP. The facies and rates of accretion for the top 4 m of Rodrigues reef are consistent with a high-energy environment dominated by slow growing coralline algae. There is a prominent algal ridge feature on the windward reef flat indicating persistent high-energy

conditions probably related to the south east trade winds. The large aeolian dune deposits on the Southern and Eastern coasts of Rodrigues indicate that the modern day Holocene reef probably caps an older Pleistocene reef. Holocene accretion rates from drill cores in the Western Indian ocean together with a reef area estimate of 18,530 km^2 (Spalding *et al.*, 2001) indicate that oceanic islands in the region have accumulated at least 217 Gt $CaCO_3$ during the Holocene. From first approximations, this may represent approximately 10 % of the global total for this period and suggests that Western Indian oceanic island reefs could have released approximately 57 Gt CO_2 to the Holocene atmosphere. These estimates are calculated from relatively few published drill cores from the region and it is clear that there is a large gap in knowledge relating to the evolution of Holocene reefs in the Indian Ocean. A greater understanding of reef growth and area in this region is required before a truly accurate picture of $CaCO_3$ accumulation in the region can be established.

4.9 References

Adey, W. H. (1986) Coralline algae as indicators of sea level. In O.V.D. Plassche (ed), *Sea Level Research A Manual for the collection and evaluation of data*. Galliard LTD., UK.

Balfour, I. B. (1879) An account of the petrological, botanical and zoological collections made in Rodriguez during the transit of Venus expeditions of 1874-75. *Roy. Soc. Philos. Trans. London.*, **168**, 289-301.

Bard, E., Hamelin, B., Arnold, M., Montaggioni, L., Caboich, G., Faure, G. and F. Rougerie (1996) Deglacial sea-level record from Tahiti corals and the timing of global meltwater discharge. *Nature*, **382,** 241-244.

Barker, S., Higgins, J. A. and H. Elderfield (2003) The future of the carbon cycle: review, calcification response, ballast and feedback on atmospheric CO_2. *Phil. Trans. R. Soc. Lond. A,* **361**, 1977-1999.

Battistini, R. (1964) Etude geomorphologique de l'extreme-sud de Madagascar. *Editions Cujas*, Paris.

Bellwood, D. R. and T. P. Hughes (2001) Regional Scale Assembly Rules and Biodiversity of Coral Reefs. *Science*, **292**, 1532-1535.

Berger, W. H. (1982a) Increase of CO_2 in the atmosphere during deglaciation the coral reef hypothesis. *Naturwissenschaften*, **69**, 87-88.

Berger, W. H. (1982b) Deglacial CO_2 build-up: constraints on the coral reef model. *Pal. Pal. Pal.,* **40,** 235-253.

Bonneville, A., Barriot, J. P. and R. Bayer (1988) Evidence from geoid data of a Hot Spot origin for the southern Mascarene Plateau and Mascarene islands (Indian Ocean). *J. Geophys. Res.*, **93,** B5, 1499-4212.

Braithwaite, C. J. R., Montaggioni, L. F., Camoin, G. F., Dalmasso, H., Dullo, W. C. and A. Mangini (2000) Origins and development of Holocene coral reefs: a revisited model based on reef boreholes in the Seychelles, Indian Ocean. *Int. J. Earth. Sci.,* **89**, 431-445.

Caboich, G. F., Montaggioni, L. F. and G. Faure (1995) Holocene initiation and development of New Caledonian fringing reefs, S.W. Pacific. *Coral Reefs,* **14,** 131-140.

Camoin, G. F., Colonna, M., Montaggioni, L. F., Casanova, J., Faure, G. and B. A. Thomassin (1997) Holocene sea level changes and reef development in the south-western Indian Ocean. *Coral Reefs,* **16**, 247-259.

Camoin, G. F., Montaggioni, L. F. and C. J. R. Braithwaite (2004) Late glacial to post glacial sea levels in the Western Indian Ocean. *Mar. Geol.*, **206**, 119-146.

Chave, K. E., Smith, S. V. and K. J. Roy (1972) Carbonate production by coral reefs. *Mar. Geol.*, **12**, 123 – 140

Cole, J. (2003) Global Change: Dishing the dirt on coral reefs. *Nature,* **421**, 705-706.

Colonna, M., Casanova, J., Dullo, W. C. and G. Camoin (1996) Sea level changes and delta ^{18}O record for the past 34,000 years from Mayotte Reef, Indian Ocean. *Quat. Res.*, **46,** 335-339.

Cortes, J., MacIntyre, I. G. and P. W. Glynn (1994) Holocene growth history of an Eastern Pacific fringing reef, Punta Islotes, Costa Rica. *Coral Reefs,* **13**, 65-73.

Darwin, C. (1842) *The structure and distribution of coral reefs*. London: Smith, Elder and Company.

Davies, D. and T. J. G. Francis (1964) The crustal structure of the Seychelles Bank. *Deep-Sea Res*., **11**, 921-927.

Davies, P. S., Stoddart, D. R. and D. C. Sigee (1971) Reef forms of Addu Atoll, Maldive Islands. *Symp. Zool. Soc. Lond.*, **29**, 217-259.

Davies, P. J. (1983) Reef Growth. In D. J. Barnes (ed), *Perspectives on Coral Reefs*. Aust. Inst. Mar. Sci., Brian Clouston Publishing, Manuke, ACT, Australia, pp 69- 106.

Davies, P. J. and D. Hopley (1983) Growth facies and growth rates of Holocene reef in the Great Barrier Reef. *B.M.R. J. Aust. Geol. Geophys.*, **8**, 237-251.

Davies, P. J., Marshall, J. F. and D. Hopley (1985) Relationships between reef Growth and sea level in the Great Barrier Reef. *Proc. 5th Int. Coral Reef Congr. Tahiti*, **3**, 95-103.

Davis, W. M. (1928) The coral reef problem. *Am. Geog. Soc. Special Pub.*, **9**, 569.

Dullo, W-C., Camoin, G. F., Blomeier, D., Colonna, M., Eisenhauer, A., Faure, G., Casanova, J. and B. A. Thomassin (1998) Morphology and sediments of the foreslopes of Mayotte, Comoro Island: direct observations from a submersible. *IAS Spec. Publ.*, **25**, 219-236.

Eisenhauer, A., Wasserburg, G. J., Chen, J., Bonani, G. J., Collins, L. B., Zhu, Z. R. and K. H. Wyroll (1993) Holocene sea level determination relative to the Australian continent: U-Th (TIMS) and ^{14}C (AMS) Dating of coral cores from Abrolhos Islands. *Earth Planet. Sci. Lett.*, **114,** 529-547.

Fairbanks, R. G. (1989) A 17, 000 year glacio-eustatic sea level record: influence of glacial melting rates on the Younger Dryas event and deep ocean circulation. *Nature*, **342**, 637-642.

Faure, G. (1974) Morphology and bionomy of the coral reef discontinuities in Rodriguez island (Mascarene Archipelago, Indian Ocean). *Proc. 2nd Int. Coral Reef Symp, Brisbane*, Great Barrier Reef Committee, **2**, 161-172.

Faure, G. and L. F. Montaggioni (1970) Le récif coralline de St-Pierre-de-la Réunion (Océan Indien): géomorphologie et repartition des peuplements. *Rec. Trav. Stn. Mar. Endoume (H.S. Suppl.)*. **10**, 271-284.

Farrow, G. E. and K. M. Brander (1971) Tidal studies of Aldabra. *Phil. Trans. Roy. Soc. Lond. B,* **260**, 93-121.

Francis, T. J. G. and G. G. Shor (1966) Seismic refraction measurements in the Northwest Indian Ocean. *J. Geophys. Res.*, **71**, 427.

Frankignoulle, M., Canon, C. and J. P. Gattuso (1994) Marine calcification as a source of CO_2: positive feedback of increasing atmospheric CO_2. *Limnol. Oceanogr.*, **39**, (2), 458-462.

Gardiner, J. S. (1936) The reefs of the Western Indian Ocean. II. The Mascarene region. *Linnean. Soc. Cond. Trans. (Zool).*, **19**, 426-436.

Gattuso, J. P., Pichon, M., Delesalle, B. and M. Frankignoulle (1993) Community metabolism and air-sea CO_2 fluxes in a coral reef ecosystem (Moorea, French Polynesia). *Mar. Ecol. Prog. Ser*., **96**, 259-267.

Gattuso, J. P., Frankignoulle, M. and S. V. Smith (1999) Measurement of community metabolism and significance of coral reefs in the CO_2 source-sink debate. *Proc. National Acad. Sci. USA.*, **96,** (23), 13017-13022.

Gattuso, J. P. and R. W. Buddemeier (2000) Calcification and CO_2. *Nature*, **407**, 311-313.

Guilcher, A. (1956) Etude géomorphologique des récifs corallines du Nord-Ouest de Madagascar. *Ann. Inst. Oceanogr. Paris*, **33**, 2, 65-136.

Guilcher, A. (1958) Development on the geomorphology of the reefs corallines of Madagascar and dependences. *Mem. Inst. Sci. Madagascar*. F, **3**, 89-115.

Guilcher, A., Berthois, L., Le Calvez, Y., Battistini, R. and A. Crosnier (1965) Les récifs corallines et la lagoon de l'lle Mayotte (Archipel des Comores, Océan Indien). *Mem. ORSTOM.*, **11**, 1-120.

Hay, B. J. and J. R. Southam (1977) Modulation of marine sedimentation by continental shelves. In N. R. Anderson and Malahoff, A. (eds), *The Fate of Fossil Fuel CO_2 in the Oceans.* Plenum Press, New York, pp 569-604.

Higgin, E. (1849) Remarks on the country, products and appearance of the island of Rodriguez with opinions as to its future colonization. *Geographical J.*, **19**, 17.

Hopley, D. (1982) *The geomorphology of the Great Barrier Reef: Quaternary development of coral reefs.* John Wiley, NY.

Houghton, J. T., Ding, Y., Griggs, D. J., Noguer, M., van der Linden, P. J., Dai, X., Maskell, K. and C. A. Johnson (eds) (2001) *Climate Change 2001: the scientific basis. Contribution of Working Group I to the Third assessment Report of the International Panel on Climate Change*. Cambridge University Press, Cambridge, United Kingdom and New York, USA, pp 881.

Hubbard, D. K., Miller, A. I. and D. Scaturo (1990) Production and cycling of $CaCO_3$ in a shelf edge reef system (St Croix, US Virgin Islands): applications to the nature of reef systems in the fossil record. *J. Sed. Petrol*., **60**, 3, 335-360.

Iglesias-Rodriguez, M. D., Armstrong, R., Feely, R., Hood, R., Kleypas, J., Milliman, J. D., Sabine, C. and J. Sarmiento (2000) Progress made in study of ocean's calcium carbonate budget. *Eos*, **83**, 34, 365 – 375.

Jennings, S., Marshall, S., Cuet, P. and O. Naim (2000) Chapter 13 The Seychelles. In T. R. McClanahan, C. R. C. Sheppard and D. O. Obura (eds), *Coral Reefs of the Indian Ocean their Ecology and Conservation.* Oxford University Press, pp 383-407.

Kayanne, H. (1992) Deposition of $CaCO_3$ into Holocene reefs and its relation to sea level rise and atmospheric CO_2. *Proc. 7th Int. Coral Reef Symp. Guam.*, 1, 50-55.

Keir, R. S. and W. H. Berger (1984) Late Holocene carbonate dissolution in the equatorial Pacific: reef growth or neoglaciation? In E. T. Sundiquist and W. S. Broecker (eds), *The carbon cycle and atmospheric CO_2 natural variations archean to present. Geophysics. Monograph. Ser*., **32**, pp. 208 – 219.

Kinsey, D. W. (1981) The Pacific – Atlantic reef growth controversy. *Proc. 4th Int. CR. Symp. Manila*, **1,** pp. 493 – 495.

Kinsey, D. W. and D. Hopley (1991) The significance of coral reefs as global carbon sinks – response to greenhouse. *Pal. Pal. Pal*., (Global and Planetary change section) **89**, 363 – 377.

Kleypas, J. A. (1997) Modeled estimates of global reef habitat and CO_2 production since the last glacial maximum. *Paleocean.*, **12**, 533 – 545.

Kleypas, J. A., Buddemeier, R. W., Archer, D., Gattuso, J. P., Langdon, C. and B. N. Opdyke (1999) Geochemical consequences of increased atmospheric CO_2 on coral reefs. *Science*, **284**, 118 – 120.

Lacroix, A. (1923) *Le volcan actif de L'ile de la Reunion et ses products.* Paris,Gauthier-Villers.

Lambeck, K. (1993) Glacial rebound and sea-level change: an example of a relationship between mantle and surface processes. *Tectonophysics*, **223**, 15-37.

Lambeck, K. and Chappell, J. (2001) Sea level change through the last glacial cycle. *Science*, **292**, 679.

Langdon, C., Takahashi, T., Sweeney, C., Chipman, D., Goddard, J., Marubini, F., Aceves, H., Barnett, H. and M. J. Atkinson (2000) Effect of calcium carbonate saturation state on the calcification rate of an experimental coral reef. *Glob. Biogeochem. Cy.*, **14**, 639-654.

MacIntyre, I. G. (1988) Modern coral reefs of western Atlantic: new geological perspective. *Am. Ass. Petrol. Geol. Bull*., **72**, 1360-1369.

Mathews, D. H. and D. Davies (1966) Geophysical studies of the Seychelles Bank. *Phil. Trans. Roy. Soc. Lond. Ser. A*., **259**, 227-239.

McCulloch, M., Fallon, S., Wyndham, T., Hendy, E., Lough, J. and D. Barnes (2003) Coral record of increased sediment flux to the inner Great Barrier Reef since European Settlement. *Nature*, **421**, 727-730.

McDougall, I., Upton, B. G. J. and W. J. Wadsworth (1965) A geological reconnaissance of Rodriguesz island, Indian Ocean. *Nature*, **206**, 26-27.

Mckenzie, D. and J. G. Sclater (1971) The evolution of the Indian Ocean since the Late Cretaceous. *Geophysi. J. R. Astr. Soc*., **25**, 437-528.

Milliman, J. D. (1974) *Marine Carbonates. Recent sedimentary carbonates 1*. Springer-Verlag, NY.

Milliman, J. D. (1993) Production and accumulation of calcium carbonate in the ocean: budget of a nonsteady state. *Global Biogeochem. Cy*., **7**, 927 – 957.

Montaggioni, L. F. (1970) Essai de reconstitution paleogéographique de I'ile Rodrigue (Archipel des Mascareignes, Océan Indien) *Acad. Sci. Paris.* (D)., **271**, 1741-1744.

Montaggioni, L. F. (1974) Coral reefs and quaternary shorelines in the Mascarene Archipelago (Indian Ocean). *Proc. 2nd Int. Coral Reef Symp. Brisbane*, Great Barrier Reef Committee, **1**, 579-593.

Montaggioni, L. F. (1988) Holocene reef growth history in mid-plate high volcanic islands. *Proc. 6th Int. Coral Reef Symp. Australia*, **3**, 455-461.

Montaggioni, L. F. (2000) Postglacial reef growth. *Earth Planet. Sci.,* **331,** 319-330.

Montaggioni, L. F. and G. Faure (1980) Les récifs corallines des Mascareignes (Océan Indien). *Collections des Travaux du Centre Universitaire,* Université de la Réunion.

Montaggioni, L. F. and G. Faure (1997) Response of reef coral communities to sea level rise: A Holocene model from Mauritius (Western Indian Ocean). *Sediment.*, **44**, 1053 – 1070.

Morgan, W. J. (1978) Rodriguesz, Darwin, Amsterdam, a second type of hot spot island. *J. Geophys. Res*., **83**, 5355-5360.

Naim, O., Pascale, C. and V. Mangar (2000) Chapter 12 The Mascarene Islands. In T. R. McClanahan, C. R. C. Sheppard and D. O. Obura (eds), *Coral Reefs of the Indian Ocean Their Ecology and Conservation.* Oxford University Press, New York.

Nakada, M. and K. Lambeck (1991) Late Pleistocene and Holocene sea level changes in the Australian region and mantle rheology. *Geophys. J*., **96**, 467-517.

Opdyke, B. N. (2000) Shallow water carbonate deposition and its effect on the carbon cycle. In T. M. L. Wigley and D. S. Schimel (eds), *The Carbon Cycle.* Cambridge University Press, Cambridge.

Opdyke, N. B. and J. C. G. Walker (1992) Return of the coral reef hypothesis: Basin to shelf partitioning of $CaCO_3$ and effect on Holocene atmospheric CO_2. *Geology*, **20**, 733-736.

Peltier, W. R. (1991) The ICE-3G model of late Pleistocene deglaciation: construction, verification, and applications. In R. Sabadini (ed), *Isostasy, sea level and mantle rheology*. NATO ASI, C, **334**, Kluwer.

Pichon, M. (1967) Caractéres généraux des peuplements benthiques des récifs et lagoons de l'ile Maurice (Océan Indien). *Cahiers de l'ORSTOM (série Océanographie)*, **5**, 31-45.

Pirazzoli, P. A. (1991) *World Atlas of Holocene sea level changes*. Elsevier Oceanography Series, Amsterdam.

Rajkumar, R. and A. H. Parulekar (2001) Biology of Corals and Coral Reefs. In R. S. Gupta and E. Desa (eds), *The Indian Ocean – A Perspective*, 2, A. A. Balkema Publishers, Tokyo.

Roberts, C. M., McClean, C. J., Veron, J. E. N., Hawkins, J. P., Gerald, R. A., McAllister, D. E., Mittermeier, C. G., Schueler, F. W., Spalding, M., Wells, F., Vynne, C. and T. B. Werner (2002) Marine Biodiversity Hotspots and Conservation Priorities for Tropical Reefs. *Nature*, **295**, 1280-1284.

Ryan, D. A., Opdyke, B. N. and J. S. Jell (2001) Holocene sediments of Wistari Reef towards a global quantification of coral reef related neritic sedimentation in the Holocene. *Pal. Pal. Pal.*, **175,** 1-12.

Schlanger, W. (1981) The paradox of drowned reefs and carbonate platforms. *Geol. Soc. Am. Bull. Part 1*, **92**, 197-211.

Sewell, R. B. S. (1935) Studies on coral and coral-formations in Indian waters. Geographic and Oceanographic Research in Indian Waters No 8. *Memoirs Asiatic Soc. Bengal*, **9**, 461-539.

Sheppard, C. R. C. (2000) The Chagos Archipelago. In T. R. McClanahan, C. R. C. Sheppard and D. O. Obure (eds), *Coral reefs of the Indian Ocean: Their Ecology and Conservation.* Oxford University Press, Oxford, pp 445-468.

Sheppard, C. R. C. (2003) Predicted recurrences of mass coral mortality in the Indian Ocean. *Nature*, **425**, 294-297.

Shor, G. G. and D. D. Pollard (1963) Seismic investigations of Seychelles and Saya de Malha Banks, NW Indian Ocean. *Science*, **142**, 48-49.

Smith, S. V. and D. W. Kinsey (1976) Calcium carbonate production, coral reef growth and sea level change. *Science*, **194**, 937-939.

Smith, S. V. (1978) Coral reef area and the contributions of reefs to the processes and resources of the world's oceans. *Nature*, **273**, 225-226.

Snell, H. J. and W. H. T. Tams (1920) The natural history of the island of Rodriguez. *Camb. Philos. Soc. Trans.*, **9**, 283-292.

Spalding, M. D., Ravilious, C. and E. P. Green (2001) *World Atlas of Coral Reefs*. Prepared at the UNEP World Conservation Monitoring Centre. University of California Press, Berkeley, USA.

Stoddart, D. R. (1966) Reef Studies at Addu Atoll, Maldive Islands. *Atoll Res. Bull.*, **116**, 1-107.

Stoddart, D. R. (1971) Environment and history in Indian Ocean reef morphology. In D. R. Stoddart and M. Yonge (eds), *Regional variation in Indian Ocean Coral Reefs.* Symposia of the Zoological Society of London, 28, London Academic Press, pp 3-38.

Stoddart, D. R. (1973) Chapter 2 Coral Reefs of the Indian Ocean. In O. A. Jones and R. Endean (eds), *Biology and Geology of Coral Reefs*, vol. 1, Geology 1, Academic Press, NY, pp 51-87.

Stuiver, M. and P. J. Reimer (1993) Extended ^{14}C database and revised CALIB radiocarbon calibration program. *Radiocarbon*, **35**, 215-230.

Upton, B. G. J., Wadsworth, W. J. and T. C. Newman (1967) The petrology of Rodriguez Island, Indian Ocean. *Geol. Soc. Am. Bull.*, **78**, 1495-1506.

Zeebe, R. E. and D. A. Wolf-Gladrow (2001) *CO_2 in Seawater: Equilibrium, Kinetics, Isotopes*. Elsevier Oceanography Series, 65, Amsterdam, pp 346.

Ware, J. R., Smith, S. V. and M. L. Reaka – Kudla (1991) Coral reefs: sources or sinks of atmospheric CO_2. *Coral Reefs*, **11**, 127 – 130.

Wollast, R., Garrels, R. M. and F. T. Mackenzie (1980) Calcite-seawater reactions in ocean surface waters. *Am. J. Sci.*, **280**, 831-848.

Woodroffe, C. D., McLean, R. F., Polach, H. and E. Wallensky (1990) Sea level and coral atolls: Late Holocene emergence in the Indian Ocean. *Geology*, **18**, 62-66

4.10 Acknowledgments

This research has been supported by The Royal Geographic Society, The Royal Society, National Environment Research Council (NERC), the *Shoals of Capricorn* Marine Research Programme (this is Shoals Contribution no. P046), Australian National University Marine and Earth Sciences, Department and Australian National University Nuclear Physics Department. We especially thank Kate Davis, for drafting figures 1 and 2, and Dr Vladeimier Levchenko, Dr Matt Cooper, Dr Daniel Marie and the Rodrigues Research Station.

Chapter Five

The Impact of Coral Reef $CaCO_3$ Accumulation on Holocene Atmospheric Carbon Dioxide Concentration.

Plate 5.1 Heron Island, Southern Great Barrier Reef, Australia (Heron Island Research Station postcard).

Chapter 5

The Impact of Coral Reef $CaCO_3$ Accumulation on Holocene Atmospheric Carbon Dioxide Concentration.

Reference: Rees S. A., Opdyke, B. N. and P. A. Wilson (manuscript submitted 06.08.05) The Impact of Coral Reef $CaCO_3$ Accumulation on Holocene Atmospheric Carbon Dioxide Concentration. *Global Biogeochemcial Cycles*.

5.1 Abstract

We present a re-evaluation of the contribution of coral reef-derived carbon dioxide (CO_2) to the Holocene atmosphere. Our new estimates make use of accretion rate data from cored coral reef sequences that we have compiled from the published literature. The cumulative calcium carbonate ($CaCO_3$) accumulation within coral reefs globally during the past 10 kyr BP is 7970 Gt (~ 0.1 Gt C yr^{-1}) about half the flux of carbon to both the global ocean from rivers and buried in deep sea sediments as $CaCO_3$. This mass of $CaCO_3$ accumulation would have made approximately 2100 Gt CO_2 available for release to the atmosphere over the Holocene. Yet, the observed natural increase in atmospheric CO_2 concentration 10 kyr BP to pre-industrial revolution is only a fraction of this amount. The rate of this natural flux (~0.06 Gt C as CO_2 yr^{-1}) is dwarfed by the anthropogenic flux of CO_2 to the atmosphere (currently ~ 6.3 Gt C as CO_2 yr^{-1}). Present day reefs release only about 0.3 % current anthropogenic emissions and even the peak Holocene reef flux amounted to only 1.4 % of present day anthropogenic release.

5.2 Introduction

Ever since ice core records have demonstrated the close correlation between changes in atmospheric CO_2 concentration and temperature on glacial-interglacial timescales, the cause of the CO_2 change has become the focus of much debate (Barnola *et al.*, 1987; Petit *et al.*, 1999; Shackleton, 2000). Many mechanisms have been hypothesized to explain the changes in atmospheric CO_2 concentration over the glacial-interglacial cycle (Archer *et al.*, 2000). However, no one mechanism appears capable of fully explaining the magnitude of the observed changes in atmospheric CO_2 in the ice core and sedimentary record (Broecker and Henderson, 1998; Sigman and Boyle, 2000; Houghton *et al.*, 2001). One of the hypotheses put forward to help explain the

magnitude of the deglacial increase in atmospheric CO_2 is the Coral Reef Hypothesis. This hypothesis proposes that the expansion and acceleration of coral reef growth during deglaciation acts as a positive feedback on atmospheric CO_2 concentration because CO_2 is released as a bi-product of calcification (Berger, 1982a, 1982b; Berger and Killingley, 1982; Opdyke and Walker, 1992; Walker and Opdyke, 1995; Kleypas, 1997; Opdyke, 2000; Ryan *et al.,* 2001; Vecsei and Berger, 2003).

In the marine environment, upon calcification about 0.6 mol of CO_2 is liberated per mole of solid $CaCO_3$ deposited (Equation 5.1a). As a consequence of the buffering effect of seawater, the remaining 0.4 mol of CO_2 formed recombines with carbonate ions and water to form bicarbonate (hydrogen carbonate) which remains in solution (Equation 5.1b; Ware *et al.,* 1991; Zeebe and Wolf-Gladrow, 2001).

Equation 5.1

$$Ca^{2+}_{(aq)} + 2HCO_3^-{}_{(aq)} \xrightarrow{\text{(calcification)}} CaCO_{3\,(s)} + H_2O_{(aq)} + CO_{2(aq)}$$

$CO_{2(aq)}$ [a]

$$CO_{2(aq)}{}^{b} + CO_3^{2-}{}_{(aq)} + H_2O_{(aq)} \longrightarrow 2HCO_3^-{}_{(aq)}$$

In Equation 5.1, $2HCO_3^-$ is bicarbonate or hydrogen carbonate, $CaCO_3$ is calcium carbonate, CO_2 is carbon dioxide and CO_3^{2-} is carbonate ion. [a] 0.6 mol available for release to the atmosphere. [b] 0.4 mol recombines to form aqueous hydrogen carbonate.

The fate of the 0.6 mol of CO_2 released has been debated. In many field studies on reef ecosystems, CO_2 has been measured passing across the air sea interface to the atmosphere (Smith and Pesret, 1974; Smith and Jokiel, 1978; Gattuso *et al.,* 1993; 1996; 1997; Frankignoulle *et al.,* 1996, Kawahata *et al.,* 1997; 1999; 2000; Suzuki *et al.,* 1997). In some others the CO_2 flux appears to be in the opposite direction (atmosphere to ocean) (Kayanne *et al.,* 1995; Yamamuro *et al.,* 1995; Kraines *et al.,* 1997; Chrisholm and Barnes, 1998). This apparent fundamental discrepancy reflects the overall health of the ecosystem being studied (Gattuso *et al.,* 1999). CO_2 absorption is expected in the case of unhealthy, stressed fringing reefs exposed to high nutrient concentrations and turbidity (often the result of anthropogenically induced terrestrial run off and pollution). These polluted reefs are not representative of the natural global picture of Holocene reef growth because the stressed reef communities are dominated by non-calcareous photosynthesising green algae. These algae absorb CO_2 during photosynthesis thus potentially drawing down the CO_2 concentration in surface waters

(Gattuso *et al.,* 1999). Additional field studies are needed to refine the picture of CO_2 flux across the ocean-atmosphere interface for all reef types worldwide over a variety of time scales to incorporate, for example, seasonal changes (Frankignoulle *et al.,* 1994). However, healthy coral reefs are a source of CO_2 to the atmosphere and we assume that all of the CO_2 produced by coral reefs is made available to the atmosphere (Equation 5.1) and passes across the sea-air interface acting, all things being equal, to increase the atmospheric CO_2 concentration (Ware *et al.,* 1991; Opdyke and Walker, 1992; Gattuso *et al.,* 1993, 1999; Frankignoulle and Gattuso, 1993; Frankignoulle *et al.,* 1994; Kawahata *et al.,* 1997; 2000; Barker *et al.,* 2003; Rees *et al.,* 2005).

5.2.1 A Note on the Coral Reef Hypothesis

Some authors have dismissed the Coral Reef Hypothesis as a process contributing to the deglacial atmospheric CO_2 rise observed in ice core records because it is sea-level led and thus cannot explain the initiation of deglaciation (Mylroie, 1993; Broecker and Henderson, 1998). But to some extent this misrepresents the hypothesis as originally conceived because it was initially proposed as a positive feedback mechanism on deglacial increases in the concentration of atmospheric CO_2 as follows. As sea level rose and flooded the continental shelves during the last deglaciation, large shallow areas became available for re-colonisation by coral reefs. In order to remain in the photic zone (to maximise the photosynthetic processes of their algal symbionts) reef corals responded to sea level rise by growing vertically. During calcification, CO_2 was released lowering the surface ocean pH, the increase in the partial pressure of CO_2 resulted in CO_2 escape to the atmosphere. The accommodation space created by sea level rise allowed an increase in reef carbonate sedimentation. This would have made a substantial quantity of CO_2 available to the atmosphere amplifying the deglacial atmospheric CO_2 increase and inducing further warming, ice melt and continued sea level rise.

5.2.2 Carbonate Budgets

Recent renewed interest in the role of the basin-to-shelf fractionation of carbonate during glacial interglacial cycles requires the mass balance of coral reef carbonate be confidently quantified (Ridgwell *et al.,* 2003; Coxall *et al.,* 2005; Marchitto *et al.,* 2005; Ridgwell and Zeebe, 2005). Currently, most carbon cycle budgets do not include a breakdown of the pelagic and neritic carbonate reservoirs and fluxes (Sigman and

Boyle, 2000; Houghton *et al.*, 2001). Many studies have attempted to estimate the contribution of calcium carbonate ($CaCO_3$) to the global carbon budget (Milliman, 1974, 1993; Hay and Southam, 1977; Smith, 1978; Berger, 1982a, 1982b; Kinsey and Hopley, 1991; Kayanne, 1992; Opdyke and Walker, 1992; Milliman and Droxler, 1996; Kleypas, 1997; Opdyke, 2000; Vecsei and Berger, 2003; Vecsei, 2004b; Rees *et al.*, 2005). Yet, the size of the Holocene shallow water carbonate reservoir is still not well constrained (Opdyke, 2000; Iglesias-Rodriguez *et al.*, 2000; Vecsei, 2004a; Ridgwell and Zeebe, 2005). Various methods have been employed to calculate a global Holocene $CaCO_3$ budget (see Vecsei, 2004a for a review). Most budgets have been calculated using either i) $CaCO_3$ sediment accumulation rates estimated from the stratigraphic record (Opdyke and Walker, 1992; Opdyke, 2000; Ryan *et al.*, 2001) or ii) modern day reef productivity values measured using the alkalinity method (Smith, 1978; Kinsey and Hopley, 1991; Vecsei and Berger, 2003; Vecsei, 2004b). However, estimates of $CaCO_3$ fluxes, both production and accumulation have uncertainties of at least 100 % (Iglesias-Rodriguez *et al.*, 2000). Most uncertainties arise because various authors have had little choice but to i) manipulate recycled data of variable quality and resolution and ii) make assumptions regarding the proportion of $CaCO_3$ production that is retained within a reef (Milliman, 1993).

5.2.3 Extrapolating Growth and Productivity Rates

Many budgets are inaccurate because they rely on data from only a few regions of the globe and extrapolate either production or accumulation rate data from one reef province to another where no data are available. For example, Milliman (1974) used $CaCO_3$ deposition rates mainly from the Caribbean (Florida, Bahamas, Bermuda, Jamaica, British Honduras but also Western Australia and Hawaii) to represent global Holocene reef growth. This approach does not give adequate global coverage because it grossly under-represents the largest reef province in the world, the Indo-Pacific. Vecsei (2004a) extrapolated production estimates from i) East Pacific reef flats to represent reefs of the whole Pacific Ocean except the Great Barrier Reef, ii) Southwest Indian Ocean reef flats to represent all Indian Ocean reefs and iii) Atlantic fore-reefs to represent all Indo-Pacific reefs. While the practice of extrapolation in this way may have been necessary in the past it is clearly not ideal because reef growth has varied significantly in response to various factors including variations in sea level rise, substrate type, antecedent topography, sea surface temperature, nutrients, wave energy,

light, turbidity, aragonite saturation state and larval recruitment (Kleypas, 1997; Montaggioni, 2005; Lambeck and Chappell, 2001).

5.2.4 Productivity vs Accumulation

Various $CaCO_3$ budgets have used reef production values (estimated by the alkalinity method, Smith and Kinsey, 1978) to calculate coral reef $CaCO_3$ accumulation and consequent CO_2 release to the atmosphere (Chave *et al.*, 1972; Milliman, 1974, 1993; Smith, 1978; Kinsey and Hopley, 1991; Iglesias-Rodriguez *et al.*, 2000; Vecsei and Berger, 2003; Vecesi, 2004b). Productivity values represent an estimate of $CaCO_3$ formed *in situ* during a specific time interval. Subsequently a fraction of this produced $CaCO_3$ is lost because of erosion and dissolution and this loss may amount to 20 to 25 % of the carbonate produced (Hubbard *et al.*, 1990; Milliman, 1993). But in practice reef carbonate losses are still very poorly defined globally (Kleypas, 1997). The practice of extrapolating modern day coral reef production values into the past to calculate a marine $CaCO_3$ budget over a full glacial-interglacial cycle is also likely to be misleading because of the effect of changes in the *loci* and rates of coral reef sedimentation during transgression (Kinsey, 1981; Davies *et al.*, 1985; Kinsey and Hopley, 1991; Montaggioni, 2000). Finally, implied vertical growth rates estimated from net productivity rates are often substantially lower than accumulation rates seen in the sedimentary record and may be in error by up to 50 % (Smith, 1983; Davies and Hopley, 1983). For example, the modern day accumulation rate inferred by the alkalinity method is approximately 3 m kyr^{-1} compared to rates measured in reef cores of up to 8 m kyr^{-1} (Davies and Marshall, 1980; Davies, 1983).

Milliman (1993) suggested that the key problem in estimating the shallow water carbonate budget is documenting the *loci* and rates of production and accumulation during the Holocene. A more conservative way to estimate coral reef $CaCO_3$ accumulation is to use accretion rates calculated from radiometrically dated coral reef cores, as opposed to productivity estimates. Accretion rates represent only retained $CaCO_3$ (net production) and are thus more representative of $CaCO_3$ accumulation during the Holocene (Smith and Kinsey, 1976; Schlanger, 1981; Opdyke and Walker, 1992; Rees *et al.*, 2005). This method allows an estimate of the $CaCO_3$ mass balance to be made from actual rates measured in the stratigraphic record avoiding questionable extrapolation temporally or spatially if one uses sea level curves or predictive models. Accumulation rates measured in the geological record may underestimate the maximum

potential reef accretion rate by up to 40 % (Davies and Hopley, 1983). Recently, Vecsei (2004a) proposed that assumptions regarding the carbonate content (%) of reefal sediments may lead to overestimates in calculations that utilize accretion rate data. Logistical problems associated with reef drilling and radiometric dating mean that reef growth is measured over relatively few points which may hinder estimation of the $CaCO_3$ mass balance (Hopley, 1982).

5.2.5 Variation in Holocene Accumulation Rates

Accumulation rates estimated from radiocarbon dated cores for late Holocene reef sequences are slower than those for the early to mid-Holocene. For example, modern day accretion rates of 1.3 to 4.2 m kyr^{-1} in Panama contrast with rates of 7.5 to 10 m kyr^{-1} in the mid-Holocene (Glynn and Macintyre, 1977; Davies, 1983), and at One Tree Reef (Great Barrier Reef) early to mid-Holocene accretion rates of 3 to 7 m kyr^{-1} contrast with current rates of 3 m kyr^{-1} (Kinsey, 1979; Davies and Marshall, 1980). During the early Holocene, reefs catching up with sea level rise were generally covered with at least 5 m or more of water. Therefore, a smaller fraction of the $CaCO_3$ produced was lost to erosion caused by wave action near the sea surface and a greater fraction of the sediment produced became incorporated into the reef structure than today. As reefs approached modern day sea level the amount of accommodation space is decreased and excess production is transported leeward. The sediment ultimately forms lagoonal sands and leeward accretionary wedges (Ryan *et al.,* 2001). Reefs presently at sea level do not accrete vertically because there is no space left to accommodate this direction of growth. Instead the dominant vector of accretion on modern reefs is lateral. The majority of the $CaCO_3$ produced on modern reef flats is eroded and transported leeward where it is responsible for infilling lagoons and creating leeward accretionary wedges.

5.2.6 Global Reef Area Estimates

Past estimates of coral reef $CaCO_3$ accumulation during the Holocene have been obscured by outdated estimates of global reef area and the inclusion or exclusion of non-reef areas such as carbonate banks and carbonate dominated embayments (Chave *et al.,* 1972; Milliman, 1974, 1993; Smith, 1978; Keir and Berger, 1985; Kinsey and Hopley, 1991; Opdyke and Walker, 1992; Iglesias-Rodriguez *et al.*, 2000; Vecsei and Berger, 2003; Vecsei, 2004b). For example, Smith's (1978) coral reef area estimate (6×10^5 km^2) was derived simply from estimates of shallow water (0 to 30 m) areas in

tropical regions, whereas Milliman (1974) calculated global reef area (1.4×10^6 km^2) as the area of reported atolls globally multiplied by two plus the area of the Great Barrier Reef and the Bahamas. Neither of these two estimates are an accurate estimation of actively calcifying reefs of the present day and no correction for changes in reef area was applied when these estimates were extrapolated into the Holocene (Milliman, 1974, 1993; Smith, 1978). The most comprehensive reef area estimate to date is that of Spalding *et al.* (2001) of 2.843×10^5 km^2 calculated using remote sensing techniques and navigation charts. Spalding *et al.*'s (2001) reef area estimate defines the area of reef near the sea surface shown on charts as breaking waves, the reef flat and crest. This estimate is conservative with respect to $CaCO_3$ budget studies because it does not include submerged reefs (drowned), reefal shoals, drowned reefs, lagoons or fore-reefs.

5.2.7 Our Approach

We present a new calculation for the global Holocene coral reef $CaCO_3$ mass balance using published coral reef accumulation rate data. This reassessment is made possible by i) the increase in the volume and geographical coverage of accumulation rate data available in the published literature and ii) the new global reef area estimate of 2.843×10^5 km^2 (Spalding *et al.*, 2001). The consequent flux of CO_2 to the Holocene atmosphere resulting from coral calcification is estimated using the seawater buffering factor (~0.6 mol CO_2 released for every mole of $CaCO_3$ laid down in the marine environment) established by Ware *et al.* (1991). We ignore the suggested slight increase in this factor since the LGM (Frankignoulle *et al.*, 1994). The present study improves upon past estimates of the Holocene coral reef $CaCO_3$ mass balance and potential release of CO_2 to the atmosphere because it i) uses data from the geological record representative of reef growth during the Holocene (not extrapolated present day values) and ii) provides both a temporal and spatial perspective of the flux of $CaCO_3$ into reefs and release of CO_2 to the atmosphere.

5.3 Materials and Methods

Information regarding the ages (^{14}C and U-Th) and depths of coral material (interpreted as being in growth position when cored) from over 300 reef drill cores (from 133 reefs worldwide) were compiled and manipulated to calculate coral reef accretion (growth or accumulation) rates throughout the Holocene. Accretion rates are calculated by dividing the thickness of the carbonate sediment by the time interval over

which the sediments were deposited. The accretion rates estimated here relate to vertical reef growth and are expressed in m kyr^{-1}. In order to reduce errors associated with use of second hand recycled data, we calculated accretion rates from radiometric ages and depth values, (the 'raw data', in each publication) to ensure consistency in methods of calculation. Here, a 'reef' is defined as a three dimensional structure comprised of calcium carbonate sediment (rock, sands and muds) generated by calcification of scleractinian corals and coralline algae in the tropical marine environment which remains as solid $CaCO_3$ and is not dissolved, it does not include non-reef habitats for example, banks, platforms and carbonate dominated embayments (Rees *et al.,* 2005). Reef accretion is defined as the sum of the operative constructional and destructional processes, net framework production (Davies and Hopley, 1983).

5.3.1 Calculation of the Global $CaCO_3$ Mass Balance

The mean accretion rates calculated were used to estimate the mass of $CaCO_3$ using Equation 5.2 (Rees *et al.*, 2005).

Equation 5.2

$$\mathbf{M = R * A * D * P}$$

In Equation 5.2, M is the mass of $CaCO_3$ accumulated; R is the mean accretion rate (m kyr^{-1}); A is reef area (km^2) estimated from Spalding *et al.* (2001); D is the average density of coral reef $CaCO_3$ (2.9 g cm^{-3}, equivalent to 1.4×10^6 g $CaCO_3$ m^{-3}; Kinsey and Hopley, 1991); P, the average porosity of coral reef sediments is 50 % (Kinsey and Hopley, 1991; Ryan *et al.*, 2001).

5.3.2 Coral Reef Area

Various authors have used estimates of coral reef area to calculate the global coral reef $CaCO_3$ budget (Milliman, 1974, 1993; Smith, 1978; Kinsey and Hopley, 1991; Opdyke and Walker, 1992; Kleypas, 1997; Opdyke, 2000; Vecsei and Berger, 2003; Vecsei, 2004b; Rees *et al.,* 2005). The magnitude of the coral reef area estimates depend on the author's definition of coral reef area (Figure 5.1). To estimate the area of coral reef authors have to decide which definition most appropriately describes the part of the reef they are interested in. Previous estimates of coral reef area are probably reasonably correct however, accurate quantification of the global carbonate budget can only be achieved if the appropriate definition of coral reef area is used.

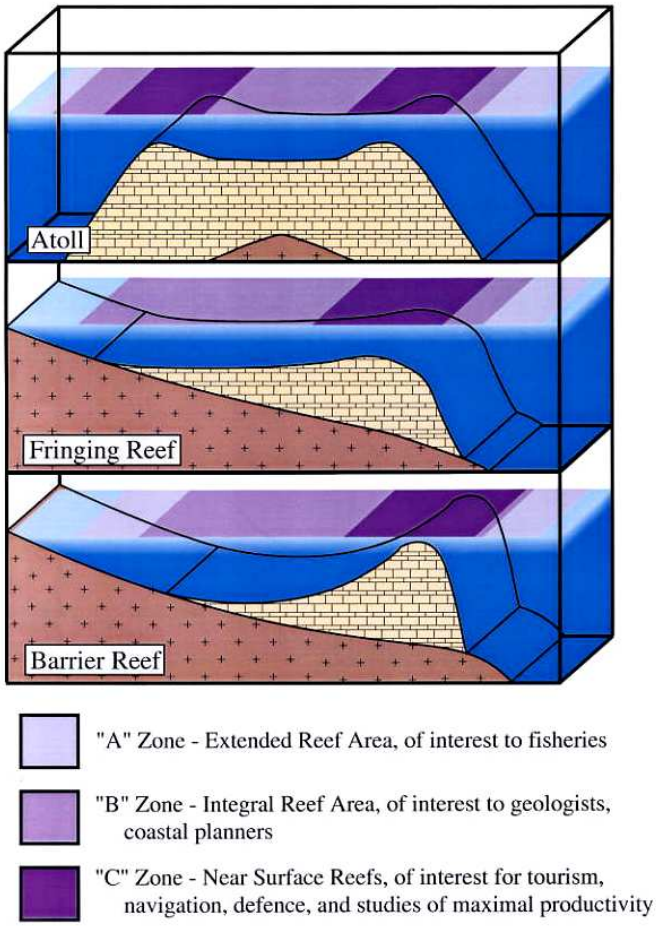

Figure 5.1 Three different definitions of `reef area' (from Ryan *et al.*, 2001). Zone A, the extended reef area, is of interest to fisheries. Zone B, integral reef area which includes thick deposits of calcium carbonate, is of specific interest to geologists, geochemists, and coastal planners. Zone C, the central and shallowest zone, is the near surface reefs that are easily imaged by satellite and is the definition used by Spalding *et al.* (2001) to estimate global reef area.

The present day coral reef area estimate used is calculated from remote sensing and navigation charts (Spalding *et al.*, 2001), the reef flat area was defined as the dark areas around a reef within a 1 km^2 grid (see definition C, Figure 5.1 or definition C, figure 3 in Spalding and Grenfell, 1997; Spalding *et al.*, 2001). This estimate defines areas that are presently at the sea surface and thus includes the reef flat and crest areas but not lagoons or leeward accretionary wedges. Spalding *et al.*'s (2001) estimate is conservative because lagoon and leeward accretionary wedge features often contain comparable amounts of $CaCO_3$ to the reef margins (Ryan *et al.*, 2001; Dickinson, 2004). To allow regional comparisons of the response of reef growth to sea level change to be made, global reef coverage was divided into six reef provinces; Great Barrier Reef (GBR); Western Pacific Ocean (WPO); Atlantic-Caribbean (AC); Western Indian

Ocean (WIO); Eastern Indian Ocean (EIO) and East Pacific Ocean (EPO; Figure 5.2; Table 5.1).

Table 5.1. Reef area estimates used in the mass balance calculations. [a] The Great Barrier Reef area estimate is calculated using the Australian reef area estimate from Spalding *et al.* (2001), minus the area of Ningaloo, the Houtman Abrolhos Islands, Christmas Island and Cocos-Keeling Islands (Sheppard and Wells, 1988). [b] The East Indian Ocean reef area estimate is the sum of reef areas of Ningaloo reef, Houtman Abrolhos Islands, Cocos-Keeling Islands and Christmas Island (Sheppard and Wells, 1988).

Reef Province	Reef Area ($\times 10^4$ km^2)
Great Barrier Reef [a]	4.492
Western Pacific Ocean	9.894
Atlantic Caribbean Ocean	2.055
Western Indian Ocean	1.853
East Pacific Ocean	2.68
East Indian Ocean [b]	4.04

Only reef area estimates (A) of those regions for which representative accretion rate data were available were used to calculate the $CaCO_3$ mass balance (Table 5.1). The global reef area calculated by Spalding *et al.* (2001) is 28.43×10^4 km^2; the total area used in this study is 18.97×10^4 km^2. This leaves 9.464×10^4 km^2 of reef area not represented, of which Indonesia is the largest unrepresented area (5.102×10^4 km^2). This highlights the need for more drilling investigations worldwide to be carried out in areas not presently adequately represented with respect to accretion rates, for example, Indonesia, the Philippines and the East Pacific (Figure 5.2).

Data pertaining to Holocene coral reef growth on the African continent, Red Sea, Arabian Sea, Indonesia, Philippines, Brazil, Sri Lanka and India could not be found in the published literature, hence these regions were also excluded from our mass balance estimate. Only sparse data were available for the East Indian Ocean and East Pacific Ocean. There are few drilling investigations relating to the time interval preceding 10 kyr BP. This is probably because many older reefs were submerged during the transgression (for example, Barbados, Fairbanks (1989); Grand Cayman, Blanchon *et al.*, (2002)) and are therefore too deep to drill using small portable drilling rigs (Caboich *et al.*, 2003).

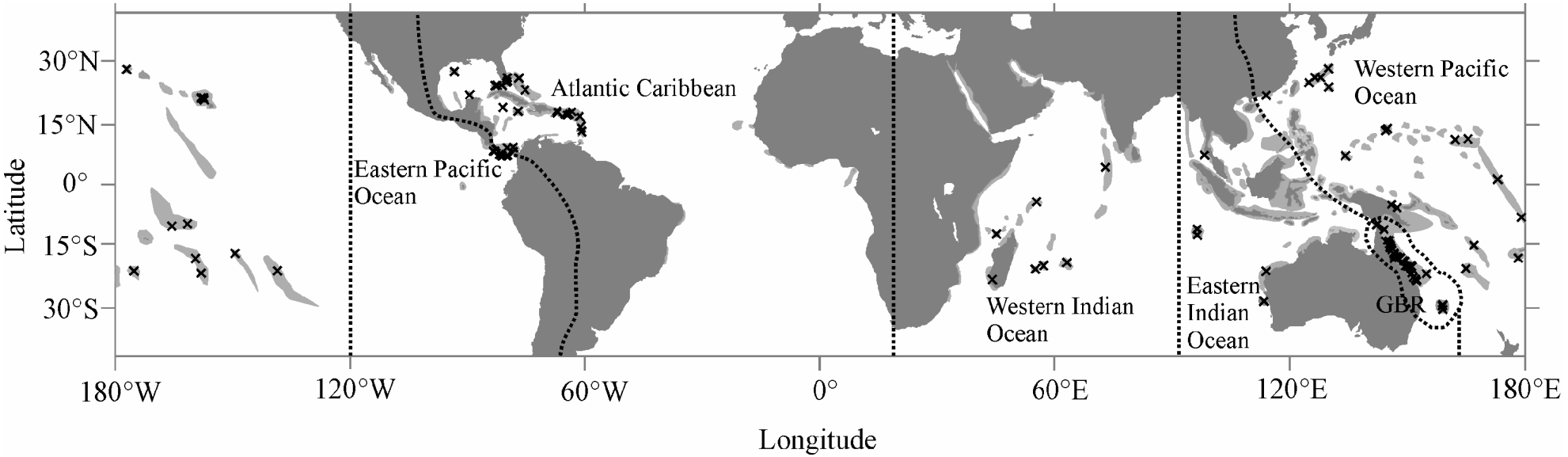

Figure 5.2. Locations of reefs drilled in the published literature and division of globe into reef provinces. Lightly Shaded area indicates present reef distribution, crosses indicate drill cores, dotted line indicates margins of reef provinces; GBR – Great Barrier Reef.

The data available for reef growth before 10 kyr BP come from uplifted reef terraces (for example, Huon Peninsula, Chappell and Polach, 1991) and a handful of deep drilling studies (for example, Tahiti, Bard *et al.*, 1996). Reef growth during this time interval is inadequately represented in the published literature compared to the Holocene, therefore we have not attempted to estimate a mass balance of $CaCO_3$ for the early deglaciation (19 – 10 kyr BP).

5.3.3 Calculation of Accretion Rates

Reefs are thought to grow most aggressively and extensively along their windward margins (Davies and Marshall, 1980). The dataset compiled here includes data from both windward and leeward margins because the reef area estimate of Spalding *et al.* (2001) represents shallow reef flat and crest areas of both the leeward and windward margins. Use of only windward margin accretion rates would overestimate the mass of $CaCO_3$ accumulated. To be conservative we use mean framework accretion rates, calculated from both windward and leeward margins. In addition to sea level rise accretion rates are affected by environmental factors including; substrate type; substrate availability; nutrient availability; larval recruitment; light; turbidity; temperature; aragonite saturation state and salinity (Davies *et al.*, 1985; Blanchon and Shaw, 1995; Kleypas, 1997; Montaggioni, 2005). Recently, the potential for single drill cores through modern reef flats to mis-represent the accretion history of an overall reef mass was elegantly highlighted in a series of numerical modelling experiments of reef architecture (Blakeway, 2000; Blanchon and Blakeway, 2003). However, these studies conclude that there is little evidence in the published literature that reef coring artificially exaggerates accretion rates.

5.3.4 Manipulation of Radiometric Ages

During the compilation of our new dataset it became clear that very few authors have reported their ^{14}C data in calibrated years. Indeed either explicitly or by inference most data is reported as marine radiocarbon age. A few authors have dated coral cores using the U-Th dating technique. Problems arise in using accretion rates determined by the two methods because of the systematic offset between the two methods (^{14}C ages are younger than U-Th ages) established by Bard *et al.* (1990). It was more convenient for the purposes of this study to convert dates expressed on an absolute time scale to marine radiocarbon ages. This was accomplished by converting calibrated ages and U-Th ages

to marine radiocarbon ages using the plots of Stuiver and Braziunas (1993). Marine radiocarbon ages which had been converted to terrestrial radiocarbon ages by subtracting 400 years were back corrected to the original marine ages by adding 400 years.

Two methods were employed to calculate the flux of $CaCO_3$ into reef sediments and the mass of CO_2 available for release to the Holocene atmosphere.

5.4 Method 1: Comparison with Opdyke and Walker (1992)

We employed a global mean framework accretion rate deemed representative of the Holocene as a whole and the present day reef area estimate of Spalding *et al.* (2001) to calculate the mass balance of Holocene reef calcium carbonate. This method allows us to compare our results directly with those of Opdyke and Walker (1992) and thereby evaluate the effect of the updated dataset on the coral reef carbonate mass balance (Table 5.2). Opdyke and Walker (1992) calculated a mean Holocene neritic $CaCO_3$ accumulation rate using 220 rate values normalised to 5 kyr duration for a variety of carbonate systems including reefs, ooids, muds and sands. Our study (method 1) calculates a mean coral reef carbonate accretion rate from 1764 rate values (300 coral reef sequences) normalised to 5 kyr duration (Table 5.2). The typical duration of the phase of rapid accretion recorded in most Holocene reef cores is 5 kyr (Opdyke and Walker, 1992; Opdyke and Wilkinson, 1993; Rees *et al.*, 2005). A Holocene coral reef $CaCO_3$ mass balance was calculated using Equation 2, the consequent release of CO_2 to the atmosphere was estimated using the conversion factor of Houghton *et al.* (1994; Table 5.2).

5.5 Method 2: Temporal and Spatial Variation within the Holocene

In order to compare our estimates of coral reef CO_2 with recorded atmospheric CO_2 concentrations in ice cores (Indermuhle *et al.*, 1999) we also calculated regional mean framework accretion rates for 5 time slices within the Holocene. It was necessary to assign accretion rates to a suitable interval of time which would allow the pattern of accretion rate variation to be established. The Holocene was divided into 2 kyr time slices (10 to 8 kyr BP; 8 to 6 kyr BP; 6 to 4 kyr BP; 4 to 2 kyr BP and 2 to 0 kyr BP). This reflects a compromise between the desire to obtain a high resolution record of the temporal changes in accretion rates through the Holocene and constraints of the growth rate data available from the published literature. The typical growth pattern exhibited by

Holocene reefs of the Australian Great Barrier Reef is represented by the cartoon shown in Figure 5.3a. The schematic sigmoidal growth curve shows; an initiation period of slow growth followed by a period of accelerated growth when the reef is keeping-up or catching-up to sea level and the final maturation phase exhibiting slow accretion rates because of a lack of accommodation space, retardation of growth and possible facies changes induced by increased hydrodynamic energy as the reef approaches the modern day sea surface (Figure 5.3a; Davies and Marshall, 1980; Davies and Hopley, 1983). Although, this growth curve may only be representative when reef growth is mainly biologically controlled and free from external physical or chemical influences such as terrestrial run off or anomalous sea surface temperatures (Davies and Hopley, 1983; Collins *et al.*, 1993), it is reasonable to expect that these changes in growth rate should approximate a bell-shaped curve when accretion rates are plotted against time (Figure 5.3b).

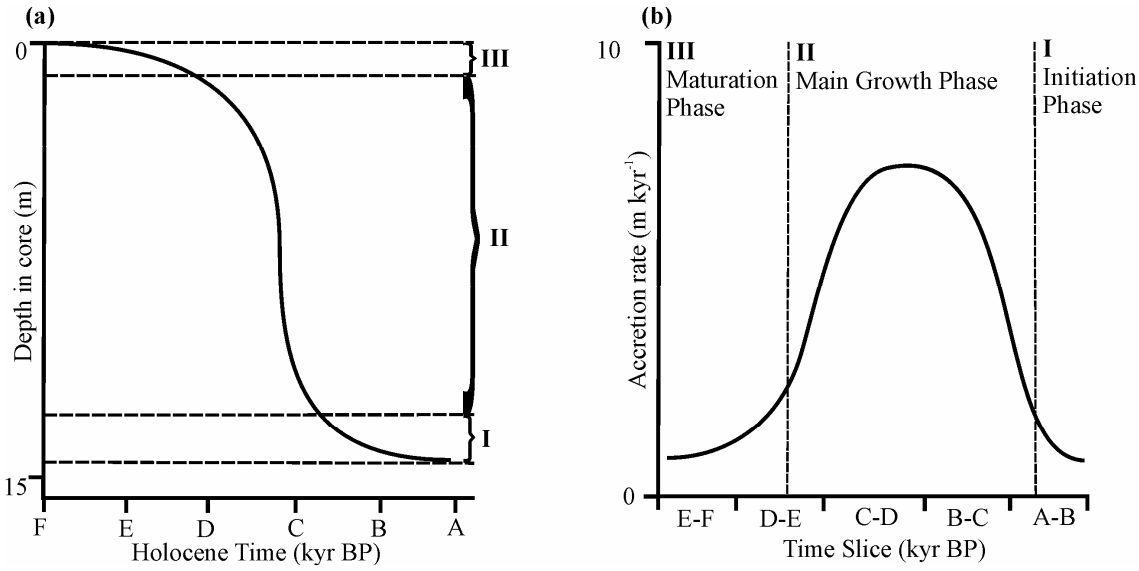

Figure 5.3. (a) Schematic of the hypothetical sigmoidal growth curve (Davies and Marshall, 1980; Davies and Hopley, 1983). (b) Schematic of the predicted bell-shaped curve of the changes in reef accretion rates during the Holocene, reflecting the hypothetical growth curve in Figure 5.3a.

5.5.1 Time Slices

One objective of reef coring has been to establish sea level curves for various regions of the world. These studies require that cores are very well dated and often provide a high resolution record of reef growth (Bard *et al.*, 1996; Camoin *et al.*, 2004). However, dating procedures are expensive and time consuming. As a result, many of the drill cores taken for other purposes report relatively few radiocarbon ages. The radiometric data available rarely fit into the 2 kyr time slice 'bins' neatly. Therefore, it

was necessary to use discretion in 'binning' the accretion rates into the appropriate time slice. It was essential to select accretion rates calculated over short durations (high resolution data). Accretion rates calculated over time periods of up to 4 kyr were used to i) allow more data to be included per time slice and ii) to reduce the uncertainties associated with using ^{14}C and U-Th measurements over very short time intervals (Opdyke, 2000). Accretion rates calculated over long durations are usually slower than those calculated over short durations. This occurs because rates calculated over long durations are more likely to encompass periods of hiatal time and erosional events as well as accumulation (Sadler, 1981; Opdyke and Wilkinson, 1993; Opdyke, 2000). This observation is important when trying to assess the accumulation of a typical mass of sediment where one would normally use rates determined over longer durations. However, we required a rate most accurately representing accretion during a 2 kyr time slice. If low resolution data (accretion rates calculated using durations longer than 4 kyr) are used they may artificially suppress the higher accretion rates in phase II and exaggerate the slower rates in phases I and III (Figures 5.3a and b). This could potentially obscure the true pattern and magnitude of Holocene coral reef $CaCO_3$ accumulation. Elsewhere it has been noted that early Holocene (8 to 6 kyr BP) reef accretion rates are consistently higher than those of the last 3 to 2 kyr BP (Davies *et al.*, 1985; Kinsey and Hopley, 1991; Ryan *et al.*, 2001). It as therefore important to split the Holocene into time slices to accurately calculate the global $CaCO_3$ mass balance.

5.5.2 Statistical Manipulation of the Data

Reef accretion rates vary within a core; margin; reef and between reefs in the same reef province, it is therefore necessary to calculate a rate representative of the majority of reefs in a province for each time slice. We made as few statistical assumptions as possible. Trimmed mean accretion rates, the mean calculated after the removal of outlier data, were calculated for time slices where 10 or more rate values were available (Figures 5.4 a-f). For time slices where less than 10 rate values were available the true or arithmetic mean was calculated after removal of individual spuriously high rates (Figures 5.4 a-f). For example, for the East Indian Ocean time slice 6 to 4 kyr BP, 7 rate data were available; 0.73, 0.82, 0.98, 2.4, 4.8, 7.5 and 29.3 m kyr^{-1}. Coral core accretion rates usually fall within the range of 0 to 10 m kyr^{-1}. Therefore, the rate of 29.3 m kyr^{-1} was considered to be unreliably high and was therefore removed before the arithmetic mean rate was calculated to reduce potential bias in the small dataset by extreme outlier

values (Figure 5.4 e). Figures 5.4 a-f illustrate the variation in the rates calculated from the literature. Figures 5.4 a-f also highlight the need for more radiocarbon dated cores to be obtained which will enable a statistically robust calculation of mean accretion rates for all of the time slices within each reef province. Figures 5.4 a-f highlight those provinces and time slices for which few accretion rate values, if any, are available. For example, the time slice, 10 to 8 kyr BP, is under represented with respect to accretion rate values in all of the reef provinces.

The mean accretion rates calculated are not definitive rates representative of each time slice for each reef province, the rates may change appreciably as more drill core data become available (Figure 5.5). However, we have attempted to take as conservative and methodical an approach to data manipulation as possible. The methods employed here represent a first step towards revising the carbonate budget with statistically robust data. In total, accretion rate data from over 300 reef cores representing over 130 reefs globally were used to estimate the global Holocene $CaCO_3$ mass balance (Figure 5.6).

5.5.3 Temporal Variation in Reef Area

The area available for reef growth has changed during the Holocene in response to sea level rise and other environmental factors including turbidity, light, salinity, nutrients and temperature. Kleypas (1997) used a predictive model (ReefHab) to estimate the changes in area available for reef growth from the LGM to present. Results indicate that, as the continental shelves became flooded by sea level rise, the area available for reef colonisation increased rapidly to a maximum at 6 ka. Between 6 ka and present, the area available for reef colonisation decreased slightly to between 5.84 and 7.46×10^5 km^2. The most recent estimate of Spalding *et al.* (2001) suggests that present day reef area is 2.84×10^5 km^2. To obtain a temporal perspective of the changes in $CaCO_3$ accumulation through the Holocene, the proportional changes in reef area revealed by Kleypas's (1997) ReefHab model were used to redefine the reef province area estimates for each time slice representing the early to mid-Holocene in Method 2 (Equation 5.2). For example, the ReefHab model predicts that between 4 and 6 kyr BP the area available for reef growth was 106 % of present day reef area. To calculate reef area for the GBR for the time slice 4-6 kyr BP, the present day reef area for GBR from Spalding *et al*. (2001) of 44917 km^2 was multiplied by 1.06 to give the reef area in the GBR between 4 and 6 kyr BP (47612 km^2). The aim of this step was to reduce potential errors associated with the extrapolation of the present day reef area estimates back into

the Holocene when attempting to calculate the $CaCO_3$ accumulated during the early Holocene. In the early Holocene, coral growth was reduced because either less accommodation space was available for coral colonisation (large areas of substrate had yet to be flooded by the transgression) or the rate of sea level rise was too rapid for reef growth to keep-up.

5.5.4 Comparison with the Ice Core Records

In order to put the coral reef CO_2 release into perspective with respect to the Taylor Dome ice core record, the flux of CO_2 available to the atmosphere per time slice was converted into a decadal parts per million by volume (ppmv) change in atmospheric CO_2 concentration using the conversion factor of Houghton *et al.* (1994; Indermuhle *et al.*, 1999; Figure 5.7). The Taylor Dome ice core record data are reported as absolute calendar ages; so we have converted these marine radiocarbon ages using the plots of Stuiver and Braziunas (1993). The one-way flux of coral reef CO_2 was plotted as a cumulative decadal change in CO_2 (ppmv) against the Taylor Dome record starting from the initial concentration at 10 kyr BP, assuming that all other fluxes and reservoirs associated with the atmospheric CO_2 pool remained constant during the last 10 kyr (Figure 5.7).

5.5.5 Porosity

Vecsei (2004a) proposed that inaccurate porosity estimates are one of the main sources of error in calculating the mass of reef $CaCO_3$. It has been suggested that the porosity of reef sediments may range from 20 to 80 % (Kinsey and Hopley, 1991; Hubbard *et al.*, 1998; Vecsei, 2004a). Assuming a porosity (P) value of 50 % for reef sediments may lead to overestimates of the mass of $CaCO_3$ accumulated (Vecsei, 2004a). To estimate the effect of porosity variation on the amount of coral reef CO_2 released, Method 2 calculations were carried out using porosity value of 77 % estimated by Hubbard *et al.* (1998) for high porosity *Acropora palamata* open framework (Figure 5.7).

5.6 Results

5.6.1 Method 1: Comparison with Opdyke and Walker (1992)

Using the same method as Opdyke and Walker (1992) we calculate a mean global Holocene reef framework accretion rate of 1.2 m kyr^{-1}, a global $CaCO_3$ mass balance of 1650 Gt over 5 kyr duration and estimate that coral reefs could have released approximately 436 Gt of CO_2 to the Holocene atmosphere over 5 kyr (Table 5.2). All other things being equal, this flux would have led to an increase in atmospheric CO_2 concentration of 57 ppmv, with an average flux of 0.011 ppmv yr^{-1} or 0.024 Gt C as CO_2 per year (Table 5.2).

Table 5.2. Global Mass and Flux of $CaCO_3$ Estimated for the Holocene (Method 1). [a] Global Holocene mean accretion rate calculated from 1764 accretion rates complied from published literature, normalised to 5 kyr duration. [b] Sum of reef area estimates for reef provinces from Spalding *et al.* (2001) and Sheppard and Wells (1988). [c] Mass $CaCO_3$ (Gt) accumulated in 5 kyr calculated using Equation 5.2. [d] Flux CO_2 available for release to the atmosphere resulting from coral reef calcification, calculated by applying Ware *et al.*'s (1991) seawater buffering factor. 5 kyr is the general duration of reef growth during the Holocene (Opdyke and Wilkinson, 1993; Rees *et al.*, 2005). [e] Calculated using conversion of Houghton *et al.* (1994) of 0.478 ppmv increase per Gt C released as CO_2.

Mean Accretion Rate [a] m kyr^{-1}	Reef Area [b] km^2	$CaCO_3$ Accumulated [c] Gt	Flux $CaCO_3$ 10^{13} mol yr^{-1}	CO_2 in 5 kyr [d] Gt	Total ppmv Change [e]
1.2	189600	1650	0.33	436	57

5.6.2 Method 2: Temporal and Spatial Variation within the Holocene

Coral reef mean framework accretion rates have varied both between reef provinces (spatially) and through the Holocene (temporally) (Figures 5.4 a-f, 5.5 and 5.6). All provinces show a similar overall pattern of decreasing accretion rates through the Holocene between 8 and 0 kyr BP (Figures 5.5 and 5.6). No accretion rate data could be found to represent the East Pacific reef province prior to 6 kyr BP and the East Indian Ocean prior to 8 kyr BP. The East Pacific reef province exhibits an unusual pattern of variation in accretion rates through the Holocene, the mean accretion rate for the 2 to 0 kyr BP time slice is higher than that for the 4 to 2 kyr BP time slice (Figures 5.5 and 5.6).

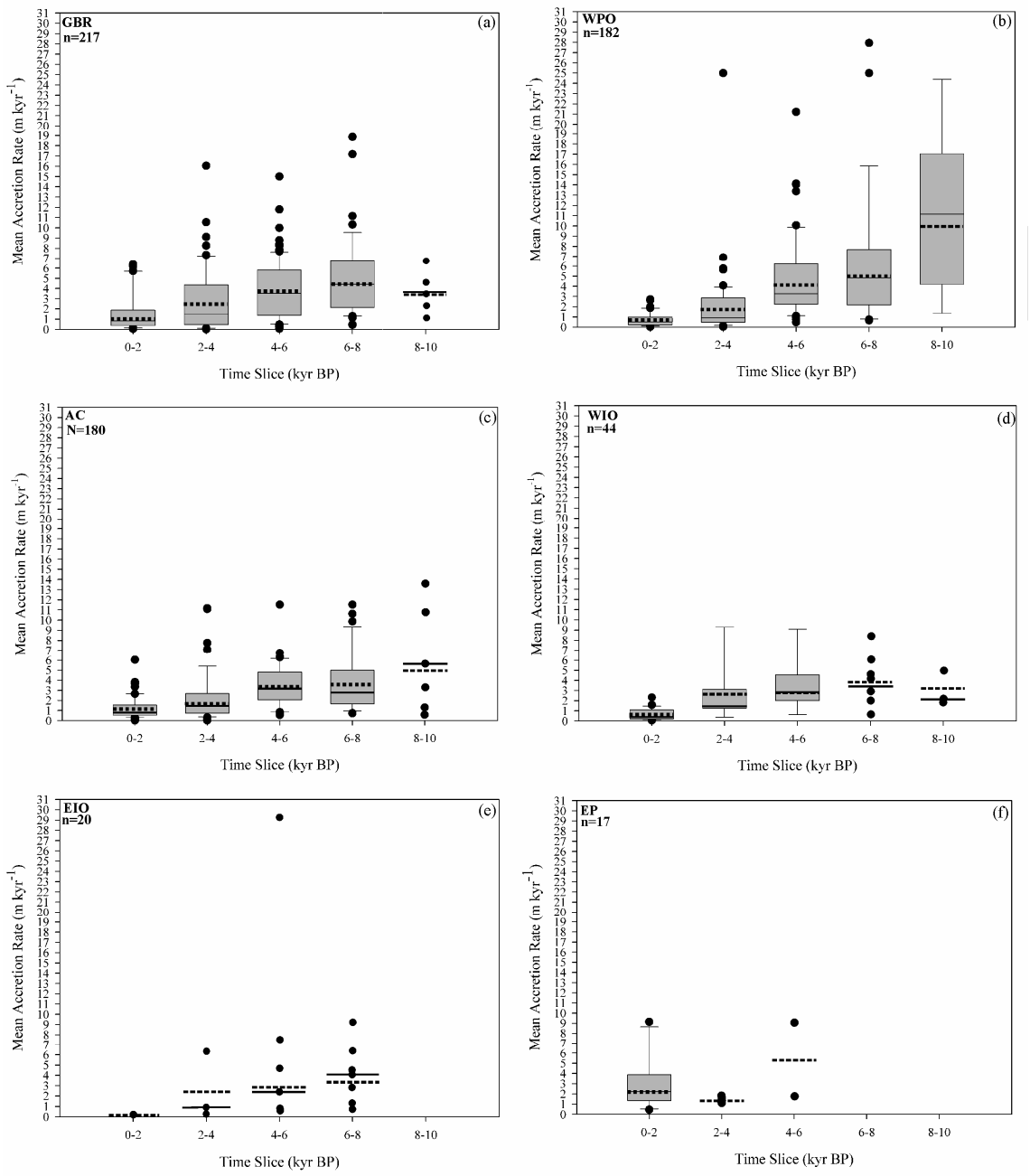

Figure 5.4 a-f. Box plots of the variation in the accretion rate data used to calculate the trimmed and arithmetic mean accretion rates for each time slice for each reef province. (a) Great Barrier Reef, (b) Western Pacific Ocean, (c) Atlantic-Caribbean, (d) Western Indian Ocean, (e) East Indian Ocean and (f) East Pacific. The accretion rates used in the mass balance calculations are represented by dotted lines (trimmed means) and dashed lines (arithmetic means). The unbroken horizontal line indicates the median, if it is the same as the trimmed or arithmetic mean it is not shown. The inter-quartile range for each time slice is indicated by the vertical unbroken lines and outlier data indicated by filled circles.

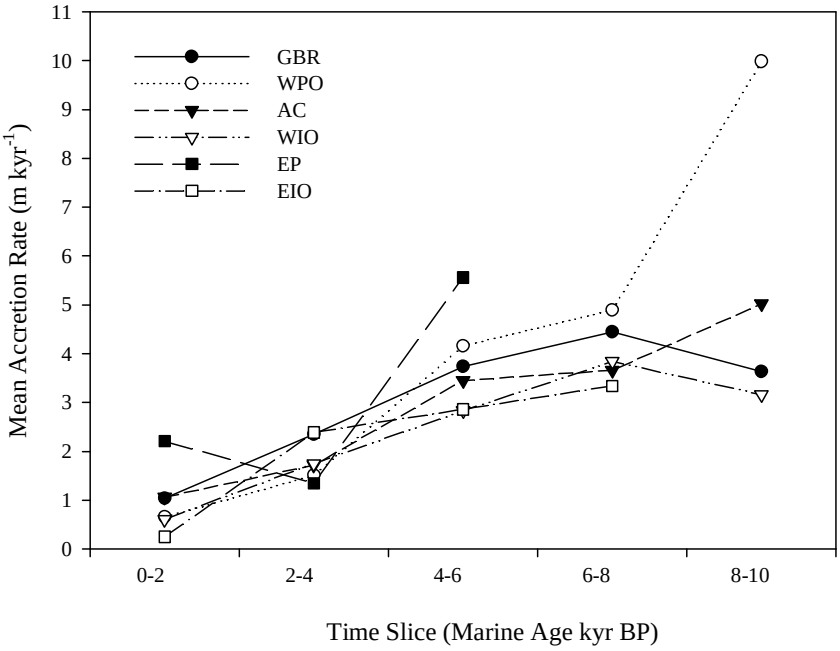

Figure 5.5. Variation in mean framework accretion rates through the Holocene for each reef province using Method 2. Time scale is marine radiocarbon age. GBR – Great Barrier Reef, WPO – Western Pacific Ocean, AC – Atlantic Caribbean, WIO – Western Indian Ocean, EP – East Pacific Ocean, EIO – Eastern Indian Ocean.

The accretion rates of both the Western Indian Ocean and the Great Barrier Reef are lower for the 10 to 8 kyr BP time slice than for the 8 to 6 kyr BP time slice, similar to the hypothetical growth curves in Figures 5.3 (Figures 5.5 and 5.6). The Western Pacific reef province exhibits the highest mean accretion rate (9.98 m kyr^{-1}) between 10 and 8 kyr BP (Figures 5.5 and 5.6). Rates of vertical accretion exhibit a positive correlation with rates of sea level rise in the Great Barrier Reef, Western Pacific Ocean, Atlantic Caribbean, Western Indian Ocean and the Eastern Indian Ocean (Figures 5.6 a-e). Higher vertical accretion rates coincide with rapid rates of sea level rise in response to the increase in accommodation space available for reef growth and the need for corals to remain in the photic zone (Figures 5.6 a-e). Rates of vertical accretion decrease as the rate of sea level rise slows or once sea level stabilized at its modern level. Figures 5.6 a-f indicate the importance of the rate of sea level rise on the rate of reef accretion. We conservatively estimate the total amount of $CaCO_3$ accumulated by coral reefs during the Holocene to be 7970 Gt (Table 5.3).

The majority of $CaCO_3$ accumulation occurred in the early to mid-Holocene between 10 and 4 kyr BP, $CaCO_3$ accumulation during the late Holocene (between 2 and 0 kyr BP) was much less significant (Table 5.3; Figure 5.7). The Western Pacific

province accumulated the majority of global $CaCO_3$ during the Holocene (Figure 5.7; Table 5.3). The global mass balance of $CaCO_3$ accumulated through the Holocene is a reflection of the pattern of variation in the accretion rates (Figures 5.5, 5.6 and 5.7; Table 5.3). The mean accumulation rates are, to first order, similar between the reef provinces, hence the regional contributions to the global mass balance are dominated by the area term (Figure 5.7; Table 5.3). The flux of CO_2 available to the atmosphere during the Holocene ranged from 7.31 to 1.32 × 10^{12} mol yr^{-1} (643 to 116 Gt CO_2 per 2 kyr time slice) between 10 and 8 kyr BP and between 2 and 0 kyr BP (Table 5.4).

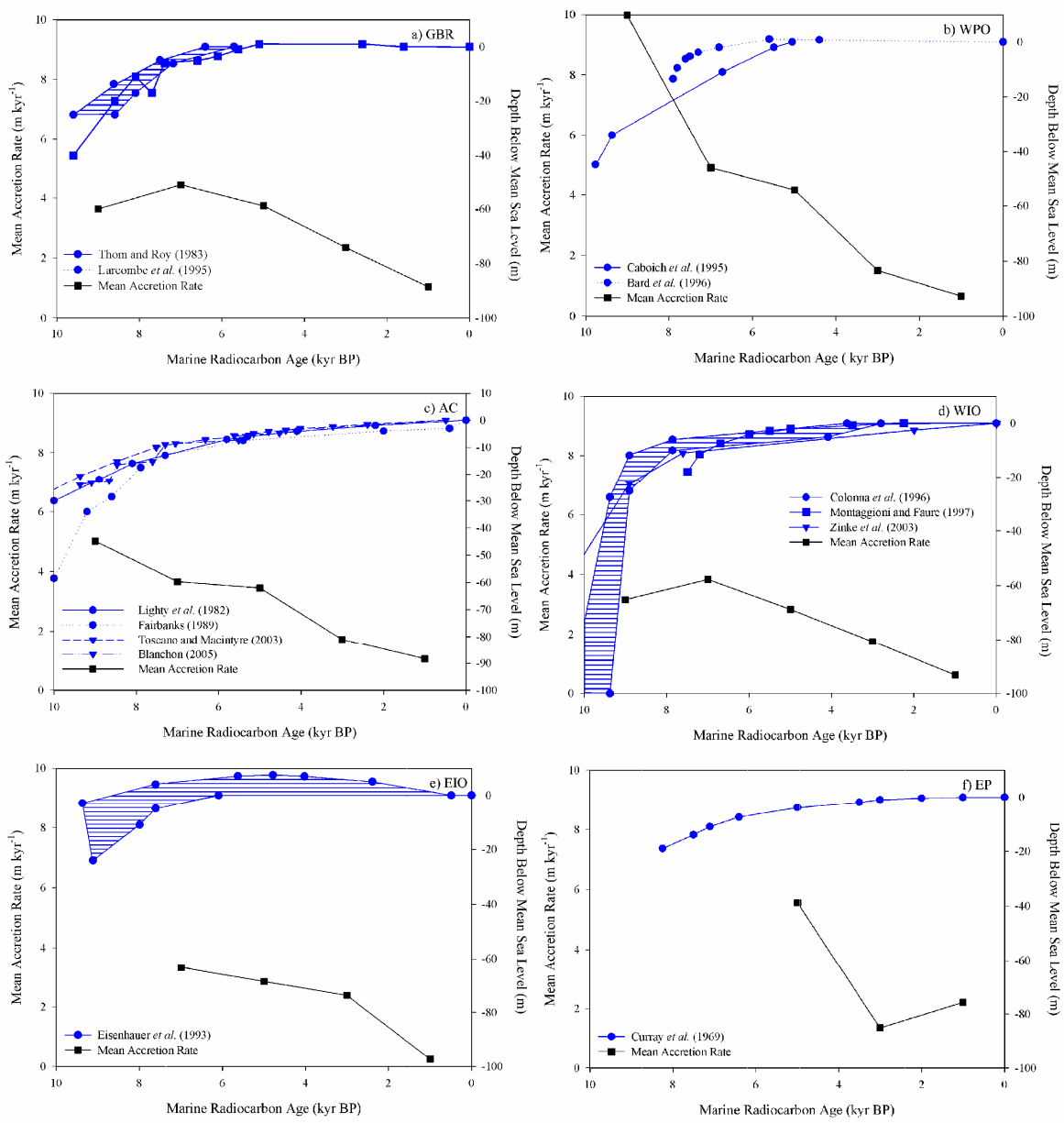

Figure 5.6 Variation in sea level curves (blue) and mean framework accretion rates (black) through the Holocene for each reef province using Method 2. (a) Great Barrier Reef (modified from Thom and Roy (1983)'s relative sea level envelope (shaded area) for north east Australia and Larcombe *et al.*'s (1995)

relative sea level curve for the Central Great Barrier Reef, between Hayman Island and Cape Tribulation, established using 364 radiocarbon dates from a variety of materials from across the shelf), (b) Western Pacific Ocean (modified from Caboich *et al.*'s (1995) New Caledonian relative mean sea level curve and Bard *et al.*'s (1996) Tahiti sea level curve both established using radiometrically dated coral cores), (c) Atlantic-Caribbean (modified from Fairbanks's (1989) Barbados (western tropical Atlantic) sea level curve established using radiometrically dated coral cores, Lighty *et al.'s* (1982) western tropical Atlantic sea level curve established using radiometrically dated coral cores from a variety of locations, Toscano and Macintyre's (2003) revised Lighty *et al.'s* (1982) sea level curve based on radiometrically dated coral cores and mangrove peat samples and Blanchon's (2005) stepped-wise sea level curve for the Western Atlantic), (d) Western Indian Ocean (modified from: Zinke *et al.*'s (2003) sea level curve established using radiometrically dated coral and lagoon sediment cores from Mayotte, Montaggioni and Faure's (1997) Mauritius Island sea level curve established using radiometrically dated coral cores from Pointe-au-Sable reef and Colonna *et al.*'s (1996) sea level envelope established using radiometrically dated coral drill cores and submersible samples from Mayotte Reef), (e) East Indian Ocean (modified from Eisenhauer *et al.'s* (1993) sea level envelope (shaded area) for Morley Reef, Abrolhos Islands established using radiometrically dated coral cores. The lower curve assumes the corals grew at sea level, the top curve assumes the corals grew at depth under water) and (f) East Pacific (modified from Curray *et al.*'s (1969) sea level curve for the Pacific coast of Mexico). Time scale is marine radiocarbon age.

Table 5.3. Reefal $CaCO_3$ Accumulated in each Reef Province per Time Slice (Method 2). [a] RP, Reef Province; GBR, Great Barrier Reef; WPO, Western Pacific Ocean; AC, Atlantic-Caribbean; WIO, Western Indian Ocean; EIO, East Indian Ocean and EPO, East Pacific Ocean. [b] Reef area estimates from Spalding *et al.* (2001) and Sheppard and Wells (1988). [c]Note time scale is marine radiocarbon age (kyr BP).

RP [a]	RA[b] 10^4 km^2	$CaCO_3$ Accumulated in each Reef Province per Time Slice [c] Gt					Holocene $CaCO_3$ Total Gt
		2-0	4-2	6-4	8-6	10-8	
GBR	4.492	135.5	324.5	472.6	474.2	302.6	1709.4
WPO	9.894	189.4	459.3	1157.8	1150.2	1832.7	4789.6
AC	2.055	63.2	108.7	199.4	178.9	191.5	741.6
WIO	1.853	32.8	99.7	147.5	169.2	108.7	557.9
EPO	0.268	17.2	11.1	41.9	0	0	70.2
EIO	0.404	2.93	29.7	32.5	32.1	0	97.3
Global Total	18.97	440.9	1032.9	2051.7	2004.9	2435.4	**7965.9**

The greatest flux of CO_2 to the atmosphere occurred between 10 and 8 kyr BP (7.31×10^{12} mol yr^{-1}) and compares to only 1.32×10^{12} mol yr^{-1} between 2 and 0 kyr BP (Table 5.4). The total amount of CO_2 available for release during the Holocene as a consequence of coral reef calcification is 2100 Gt CO_2, which, all other things being

equal would have resulted in a 274 ppmv increase in Holocene atmospheric CO_2 concentration (Table 5.4; Figure 5.8). Use of a reef porosity of 77 % instead of 50 % yields significantly less CO_2 to the atmosphere (only 126 ppmv; Figure 5.8).

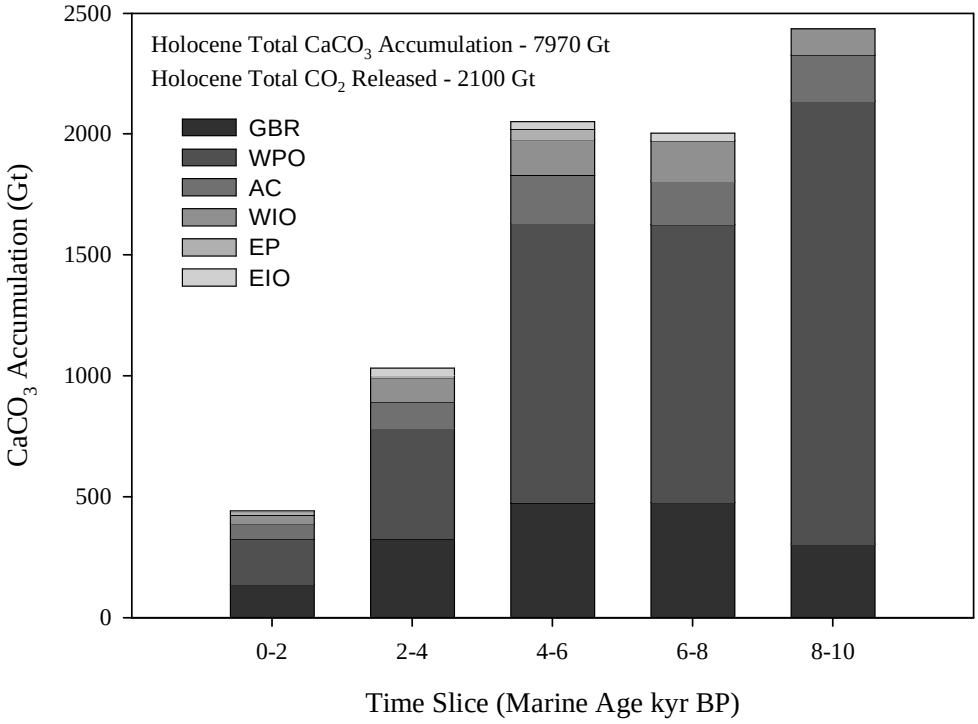

Figure 5.7. Coral reef $CaCO_3$ accumulated in each reef province during each time slice using Method 2. Note time scale is marine radiocarbon age.

Table 5.4. CO_2 Available for Release to the Atmosphere during the Holocene (Method 2). [a] Note time scale is marine radiocarbon age. [b] Assuming all CO_2 available for release, calculated using the seawater buffering factor of (Ware *et al.*, 1991), passes across the air-sea interface. [c] Calculated assuming Houghton *et al.'s* (1994) conversion of 0.0478 ppmv increase in atmospheric CO_2 concentration per Gt C released as CO_2.

Time Slice [a] kyr BP	Flux CO_2 to Atmosphere [b] 10^{12} mol yr^{-1}	CO_2 Released in Time Slice Gt	Flux CO_2 to Atmosphere Gt C yr^{-1}	Flux CO_2 to Atmosphere [c] ppmv yr^{-1}	Ppmv Change
2-0	1.32	116.4	0.016	0.008	15.2
4-2	3.10	272.7	0.037	0.018	35.5
6-4	6.16	541.7	0.074	0.035	70.6
8-6	6.02	529.3	0.072	0.035	69.0
10-8	7.31	643	0.088	0.042	83.8
Global Holocene Total		**2103**			**274.2**

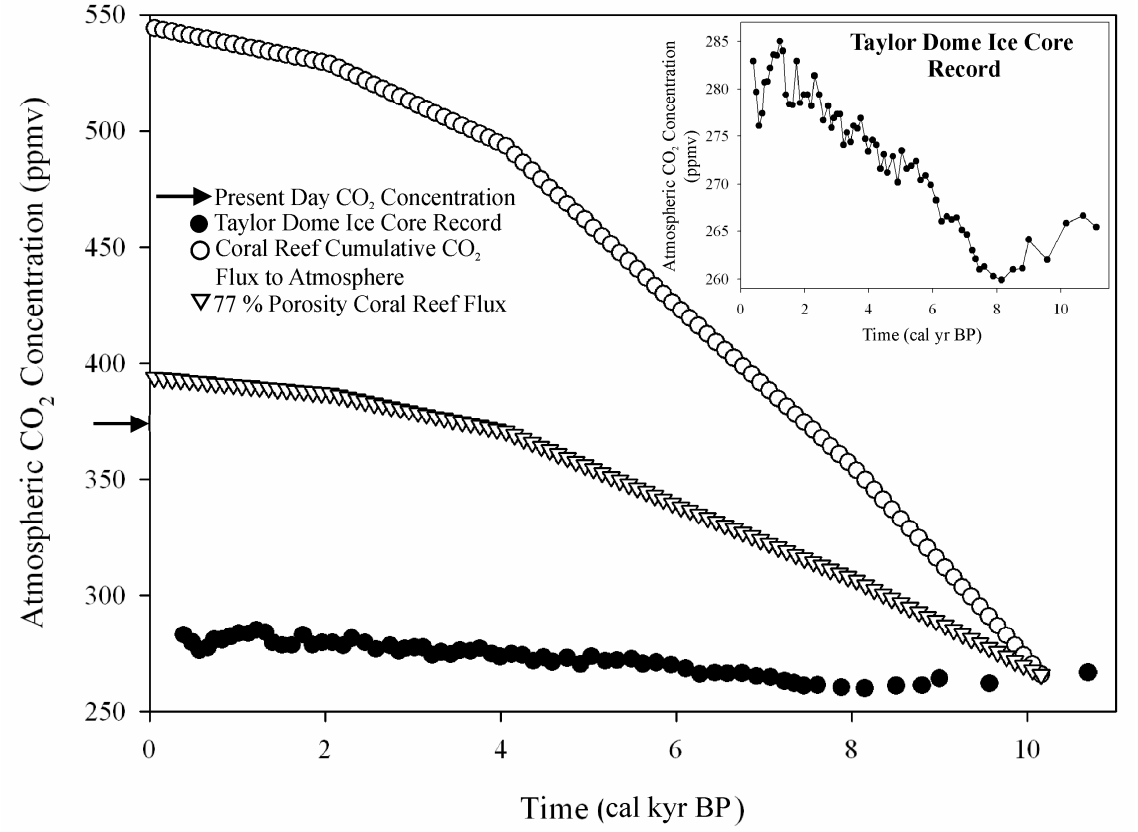

Figure 5.8. 'Coral reef' CO_2 release to the atmosphere compared to the actual change in atmospheric CO_2 concentration measured in the Taylor Dome ice core record (Indermuhle *et al.*, 1999) and the present day atmospheric CO_2 concentration of 375 ppmv, arrow (CDIAC, 2005), assuming all 'coral-reef' derived CO_2 available for release passes across the air-sea interface. Filled circles indicate the effect of adding the cumulative decadal flux of reef released CO_2 to the Holocene atmosphere to an initial concentration at 10 kyr BP (assuming that all other fluxes and reservoirs remain constant). The conversion factor of Houghton *et al.* (1994) each Gt C as CO_2 added to the atmosphere corresponds to an increase in atmospheric CO_2 concentration of 0.478 ppmv. Open triangles indicate the 23 % framework, 77 % porosity *Acropora palmata* reef CO_2 flux (Hubbard *et al.*, 1998; Vecsei, 2004a).

5.7 Discussion

5.7.1 Method 1: Comparison with Opdyke and Walker (1992)

Using Method 1 we calculate a mean accretion rate (normalised to 5 kyr duration) for Holocene coral reefs of 1.2 m kyr^{-1} from over 1700 rate values (Table 5.2). This compares with rates calculated by previous studies of 1.6 m kyr^{-1} from over 60 carbonate sequences (Opdyke and Walker, 1992) and 1.1 ± 0.5 m kyr^{-1} estimated from 220 rate values (Opdyke and Wilkinson, 1993; Opdyke, 2000) for shallow water carbonate environments including reefs, ooids, carbonate mud and sand. Our new mean accretion rate is consistent with the assertion that the mean Holocene accretion rate is

well above the long term average carbonate sediment accretion rate of 0.014 to 0.03 m kyr^{-1} (8 to 9 × 10^{12} mol yr^{-1} or 14 to 30 m m.yr^{-1}) (Wilkinson *et al.*, 1991; Opdyke, 2000). These high rates indicate that the increase in interglacial (Holocene) carbonate deposition is likely to significantly affect both the carbon and alkalinity budgets of the ocean (Tables 5.2 and 5.5; Walker and Opdyke, 1995).

Table 5.5. Previous Estimates of Holocene Average Neritic Accretion Rates. [a] Neritic facies including coral reefs, ooids, mud and sand carbonate embayments.

Reference	Year	Carbonate Type	Average Accretion Rate (m kyr^{-1})
Method 1		Coral reef	1.2
Opdyke	2000	Neritic facies[a]	1.1 ± 0.5
Opdyke and Wilkinson	1993	Neritic facies[a]	1.1 ± 0.5
Opdyke and Walker	1992	Neritic facies[a]	1.6
Milliman	1974	Neritic facies[a]	0.4

The new Holocene mean accretion rate (1.2 m kyr^{-1}) yields a global $CaCO_3$ mass balance of 1650 Gt $CaCO_3$ at a rate of 3.3 × 10^{12} mol $CaCO_3$ yr^{-1} (Tables 5.2 and 5.5). This would have made approximately 436 Gt CO_2 available for release to the atmosphere over 5 kyr, at an average rate of 0.024 Gt C as CO_2 yr^{-1}. This corresponds to a 57 ppmv change in atmospheric CO_2 concentration at an average rate of 0.011 ppmv yr^{-1}. This flux estimate compares favourably with the flux of 0.02 ppmv yr^{-1} calculated by Kleypas (1997) using Milliman and Droxler's (1996) current rate of coral reef $CaCO_3$ production (0.9 Gt $CaCO_3$ yr^{-1}). Kleypas (1997) estimates that coral reef calcification could have lead to a 295 ppmv change in atmospheric CO_2 concentration since the LGM. The Holocene mass balance calculated by Method 1 is conservative because it i) only represents reefal $CaCO_3$ accumulated over 5 kyr of Holocene time, and ii) incorporates a mean accretion rate that is low compared to peak growth rates observed during the early to mid-Holocene (Figures 5.4 a-f and 5.5).

5.7.2 Method 2: Temporal and Spatial Variation within the Holocene

5.7.3 Accretion Rate Variation

Coral reef mean vertical accumulation rates have varied both within the Holocene and between different reef provinces of the world during the Holocene, in agreement

with reef drill core literature (Figure 5.5; Davies *et al.*, 1985; Ryan *et al.*, 2001; Montaggioni, 2005). The variation in mean accretion rates through time (Figure 5.5) is consistent with the hypothetical sigmoidal growth curve of Davies and Marshall (1980; Figure 5.3). Reef carbonate accumulated fastest between 10 and 4 kyr BP and slowest between 2 and 0 kyr BP (Figure 5.5). The highest accretion rates for the majority of reef provinces encompass the Holocene climatic optimum between 8 and 6 kyr BP, the so-called global reef initiation period around 8 ka and an interval of rapidly rising sea level between 18 and 6 ka (11.25 m kyr^{-1}; Figures 5.5 and 5.6a-f; Davies *et al.*, 1985; Davies and Montaggioni, 1985; Ridgwell *et al.*, 2003; Montaggioni 2005). Reef growth in all provinces slowed dramatically after 4 kyr BP, for example, the mean accretion rate for the Great Barrier Reef province decreased from 3.7 m kyr^{-1} between 6 and 4 kyr BP to 1 m kyr^{-1} between 2 and 0 kyr BP (Figures 5.5 and 5.6a). As reefs grew to within 2 m of modern sea level, vertical growth was inhibited by a lack of accommodation space and increased wave stress. In the Indo-Pacific sea level reached its current level around 6 kyr BP (Montaggioni, 2005), reef growth response to this can be seen in a decrease in accretion rates after 6 kyr BP in the Great Barrier Reef and Western Pacific (Figures 5.4 a; b; 5.5; 5.6a and b). In the Atlantic Caribbean, sea level only stabilised relatively recently, reef accretion rates for this reef province show a relatively constant range over the Holocene and only decrease slightly after 2 kyr BP (Figures 5.4; 5.5 and 5.6c; Toscano and Macintyre, 2003).

5.7.4 Atlantic vs Pacific Controversy

It has been suggested that, throughout the Holocene, the reefs of the Atlantic-Caribbean accreted more rapidly than those of the Western Pacific (Adey, 1978; Kinsey, 1981). The mean accretion rates computed here do not support this suggestion (Figures 5.5 and 5.6a-f). In fact, we find that the accretion rates for the Western Pacific province are higher than those of the Atlantic-Caribbean province during the early to mid Holocene (10 to 4 kyr BP) ranging from 9.98 to 4.16 m kyr^{-1} and 5.02 to 3.45 m kyr^{-1} respectively (Figures 5.5 and 5.6a-f). Our findings support the view that the controversy can be traced to the erroneous comparison of accretion rates recorded in Atlantic-Caribbean reef cores with predicted rates calculated by extrapolating present day productivity values into the Holocene for the Western Pacific (Kinsey, 1981).

The rate of sea level rise in the Western Pacific Ocean was rapid between 10-6 kyr BP and sea level stabilized at its modern level around 6 kyr BP, this is reflected in the

pattern of vertical accretion rates (Figure 5.6 b). In the Atlantic Caribbean sea level rise was slower than that of the Western Pacific Ocean during the Holocene, modern sea level being reached within the last 1000 years (Figures 5.6 b and c). The slower continual sea level rise may explain the relatively slower reef accretion rates in the Atlantic Caribbean compared to the Western Pacific Ocean.

5.7.5 East Pacific Reef Province

East Pacific reefs show, on average, the lowest Holocene accumulation rates (Figures 5.5 and 5.6). There is a lack of drill core data for East Pacific reefs prior to 6 kyr BP. This is because the majority of the shelf areas in this province were only flooded between 7 and 6 kyr BP and reef initiation apparently lagged transgression by about 1 kyr (Figures 5.6a-f; Macintyre *et al.,* 1992; Cortes *et al.,* 1994). The mean accretion rates for the East Pacific do not follow the hypothetical sigmoidal growth curve shape outlined above (Figures 5.3a; b, 5.5 and 5.6a-f), indicating that factors other than sea level rise have played a significant role in determining the growth potential of these reefs. The factors limiting the growth potential of East Pacific reefs (e.g. Pacific coasts of Panama and Costa Rica) include a lack of antecedent carbonate structures, the occurrence of severe El Nino warming events, annual upwelling of cool nutrient rich waters, a shallow and fluctuating thermocline, a limited number of coral species, turbidity and siliciclastic sedimentation and a relatively narrow continental shelf (Cortes *et al.,* 1994). The lack of accretion rate data for the East Pacific, resulting from environmental disturbances, reinforces the view that reef accretion is not only a reflection of relative sea level variations (Montaggioni, 2000; 2005).

5.7.6 Accretion vs Productivity

The practice of extrapolating present day productivity values back into the Holocene has often led authors to be understandably very conservative when choosing values to represent past reef growth. For example, Vecsei and Berger (2003) and Vecsei, (2004b) used 1 kg $CaCO_3$ m^{-2} yr^{-1} (1 G) to represent productivity between 6 and 0 kyr BP and only double the modern day productivity value (2 kg $CaCO_3$ m^{-2} yr^{-1}; 2 G) to represent global reef production between 8 and 6 kyr BP, the main phase of reef accretion (Figures 5.3a and b and 5.5). In contrast, Smith and Kinsey (1976) indicate the mean productivity rate for modern day fore-reefs to be 4 kg $CaCO_3$ m^{-2} yr^{-1} (4 G; equivalent to 3 to 5 m kyr^{-1} vertical accretion). It has been suggested that reefs in the

early to mid-Holocene could have exhibited production rates nearer to 10 kg $CaCO_3$ m^{-2} yr^{-1} (10 G equivalent to 7 to 10 m kyr^{-1} vertical accretion) (Kinsey, 1981; Ryan *et al.*, 2001). Although Vecsei and Berger's (2003) values of 1 to 2 kg $CaCO_3$ m^{-2} yr^{-1} (1 to 2 G), equivalent to approximately 1 to 1.5 m kyr^{-1} vertical growth, are in agreement with our mean accretion rate for the 2 to 0 kyr BP time slice. We find that these low rates are not representative of reef accretion in the early to mid-Holocene (Figure 5.5). Davies and Hopley (1983) calculated, from reef drill cores, that Holocene accretion rates for the Great Barrier Reef vary between 1 and 16 m kyr^{-1} with a mode of 4 to 6 m kyr^{-1}. Indeed, Vecsei (2004a) acknowledges that the $CaCO_3$ production of individual reefs is not well known and that global carbonate production can only be crudely assessed. Perhaps a better estimate of production for the early to mid-Holocene would be 4 to 10 G, (equivalent to 3 to 7 m kyr^{-1} vertical accretion) because the majority of the mean accretion rates that we calculated for this time period (10 to 4 kyr BP) fall within this range (Figure 5.5). Our dataset suggests that using modern productivity values to estimate Holocene $CaCO_3$ fluxes will underestimate the true accumulation of reef $CaCO_3$ in the early to mid-Holocene by up to an order of magnitude. The values that Vecsei and Berger (2003) use to represent reef production (1 kg $CaCO_3$ m^{-2} yr^{-1}; 1 G) may be suitable for the last 2 kyr but they are not representative of production during the early to mid-Holocene (between 10 and 4 kyr BP; Figure 5.5).

5.7.7 Spatial and Temporal Variation in $CaCO_3$ production

The pattern of variation in the mean accretion rates calculated here (Figures 5.4 a-f and 5.5) compares favourably with the hypothetical sigmodial curves of Davies and Marshall (1980; Figure 5.3). Globally the majority of coral reef carbonate was accumulated during the early to mid-Holocene (Figure 5.7). The reef area estimate has the greatest influence on the final $CaCO_3$ mass balance and estimate of CO_2 available for release and this highlights the need for confidence in the reef area estimates.

5.7.8 Our Estimates Compared to previous Budgets

The two methods employed here calculate different global coral reef $CaCO_3$ mass balance estimates (Tables 5.3 and 5.4). This is to be expected because the compiled data were manipulated in different ways, Method 1 used a larger dataset (1764 rate values normalized to 5 kyr duration) to estimate a mean Holocene accumulation rate. Whereas Method 2 disregards low resolution data (rates calculated over durations longer than 4

kyr) but incorporates a temporal perspective. Previous estimates of the carbonate flux into neritic sediments range from 0.03 to 0.23 × 10^{13} mol yr^{-1} and our estimates fall within the upper limits of this range (Table 5.6).

Table 5.6. Global Coral Reef $CaCO_3$ Flux Estimates. [a] average Holocene flux estimated to be 0.8 × 10^{13} mol $CaCO_3$ yr^{-1}. [b] Western Indian Ocean reefs only. [c] reef only carbonate accumulation of 0.504 × 10^{13} mol $CaCO_3$ yr^{-1} .

Author	Year	Flux of $CaCO_3$ (× 10^{13} mol yr^{-1})
This study Method 1		0.33
This study Method 2		0.22-1.2 [a]
Rees *et al.*	2005	0.043[b]
Vecsei	2004b	0.3
Vecsei and Berger	2003	0.3
Ridgwell *et al.*	2003	0.03 and 0.015
Ryan *et al.*	2001	1.3
Opdyke	2000	1.7
Kleypas	1997	0.6
Milliman and Droxler	1995	0.7
Munhoven and François	1996	1.45
Walker and Opdyke	1995	2-2.3
Munhoven and François	1994	1.1
Milliman	1993	0.5
Opdyke and Walker	1992	1.4-1.9
Kayanne	1992	0.03
Kinsey and Hopley	1991	1.1
Keir and Berger	1985	1.4
Schlanger	1981	0.8
Smith	1978	0.6
Hay and Southam	1977	1.3 [c]
Milliman	1974	0.5

Our estimated fluxes of $CaCO_3$ into reefs compare favourably with previous work but our estimates focus on only coral reefs *sensu strictu* and represent the best constrained coral reef mass balance to date (Table 5.6). Previous mass balance studies have included wider neritic facies, for example, ooids, carbonate muds and sands (Milliman, 1993; Opdyke and Walker, 1992; Vecsei and Berger, 2003). Our new estimates give a better indication of the mass balance of reefal $CaCO_3$ accumulation and flux of CO_2 to

atmosphere than previous estimates because we use i) the more accurate reef area estimate of Spalding *et al.* (2001), ii) a larger dataset of reef only data (to which the reef area estimate relates) and iii) is not subject to potential errors associated with the practice of extrapolating modern day productivity values back into the Holocene.

5.7.9 Glacial-Interglacial Lysocline Depth Changes

Critics of the coral reef hypothesis have argued that estimates of neritic carbonate deposition are too large to be reconciled with the deep sea sedimentary record. Increases in coral reef $CaCO_3$ deposition leads to a reduction in the surface ocean carbonate ion concentration, which when transferred, by ocean mixing, to the deep ocean leads to a shoaling of the lysocline to restore the ocean pH. Shoaling of the lysocline increases the area where dissolution of deep sea carbonate sediment occurs. Changes in the preservation of $CaCO_3$ in deep sea cores record changes in lysocline depth. During interglacials, when coral reef sedimentation is high, the depth of the lysocline is shallower and deep sea carbonate sediments are poorly preserved. Conversely, during glacial periods, when the shelves are exposed and the area available for coral reef growth is significantly reduced, the lysocline deepens increasing deep sea carbonate preservation.

Past estimates of increased neritic carbonate accumulation since the LGM required a change in the depth of the lysocline of between 1 and 2 km (Opdyke and Walker, 1992; Archer and Maier-Reimer, 1994; Walker and Opdyke, 1995; Ridgwell *et al.*, 2003). Evidence from deep sea sediment cores reveal an average global glacial interglacial (for the last 800 kyr) lysocline depth change of only approximately 0.4 to 0.8 km (Farrell and Prell, 1989). Many authors refer to this discrepancy to refute the Coral Reef Hypothesis (Archer and Maier-Reimer, 1994; Sigman and Boyle, 2000). Contrary to these assumptions, cores from the western equatorial Pacific and Atlantic infer local lysocline depth changes of up to 2.1 km (Balsam, 1983; Berger and Keir, 1984; Farrell and Prell, 1989). The results of a coupled model of the global carbon cycle proposed that significant rapid deepening of the lysocline during interglacials may not necessarily be preserved in the deep sea sedimentary record (Walker and Opdyke, 1995). These investigations call into question the assumption that the sedimentary record provides irrefutable evidence to dispute the magnitude and effect of coral reef accumulation on the global carbon cycle.

Opdyke and Walker (1992) estimated that the flux of $CaCO_3$ to neritic sediments (1.4 to 1.9 × 10^{13} mol yr^{-1}) would have caused the lysocline to shallow by approximately 1.5 km. Here we estimate that coral reefs alone could have accumulated 0.33 × 10^{13} mol $CaCO_3$ yr^{-1} during 5 kyr duration (Method 1) or between 0.22 and 1.2 × 10^{13} mol $CaCO_3$ yr^{-1} (average 0.8 × 10^{13} mol $CaCO_3$ yr^{-1}; Method 2) during the Holocene (Table 5.5). Using Opdyke and Walker's (1992) model results as a guide we note that our new coral reef mass balance estimates would have resulted in lysocline depth change of between 0.5 and 1 km, more consistent with the deep sea record (Farrell and Prell, 1989).

5.8 Unaccounted for Carbonate and Potential Sources of Error

5.8.1 Under-Represented Reef Areas

Figure 5.2 highlights the regions of the world where the pattern of Holocene reef growth is still under represented with respect to radiometric dated drill cores, specifically Indonesia, the Red Sea and the Arabian Gulf. The reefs of the Red Sea, Arabian Gulf and Gulf of Aden comprise an area of approximately 2.16 × 10^4 km^2 (Spalding *et al.*, 2001), Indonesian reefs cover approximately 5.102 × 10^4 km^2. These areas, which account for approximately 26 % of global reef area, are not included in our coral reef $CaCO_3$ mass balance. Kinsey and Hopley (1991) estimated that the Red Sea, South East Asia and the Persian Gulf currently produce 320 × 10^6 t $CaCO_3$ yr^{-1} (3.2 × 10^8 mol yr^{-1}), approximately one third of global $CaCO_3$ production, using Smith's (1978) reef area estimate and conservative productivity values. Riegl and Piller (1999) suggest that Northern Red Sea coral carpets accretion rates range from 1 to 2 m kyr^{-1}. They propose that coral carpets may accumulate proportionally more carbonate than coral reefs because of their greater aerial extent and retention of sediments.

5.8.2 Leeward Accretionary Wedge and Lagoon Carbonate

The methods used to estimate the global mass balance of reefal $CaCO_3$ in this study are conservative because accretion rates only record sediment accumulated within the reef margins (windward and leeward). Once reefs approach sea level *in situ* sediment accumulation is reduced by lack of accommodation space and erosion as a result of increased hydrodynamic energy near the sea surface. Large volumes of sediment are eroded and transported to leeward infilling lagoons and forming leeward

accretionary wedge features (Ryan *et al.*, 2001). Erosion of modern day reefs, presently at sea level, commonly removes between 10 and 25 % of the carbonate sediment produced; most of which is transported to leeward (Hubbard *et al.*, 1990; Milliman, 1993). The mass of carbonate within lagoons and leeward accretionary wedges implies that productivity was much higher during the early to mid-Holocene than that measured on reef flats today (Ryan *et al.*, 2001; Dickinson, 2004; Rees *et al.*, 2005). Ryan *et al.* (2001) proposed that leeward accretionary wedges may effectively double the area of reefal carbonate accumulation implying a doubling of the present reef area estimate (2.843×10^5 km^2; Spalding *et al.*, 2001) to 5×10^5 km^2. Interestingly this doubled area estimate agrees with Kleypas's (1997) ReefHab model prediction of present reef area between 5.82 and 7.46×10^5 km^2. Spalding *et al.*'s (2001) reef area estimate is derived from only shallow, physically well developed reefs and represents only reef flats and crests (the areas of highest productivity) it does not include lagoon or reef slope areas and is therefore considered conservative (see Figure 1 in Ryan *et al.*, 2001).

5.8.3 Unaccounted for Tropical Carbonate

In the context of the global Holocene shallow water $CaCO_3$ mass balance our estimates are conservative because they do not include other neritic carbonates, for example, ooids, carbonate embayments, mud, sands and *Halimeda* bioherms. Together, the first three of these carbonate sediment types are estimated to have a combined area of between 2 and 5×10^5 km^2 and are estimated to add 0.44×10^{13} mol $CaCO_3$ yr^{-1} to the total nertic $CaCO_3$ flux (Opdyke and Walker, 1992; Opdyke, 2000). It has been suggested that the amount of $CaCO_3$ within *Halimeda* bioherms may be comparable that of the reef platforms in the Great Barrier Reef province (Flood, 1984; Marshall and Davies, 1988). Presently the aerial extent and contribution *Halimeda* bioherms make to the global carbonate budget are still unknown (Milliman, 1993; Rees *et al.*, 2005).

5.8.4 The Reef Area Estimate

Spalding *et al.* (2001) do not indicate the error range for their reef area estimate, this precludes the inference of error for our estimates of the $CaCO_3$ mass balance and CO_2 available to the atmosphere. However, if we tentatively use Spalding *et al.*'s (2001) assertion that the reef area estimate will probably not exceed 3×10^5 km^2 given further refinement, this estimates a ± 6 % error in the reef area estimate and gives at least a 6 % error to our estimates (Tables 5.3 and 5.4; Figures 5.7 and 5.8). Assuming an error of ±

6 % we calculate the amount of $CaCO_3$ accumulated during the Holocene is 7970 ± 478 Gt $CaCO_3$. This would have released 2100 ± 126 Gt CO_2 to the Holocene atmosphere resulting in an increase in the atmospheric CO_2 concentration of 274 ± 16 ppmv.

5.8.5 Coral Reef Accretion prior to 10 kyr BP

Our estimates of the deglacial $CaCO_3$ mass balance and CO_2 flux to the atmosphere are conservative because only data pertaining to the last 10 kyr BP has been used. The discovery of reefs older than 10 kyr BP (submerged, drowned and uplifted) and those in marginal environments indicates that reef growth may have been more prolific prior to 10 kyr BP than previously thought (Kleypas, 1997; Montaggioni, 2000; 2005). For example, submerged reefs have been documented in Florida, Hawaii, Grand Cayman, Great Barrier Reef, Mayotte and Barbados (Davies and Montaggioni, 1985; Macintyre *et al.,* 1991; Blanchon and Shaw, 1995; Dullo *et al.,* 1998; Blanchon *et al.,* 2002; Webster *et al.,* 2004; Camoin *et al.,* 2004). Indeed Montaggioni (2000; 2005) identified 4 reef generations since the LGM, RGO (23 to 19 kyr BP), RGI (17.5 to 14.7 kyr BP), RGII (13.8 to 11.5 kyr BP) and RGIII (10 to 0 kyr BP) which were interrupted by meltwater pulses when sea level rise outpaced reef growth and drowned the reef growth phases. Montaggioni (2005) interestingly points out that reef generations RGI, RGII and RGIII roughly coincide with rapid atmospheric CO_2 increases. Accretion rates for the time interval prior to 10 kyr BP associated with submerged reefs (Mayotte, Camoin *et al.,* 2004), deeper drill holes (Barbados, Fairbanks, 1989; Bard *et al.,* 1990; Tahiti, Caboich *et al.,* 2003) and uplifted terraces (Huon Penninsula, Chappell and Polach, 1991) have not been included in this assessment because the data are too few and may not be globally representative. Kleypas's (1997) ReefHab model predicted the area of these late Pleistocene reefs would probably only have been between 20 % (17 kyr BP) and 60 % (11 kyr BP) of present day reef area.

5.8.6 Sea-Air Flux of CO_2

The fate of the 0.6 mol of CO_2 produced by the deposition of 1 mole $CaCO_3$ is still debated, we have assumed that the 0.6 mol CO_2 available does pass across the air-sea interface (Equation 5.2). It is possible that not all of the available CO_2 is released to the atmosphere, however, even if it remained in solution it would, nevertheless, affect the atmospheric CO_2 concentration by having a negative effect on the oceans capacity to absorb more CO_2 (Frankignoulle *et al.,* 1994).

5.8.7 Reef Porosity Variation

The assumption that reef framework porosity is 50 % may not be globally representative and may lead to the $CaCO_3$ mass balance being overestimated (Kinsey and Hopley, 1991; Hubbard *et al.*, 1998; Vecsei, 2004a). Here we chose 50 % porosity because it allowed us to compare our results with those of previous authors (Kinsey and Hopley, 1991; Opdyke and Walker, 1992; Opdyke, 2000; Ryan *et al.*, 2001; Rees *et al.*, 2005). Kinsey (1981) proposed that rapid reef growth is usually less consolidated and creates a higher porosity framework than slow reef growth. To illustrate the potential error associated with the variation in reef porosity the coral reef mass balance and flux of CO_2 to the atmosphere were recalculated assuming a porosity of 77 % (open triangles, Figure 5.8). This modification yields only 126 ppmv CO_2 released to the atmosphere during the Holocene (Figure 5.8). The assumption of 50 % porosity may be considered realistic if the carbonate sediments stored within reef lagoons and leeward accretionary wedges are taken into account. These sediments have been shown to be of approximately equal volume to the reef platform itself and including these re-deposited sediments could effectively cancel out any underestimation of porosity within the reef itself (Ryan *et al.*, 2001; Dickinson, 2004).

5.9 Coral Reef CO_2 Flux to the Atmosphere

The greatest flux of CO_2 to the atmosphere is estimated to have occurred between 10 and 4 kyr BP and ranges from 0.088 to 0.074 Gt C as CO_2 yr^{-1} (Table 5.4). Our estimated flux of C as CO_2 released to the atmosphere between 2 and 0 kyr BP (0.016 Gt C as CO_2 yr^{-1}) compares favourably with Ware *et al.*'s (1991) estimate for present day reefs (0.02 to 0.08 Gt C as CO_2 yr^{-1}) calculated using productivity measurements. Yet, Ware *et al.*'s (1991) calculations utilized Smith's (1978) reef area estimate (6×10^5 km^2) which is double Spalding *et al.*'s (2001) estimate (2.843×10^5 km^2). Combining the productivity values used by Ware *et al.* (1991) and the reef area estimate of Spalding *et al.* (2001), we calculated that present day reefs release between 0.01 and 0.04 Gt C as CO_2 yr^{-1} to the atmosphere. It is important to note that this new estimate, like Ware *et al.*'s (1991) initial estimate, does not account for carbonate losses to erosion and dissolution and therefore overestimates the true flux of CO_2 to the modern atmosphere. However, our estimate of 0.016 Gt C as CO_2 yr^{-1} between 2 and 0 kyr BP compares well with the new range calculated here (between 0.01 and 0.04 Gt C as CO_2 yr^{-1}; Table 5.4). Our calculations were estimated using accretion rates estimated for the last 2 kyr, when

the majority of reefs had already reached modern day sea level and reef morphology and community composition were probably very similar to the present day situation. Our estimates of the fluxes of CO_2 to the atmosphere during the early and mid-Holocene (0.088, 0.072 and 0.074 Gt C yr^{-1} for time slices 10 to 8, 8 to 6 and 6 to 4 kyr BP respectively) are higher than those for late Holocene (0.016 Gt C as CO_2 yr^{-1} between 2 and 0 kyr BP; Table 5.4). Reefs in the early Holocene were growing at a faster rate and trying to keep-up or catch-up with sea level rise, reef growth slowed in the late Holocene as reefs grew within 2 to 3 m of sea level as a result of increased hydrodynamic energy near the surface (Figure 5.5; Davies and Hopley, 1983; Ryan *et al.,* 2001). The fluxes of CO_2 calculated here (0.016 to 0.088 Gt C as CO_2 yr^{-1}; Table 5.4) are comparable to the average Holocene flux calculated by Kleypas (1997) using the ReefHab model (0.048 Gt C as CO_2 yr^{-1}). The total amount of CO_2 released to the Holocene atmosphere by reef calcification is estimated to be 2100 Gt CO_2 (573 Gt C as CO_2), which is more than double Vecsei and Berger's (2003) estimate (225 Gt C as CO_2). This is probably because Vecsei and Berger (2003) were very conservative in their choice of production estimates used in their calculations.

5.10 Coral Reef CO_2 flux compared to Ice Core Records

The total amount of CO_2 released by coral reef calcification during the Holocene corresponds to a 274 ppmv cumulative change in atmospheric CO_2 assuming no compensatory sink. This figure is similar to that estimated by Kleypas's (1997) ReefHab model of a 295 ppmv change since the LGM (Figure 5.8). The cumulative concentration of reef derived CO_2 was plotted against the Taylor Dome ice core record using 10 kyr BP as a starting reference atmospheric CO_2 concentration and assuming all other components of the carbon cycle remained the same (Figure 5.8). Our estimated CO_2 change, assuming no compensatory sink (274 ppmv) exceeds the change recorded in the Taylor Dome ice core record of 20 ppmv for the Holocene by an order of magnitude (Indermuhle *et al.,* 1999). The coral reef-derived CO_2 would not have simply pooled in the atmosphere, indeed there is no pulse of CO_2 of the magnitude we calculate, recorded in the Taylor Dome ice core record (Figure 5.8). The atmospheric CO_2 reservoir is dynamic; any increase in one reservoir or flux will be mediated by other processes or reservoirs within the carbon cycle, for example, one third of the anthropogenic release of CO_2 to the atmosphere has already been absorbed by the oceans (Houghton *et al.,* 2001). Indeed several carbon cycle models have combined

coral reef growth with other components of the carbon cycle, for example, calcium carbonate compensation, continental silicate rock weathering and terrestrial biosphere/vegetation re-growth, in an attempt to explain both the deglacial ice core and deep sea sedimentary records (Archer and Maier-Reimer, 1994; Munhoven and Francois, 1994; 1996; Ridgwell *et al.*, 2003; Marchitto *et al.*, 2005). A recent global atmosphere ocean-sediment, carbon cycle modelling study has indicated that a large volume of early Holocene reef released CO_2 could have been absorbed by an increase in terrestrial biosphere re-growth (Ridgwell *et al.*, 2003; Vecsei and Berger, 2003; Vecsei, 2004b).

5.11 Coral Reef and Anthropogenic CO_2 Fluxes

It has been suggested that the coral reef CO_2 flux to the deglacial atmosphere is trivial on a geological time scale given the error terms associated with the global CO_2 budget because it approximates only 0.4 to 1.4 % of the anthropogenic flux (Ware *et al.*, 1991). If we compare the magnitude of the coral reef flux into reefs and the atmosphere with various other natural fluxes and reservoirs, a different picture emerges, (Tables 5.7 and 5.8).

Table 5.7. Comparison of our Coral Reef carbon fluxes with other Natural Carbon Fluxes during the Holocene. [a] Gt C yr^{-1}.

Flux	Pg C yr^{-1} [a]	Reference
River input dissolved $CaCO_3$ to ocean	0.2	Holmen, (1992); Sigman and Boyle, (2000)
DIC surface ocean to deep ocean	1	Holmen, (1992); Sigman and Boyle, (2000)
Deep ocean $CaCO_3$ to burial	0.2	Holmen, (1992); Sigman and Boyle, (2000)
$CaCO_3$ into coral reefs	0.1	Method 2
Coral reef CO_2 into atmosphere	0.06	Method 2

The flux of carbon into coral reef carbonate is half the flux of carbon into the ocean from riverine input and half the burial of carbon as $CaCO_3$ to the deep ocean during the Holocene (Table 5.7). It is also clear that the amount of carbon locked-up in coral reefs and released to the atmosphere by coral reef calcification during the Holocene are comparable to the amount of carbon in the present day terrestrial biosphere and surface ocean DIC (Table 5.8).

Table 5.8. Comparison of our coral reef carbon mass balance with other Natural Reservoirs during the Holocene. [a] Gt C.

Reservoir	Pg C [a]	Reference
Atmosphere	600	Holmen, (1992); Sigman and Boyle, (2000)
Present day atmosphere as CO_2	720	Powlson 2005
Surface ocean DIC	700	Holmen, (1992); Sigman and Boyle, (2000)
Deep Ocean DIC	38,000	Holmen, (1992); Sigman and Boyle, (2000)
Sediments and crust (Ca,Mg) $CaCO_3$	48,000,000	Holmen, (1992); Sigman and Boyle, (2000)
Terrestrial	2100	Holmen, (1992); Sigman and Boyle, (2000)
Increase in the terrestrial biosphere since the LGM	700-1350	Sigman and Boyle, (2000); Adams *et al.* (1990); Crowley, (1995)
Present day soil reservoir (organic carbon)	1500	Powlson 2005
Present day carbon in vegetation	600	Powlson 2005
Coral reef $CaCO_3$ (increase in the size of the reservoir during the Holocene)	956	Method 2
Coral reef CO_2 increase in atmosphere	574	Method 2

Currently, most carbon cycle models and budgets do not include an independent coral reef component (Sigman and Boyle, 2000; Houghton *et al.,* 2001). The current rate of coral reef CO_2 release calculated by this study is approximately 0.3 % of present day anthropogenic fuel emissions of 6.3 ± 0.4 Pg C yr^{-1} (Houghton *et al.,* 2001). The flux of CO_2 estimated here may be minor in comparison to the present anthropogenic flux, however, it is intimately related to atmospheric CO_2 and the ocean carbonate system, as such accurate quantification is a pre-requisite to understanding the global carbon cycle (Milliman, 1993; Ridgwell *et al.,* 2003; Ridgwell and Zeebe, 2005).

5.12 Future Work

This study (Method 2) is an improvement on past budget studies because i) it is calculated using only coral reef data, ii) the dataset contains over 300 reef sequences from 133 reefs and has global coverage, iii) it has a temporal perspective, the Holocene has been spilt into 2 kyr time slices, iv) it incorporates the proportional change in reef area associated with the transgression (Kleypas, 1997) and vi) it utilizes the most accurate and up to date reef area estimate (Spalding *et al.,* 2001).

Future improvements in the global mass balance could be achieved by breaking down each of the reef provinces into smaller regions, for example, splitting the Western Pacific into North Western and South Western Pacific to distinguish between various reef types of this vast province. The north Western Pacific (Japan) consists of mainly

fringing reefs whereas the south Western Pacific is dominated by atolls. Splitting the Atlantic-Caribbean into East and West Caribbean would allow elucidation of the different responses to reefs with different ecological compositions (Macintyre, 1988; Kleypas, 1997). Future refinement of the marine $CaCO_3$ budget will only be made possible by future drilling investigations and a comprehensive breakdown of the reef area estimate which encompasses details of each reef in a region and reef type. Although the CO_2 estimated here is small compared to, for example, the anthropogenic flux it is significant relative to other similar natural fluxes and it is important to note that these reef ecosystems have an uncertain future (Kleypas *et al.,* 1999; Feely *et al.,* 2004). The role coral reefs play in both the global carbon cycle and climate system should be included in modelling studies predicting future CO_2 scenarios.

5.13 References

Adams, J. M., Faure, H., Faure-Denard, L., McGlade, J. M. and F. I. Woodward (1990) Increases in terrestrial carbon storage from the Last Glacial Maximum to the present. *Nature*, **348**, 711-714.

Adey, W. H. (1978) Coral reef morphogenesis: a multidimensional model. *Science,* **202**, 831-837.

Archer, D. and E. Maier-Reimer (1994) Effect of deep-sea sedimentary calcite preservation on atmospheric CO_2 concentration. *Nature,* **367**, 260-263.

Archer, D., Winguth, A., Lea, D. and N. Mayoral (2000) What caused the glacial/ interglacial atmospheric CO_2 cycles? *Reviews of Geophysics*, **38,** 2, 159–189.

Balsam, W. B. (1983), Carbonate dissolution on the Muir Seamount (western North Atlantic): Interglacial/glacial changes. *J. Sediment. Petrol.,* **53**, 719-731.

Bard, E., Hamelin, B., Fairbanks, R. G. and A. Zindler (1990) Calibration of the ^{14}C timescale over the past 30,000 years using mass spectrometric U-Th ages from Barbados corals. *Nature,* **345**, 405-410.

Bard, E., Hamelin, B., Arnold, M., Montaggioni, L., Caboich, G., Faure, G. and F. Rougerie (1996) Deglacial sea level record from Tahiti corals and the timing of global melt water discharge. *Nature,* **382**, 241-244.

Barker, S., Higgins, J. A. and H. Elderfield (2003) The future of the carbon cycle: review, calcification response, ballast and feedback on atmospheric CO_2. *Phil. Trans. R. Soc. Lond. A,* **361**, 1977-1999.

Barnola, J. M., Raynaud, D., Korotkevic, Y. S. and C. Lorius (1987) Vostok ice core provides 160,000 years record of atmospheric CO_2. *Nature,* **329**, 408-414.

Berger, W. H. (1982a) Increase of CO_2 in the atmosphere during deglaciation the coral reef hypothesis. *Naturwissenschaften,* **69**, 87-88.

Berger, W. H. (1982b) Deglacial CO_2 build-up: constraints on the coral reef model. *Pal. Pal. Pal.,* **40,** 235-253.

Berger, W. H. and R. S. Keir (1984) Glacial-Holocene changes in atmospheric CO_2 and the deep-sea record. In J. E. Hansen and T. Takahasi (eds), *Climate Sensitivity*. *Geophys. Monogr. Ser.*, **29**, AGU Washington, D. C., pp 337-351.

Berger, W. H. and J. S. Killingley (1982) Box cores from the equatorial Pacific: ^{14}C sedimentation rates and benthic mixing. *Mar. Geol.,* **45**, 93-125.

Blakeway, D. (2000) Artefacts in reef-accretion curves derived from core: A simulation study. *Proc. 9th Int. Coral Reef Symp. Bali. Indonesia,* **1**, 217-221.

Blanchon, P., Jones, B. and D. C. Ford (2002) Discovery of a submerged relic reef and shoreline off Grand Cayman: Further support for an early Holocene jump in sea level. *Sediment. Geol.,* **147**, 253-270.

Blanchon, P. (2005) Comments on "Corrected western Atlantic sea-level curve for the last 11,000 years based on calibrated ^{14}C dates from *Acropora palmata* framework and intertidal mangrove peat" by Toscano and Macintyre [Coral Reefs (2003) 22: 257-270]. *Coral Reefs*, **24**, 183-186.

Blanchon, P. and J. Shaw (1995) Reef drowning during the last deglaciation: evidence for catastrophic sea-level rise and ice sheet collapse. *Geology,* **23**, 4-8.

Blanchon, P. and D. Blakeway (2003) Are catch-up reefs an artifact of coring? *Sediment.*, **50**, 1271-1274.

Broecker, W. S. and G. M. Henderson (1998) The sequence of events surrounding termination II and their implications for the cause of glacial-interglacial CO_2 changes. *Paleocean.,* **13**, 4, 352-364.

Cabioch, G., Montaggioni, L. F. and G. Faure (1995) Holocene initiation and development of New Caledonian fringing reefs, SW Pacific. *Coral Reefs*, **14**, 131-140.

Cabioch, G., Banks-Cutler, K. A., Beck, W. J., Burr, G. S., Corrège, T., Edwards, R. L. and F. W. Taylor (2003) Continuous reef growth during the last 23 cal kyr BP in a tectonically active zone (Vanuatu, South West Pacific). *Quat. Sci. Revs.,* **22**, 1771–1786.

Camoin, G. F., Montaggioni, L. F. and C. J. R. Braithwaite (2004) Late glacial to post glacial sea levels in the Western Indian Ocean. *Mar. Geol.*, **206**, 119-146.

CDIAC Carbon Dioxide Information Analysis Center (2005) http://cdiac.esd.orn/gov.html

Chappell, J. and H. Polach (1991) Post glacial sea level rise from a coral record at Huon Peninsula, Papua New Guinea. *Nature,* **349**, 147-149.

Chave, K. E., Smith, S. V. and K. J. Roy (1972) Carbonate production by coral reefs. *Mar. Geol.,* **12**, 123-140.

Chrisholm, R. M. and D. J. Barnes (1998) Anomalies in coral reef community metabolism and their potential importance in the reef CO_2 source-sink debate. *Proc. Nat. Acad. Sci. USA.*, **95**, 6566-6569.

Collins, L. B., Zhu, Z. R., Wyrwoll, K-H., Hatcher, B. G., Playford, P. E., Eisenhauer, A., Chen, J. H., Wasserburg, G. J. and G. Bonani (1993) Holocene growth history of a reef complex on a cool-water carbonate margin: Easter Group of the Houtman Abrolhos, Eastern Indian Ocean. *Mar. Geol.,* **115**, 29-46.

Colonna, M., Casanova, J., Dullo, W-C. and G. Camion (1996) Sea-Level Changes and $\delta^{18}O$ Record for the past 34,000 yr from Mayotte Reef, Indian Ocean. *Quat Res*, **46**, 335-339.

Cortes, J., Macintyre, I. G. and P. W. Glynn (1994) Holocene growth history of an Eastern Pacific fringing reef, Punta Islotes, Costa Rica. *Coral Reefs,* **13**, 65-73.

Coxall, H. K., Wilson, P A., Pälike, H., Lear, C. H. and J. Backman (2005) Rapid stepwise onset of Antarctic glaciation and deeper calcite compensation in the Pacific Ocean. *Nature,* **433**, 53-57.

Crowley, T. J. (1995) Ice-Age terrestrial carbon changes revisited. *Glob. Biogeochem. Cy.,* **9**, 377-389.

Curray, J. R., Emmel, F. J. and P. J. S. Crampton (1969) Holocene history of a strand plain, lagoonal coast, Nayarit, México. In A. Ayala-Castañares and F. B. Phleger (eds), *Coastal Lagoons, a symposium-UNAM-UNESCO*. México, D.F., 1967: México University Nac. Autońoma, pp 63-100.

Davies, P. J. (1983) Reef Growth. In D. J. Barnes (ed), *Perspectives on Coral Reefs*. Aust. Inst. Mar. Sci. Brian Clouston Publishing, Manuke, ACT, Australia, pp 69-106.

Davies, P. J. and J. F. Marshall (1980) A model of epicontinental reef growth. *Nature*, **287**, 37-38.

Davies, P. J. and D. Hopley (1983) Growth facies and growth rates of Holocene reef in the Great Barrier Reef. *B. M. R. J. Aust. Geol. Geophys.*, **8**, 237-251.

Davies, P. J., Marshall, J. F. and D. Hopley (1985) Relationships between reef growth and sea level in the Great Barrier Reef. *Proc. 5th Int. Coral Reef Congr. Tahiti*, **3**, 95-103.

Davies, P. J. and L. F. Montaggioni (1985) Reef growth and sea level change: the environmental signature. *Proc. 5th Int. Coral Reef. Congr. Tahiti*, **3**, 477-511.

Dickinson, W. R. (2004) Impacts of Eustasy and hydro-isostasy on the evolution and landforms of Pacific atolls. *Pal. Pal. Pal.*, **213**, 3-4, 251-269.

Dullo, W-C., Camoin, G. F., Blomeier, D., Colonna, M., Eisenhauer, A., Faure, G., Casanova, J. and B. A. Thomassin (1998) Morphology and sediments of the fore slopes of Mayotte, Comoro Island: direct observations from a submersible. *I. A. S. Spec. Publ.*, **25**, 219-236.

Eisenhauer, A., Wasserburg, G. J., Chen, J. H., Bonani, G., Collins, L. B., Zhu, Z. R. and K. H. Wyrwoll (1993) Holocene sea-level determination relative to the Australian continent: U/Th (TIMS) and ^{14}C (AMS) dating of coral cores form the Abrolhos Islands. *Earth Planet. Sci. Lett*., **114**, 529-547.

Fairbanks, R. G. (1989) A 17,000-year glacio-eustatic sea level record: influence of glacial melting rates on the Younger Dyras events and deep ocean circulation. *Nature*, **342**, 637-642.

Farrell, J. W. and W. L. Prell (1989) Climate change and $CaCO_3$ preservation: an 800,000 year bathymetric reconstruction from the central equatorial Pacific ocean. *Paleocean.*, **4**, 447-466.

Feely, R. A., Sabine, C. L. Lee, K. Berelson, W. Kleypas, J. A. Fabry, V. J. and F. J. Millero (2004) Impact of Anthropogenic CO_2 on the $CaCO_3$ System in the Oceans. *Science*, **305**, 362-366.

Flood, P. G. (1984) *A geological guide to the northern Great Barrier Reef*. Australasian Sedimentologists Group Field Guide Series, 1, Sydney, Geological Society of Australia.

Frankignoulle, M. C. and J. P. Gattuso (1993) Air-Sea CO_2 exchanges in coastal ecosystems. In R. Wollast, F. T. Mackenzie and L. Chou (eds), *Interactions of the carbon, nitrogen, phosphorus and sulphur biogeochemical cycles and global change*. NATO ASI Series, 14, Springer-Verlag. New York, Berlin, pp 233-248.

Frankignoulle, M., Canon, C. and J. P. Gattuso (1994) Marine calcification as a source of CO_2: positive feedback of increasing atmospheric CO_2. *Limnol. Oceanogr.*, **39**, 2, 458-462.

Frankignoulle, M., Gattuso, J. P., Biondo, R., Bourge, I., Copin-Montégut, G. and M. Pichon (1996) Carbon fluxes in coral reefs. II. Eulerian study of inorganic carbon dynamics and measurement of air-sea CO_2 exchanges. *Mar. Ecol. Prog. Ser.*, **145**, 123-132.

Gattuso, J. P., Pichon, M., Delesalle, B. and M. Frankignoulle (1993) Community metabolism and air-sea CO_2 fluxes in a coral reef ecosystem (Moorea, French Polynesia). *Mar. Ecol. Prog. Ser*., **96**, 259-267.

Gattuso, J. P., Pichon, M., Delesalle, B., Canon, C. and M. Frankignouelle (1996) Carbon fluxes in coral reefs. I. Lagrangian measurement of community metabolism and resulting air-sea CO_2 disequilibrium. *Mar. Ecol. Prog. Ser.*, **145**, 109-121.

Gattuso J. P., Payri, C. E., Pichon, M., Delesalle, B. and M. Frankignoulle (1997) Primary production, calcification and air-sea CO_2 fluxes of a macroalgal-dominated coral reef community (Moorea, French Polynesia). *J. Phycology*, **33**, 5, 729-738.

Gattuso, J. P., Frankignoulle, M. and S. V. Smith (1999) Measurement of community metabolism and significance of coral reefs in the CO_2 source-sink debate. *Proc. Nat. Acad. Sci. USA.*, **96**, 23, 13017-13022.

Glynn, P. W. and I. G. Macintyre (1977) Growth rate and age of coral reefs on the Pacific coast of Panamá. *Proc. 3rd Int. Coral Reef Symp.*, **2**, 251-259.

Hay, B. J. and J. R. Southam (1977) Modulation of marine sedimentation by continental shelves. In N. R. Anderson and A. Malahoff (eds), *The Fate of Fossil Fuel CO_2 in the Oceans.* Plenum Press, New York, pp 569-604.

Holmen, K. (1992) The global carbon cycle. In S. S. Butcher, R. J. Charlson, G. H. Orians and G. V. Wolfe (eds), *Global Biogeochemical Cycles*. Academic Press, New York, pp 239-262.

Hopley, D. (1982) *The geomorphology of the Great Barrier Reef: Quaternary development of coral reefs.* John Wiley, NY.

Houghton, J. T., Meira Filho, L. G., Bruce, J., Lee, H., Callander, B. A., Hartis, E., Harris, N. and K. Muskell (1994) IPCC: *Radiative forcing of Climate Change and an Evaluation of the IPCC IS92 Emission Scenarios*. Cambridge Univ. Press, New York.

Houghton, J. T., Ding, Y., Griggs, D. J., Noguer, M., van der Linden, P. J., Dai, X., Maskell, K. and C. A. Johnson (2001) *Climate Change 2001: The Scientific Basis, Contributions of Working Group 1 to the Third Assessment Report of the Intergovernmental Panel on Climate Change.* Cambridge University Press, Cambridge, United Kingdom and New York, USA, pp 881.

Hubbard, D. K., Miller, A. I. and D. Scaturo (1990) Production and cycling of $CaCO_3$ in a shelf edge reef system (St Croix, US Virgin Islands): applications to the nature of reef systems in the fossil record. *J. Sediment. Petrol.*, **60**, 3, 335-360.

Hubbard, D. K., Burke, R. B. and I. P. Gill (1998) Where's the reef: the role of framework in the Holocene. *Carbonate and Evaporites*, **13**, 1, 3-9.

Iglesias-Rodriguez, M. D., Armstrong, R., Feely, R., Hood, R., Kleypas, J. A. Milliman, J. D., Sabine, C. and J. Sarmiento (2000) Progress made in study of ocean's calcium carbonate budget. *Eos*, **83**, 34, 365-375.

Indermuhle, A., Stocker, T. F., Joos, F., Ficher, H., Smith, H. J., Wahlen, M., Deck, B., Mastroianni, D., Tschumi, J., Blunier, T., Meyer, R. and B. Stauffer (1999) Holocene carbon cycle dynamics based on CO_2 trapped in ice at Taylor Dome, Antarctica. *Nature*, **398**, 121-126.

Kawahata, H., Suzuki, A. and K. Goto (1997) Coral Reef ecosystems as a source of atmospheric CO_2: evidence from PCO_2 measurements of surface waters. *Coral Reefs*, **16**, 261-266.

Kawahata, H., Suzuki, A. and K. Goto (1999) PCO_2 spatial distribution in coral reefs of Majuro Atoll, Marshall Islands. *Geochem. J.*, **33**, 295–303.

Kawahata, H., Suzuki, A., Ayukai, T. and K. Goto, (2000) Distribution of the fugacity of carbon dioxide in the surface seawater of the Great Barrier Reef. *Mar. Chem.*, **72**, 257–272.

Kayanne, H. (1992) Deposition of $CaCO_3$ into Holocene reefs and its relation to sea level rise and atmospheric CO_2. *Proc. 7th Int. Coral Reef Sym., Guam,* **1**, 50-55.

Kayanne, H., Suzuki, A. and H. Saito, (1995) Diurnal changes in the partial pressure of carbon dioxide in coral reef water. *Science,* **269**, 214-216.

Keir, R. S. and W. H. Berger (1985) Late Holocene carbonate dissolution in the equatorial Pacific: reef growth or neoglaciation? In E. T. Sundiquist and W. S. Broecker (eds), *The carbon cycle and atmospheric CO_2 natural variations archean to present. Geophysics. Monograph. Ser.,* **32**, 208-219.

Kinsey, D. W. (1979) *Carbon Turnover and Accumulation by Coral Reefs.* Unpublished PhD Thesis, University of Hawaii, pp 248.

Kinsey, D. W. (1981) The Pacific-Atlantic reef growth controversy. *Proc. 4th Int. Coral Reef Symp. Manila, 1,* 493-495.

Kinsey, D. W. and D. Hopley (1991) The significance of coral reefs as global carbon sinks – response to greenhouse. *Pal. Pal. Pal.*, (Global and Planetary change section), **89**, 363-377.

Kleypas, J. A. (1997) Modelled estimates of global reef habitat and CO_2 production since the last glacial maximum. *Paleocean., **12***, 533-545.

Kleypas, J. A., Buddemeier, R. W., Archer, D., Gattuso, J. P., Langdon, C. and B. N. Opdyke (1999) Geochemical consequences of increased atmospheric CO_2 on coral reefs. *Science,* **284**, 118-120.

Kraines, S., Suzuki, Y., Omori, T., Shitashima, K., Kanahara, S. and H. Komiyama (1997) Carbonate dynamics of the coral reef system at Bora Bay, Miyako Island. *Mar. Ecol. Prog. Ser.,* **156**, 1–16.

Lambeck, K. and J. Chappell (2001) Sea level change through the last glacial cycle. *Science,* **292**, 679.

Larcombe, P., Carter, R. M., Dye, J., Gagan, I. M. K. and D. P. Johnson (1995) New evidence for episodic post-glacial sea-level rise, central Great Barrier Reef, Australia. *Mar. Geol.,* **127**, 1-44.

Lighty, R. G., Macintyre, I. G. and R. Stuckenrath (1982) *Acropora palmata* Reef Framework: A Reliable Indicator of Sea Level in the Western Atlantic for the Past 10,000 Years. *Coral Reefs*, **1**, 125-130.

Macintyre, I. G. (1988) Modern coral reefs of the Western Atlantic. New geological perspective. *AAPG Bull*, **72**, 1360-1369.

Macintyre, I. G., Rutzler, K., Norris, J. N., Smith, K. P., Cairns, S. D., Bucher, K. E. and R. S. Steneck (1991) An early Holocene reef in the western Atlantic: submersible investigations of a deep relict reef off the west coast of Barbados, W. I. *Coral Reefs,* **10**, 167-174.

Macintyre, I. G., Glynn, P. W. and J. Cortés (1992) Holocene Reef History in the Eastern Pacific: Mainland Costa Rica, Cano Island, Cocos Island, and Galápagos Islands. *Proc. 7th Int. Coral Reef Symp., Guam,* **2**, 1174-1184.

Marchitto, T. M., Lynch-Stieglitz, T. J. and S. R. Hemming (in press) Deep Pacific $CaCO_3$ compensation and glacial–interglacial atmospheric CO_2. *Earth Planet. Sci. Lett.*

Marshall, J. F. and P. J. Davies (1988) *Halimeda* Bioherms of the Northern Great Barrier Reef. *Coral Reefs,* **6**, 139-148.

Milliman, J. D. (1974) *Marine Carbonate, Recent sedimentary carbonates, 1*. Springer-Verlag, N.Y.

Milliman, J. D. (1993) Production and accumulation of calcium carbonate in the ocean: budget of a non-steady state. *Glob. Biogeochem. Cy*., **7**, 927-957.

Milliman, J. D. and A. W. Droxler (1996) Neritic and pelagic carbonate sedimentation in the marine environment: ignorance is not bliss. *Geol. Rundsch.*, **85**, 495-511.

Montaggioni, L. F. (2000) Postglacial reef growth. *Earth Planet. Sci.*, **331**, 319-330.

Montaggioni, L. F. (2005) History of Indo-Pacific coral reef systems since the last glaciation: Development patterns and controlling factors. *Earth-Sci. Revs.*, **71**, 1-2, 1-75.

Montaggioni, L. F. and G. Faure (1997) Response of reef coral communities to sea-level rise: a Holocene model from Mauritius (Western Indian Ocean). *Sediment.*, **44**, 1053-1070.

Munhoven, G. and L. M. François (1994) Glacial-interglacial changes in continental weathering possible implications for atmospheric CO_2. In Zahn *et al.*, (eds), *Carbon Cycling in the Glacial Ocean: Constraints on the Ocean's Role in Global Change*. Springer-Verlag, Berlin. pp 39-58.

Munhoven, G. and L. M. François (1996) Glacial-interglacial variability of atmospheric CO_2 due to changing continental silicate rock weathering: A model study. *J Geophysical Res*, **101**, D16, 21,423-21,437.

Mylroie, J. E. (1993) Return of the coral reef hypothesis: Basin to shelf partitioning of $CaCO_3$ and its effect on atmospheric CO_2: Comment. *Geology*, **21**, 475.

Opdyke, B. N. (2000) Shallow water carbonate deposition and its effect on the carbon cycle. In T. M. L. Wigley and D. S. Schimel (eds), *The Carbon Cycle*. Cambridge University Press, Cambridge.

Opdyke, B. N. and J. C. G. Walker (1992) Return of the coral reef hypothesis: Basin to shelf partitioning of $CaCO_3$ and effect on Holocene atmospheric CO_2. *Geology*, **20**, 733-736.

Opdyke, B. N. and B. H. Wilkinson (1993) Carbonate mineral saturation state and cratonic limestone accumulation. *Am. J. Sci.*, **293**, 217-234.

Petit, J. R., Jouzel, J., Raynaud, D., Barkov, N. I., Barnola, J. M., Basile, I., Bender, M., Chappellaz, J., Davis, M., Delaygue, G., Delmatte, M., Kotlyakov, V. M., Legrand, M., Lipenkov, V. U., Lorius, C., Pepon, L., Ritz, C., Saltzmane, E. and M. Stievenard (1999) Climate and atmospheric history of the past 420,000 years from the Vostock ice core, Antarctica. *Nature*, **399**, 429-435.

Powlson, D. (2005) Will soil amplify climate change? *Nature*, **433**, 204-205.

Rees, S. A., Opdyke, B. N., Wilson, P. A. and L. K. Fifield (2005) Coral Reef sedimentation on Rodrigues and the Western Indian Ocean and its impact on the carbon cycle. *Phil. Trans. R. Soc. Lond. A*, **363**, 101-120.

Ridgwell, A. J., Watson, A. J., Maslin, M. A. and J. O. Kaplan (2003) Implications of coral reef build-up for the late quaternary carbon cycle. *Palaeocean.*, **18**, 4, 1083.

Ridgwell, A. J. and R. E. Zeebe (2005) The role of the global carbonate cycle in the regulation and evolution of the Earth system. *Earth Planet. Sci. Lett.*, **234**,299 - 315

Riegl, B. and W. E. Piller (1999) Coral frameworks revisited-reefs and coral carpets in the northern Red Sea. *Coral Reefs*, **18**, 241-253.

Ryan, D. A., Opdyke, B. N. and J. S. Jell (2001) Holocene sediments of Wistari Reef towards a global quantification of coral reef related neritic sedimentation in the Holocene. *Pal. Pal. Pal.*, **175**, 1-12.

Sadler, P. M. (1981) Sediment accumulation rates and the completeness of stratigraphic sections. *Jn. Geol*, **89**, 569-584.

Schlanger, W. (1981) The paradox of drowned reefs and carbonate platforms, *Geol. Soc. Am. Bull. Part 1*, **92**, 197-211.

Shackleton, N. J. (2000) The 100,000-year ice age cycle identified and found to lag temperature, carbon dioxide and orbital eccentricity. *Science*, **289**, 1897-1902.

Sheppard, C. and S. M. Wells (1988) *Coral reefs of the world, Vol 2*. Indian Ocean, Red Sea and Gulf, IUCN, Conservation Monitoring Centre. International Union for Conservation of Nature and Natural Resources, Switzerland.

Sigman, D. M. and E. A. Boyle (2000) Glacial/interglacial variations in atmospheric carbon dioxide. *Nature*, **407**, 859-869.

Smith, S. V. (1978) Coral reef area and the contributions of reefs to the processes and resources of the world's oceans. *Nature*, *273*, 225-226.

Smith, S. V. (1983) Coral Reef Calcification. In D. J. Barnes (ed), *Perspectives on Coral Reefs*. Brian Cloustan Publishing, Manuka, ACT, Australia, pp 240-247.

Smith, S. V. and D. W. Kinsey (1976) Calcium carbonate production, coral reef growth and sea level change. *Science*, **194**, 937-939.

Smith, S. V. and D. W. Kinsey (1978) Calcification organic carbon metabolism as indicated by carbon dioxide. In D. R. Stoddart and R. E. Johannes (eds), *Coral Reefs: research Methods*. UNESCO, Paris, pp 469-484.

Smith, S. V. and P. L. Jokiel (1978) Water composition and biogeochemical gradients in the Canton Atoll lagoon. *Atoll Res. Bull.*, **221**, 15-53.

Smith, S. V. and F. Pesret (1974) Processes of carbon dioxide flux in the Fanning Island Lagoon. *Pac. Sci.*, **28**, 255-245.

Spalding, M. D. and A. M. Grenfell (1997) New estimates of global and regional coral reef areas. *Coral Reefs*, **16**, 225-230.

Spalding, M. D., Ravilious, C. and E. P. Green (2001) *World Atlas of Coral Reefs*. Prepared at the UNEP World Conservation Monitoring Centre. University of California Press, Berkeley, USA.

Stuiver, M. and T. F. Braziunas (1993) Modelling atmospheric ^{14}C influences and ^{14}C ages of marine samples to 10,000 BC. *Radiocarbon*, **35**, 1, 137-189.

Suzuki, A., Kawahata, H. and G. Goto (1997) Reef water CO_2 system and carbon cycle in Majuro Atoll, The Marshall Islands in the Central Pacific. *Proc. 8th Int. Coral Reef Symp.* (Smithsonian Tropical Research Institute, Balboa, Panamá), 971-976.

Thom, B. G. and J. Chappell (1975) Holocene sea-levels relative to Australia. *Search*, **6,** 90-93.

Thom, B. G. and P. S. Roy (1983) Sea-level change in New South Wales over the past 15,000 years. In D. Hopley (ed), *Australian Sea Levels in the Last 15,000 years: A Review*. Dept. Geography, James Cook University, Monograph Series, Occasional Paper No. 3, Townsville, Australia, pp 64-84.

Toscano M. A. and I. G. Macintyre (2003) Corrected western Atlantic sea-level curve for the last 11,000 years based on calibrated ^{14}C dates from *Acropora palmata* framework and intertidal mangrove peat. *Coral Reefs*, **22**, 257–270

Vecsei, A. (2004)a A new estimate of global reefal carbonate production including the fore-reefs. *Global Planet. Change*, **43**, 1-18.

Vecsei, A. (2004)b Holocene carbon fluxes from reef and peat accumulation: on the way to balancing the carbon cycle. *8th Int. Conf. Paleoceanography*. 5-10 September 2004, Biarritz, France, Program and Abstracts, 100, Bordeaux 1 University.

Vecsei, A. and W. H. Berger (2003) Increase of atmospheric CO_2 during deglaciation: Constraints on the coral reef hypothesis from patterns of deposition. *Global Biogeochem. Cy.*, **18**, 1, GB1035 (DOI:10.1029/2003GB002147).

Walker, J. C. G. and B. N. Opdyke (1995) Influence of variable rates of neritic carbonate dissolution on atmospheric CO_2 and pelagic sediments. *Paleocean.*, **10**, (3), 415-427.

Ware, J. R., Smith, S. V. and M. L. Reaka – Kudla (1991) Coral reefs: sources or sinks of atmospheric CO_2. *Coral Reefs*, **11**, 127-130.

Webster, J. M., Clague, D. A., Rier-Coleman, K., Gallup, C., Braga, J. C., Potts, D., Moore, J. G., Winterer, E. L. and C. K. Paull (2004) Drowning of the -150 m reef off Hawaii: A casualty of global meltwater pulse 1A? *Geology*, **32**, 3, 249-252.

Wilkinson, B. H., Opdyke, B. N. and T. Algeo (1991) Time partitioning in cratonic carbonate rocks. *Geology*, **19**, 1093-1096.

Yamamuro, M., Kayanne, H. and M. Minagawa (1995) Carbon and nitrogen stable isotopes of primary producers in coral reef ecosystems. *Limnol. Oceanogr.*, **40**, 617–621.

Zeebe, R. E. and D. A. Wolf-Gladrow (2001) *CO_2 in Seawater: Equilibrium, Kinetics, Isotopes*. Elsevier Oceanography Series, 65, Amsterdam, pp 346.

Zinke, J., Reijmer, J. J. G., Thomassin, B. A., Dullo, W. CHr., Grootes, P. M. and H. Erlenkeuser (2003) Postglacial flooding history of Mayotte Lagoon (Comoro Archipelago, southwest Indian Ocean). *Mar Geol*, **194**, 181-196.

5.14 Acknowledgements

This research has been supported by the National Environment Research Council (NERC) and Australian National University Earth and Marine Sciences Department. The authors thank Dr L. Keith Fifield (Department of Nuclear Physics, RSPhysSE, Australian National University) for discussions regarding the manipulation of radiometric data, Dr Joanie Kleypas (National Center for Atmospheric Research, Boulder) for details of the ReefHab model results, Dr Peter Challenor (NOCS) for discussions regarding statistical manipulation of the data, Matthew Palmer (NOCS/UK Met Office) for help constructing Figure 5.1 and the National Oceanic Library staff, (NOCS).

Chapter Six

The Significance of *Halimeda* Bioherm Carbonate in the Global Budget revisited.

Plate 6.1 *Halimeda* $CaCO_3$ plates washed up on Lizard Island, NGBR.

Chapter 6

A Review of the Significance of *Halimeda* Bioherm Carbonate in the Global Budget revisited.

Reference: Rees S. A., Opdyke, B. N., Wilson, P. A. and T. Henstock (manuscript submitted 25.08.05) A Review of the Significance of *Halimeda* Bioherm Carbonate in the Global Budget revisited. *Coral Reefs.*

6.1 Abstract

Since the correlation between carbon dioxide (CO_2) levels and global temperatures was established in the ice core records, quantifying the components of the global carbon cycle has become a priority with a view to constraining models of the climate system. The link between the marine carbonate budget and atmospheric CO_2 levels draws attention to the fact that this budget is still not adequately quantified. In fact, it has been suggested that *Halimeda* bioherms on the shelf of the Northern Great Barrier Reef may contain an equal or greater volume of carbonate than the reefs themselves. The quantitative significance to the marine carbonate budget of the calcareous green alga *Halimeda* in particular is still poorly understood. We estimate that the *Halimeda* bioherms on the outer shelf of the Northern Great Barrier Reef contain at least as much (and up to 400 % more) $CaCO_3$ sediment as the adjacent ribbon reef facies. This finding, along with other discoveries of extensive biohermal features in other parts of the world (Java Sea, Timor Sea, Caribbean) highlights the fact that this part of the carbonate budget needs further investigation.

6.2 Introduction

6.2.1 Carbonate Budgets

The role of neritic carbonate within the global carbon cycle is yet to be adequately quantified (Ridgwell and Zeebe, 2005). Documenting the loci and rates of carbonate production and accumulation during the Holocene is the key to quantifying the shallow water carbonate budget (Milliman, 1993). Recently, Rees *et al.* (submitted manuscript) estimated that coral reefs have accumulated approximately 7970 Gt $CaCO_3$ over the last

10 kyr BP at an average rate of 0.8 Gt $CaCO_3$ yr^{-1}. It is widely accepted that the calcareous green alga *Halimeda* is a prominent contributor of carbonate to reef sediment facies in the tropics, however, *Halimeda* bioherms remain one of the main reservoirs of unaccounted for carbonate (Hillis-Colineax, 1980; Drew and Abel, 1983; Phipps *et al*., 1985; Milliman, 1993; Freile *et al*., 1995; Steneck and Testa, 1997; Hillis, 1997).

Milliman (1993) estimated that *Halimeda* bioherms presently accumulate approximately 0.15 Gt $CaCO_3$ yr^{-1} globally. This estimate was based on estimated numbers of *Halimeda* meadow crops per year and the assumption that, globally, bioherms cover an area of 5×10^4 km^2. Hillis (1997) attempted a first budget for modern day *Halimeda* meadows using estimates of lagoon, ridge and bioherm area and *Halimeda* crops per year (Smith and Kinsey, 1976; Smith, 1978; Milliman, 1993). Hillis (1997) estimated that global *Halimeda* bioherm production is presently 0.4 Gt $CaCO_3$ yr^{-1}, approximately 8 % and 83 % of the global carbonate and coral reef carbonate production respectively. Despite these early attempts to determine a *Halimeda* carbonate budget, the global distribution, aerial extent and role of *Halimeda* in the global carbon cycle have yet to be precisely quantified for both the present day and the past (Milliman, 1993; Rees *et al*., 2005).

Here we attempt to determine the quantitative relationship between *Halimeda* bioherm and coral reef derived carbonate accumulated during the Holocene on the outer shelf of the Northern Great Barrier Reef Province using data from seismic profiles, reef drill cores and *Halimeda* bioherm piston and vibrocore cores from the published literature (Orme *et al*., 1978; Davies and Hopley, 1983; Davies *et al*., 1985; Orme, 1985; Davies and Marshall, 1985; Marshall and Davies, 1988; Orme and Salama, 1988; Wolanski *et al*., 1988).

6.2.2 Halimeda

Halimeda is a genus of macroscopic calcareous green algae (Order Caulepales; Chlorophyta; Hillis, 1997; Heyward *et al*., 1997). The bushy plants are composed of numerous calcified (60-80 % $CaCO_3$) flat segments between 0.5-3 cm wide which are joined at un-calcified nodes (Drew, 1993). The calcified segments are shed as part of the growth - senescence cycle by disintegration of the nodes (Drew, 1993; Hillis, 1997). *Halimeda* are found in a variety of habitats from mangrove prop roots to the reef front, are common on coral reefs and can create complex habitats which serve as a refuge, nursery grounds and food for a variety of organisms (Hillis-Colineaux, 1986a; Hillis,

1997; Steneck and Testa, 1997; Heyward *et al*., 1997). *Halimeda* have been in existence since the Cretaceous and are presumed to have contributed to reef sediments for at least the last 65 Ma (Elliot, 1965; Johnson, 1969; Hillis-Colineaux, 1980; Hillis, 1997). Indeed it has been proposed that modern bioherms are reminiscent of phylloid algal bioherms of late Paleozoic reefs that presently act as hydrocarbon reservoirs (Ball *et al*., 1977; Wray, 1977; Drew and Abel, 1988; Kirkland *et al.*, 1993). Thirty species of *Halimeda* are recognised worldwide of which 19 taxa can be found on the Great Barrier Reef (Drew and Abel, 1988; Heyward *et al*., 1997). Various different terms have been used to describe the range of different structures created by *Halimeda* sediments (Table 6.1).

Table 6.1. Terms used to describe *Halimeda* sediment formations.

Term	Definition	Reference	Year
Bioherms	mounds which have relief above the sea floor but which do not exhibit a clear framework and which exist in a relatively low energy environment	Davies and Marshall	1985
Meadow	inter-reefal areas of luxuriant *Halimeda* vegetation	Drew and Abel	1988
Mounds or Banks	discrete circular mounds of *Halimeda* debris that sometimes coalesce into ridges	Drew and Abel	1988
Drapery	vertical meadow of loose sprawling plants that hang over the cemented escarpment ledges	Freile *et al.*	1995

6.2.3 Halimeda Bioherms

Significant accumulations of *Halimeda* debris have been found worldwide. Actively accreting *Halimeda* bioherms have been described in exposed and protected environments in the Eastern Java Sea, Indonesia on Kalukalukuang Bank (K bank) (Roberts *et al*., 1987a; b; 1988; Phipps and Roberts, 1988). These bioherms are approximately 20 to 30 m thick, locally 50 m high and are commonly 10 km wide. Vibrocores reveal that they are composed of *Halimeda* packstone with foraminifera-rich carbonate mud and exhibit accumulation rates varying from 2.94 to 5.9 m kyr^{-1} (Roberts *et al*., 1987a; b; Roberts and Phipps, 1988). Hine *et al*. (1988) discovered extant *Halimeda* bioherms 20 to 30 m in height (some reaching as high as 140 m) that form an almost continuous band, approximately 125 km long, in water depths of 40 to 50 m in the Southwest Caribbean (Nicaraguan Rise, Miskito Channel). These banks are composed of coarse poorly cemented packstones and grainstones of largely dead disarticulated *Halimeda* segments. *Halimeda* rich gravel deposits up to 15 m in relief

with accumulation rates averaging 0.2 m kyr^{-1} have been described on the Fly River Delta, Gulf of Papua New Guinea (Harris *et al*., 1996). A series of 8 submerged carbonate platforms, which range in size from 0.05 to 40 km^2, in the Timor Sea, North Western Australia were found to be dominated by *Halimeda* bank deposits (Heyward *et al*., 1997). Cores from these banks reveal that over 80 % of the total sediment was *Halimeda* debris.

6.2.4 Halimeda Bioherms of the Great Barrier Reef

Maxwell (1968) estimated that approximately 10 to 30 % of the reef surface in the Great Barrier Reef is composed of *Halimeda* rubble and that 5 to 65 % of the inter-reefal sediments are derived from *Halimeda*. The majority of *Halimeda* meadows are located between the latitudes of 10º30'S and 15º35'S (Far Far North Great Barrier Reef to Northern Great Barrier Reef) on the outer shelf, at depths of between 20 and 40 metres below sea level (Figures 6.1 A and B; Drew and Abel, 1983; 1988). Seismic profiling studies have revealed the absence of *Halimeda* bioherm deposits in the Princess Charlotte Bay and Bathurst Bay areas, just north of Lizard Island (Figure 6.1 B; Orme, 1983; 1985). Whereas, further north, seismic profiles reveal the presence of bioherms in the region adjacent to Lloyd Bay and the Lockhart River, between North Lloyd Island and Hibernia Entrance and between Restoration Island and Second Small Reef (12º47'S, Figure 6.1 B; John S. Jell, personal communication). Significant (1.5 to 14 m thick) *Halimeda* deposits have also been found within the Swains Reef Complex (20º53'S to 22º24'S) of the Southern Great Barrier Reef (Maxwell, 1973; Searle and Flood, 1988). Radiocarbon dating of sediments from the top 4.3 m of the Swains Reef bioherms reveal accretion rates of between 2 and 3.5 m kyr^{-1} during the last 5 kyr (Searle and Flood, 1988).

Halimeda bioherms have been investigated in detail using seismic profiling, echo sounding, vibro and piston coring and grab sampling in two regions of the Northern Great Barrier Reef, Lizard Island and Cooktown (Figures 6.2 and 6.3; Orme *et al*., 1978; Orme, 1985; Davies and Marshall, 1985; Phipps *et al*., 1985; Orme and Salama, 1988; Marshall and Davies, 1988). Seismic investigations in the Lizard Island region (between latitudes of 14º27'S and 15º02'S) reveal the presence of extensive *Halimeda* bioherms behind the ribbon reefs. These bioherms are up to 6 km wide, 100 km long and can reach thicknesses of 18.5 m at a depth of 25 m below sea level (Figure 6.2; Orme *et al*., 1978; Orme, 1983; Flood and Orme, 1988; Orme and Salama, 1988). The

bioherms are composed of *Halimeda* packstone and wackstone and reach maximum thickness of 18.5 m in the east but are less well developed in the west.

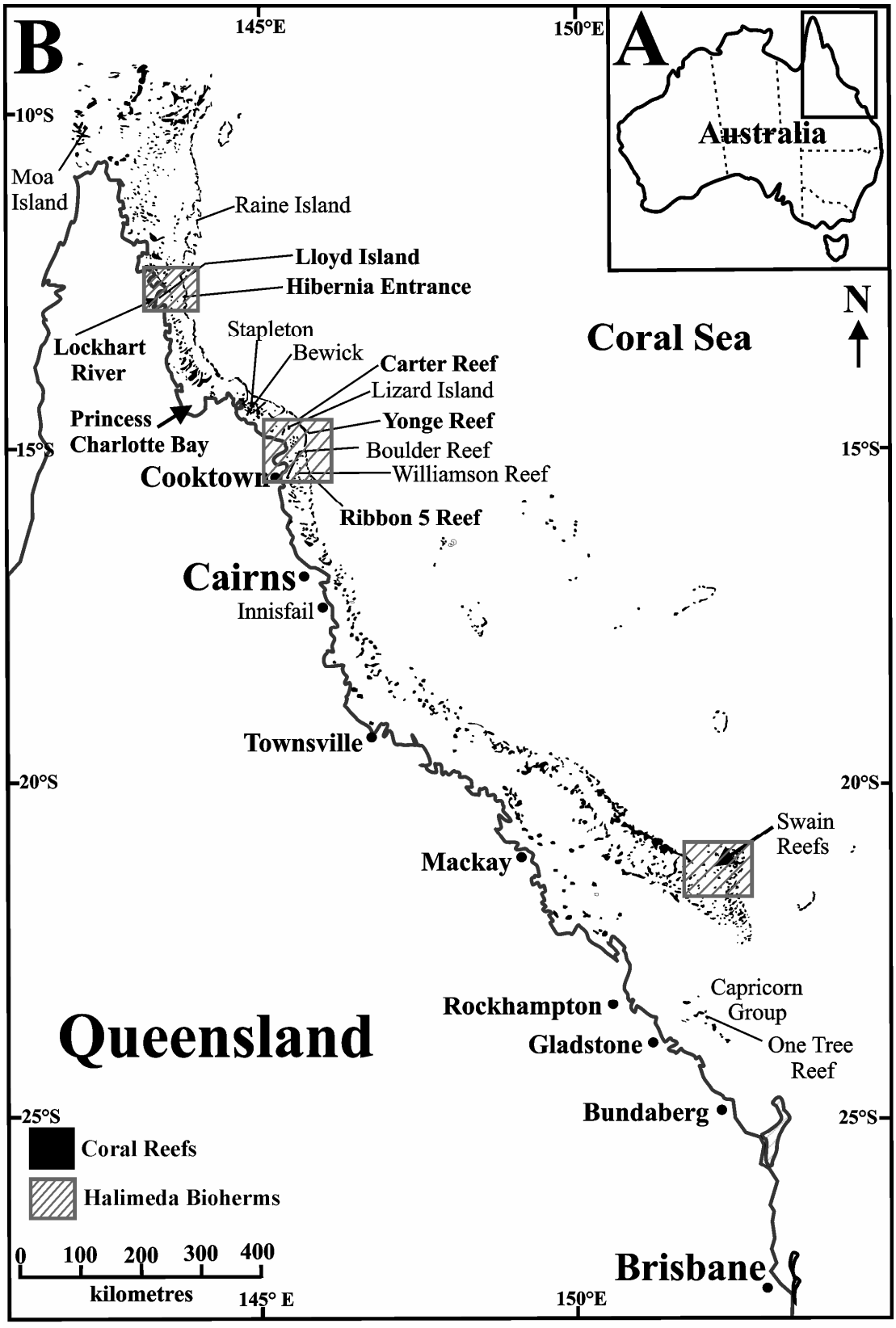

Figure 6.1 A Australia showing location of the Great Barrier Reef (modified after Flood, 1984). B The Great Barrier Reef (modified after Hopley and Davies, submitted manuscript). The majority of *Halimeda*

meadows are located between the latitudes of 10º30'S and 15º35'S (Far Far North Great Barrier Reef to Northern Great Barrier Reef).

The Lizard Island region bioherms are formed of ridges and mounds separated by hollows and channels, living *Halimeda* vegetation is found on the tops of the bioherms. Radiocarbon dating of the peat surface immediately below the bioherms reveals that they were formed during the Holocene (radiocarbon age of a peat sample 10,070 ± 180 yr BP) and were initiated some 1.5 kyr before the nearby ribbon reefs (Orme, 1985).

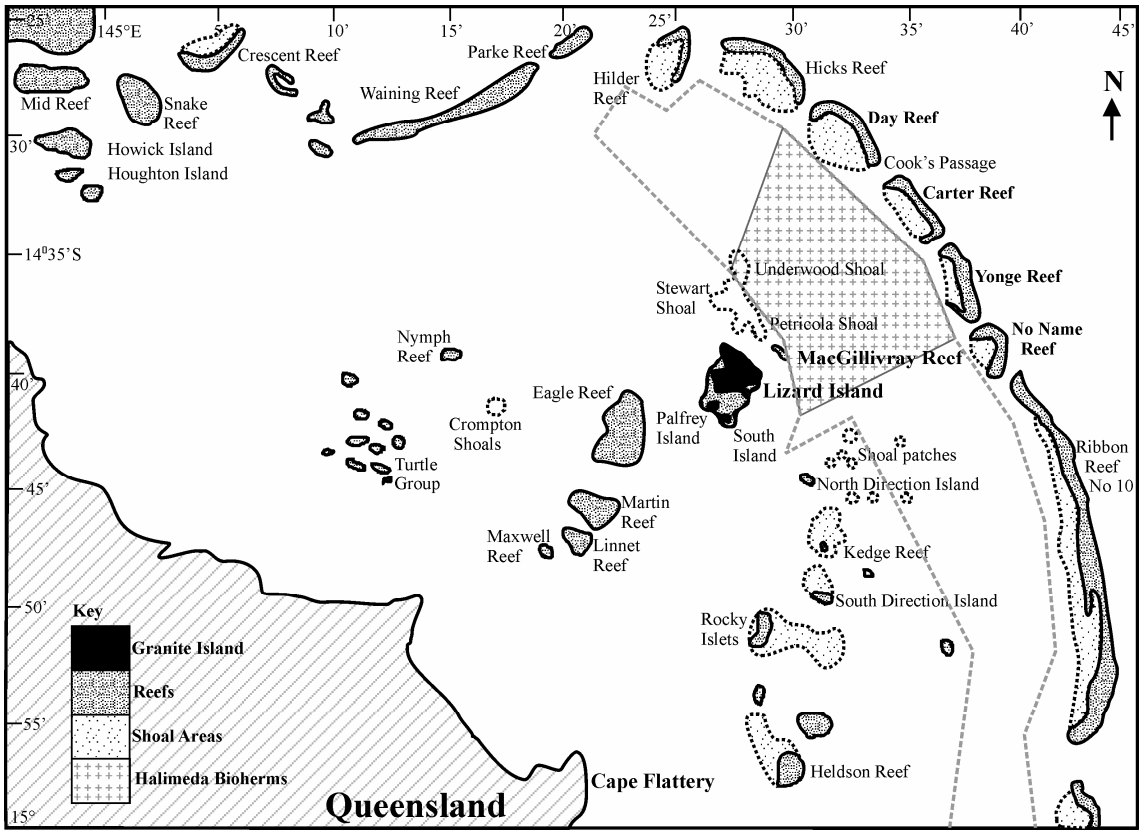

Figure 6.2. Lizard Island region, Northern Great Barrier Reef. Area enclosed by grey dashed lines indicates the extent of *Halimeda* bioherms revealed by seismic profiling (Orme *et al*., 1978; Orme, 1983; Orme and Salama, 1988), the grey stippled area indicates the area of bioherm coverage which averages 10 m thickness and was used in the calculations herein (modified after Admiralty Chart Aus 373).

On the outer shelf east of Cooktown (between latitudes 15º10'S and 15º46'S) discrete biohermal complexes are found lying 1 to 2 km directly behind the ribbon reefs (Figure 6.3; Davies and Marshall, 1985; Marshall and Davies, 1988). These were initially identified as Big Bank, Ribbon Bank and North Bank. Subsequently Big Bank was split into three separate banks (Ribbon Banks 2, 3 and 4) and renamed along with Ribbon Bank (Ribbon Bank 5) with respect to the adjacent ribbon reefs (Figure 6.3;

Davies and Marshall, 1985; Marshall and Davies, 1988; Wolanski *et al.*, 1988). Individual bioherms are composed of numerous sub-conical mounds (100 to 250 m wide) of unconsolidated sediments between 15 and 20 m in relief, individual bioherms can cover an area of several kilometres square (Marshall and Davies, 1988; Wolanski *et al.*, 1988).

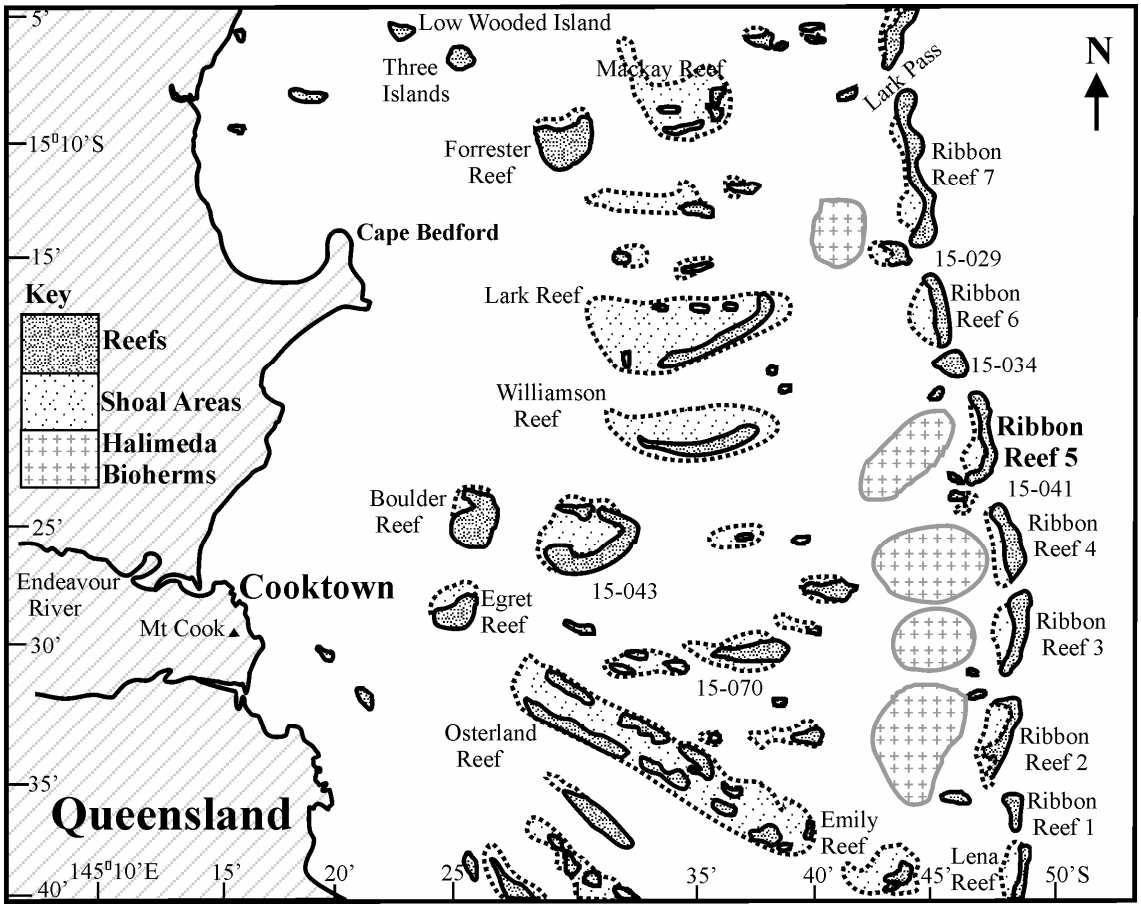

Figure 6.3 Cooktown region, Northern Great Barrier Reef, grey stippled areas indicate locations of *Halimeda* bioherms; North Bank and Ribbon Banks 2-5 (modified after the Great Barrier Reef Marine Park Authority Map BRA Q 155 February 1992).

The tops of the bioherms are covered by a forest of green algae (*Caulpera* and *Halimeda)* which effectively traps and stabilises the sediment. Radiocarbon dating vibrocores of the bioherms reveal that the bioherms are still actively accreting and vertical accretion rates have ranged between 1 and 3 m kyr^{-1} during the last 5 kyr. The bioherms are composed dominantly of *Halimeda*, cores extracted from the bioherms reveal a carbonate content averaging 75 %, the remaining 25 % comprises fine grained terrigenous material (Marshall and Davies, 1988).

In summary, the *Halimeda* bioherms in the Northern Great Barrier Reef are restricted to outer shelf areas, have thicknesses, accretion and productivity rates

comparable to and cover areas larger than individual coral reefs (Davies and Marshall, 1979; Drew, 1983; Drew and Abel, 1983; Marshall and Davies, 1988). It has been suggested that the mass of $CaCO_3$ sediment within the *Halimeda* bioherms may be greater than those of the adjacent reef platforms (Flood, 1984; Hillis, 1997).

6.2.5 Mechanism of Formation

The mechanisms of *Halimeda* bioherm formation are still debated, although it is generally agreed that their existence is related to upwelling of nutrient rich water (Drew and Abel, 1985; 1988; Phipps *et al*., 1985; Roberts *et al*., 1987a; b; 1988; Marshall and Davies, 1988; Wolanski *et al*., 1988; Phipps and Roberts, 1988; Drew, 1993; Harris *et al*., 1996). The *Halimeda* bioherms in the Northern Great Barrier Reef are thought to have been able to form because jets of up-welled nutrient-rich oceanic water intruded onto the outer shelf through the narrow passages between the ribbon reefs and formed eddies in the relative shelter behind the reefs (Drew and Abel, 1985; Marshall and Davies, 1988). Up-welling is thought to be the result of the Bernoulli Effect, with strong tidal currents lifting nutrient rich water over the shelf sills approximately 50 m below modern day sea level (Wolanski *et al*., 1988; Drew and Abel, 1988). This up-welling is only possible over sills at least 45 m below sea level, hence the assertion that local shelf bathymetry plays a significant role in controlling the formation of the bioherms (Drew and Abel, 1988; Wolanski *et al*., 1988).

Up-welling was not the only factor that affected the formation of *Halimeda* bioherms in the Great Barrier Reef. The absence of *Halimeda* bioherms in the Princess Charlotte Bay region is probably related to the input of fluvial mud from the Normandy River system, which reduces light levels and smothers vegetation (Drew and Abel, 1988). In the Southern Great Barrier Reef significant *Halimeda* deposits in the Swains Reef Complex have been associated with an influx of nutrient rich water onto the platform as a result of convergence of the ocean currents from the Capricorn Channel and the Coral Sea (Maxwell, 1968; Searle and Flood, 1988).

6.2.6 Coral Reefs

A reef is defined as a three dimensional structure of calcium carbonate sediment (rock, sands and muds) generated by Scleractinian corals and coralline algae calcification occurring in a tropical environment which remains as solid $CaCO_3$ and is not dissolved, it does not include non-reef habitats including banks, platforms and

carbonate dominated embayments (Rees *et al*., 2005). The coral reefs of the Great Barrier Reef have been extensively investigated since the mid-late 19th Century (Hopley and Davies, submitted manuscript, for a review). Reefs within the Great Barrier Reef province vary considerably in size and form, Holocene reef growth is represented by only a thin veneer, 10 to 20 m thick, commonly on top of karst Pleistocene substrates (Thom and Orme, 1976; Davies *et al*., 1977; Hopley, 1982). Coral reef drilling, radiometric dating and seismic profiling techniques have been employed to study the reefs of the Lizard Island and Cooktown regions (Davies *et al*., 1977; 1985; Hopley, 1977; 1978; 1994; Harvey and Hopley, 1981; International Consortium for Great Barrier Reef Drilling, 2001; Rees *et al.*, submitted manuscript). These investigations reveal that the Holocene ribbon reefs of the Lizard Island and Cooktown regions are approximately 9.5 m and 15 m thick respectively. Rees *et al*. (unpublished data) estimate that the coral reefs of the Great Barrier Reef (North and Northeastern Australia) accumulated 1700 Gt $CaCO_3$ during the last 10 kyr BP, approximately 21 % of the global Holocene coral reef $CaCO_3$ mass balance.

6.3 Study Area

6.3.1 The Great Barrier Reef

The Great Barrier Reef (GBR), a high energy epi-continental shelf edge reef system, is the largest reef system in the world covering an area of approximately 49 000 km^2 and comprises nearly 3000 individual reefs (Figure 1 B; Davies and Marshall, 1980; Spalding *et al*., 2001). The foundations of the Great Barrier Reef were initiated around 600 ka ago in the mid-Pleistocene and consist of a mixture of carbonate and terrigenous sediment accumulated during a succession of flooding and emergence of the continental shelf (International Consortium for Great Barrier Reef Drilling, 2001; Dunbar and Dickens, 2003). The Great Barrier Reef shelf sediments exhibit a broad semi-meridonal lithofacies zonation of terrestrial derived siliciclastic sediment on the inner shelf and an outer shelf dominated by carbonate deposition (Orme and Flood, 1980; Dunbar and Dickens, 2003). The shelf is generally covered by approximately 2 to 3 m of sediment except in areas of high carbonate deposition, for example, reefs and *Halimeda* bioherms (Orme and Flood, 1980).

6.3.2 Northern Great Barrier Reef

The Northern Great Barrier Reef extends from 9ºS to 16ºS, it is the shallowest part of the Great Barrier Reef with depths commonly less than 40 m below sea level and is generally narrow, between 24 and 60 km wide (Maxwell, 1968; Orme and Flood, 1980; Orme, 1985). This region of the Great Barrier Reef is characterised by an almost continuous line of shelf edge ribbon reefs, varying from 3 to 26 km in length and between 300 and 450 m wide (Orme and Flood, 1977; 1980; Kinsey, 1979; Flood, 1984).

The Lizard Island Region is located approximately 270 km north of Cairns, no major rivers discharge into this part of the Great Barrier Reef shelf (Figure 6.2; Flood, 1984). This area of the Great Barrier Reef province has a north-south trending line of granite continental islands (Lizard Island; North Direction Island and South Direction Island) which are surrounded by fringing reefs. It is one of a small number of areas where fringing reefs can be found growing adjacent to the mainland coast e.g. Cape Tribulation (Johnson and Carter, 1978; Orme *et al*., 1978; Partain and Hopley, 1989). Drilling, radiocarbon dating and seismic profiling investigations across the outer ribbon reefs, Carter and Yonge (15 km east of Lizard Island) reveal that these reefs reached modern sea level by approximately 5.4 kyr BP and 5.2 kyr BP respectively and that modern sea level was reached by 5.5 kyr BP (Harvey and Hopley, 1981; Hopley, 1994; Hopley and Davies, submitted manuscript). The Holocene-Pleistocene unconformity lies at approximately 19.3 m below the reef flat of the back reef at Yonge Reef and 19 m below the reef flat of the leeward edge of Carter Reef (Harvey, 1977a; b; Hopley, 1977; 1994; Harvey and Hopley, 1981; Hopley and Davies, submitted manuscript). Seismic profiling also reveals discontinuity surfaces at about 10 m below the reef flat on the windward margins of Carter reef and two mid-shelf reefs, Nymph and Three Isle (Figures 6.2 and 6.3; Harvey, 1977a; b; Orme *et al*., 1978).

In the Cooktown region (immediately east of Cooktown itself), a transect of reefs have been drilled including Boulder Reef, Williamson Reef and Ribbon Reef 5 (Figure 6.3; Davies *et al*., 1985; International Consortium for Great Barrier Reef Drilling, 2001). Radiocarbon dating indicates that reef growth in this region was initiated between 6.3 and 8.4 kyr BP on Pleistocene foundations at depths ranging from 15 to 17 m below the reef flat. Modern day sea level was established in this region by 6.5 kyr BP, the reefs reached modern day sea level between 5.9 and 6.7 kyr BP (Thom and Chappell, 1975; Stoddart *et al*., 1978; Chappell *et al*., 1983).

6.4 Materials and Methods

6.4.1 Reef Area

A 1 km^2 grid was used to estimate the area of the ribbon reefs in both the Lizard Island and Cooktown regions from the Great Barrier Reef Marine Park Authority map BRA Q 155 February 1992 (Figures 6.2 and 6.4).

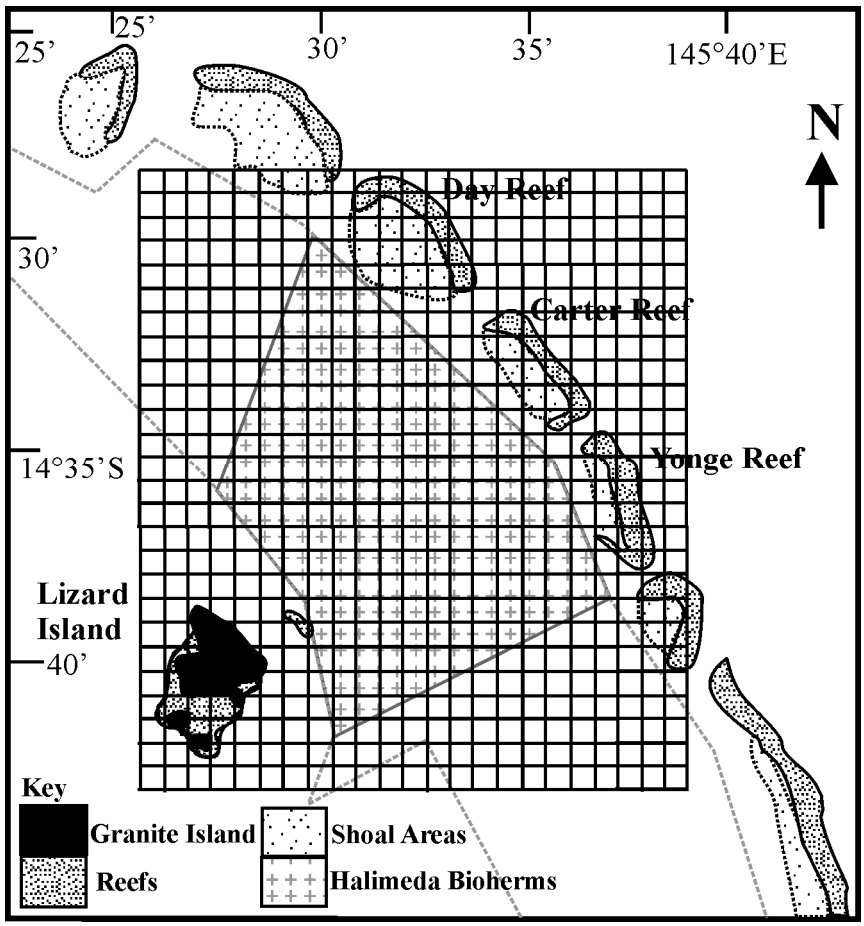

Figure 6.4 Schematic diagram showing how the area covered by the *Halimeda* bioherms and the coral reefs in the Lizard Island Region was estimated using a 1 km^2 grid. The grey dashed line indicates the area on the outer shelf where *Halimeda* bioherms are present, the grey stippled area indicates the area where the bioherms are at least 10 m thick. The black heavily stippled areas indicate the shallow coral reef flats.

The areas of the ribbon reefs in the Lizard Island and Cooktown regions are estimated to be 18.5 km^2 and 20.5 km^2 respectively (Figure 6.4; Table 6.2). The thickness of the Holocene ribbon reefs is estimated from drill cores for the Cooktown region (Davies *et al*., 1985) and from both drill cores and seismic profiling studies in the Lizard Island region (Davies *et al*., 1977; Hopley, 1977; 1994). These studies reveal that the average

thickness of the Holocene ribbon reefs is 15 m and 9.5 m for the Cooktown and Lizard Island regions respectively.

6.4.2 Reef $CaCO_3$

The mass of $CaCO_3$ for the ribbon reefs in each region was estimated using Equation 6.1.

Equation 6.1 **M = ((A * T)*2) * D * P * C**

Where M is the mass of carbonate sediments; A is reef area (km^2) estimated using a 1 km^2 grid (Figure 4; Great Barrier Reef Marine Park Authority map BRA Q 155 February 1992); T is the average thickness of the Holocene ribbon reefs (m); 2 is the factor used to correct reef volume for material exported to the leeward accretionary wedge and lagoon facies. Recent seismic profiling of Wistari Reef, Southern Great Barrier Reef, reveals that sediment accumulations in these facies, may effectively double the area used to calculate the mass of carbonate within reef systems (Ryan *et al*., 2001). D is the density of coral reef $CaCO_3$ (2.9 g cm^{-3}; Kinsey and Hopley, 1991); P is the average porosity of coral reef sediments (50 %; Ryan *et al*., 2001); C is the average carbonate content of coral reef sediments, this term can effectively be ignored because we assume the carbonate content of coral reefs to be 100 %. The mass balance of ribbon reef $CaCO_3$ estimated by equation 1 is shown in Table 6.2.

6.4.3 Halimeda $CaCO_3$

The mass of *Halimeda* bioherm $CaCO_3$ for both regions was estimated using Equation 6.2.

Equation 6.2 **M = A * T * D *P * C**

Where M is the mass of carbonate sediments; A is bioherm area (km^2); T is the average thickness of the *Halimeda* bioherms (m); D is the average density of $CaCO_3$ (2.9 g cm^{-3}; Kinsey and Hopley, 1991); P is the porosity of the bioherm sediment which we assume to be 50 %; C is the average carbonate content of the *Halimeda* bioherms (75 %; Orme, 1985; Marshall and Davies, 1988).

6.4.4 Bioherm Area

To estimate the mass of *Halimeda* bioherm $CaCO_3$ it was necessary to estimate their approximate area using previous seismic profiling, echo sounding and grab sampling studies for the Lizard Island (Orme *et al*., 1978; Orme, 1985) and Cooktown regions (Davies and Marshall, 1985; Phipps *et al*., 1985; Marshall and Davies, 1988; Wolanski *et al*., 1988). *Halimeda* bioherms in the Cooktown region appear to form more or less discrete mounds behind each of the ribbon reefs. The area covered by the Lizard Island region bioherms is harder to assess because they form a series of sinuous ridges and banks, these effectively blanket the outer shelf with thicknesses varying from 4 to 19 m over relatively short distances (Orme *et al*., 1978; Orme, 1985; Orme and Salama, 1988). Estimating the areal extent of the bioherms is also hampered by the sparcity of published seismic profiles. A 1 km^2 grid was used to estimate the area of bioherms which are consistently reported to have a thickness of 10 m or more (Figures 6.2 and 6.4). We estimate that the areas occupied by *Halimeda* bioherms are at least 184 km^2 and 118 km^2 for the Lizard Island and Cooktown regions respectively (Figure 6.4; Table 6.3).

6.4.5 Cooktown Region Bioherms

The average thickness of each bioherm in the Cooktown region was estimated from seismic and echo sounding profiles and descriptions in the published literature (Figure 6.5; Davies and Marshall, 1985; Phipps *et al*., 1985; Marshall and Davies, 1988). To interpret the seismic profiles which display the thickness of sediment in milliseconds, a figure of 1500 ms^{-1} was used to represent the velocity of the acoustic pulse following the methods of previous authors (Orme *et al*., 1978; Ryan *et al*., 2001). The thickness of each of the bioherms is not uniform; therefore the proportional area covered by sediment of varying thickness was considered when estimating of the mass balance of sediment by splitting the bioherms into boxes (Figure 6.5). For example, half of the area of a bioherm may be approximately 11.25 m thick, whereas the other half may be only 3.75 m thick (Ribbon Bank 3, Table 6.3). The mass of sediment was calculated by assuming that the bioherm sediments approximate a box shape with the area of each bioherm (width × length) multiplied by the corresponding thickness (Figure 6.5). Some bioherms were split into two boxes to estimate the appropriate volume of the bioherms as a whole e.g. Ribbon 3a, 2b (Figure 6.5; Table 6.3).

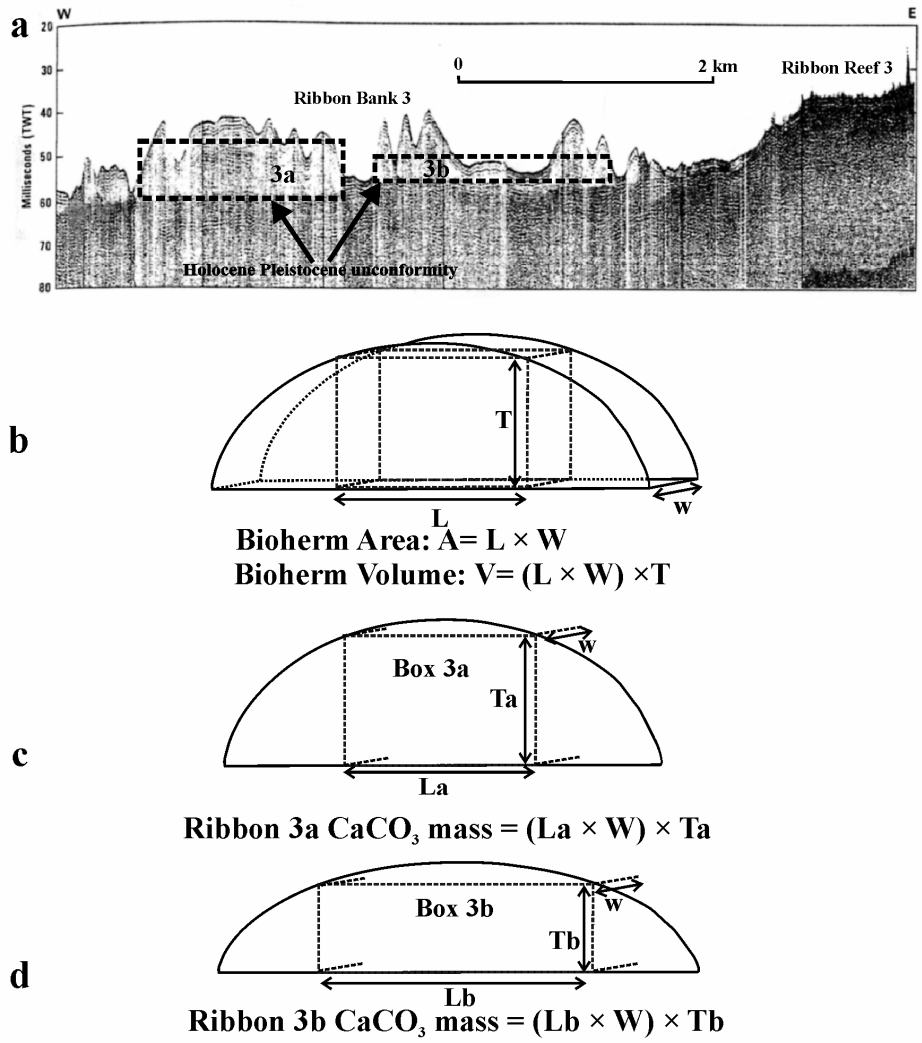

Figure 6.5a Seismic profile of *Halimeda* bioherm, Ribbon Bank 3, behind Ribbon Reef 3 in the Cooktown region (modified from Marshall and Davies, 1988 (Figure 6.2, profile B)). The black dashed rectangles (3a and 3b) outlines how Ribbon Bank 3 was split into two boxes in order to calculate the volume of carbonate sediment. b The mass of sediment was conservatively estimated by assuming that the bioherm sediments approximate a box shape with the area of each bioherm (L × W) multiplied by the corresponding thickness (T). c the volume of 3a was calculated by multiplying the area (La × W; 12.5 km^2) by the thickness of the bioherm (T, 11.25 m; Table 6.3). d the volume of 3b was calculated by multiplying the area (Lb × W; 12.5 km^2) by the thickness of the bioherm (Tb, 3.75 m; Table 6.3). The volume of Ribbon bank 3 is calculated as the sum of boxes 3a and 3b.

6.4.6 Lizard Island Region Bioherms

Seismic profiling in the Lizard Island region reveals that the thickness of the *Halimeda* deposits varies between 4.3 and 19 m, the majority of the bioherms are between 10 and 19 m thick, averaging 14.5 m thick (Orme *et al.*, 1978; Orme and Salama, 1988). We conservatively assume the average thickness of the *Halimeda* deposits in the Lizard Island region to be 10 m (Table 6.3).

6.4.7 Carbonate Content

The carbonate content of the bioherms has been investigated by vibrocoring studies in both the Lizard Island and Cooktown regions (Orme, 1985; Marshall and Davies, 1988). Marshall and Davies (1988) estimated, from twenty 5 m vibrocores taken in the Cooktown region, that the carbonate content within the bioherms averages approximately 75 %. Four vibrocores from the Lizard Island region, reveal that the carbonate content (acid soluble) within the top 4 m of the bioherms varies between 73 and 99 % (Orme, 1985). A fifth core taken from the edge of one of the bioherms reveals that the carbonate content of the bioherms increases progressively upwards above the peat substratum, varying between 20 and 90 % (core 92; Orme, 1985). We assume that the carbonate content of the bioherms in both regions is 75 %. The variation in the carbonate content of the bioherms in the Lizard Island region, between 20 and 90 %, was used to estimate the potential error in the carbonate mass balance for this region (Table 6.4).

6.5 Results and Discussion

We estimate that the ribbon reefs of the Lizard Island and Cooktown regions cover areas of approximately 18.5 and 20.5 km^2 and comprise approximately 0.52 and 0.92 Gt $CaCO_3$ respectively (Table 6.2).

Table 6.2. Dimensions and Mass of Ribbon Reef $CaCO_3$

Region	Ribbon reef	Reef area (km^2)	Thickness (m)	Mass $CaCO_3$ (Gt)
Lizard Island	Day	5.75	9.5	0.16
	Carter	5.75	9.5	0.16
	Yonge	6.75	9.5	0.19
Total		18.5		0.52
Cooktown	Ribbon 5	5	15	0.22
	Ribbon 4	5	15	0.22
	Ribbon 3	4.5	15	0.2
	Ribbon 2	5	15	0.22
	15-072	0.25	15	0.01
	15-073	0.75	15	0.03
Total		20.5		0.92

The *Halimeda* bioherms of the Lizard Island and Cooktown regions cover areas of approximately 184 and 118 km^2 and comprise approximately 2.06 and 0.86 Gt $CaCO_3$ respectively (Table 6.3).

Table 6.3. Dimensions and Mass of *Halimeda* Bioherm $CaCO_3$

Region	Bioherm complex	Area (km^2)	Thickness (m)	Mass $CaCO_3$ (Gt)
Lizard Island	Lizard Island region	184	10	2.06
Total		184		2.06
Cooktown	Ribbon 5a	8.4	8.25	0.07
	Ribbon 5b	9.1	3.75	0.04
	Ribbon 4a	21	6	0.14
	Ribbon 4b	14	3.75	0.06
	Ribbon 3a	12.5	11.25	0.16
	Ribbon 3b	12.5	3.75	0.05
	Ribbon 2a	20	11.25	0.25
	Ribbon 2b	20	3.75	0.08
Total		118		0.86

Thus, we estimate that ratio of ribbon reef to *Halimeda* bioherm $CaCO_3$ is approximately 1:4 and 1:1 for the Lizard Island and Cooktown regions respectively. If we assume that the carbonate content of the Lizard Island region bioherms ranges from 20 to 90 %, we estimate that the mass balance of *Halimeda* bioherm $CaCO_3$ is between 0.55 and 2.5 Gt (Table 6.4). The ratio of ribbon reef to *Halimeda* bioherms $CaCO_3$ may vary between 1:1 to 1:5 depending on the carbonate content of the Lizard Island bioherms (Table 6.4; Figure 6.6).

Table 6.4. Mass of $CaCO_3$ Accumulated by the Ribbon Reefs and *Halimeda* bioherms of the Lizard Island and Cooktown regions during the Holocene. [a] range between 0.55 and 2.5. [b] range between 1:1 and 1:5.

Region	Reef $CaCO_3$ (Gt)	*Halimeda* $CaCO_3$ (Gt)	Ratio of Reef : *Halimeda* $CaCO_3$
Lizard Island	0.52	2.1 [a]	1:4 [b]
Cooktown	0.92	0.86	1:1

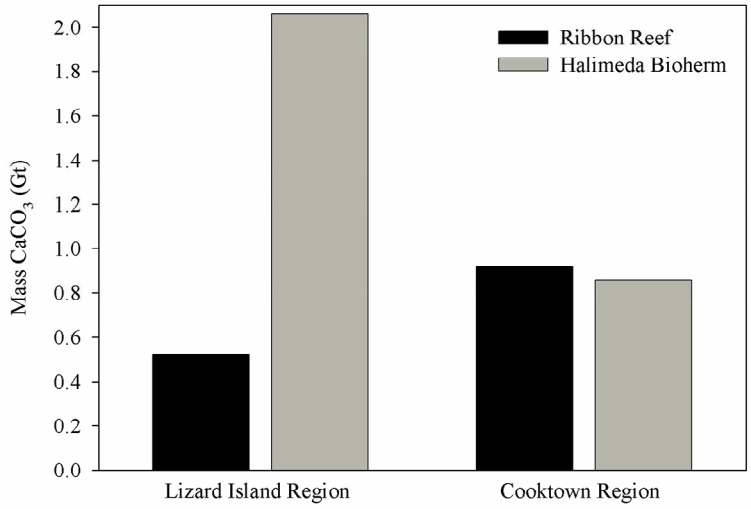

Figure 6.6 Mass of carbonate sediments accumulated within the ribbon reefs and *Halimeda* Bioherms of the Lizard Island and Cooktown Regions of the Northern Great Barrier Reef.

6.5.1 Reefs vs Bioherms

The *Halimeda* bioherms contain at least as much (and up to 400 % more) $CaCO_3$ sediment as the adjacent ribbon reefs in the Northern Great Barrier Reef (Table 4). This finding is in agreement with assertions that *Halimeda* bioherms contain more carbonate sediment than the adjacent reef platforms (Flood 1984; Hillis-Colineaux 1986b; Marshall and Davies, 1988; Freile and Hillis, 1997). The ratio of reefal to bioherm $CaCO_3$ varies within the Northern Great Barrier Reef province from 1:1 in the Cooktown region to 1:4 in the Lizard Island region. The variation in the ratio is a consequence of the differences in the thicknesses and extent of the bioherms in the two regions. For example, in the Lizard Island region the bioherms form a series of large ridges which traverse most of the outer shelf, with an average thickness of 10 m (maximum 19 m) and an area of at least 184 km^2. Whereas the Cooktown region bioherms form discrete mounds behind each ribbon reef with maximum and minimum thickness of 11.25 and 3.75 m respectively, they cover a combined area of approximately 118 km^2. The size differences in the *Halimeda* bioherms in these two regions is the result of the morphology of the shelf affecting the growth potential of the *Halimeda*. The formation of the bioherms is related to up-welling of nutrient rich waters from the Coral Sea. The timing and amount of water intruding onto the shelf during the Holocene is controlled by sea level rise and the dimensions of the reef passes (bathymetry and width). For example, Wolanksi *et al*. (1988) suggest that *Halimeda* Ribbon Bank 5 is small because it only received nutrients from one reef passage whereas the larger banks (bioherms) behind Ribbon Reefs 2, 3 and 4 were each fed by two passages (Figure 6.3). The absence of bioherms behind Ribbon Reef 1, Lena Reef and Ribbon Reef 6 and Pearl Reef results because the channels are either too wide or too shallow to induce sufficient upwelling to support bioherm development. Wolanski *et al*. (1988) suggested that the presence of ribbon reefs at least 4 km long and reef passages less than 1 km wide and 40 to 45 m deep are necessary for the development of bioherms.

6.5.2 Carbonate Budget

Rees *et al*. (submitted manuscript) estimate that the coral reefs of the Great Barrier Reef (North and Northeastern Australia) accumulated 1707 Gt $CaCO_3$ over the last 10 kyrs. This mass balance of $CaCO_3$ was estimated using the reef area estimate of 4.492×10^4 km^2 calculated using Spalding *et al*.'s (2001) reef area estimate for Australia minus

the area of Ningaloo Reef, the Houtman Abrolhos Islands, Christmas Island and Cocos-Keeling Islands (Sheppard and Wells, 1988). If we assume that 0.6 mol of CO_2 is available for release to the atmosphere per mole of $CaCO_3$ deposited in the marine environment (Ware *et al.*, 1991; Zeebe and Wolf-Gladrow, 2001), the *Halimeda* bioherms of the Lizard Island and Cooktown regions had the potential to release 0.54 and 0.23 Gt CO_2 to the atmosphere during the last 10 kyrs respectively. Previous studies have indicated that the bioherms may have begun to develop prior to the initiation of reef colonization of topographic highs on the shelf (Marshall and Davies, 1988). It has been suggested that the locus of carbonate deposition on the Northern Great Barrier Reef shelf shifted from bioherm development (between 10 and 8.5 kyr BP) when the shelf was initially flooded, to coral reef development when the eroded karst remnants of the Pleistocene ribbon reefs were transgressed and served as sites for Holocene reef colonization (Hopley, 1994). The common delay in reef colonization of newly flooded topographic highs within the Northern Great Barrier Reef is probably related to high nutrient levels which would have favoured *Halimeda* growth (Davies *et al.*, 1985; Marshall and Davies, 1988; Hopley, 1994). Indeed a *Halimeda* rich limestone unit, several meters thick and indicative of high nutrient levels, has been found at the base of many Holocene reef sections within the Great Barrier Reef including; Raine, Yonge, Boulder, Britomart, Redbill, Cockatoo and One Tree Reef (Hopley and Davies, submitted manuscript). It has been proposed that changes in oceanic circulation or climate then favoured the development of coral reefs on topographic highs between 8 and 4 kyr BP (Davies *et al.*, 1985). *Halimeda* bioherm development may have been reduced during the main phase of reef growth. Once the Holocene ribbon reefs had attained a sufficient height in relation to sea level, the area behind the ribbon reefs would have again become sheltered enough to allow *Halimeda* bioherm development which continues to this day (Davies and Marshall, 1985; Marshall and Davies, 1988; Hopley, 1994). If this model of Holocene shelf evolution is correct, *Halimeda* calcification within the Northern Great Barrier Reef may have released a pulse of CO_2 to the early Holocene atmosphere.

Kinsey and Hopley (1991) estimated that the ribbon reefs of the Great Barrier Reef cover on average 16.4 km^2 (using data from Carter Reef and Ribbon Reef 9). Using Kinsey and Hopley's (1991) estimate of the total area covered by the Great Barrier Reef ribbon reefs (approximately 1081 km^2), assuming the thickness of the ribbon reefs to be 10 m and the conservative ratio of reef to *Halimeda* bioherm $CaCO_3$

of 1:1 (Table 6.4), we estimate that the *Halimeda* bioherms of the Great Barrier Reef have accumulated at least 32 Gt $CaCO_3$ during the Holocene. This estimate for the Great Barrier Reef province, along with evidence from seismic profiling studies worldwide, give an indication of the amount of carbonate presently unaccounted for in global carbonate budgets (Roberts *et al*., 1987a; b; 1988; Phipps and Roberts, 1988; Hine *et al*., 1988; Harris *et al*., 1996; Heyward *et al*., 1997**)**.

6.5.3 Halimeda Distribution

The extent of *Halimeda* bioherm formation within the Great Barrier Reef province has yet to be adequately assessed. Detailed bathymetric sampling has revealed that *Halimeda* sediments make up to 5 to 65 % of the inter-reefal sediments on the outer shelf of the Great Barrier Reef Province (Maxwell, 1968). Drew and Abel (1983) estimated that 2000 km^2 of the Great Barrier Reef province seabed is carpeted with *Halimeda* vegetation. Standard monochrome aerial photographs of the far northern Great Barrier Reef (between 12.3ºS and 13.5ºS) reveal the presence of dark circular patches approximately 300 m in diameter. These patches were initially interpreted as submerged reefal shoals, however, it has also been suggested that they could be *Halimeda* bioherms (Drew and Abel, 1988; Hopley, 1978). Seismic profiling transects of the Northern Great Barrier Reef (from Lloyd Island to Hibernia Entrance and from Restoration Island to Second Small Reef) in the region adjacent to Portland Roads and the Lockhart River reveal the presence of substantial *Halimeda* bioherms on the outer shelf in this region (J. Jell, personal communication, 2004). Given reports of luxuriant *Halimeda* meadows principally at 20 to 40 m below sea level on the Great Barrier Reef (Drew, 1983; Drew and Abel, 1985), Hillis (1997) suggested that it is likely that additional *Halimeda* bioherms will be discovered. Hillis (1997) also proposed that dense *Halimeda* accumulations on the North-eastern Brazilian shelf may be reinterpreted as bioherms (Vicalvi and Milliman, 1977). If the ratio of *Halimeda* bioherm to coral reef carbonate on the shelf of the Northern Great Barrier Reef is even partially applicable globally then the accurate assessment of *Halimeda* distribution, through seismic profiling and vibrocoring, is a prerequisite to a comprehensive understanding of the marine carbon cycle.

6.6 References

Ball, S. M., Pollard, W. D. and J. W. Roberts (1977) Importance of phylloid algae in development of depositional topography – reality or myth. In S. H. Frost, M. P. Weiss, J. B. Saunders (eds), *Reefs and Related Carbonates – Ecology and Sedimentology. Am. Ass. Petrol. Geol. Tulsa,* **4**, 239-259.

Chappell, J., Chivas, A., Wallensky, E., Polach, H. A. and P. Aharon (1983) Holocene paleo-environmental changes, Central to North Great Barrier Reef inner zone. *Jn Aust. Geol. Geophys.*, **8**, 223-235.

Davies, P. J. and J. F. Marshall (1979) Aspects of Holocene reef growth-substrate age and accretion rate. *Search*, **10**, 276-279.

Davies, P. J. and J. F. Marshall (1980) A model of epi-continental reef growth. *Nature*, **287**, 37-38.

Davies, P. J. and D. Hopley (1983) Growth facies and growth rates of Holocene reef in the Great Barrier Reef. *BMRJ Aust. Geol. Geophys.*, **8**, 237–251.

Davies, P. J. and J. F. Marshall (1985) *Halimeda* bioherms - low energy reefs, northern Great Barrier Reef. *Proc. 5th Int. Coral Reef Congr. Tahiti*, **5**, 1-7.

Davies, P. J., Marshall, J. F., Thom, B. G., Harvey, N., Short, A. D. and K Martin (1977) Reef development Great Barrier Reef. *Proc. 3rd Int. Coral Reef Symp. Miami*, **2**, 332-337.

Davies, P. J., Marshall, J. F. and D. Hopley (1985) Relationships between reef Growth and sea level in the Great Barrier Reef. *Proc. 5th Int. Coral Reef Congr. Tahiti*, **3**, 95-103.

Drew, E. A. (1983) *Halimeda* biomass, growth rates and sediment generation on reefs in the central GBR province. *Coral Reefs*, **2**, 101-110.

Drew, E. A. (1993) Production of geological structures by the green alga *Halimeda. SPUMS J*, **23**, 2, 93-102.

Drew, E. A. and K. M. Abel (1983) Biology and sedimentology and geography of the vast inter-reefal *Halimeda* meadows within the Great Barrier Reef province. *Coral Reefs*, **2**, 101-110.

Drew, E. A. and K. M. Abel (1985) Biology, sedimentology and geography of the vast inter-reefal *Halimeda* meadows within the Great Barrier Reef Province. *Proc. 5th Int. Coral Reef Congr. Tahiti*, **5**, 15-20.

Drew, E. A. and K. M. Abel (1988) Studies on *Halimeda* I. the distribution and species composition of *Halimeda* meadows throughout the GBR province. *Coral Reefs*, **6**, 195-205.

Dunbar, G. B. and G. R. Dickens (2003) Massive siliciclastic discharge to slopes of the Great Barrier Reef Platform during sea-level transgression: constraints from sediment cores between 15°S and 16°S latitude and possible explanations. *Sed. Geol.*, **162**, 141-158.

Elliot, G. F. (1965) The interrelationships of some Cretaceaous Codiaceae (calcareous algae). *Palaeontology*, **8**, 2, 199-203.

Flood, P. G. (1984) *A geological guide to the northern Great Barrier Reef.* Australasian Sedimentologists Group Field Guide Series No. 1 Sydney Geological Society of Australia

Flood, P. G. and G. R. Orme (1988) Mixed siliciclastic/carbonatesediments of the northern Great Barrier Reef province Australia. In L. J. Doyle and H. H. Roberts (eds), *Carbonate–Clastic Transitions* Developments in Sedimentology, 42, Elsevier, Amsterdam, pp 175–205.

Freile, S. and I. Hillis (1997) Carbonate productivity by *Halimeda* incrassate in a land proximal lagoon, Pico Feo, San Blas, Panama. *Proc. 8th Int. Coral Reef Symp. Panama*, **1**, 767-772.

Freile, D., Milliman, J. D. and L. Hillis (1995) Leeward bank margin *Halimeda* meadows and draperies and their sedimentary importance on the western Great Bahama bank slope. *Coral Reefs*, **14**, 27-33.

Harris, P. T., Pattiaratchi, C. B., Keene, J. B., Dalrymple, R. W., Gardner, J. V., Baker, E. K., Cole, A. R., Mitchell, D., Gibbs, P. and W. W. Schroeder (1996) Late quaternary deltaic and carbonate sedimentation in the Gulf of Papua foreland basin: response to sea-level change. *J. Sed. Res.*, **66**, 4801-4819.

Harvey, N. (1977a) The identification of subsurface disconformities of the Great Barrier Reef, Australia between 14°S and 17°S, using shallow seismic refraction techniques. *Proc. 3rd Int. Coral Reef Symp.*, 45-51

Harvey, N. (1977b) Application of shallow seismic refraction techniques to coastal geomorphology: a coral reef example. *Catena*, **4**, 333-339.

Harvey, N. and D. Hopley (1981) Radiocarbon ages and morphology of reef tops in the Great Barrier Reef between 14º39'S and 20º45'S: Indicators of shelf neotectonics? *Proc. 4th Int. Coral Reef Symp. Manila*, **1**, 523-530.

Heyward, A., Pinceratto, E. and L. D. Smith (1997) *Big Bank Shoals of the Timor Sea: an Environmental Resource Atlas.* Australian Institute of Marine Science & BHP Petroleum, pp 115.

Hillis-Colinvaux, L. (1980) Ecology and taxonomy of *Halimeda*: primary producer of coral reefs. *Adv Mar. Bio.*, **17**, 1-327.

Hillis-Colineaux, L. (1986a) Deep water populations of *Halimeda* in the economy of an Atoll. *Bull. Mar. Sci.*, **38**, 155-169.

Hillis-Colineaux, L. (1986b) *Halimeda* growth and diversity on the deep fore-reef of Enewetak Atoll. *Coral Reefs*, **5**, 19-21.

Hillis, L. (1997) Coralgal reefs from a calcareous green alga perspective and a first carbonate budget. *Proc. 8th Int. Coral Reef Symp.*, **1**, 761-766.

Hine, A. C., Hillock, P., Harris, M. W., Mullins, H. T., Belknap, D. F. and W. C. Jaap (1988) *Halimeda* bioherms along an open seaway: Miskito Channel, Nicaraguan Rise, SW Caribbean Sea. *Coral Reefs*, **6**, 173-178.

Hopley, D. (1977) The age of the Outer Ribbon Reef Surface, Great Barrier Reef, Australia: implications for hydrostatic models. *Proc. 3rd Int. Coral Reef Symp.*, **2**, 23-28.

Hopley, D. (1978) Geomorphology of the reefs and reef islands Great Barrier Reef north of Lizard Island. In *Workshop on Northern section of Great Barrier Reef*. Great Barrier Reef Marine Park Authority Townsville, pp 129-252.

Hopley, D. (1982) *The geomorphology of the Great Barrier Reef: Quaternary development of coral reefs.* John Wiley, NY.

Hopley, D. (1994) Continental shelf reef systems. In R. W. G. Carter and C. D. Woodroffe (eds), *Coastal Evolution. Late Quaternary shoreline morphodynamics*. Cambridge University Press, Cambridge, pp 303-340.

Hopley, D. and P. J. Davies (submitted manuscript) Shallow drilling on the Great Barrier Reef and adjacent islands.

International Drilling of Consortium of the Great Barrier Reef (2001) International Consortium for Great Barrier Reef Drilling 2001 New constraints on the origin of the Australian Great Barrier Reef: results from an international project of deep coring. *Geology*, **29**, 483–486.

Johnson, J. H. (1969) *A review of the Lower Cretaceous algae*. Prof Contrib Colarado School of Mines No 6, Golden Colorado, pp 180.

Johnson, D. P. and R. M. Carter (1978) *Sedimentary framework of mainland fringing reef development, Cape Tribulation Area.* Great Barrier Reef Marine Park Authority Technical Memorandum GBRMPA-TM-14: 4-17.

Kinsey, D. W. (1979) *Carbon turnover and accumulation by coral reefs.* Unpublished PhD Thesis University of Hawaii, pp 248.

Kinsey, D. W. and D. Hopley (1991) The significance of coral reefs as global carbon sinks – response to greenhouse. *Pal. Pal. Pal.* (Global and Planetary change section), **89**, 363 – 377.

Kirkland, B. L., Moore, C. H. Jr. and J. A. D. Dickson (1993) Well preserved aragonite algae (*Eugonophyllum U'doteaceae*) form the Pennsylvanian Holder Formation. Sacramento Mountains, New Mexico. *Palaios*, **8**, 111-120.

Marshall, J. F. and P. J. Davies (1988) *Halimeda* bioherms of the Northern Great Barrier Reef. *Coral Reefs*, **6**, 139-148.

Maxwell, W. G. W. (1968) *Atlas of the Great Barrier Reef.* Elsevier, Amsterdam.

Maxwell, W. G. H. (1973) Sediments of the Great Barrier Reef. Chapter 10. In O. A. Jones and R. Endean (eds), *Biology and Geology of Coral Reefs*. Geology 1, Academic Press, New York, pp 410.

Marshall, J. F. and P. J. Davies (1988) *Halimeda* Bioherms of the Northern Great Barrier Reef. *Coral Reefs*, **6**, 139-148.

Milliman, J. D. (1993) Production and accumulation of calcium carbonate in the ocean: budget of a non-steady state. *Global Biogeochem Cy.*, **7**, 927 – 957.

Orme, G. R. (1983) Shallow structure and lithofacies of the Northern Great Barrier Reef. In J. T. Baker, R. M. Carter, P. W. Sammarco and K. P. Stark (eds), *Proc. Great Barrier Reef Conf.* JCU Press Townsville, pp 135-142.

Orme, G. R. (1985) The sedimentological importance of *Halimeda* in the development of back reef lithofacies, Northern Great Barrier Reef (Australia). *Proc. 5th Coral Reef Symp Tahiti*, **5**, 31-37.

Orme, G. R. and P. G. Flood (1977) The geological history of the Great Barrier Reef: a reappraisal of some aspects in the light of new evidence. *Proc. 3rd Int. Coral Reef Symp. Miami*, **3**, 7-43.

Orme, G. R., Flood, P. G. and G. E. G. Sargent (1978) Sedimentation trends in the lee of outer (ribbon) reefs, Northern region of the Great Barrier Reef Province. *Phil. Trans. R. Soc. Lond. A*, **291**, 85-99.

Orme, G. R. and P. G. Flood (1980) Sedimentation in the Great Barrier Reef Province, Adjacent Bays and Estuaries. In R. A. Henderson and P. J. Stephenson (eds), *The geology and geophysics of Northeastern Australia*. Geological Society of Australia Inc, Queensland Division, pp 419-434.

Orme, G. R. and M. S. Salama (1988) Form and seismic stratigraphy of *Halimeda* banks in part of the Northern Great Barrier Reef Province. *Coral Reefs*, **6**, 131-137.

Partain, B. R. and D. Hopley (1989) *Morphology and Development of the Cape Tribulation Fringing Reefs, Great Barrier Reef, Australia.* GBRMPA Tech. Mem. T.M21, pp 45.

Phipps, C. U. G., Davies, P. J. and D. Hopley (1985) The morphology of *Halimeda* banks behind the GBR east of Cooktown, Qld. *Proc. 5th Int. Coral Reef Symp. Tahiti*, **5**, 27-30.

Phipps, C. V. G. and H. H. Roberts (1988) Seismic characteristics and accretion history of *Halimeda* bioherms on Kalukalukuang bank eastern Java Sea (Indonesia). *Coral Reefs*, **6**, 149-159.

Rees, S. A., Opdyke, B. N., Wilson, P. A. and L. K. Fifield (2005) Coral Reef sedimentation on Rodrigues and the Western Indian Ocean and its impact on the carbon cycle. *Phil. Trans. R. Soc. Lond. A*, **363**, 101-120.

Rees, S. A., Opdyke, B. N., Wilson, P. A., Fifield, L. K. and V. Levchenko (submitted manuscript) Holocene Evolution of the Granite based Lizard Island and MacGillivray Reef Systems, Northern Great Barrier Reef.

Rees, S. A., Opdyke, B. N. and P. A. Wilson (submitted manuscript) The Impact of Coral Reef $CaCO_3$ Accumulation on Holocene Atmospheric Carbon Dioxide Concentration.

Ridgwell, A. J. and R. E. Zeebe (2005) The role of the global carbonate cycle in the regulation and evolution of the Earth system. *Earth Planet. Sci Lett*., **234**, 299– 315

Roberts, H. H. and C. V. Phipps (1988) Proposed oceanographic controls on modern Indonesian Reefs: A Turn-off/Turn-on Mechanism in a Monsoonal Setting. *Proc. 6th Int. Coral Reef Symp. Australia*, **3**, 529-534.

Roberts, H. H., Aharon, P. and C. V. Phipps (1988) Morphology and sedimentology of *Halimeda* bioherms from the eastern Java Sea (Indonesia). *Coral Reefs*, **6**, 161-172.

Roberts, H. H., Phipps, C. V. and L. Effendi (1987a) *Halimeda* bioherms of the eastern Java Sea, Indonesia. *Geology*, **15**, 371-374.

Roberts, H. H., Phipps, C. V. and L. Effendi (1987b) Morphology of large *Halimeda* bioherms, eastern Java Sea (Indonesia): a side scan sonar study. *Geo-marine Lett.*, **7**, 7-14.

Ryan, D. A., Opdyke, B. N. and J. S. Jell (2001) Holocene sediments of Wistari Reef towards a global quantification of coral reef related neritic sedimentation in the Holocene. *Pal. Pal. Pal.*, **175**, 1-12.

Searle, D. E. and P. G. Flood (1988) *Halimeda* bioherms of the Swain Reefs – Southern Great Barrier Reef. *Proc. 6th Int. Coral Reef Symp.*, **3**, 139-144.

Sheppard, C. and S. M Wells (1988) *Coral reefs of the world. Vol 2. Indian Ocean, Red Sea and Gulf*, IUCN, Conservation Monitoring Centre. International Union for Conservation of Nature and Natural Resources, Switzerland.

Smith, S. V. (1978), Coral reef area and the contributions of reefs to the processes and resources of the world's oceans, *Nature*, **273**, 225-226.

Smith, S. V. and D. W. Kinsey (1976) Calcium carbonate production, coral reef growth and sea level change. *Science*, 194, 937-939.

Spalding, M. D., Ravilious, C. and E. P. Green (2001) *World Atlas of Coral Reefs*. Prepared at the UNEP World Conservation Monitoring Centre. University of California Press, Berkeley, USA.

Steneck RS, Testa V (1997) Are calcareous algae important to reefs today or in the past? Symposium summary. *Proc. 8th Int. Coral Reef Symp.*, **1**, 685-688.

Stoddart, D. R., McLean, R. F., Scoffin, T. P., Thom, B. G. and D. Hopley (1978) Evolution of reefs and islands, Northern Great Barrier Reef: synthesis and interpretation. *Phil. Trans. R. Soc. Lond. B*, **284**, 149-159.

Thom B. G., and J. Chappell (1975) Holocene sea-levels relative to Australia. *Search*, **6**, 90-93.

Thom, B. G. and G. R. Orme (1976) Shallow structure of reefs from coring. In D. R. Stoddart and M. Yonge (Convenors), *The northern Great Barrier Reef a meeting for discussion*. Abstr 4. The Royal Society (London).

Vicalvi, M. A. and J. D. Milliman (1977) Carbonate sedimentation on the continental shelf off southern Brazil, with special reference to the benthic foraminifera. *Am. Ass. Petrol. Geol*., **4**, 313-328.

Ware, J. R., Smith, S. V. and M. L. Reaka-Kudla (1991) Coral reefs: sources or sinks of atmospheric CO_2. *Coral Reefs*, **1**, 127–130.

Wolanski, E. J., Drew, E. A., Abel, K. M. and J. O'Brien (1988b) Tidal jets, nutrient upwelling and their influence on the productivity of the alga *Halimeda* in the Ribbon Reefs, Great Barrier Reef. *Estuarine Coastal and Shelf Sci.*, **26**, 169-201.

Wray, J. L. (1977) *Calcareous algae, developments in palaeontology and stratigraphy*, 4. Elsevier Scientific Publishing Company, Amsterdam, Oxford, New York.

Zeebe, R. E. and D. A. Wolf-Gladrow (2001) *CO_2 in Seawater: Equilibrium, Kinetics, Isotopes*. Elsevier Oceanography Series, Amsterdam.

6.7 Acknowledgments

This research has been supported by the National Environment Research Council (NERC); the Royal Society and the Earth and Marine Sciences Department, Australian National University, Canberra. We would especially like to thank John Davis for assisting in field expedition operations, Dr John Jell for supplying various seismic profiles of the Great Barrier Reef, the Lizard Island Research Station and Staff (particularly Bob Lamb for his patience and enthusiasm during fieldwork attempts), the Australian Museum and the Great Barrier Reef Marine Park Authority.

Chapter Seven

Conclusions

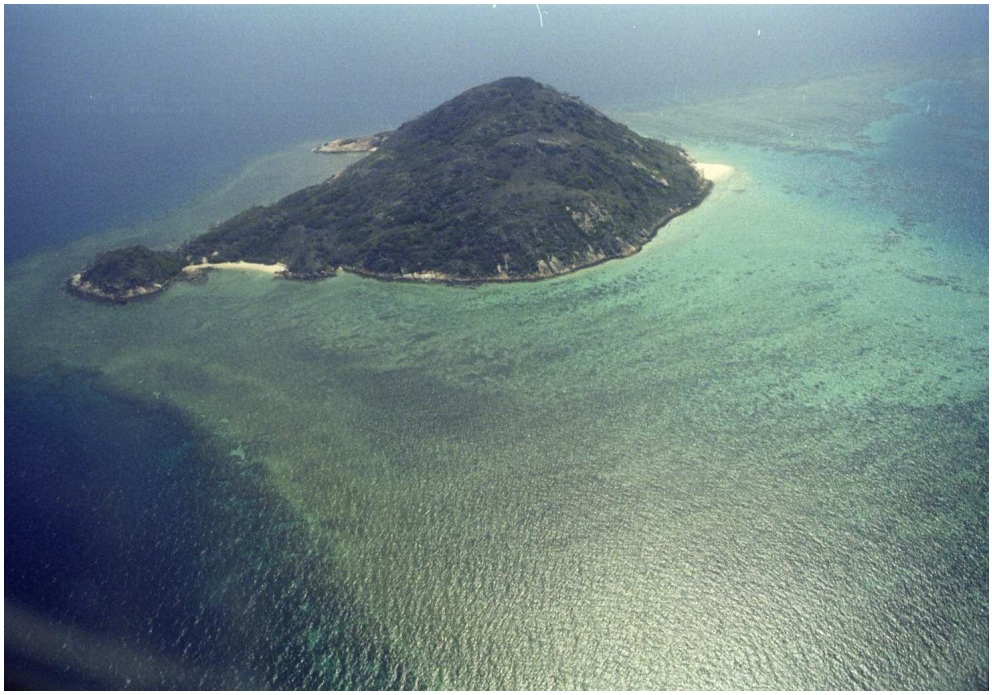

Plate 7.1 Photograph of Lizard Island windward margin and South Island.

Chapter 7

Conclusions

7.1 Conclusions

The theme of this thesis is the evolution of Holocene reefs and their role in the global carbon cycle. Chapters three and four investigate the Holocene evolution of three previously unstudied reefs, Rodrigues, Lizard Island and MacGillivray Reef. The accretion rates calculated from radiometric dating of corals obtained from drill cores through these reefs were combined in a global dataset of accretion rates compiled from the published literature. This dataset was used to estimate mean accretion rates for reef provinces and time slices within the Holocene. These mean accretion rates were used to determine the global Holocene coral reef $CaCO_3$ mass balance and flux of CO_2 available for release to the Holocene atmosphere. Chapter six investigates one of the remaining presently under-examined parts of the carbonate system, *Halimeda* bioherms.

7.1.1 Lizard Island and MacGillivray Reef

- The windward margin at Lizard Island started growing approx 6.7 kyr BP on an assumed granite basement at a depth of 4.5 m below the reef flat and approached present day sea level approximately 4 kyr BP.
- Growth of the windward margin at MacGillivray Reef was initiated by 7.6 kyr BP and reached present day sea level by approximately 5.6 kyr BP. The leeward margin at MacGillivray was initiated by 8.2 kyr BP (at a depth of 15 m below the reef flat) on an assumed granite basement, only reaching modern sea level within the last 500 years.
- Rates of vertical accretion ranged from 1.4 to 5.8 m kyr^{-1} at MacGillivray and from 0.5 to 1 m kyr^{-1} at Lizard Island. In both cases higher accretion rates were associated with the early stages of reef growth between 8.1 and 5.6 kyr BP.
- Rates of vertical accretion slowed to 1.4 m kyr^{-1} as reefs approached within 2 m of modern day sea level.
- The absence of Pleistocene reefal deposits in the cores from MacGillivray Reef, indicates the possibility that the shelf in this region may have subsided relative to modern day sea level by at least 15 m since the last interglacial (125 ka).

7.1.2 Rodrigues Island

- The windward and leeward margins of Rodrigues fringing reef approached present day sea level at approximately 3 and 1.5 kyr BP respectively. The relatively low rates of vertical reef growth within the top 4 m of the Rodrigues cores, ranging from 0.46 to 1.96 m kyr $^{-1}$, are probably related to the reef margins being exposed to increasing hydrodynamic energy conditions as they approached modern day sea level.
- There is a prominent algal ridge feature on the windward reef flat indicating persistent high-energy conditions probably related to the south east trade winds.
- The presence of large aeolian dune deposits on the southern and eastern coasts of Rodrigues Island indicate that the modern day Holocene reef probably caps an older Pleistocene reef.
- Western Indian Ocean coral reefs have accumulated at least 217 Gt $CaCO_3$ during the Holocene. From first approximations, this may represent approximately 10 % of the global total for the last 10 kyr and suggests that Western Indian Ocean reefs could have released approximately 57 Gt CO_2 to the Holocene atmosphere.

7.1.3 Carbonate Budgets

- Coral reef accretion rates have varied spatially within reef provinces and temporally during the Holocene in response to various factors including sea level rise, turbidity, substrate type, proximity to larval recruitment centres, light, salinity, nutrients and temperature
- Maximum reef accretion occurred between 10 and 4 kyr BP (6492 Gt $CaCO_3$). During this time the area available for reef growth was greatly increased by rapidly rising sea level flooding the continental shelves creating accommodation space for corals to grow into. This increase in the area available for reef growth is reflected in faster vertical accretion rates exhibited by all reefs in the early to mid-Holocene compared with the late Holocene. Around 6 kyr BP modern sea level had either been reached or the rate of sea level rise had slowed and the area available for reef growth was reduced. Between 4 and 0 kyr BP the reduction in coral reef accommodation space available for reef growth resulted in less carbonate accumulation compared to the early to mid-Holocene (1474 Gt $CaCO_3$).

- The pattern of global $CaCO_3$ accumulation temporally is a reflection of the variation in accretion rates from all reef provinces. The primary factor influencing the magnitude of the contribution of individual reef provinces to the global $CaCO_3$ mass balance is reef area.
- This thesis conservatively estimates the Holocene coral reef $CaCO_3$ mass balance to be 7970 ± 478 Gt $CaCO_3$ which would have made 2100 ± 126 Gt CO_2 available for release to the atmosphere since 10 kyr BP. This may have resulted in a 274 ± 16 ppmv change in the atmospheric CO_2 concentration.
- The cumulative calcium carbonate ($CaCO_3$) accumulation within coral reefs globally during the past 10 kyr BP (7970 Gt; ~ 0.1 Gt C yr^{-1}) is about half the flux of carbon to both the global ocean from rivers and buried in deep sea sediments as $CaCO_3$. The amount of carbon locked-up in coral reefs and released to the atmosphere by coral reef calcification during the Holocene are comparable to the amount of carbon in the present day terrestrial biosphere and surface ocean DIC.
- The CO_2 available to the Holocene atmosphere from coral reef calcification of 274 ppmv is large in comparison with the observed increase in atmospheric CO_2 concentration between the LGM and pre-industrial revolution of 80-100 ppmv. Some factor or combination of factors must have served as a sink for this coral reef released CO_2, possibly terrestrial vegetation re-growth (Figure 7.1).
- Currently, most carbon cycle models and budgets do not include an independent coral reef component. This study is an improvement on past carbonate budget studies because i) it is calculated using only coral reef data, ii) it employs an extensive dataset with global coverage, iii) it has a temporal perspective, iv) it incorporates the proportional change in reef area associated with the transgression and vi) it utilizes the most accurate and up to date reef area estimate.
- The anthropogenic flux of CO_2 to the atmosphere (currently ~ 6.3 Gt C as CO_2 yr^{-1}) is huge in comparison to natural Holocene reef emissions (Holocene average ~0.06 Gt C as CO_2 yr^{-1}), present day reefs release only 0.3 % current anthropogenic emission and even the peak Holocene reef flux amounted to only 1.4 % of present day anthropogenic release. The current rate of coral reef CO_2 release calculated by this study is approximately 0.3 % of present day anthropogenic fuel emissions of 6.3 ± 0.4 Pg C yr^{-1}.

- Future improvements in the global mass balance could be achieved by breaking down each of the reef provinces into smaller regions to distinguish between various reef types of this vast province. Refinement of the marine $CaCO_3$ budget will only be made possible by future drilling investigations and a comprehensive breakdown of the reef area estimate which encompasses details of each reef in a region and reef type.
-

7.1.4 Halimeda Bioherms

- The ribbon reefs of the Lizard Island and Cooktown regions comprise approximately 0.52 and 0.92 Gt $CaCO_3$ respectively.
- The *Halimeda* bioherms of the Lizard Island and Cooktown regions contain approximately 4.11 and 1.15 Gt $CaCO_3$ respectively.
- The ratio of coral reef to *Halimeda* bioherm $CaCO_3$ sediments varies from 1:1 to 1:4 on the Northern Great Barrier Reef. The *Halimeda* bioherms contain equal to (and up to 400 % more) $CaCO_3$ sediments than the adjacent ribbon reefs in the Northern Great Barrier Reef.
- The *Halimeda* bioherms make up a significant proportion of the outer shelf carbonate budget of the Northern Great Barrier Reef.
- Assuming the area of northern Great Barrier Reef Ribbon reefs is 1081 km^2, the *Halimeda* bioherms of the northern Great Barrier Reef have accumulated approximately 48.3 Gt $CaCO_3$ during the Holocene.

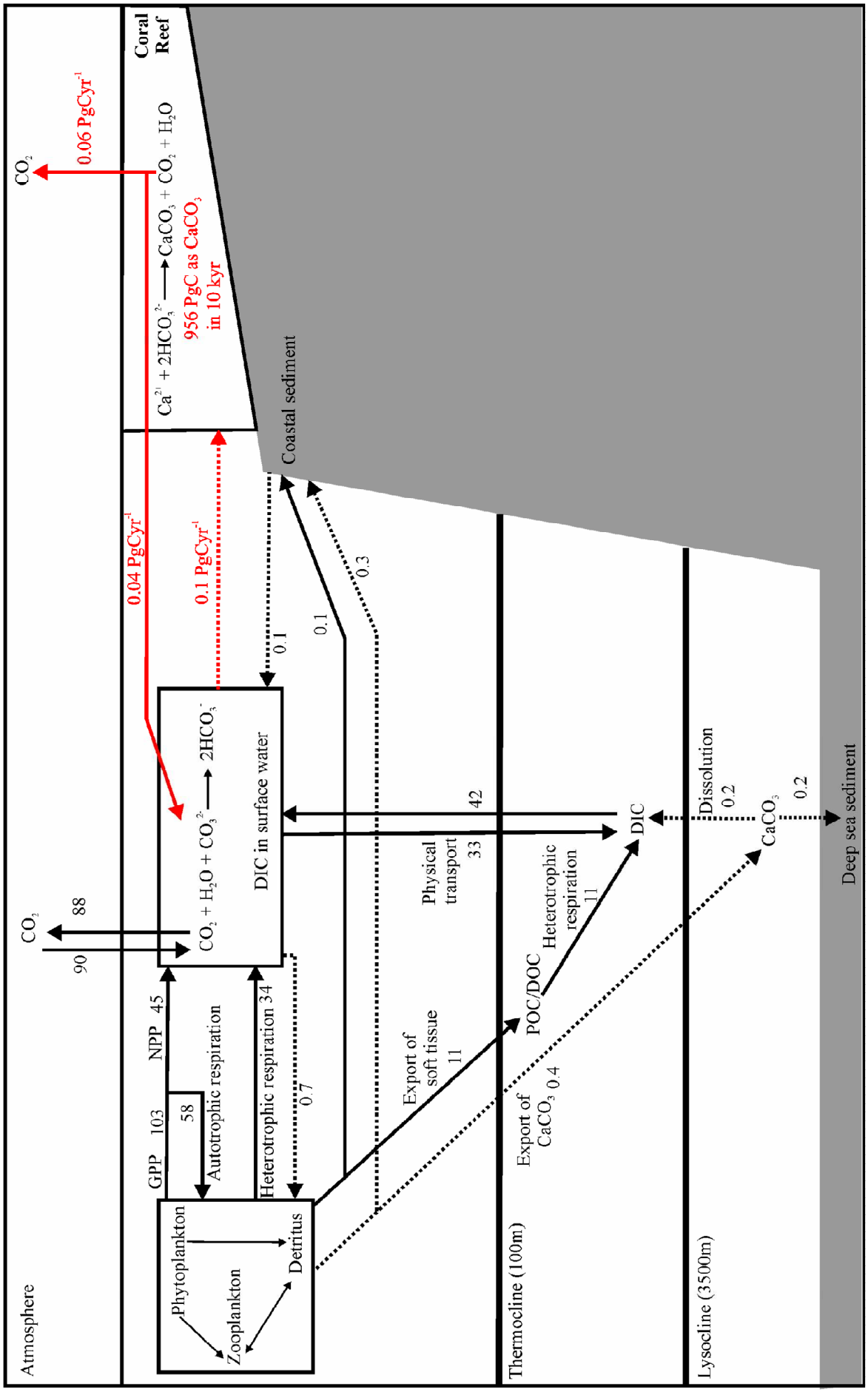
Atmosphere
Coral Reef
CO_2
0.06 PgCyr^{-1}
$Ca^{2+} + 2HCO_3^{2-} \rightarrow CaCO_3 + CO_2 + H_2O$
956 PgC as $CaCO_3$ in 10 kyr
Coastal sediment
0.04 PgCyr^{-1}
0.1 PgCyr^{-1}
0.1
0.1
0.3
CO_2
88
90
$CO_2 + H_2O + CO_3^{2-} \rightarrow 2HCO_3^-$
DIC in surface water
42
Physical transport
33
DIC
Dissolution
0.2
$CaCO_3$
0.2
Deep sea sediment
GPP 103
58
Autotrophic respiration
NPP 45
Heterotrophic respiration 34
0.7
Export of soft tissue
11
POC/DOC
Heterotrophic respiration
11
Export of $CaCO_3$ 0.4
Phytoplankton
Zooplankton
Detritus
Thermocline (100m)
Lysocline (3500m)

Figure 7.1 Ocean carbon cycle. Units of reservoirs; Pg C (Gt C) and fluxes; Pg C yr^{-1} (Gt C yr^{-1}) estimated for the 1980's (Houghton *et al.*, 2001, IPCC, Figure 3.1c). Filled lines indicate natural fluxes, dotted lines indicate fluxes of carbon as $CaCO_3$, arrows, lines and figures in red are those calculated by this PhD project. The values in brackets indicate how the fluxes have varied during the Holocene. DIC represents dissolved inorganic carbon, CO_2, CO_3^{2-} and HCO_3^-. GPP represents gross primary production; NPP represents net primary production (that left after respiration). DOC is dissolved organic carbon, POC is particulate organic carbon. The $CaCO_3$ accumulated on the shelf (coastal sediments, 0.3 Pg C yr^{-1}) represents $CaCO_3$ produced plankton and detritus, 0.1 Pg C yr^{-1} returns to the pool of DIC by dissolution. The report does not indicate if the flux of 0.3 Pg C yr^{-1} of $CaCO_3$ to coastal sediments is due to corals or to plankton. We calculate that the flux of C as $CaCO_3$ into coral reefs is 0.1 Pg C yr^{-1} (during the Holocene this could have ranged between 0.03 and 0.15 Pg C yr^{-1}; or between 0.22 to 1.2 Gt $CaCO_3$ yr^{-1}). We estimate that coral reefs accumulated 956 Pg C yr^{-1} as $CaCO_3$ during the last 10 kyr. Calcification releases 0.6 mol CO_2 available for release to the atmosphere which we estimate 0.06 Pg C yr^{-1} is available for release to the Holocene atmosphere. 0.4 mol of CO_2 released by calcification recombines with carbonate ions and water to form bicarbonate, we estimate that this constitutes a Holocene flux of 0.04 Pg C yr^{-1} back to the DIC pool.

7.2 Future Work

In light of this project I suggest the following topics for future investigation;

- Additional reef coring expeditions to a) expand knowledge into areas presently under represented, b) to investigate reef growth prior to 10 kyr BP and c) to explore submerged (drowned/give-up) reefs.
- For Holocene reef research to combine seismic profiling and reef drilling to obtain an accurate 3-D picture of Holocene reef structure for reefs worldwide and of all reef types.
- For reef area estimates to be broken down to reveal the contribution of each reef and reef type to the global total.
- Investigate the global distribution, structure and temporal pattern of accumulation of $CaCO_3$ within *Halimeda* bioherms.

7.3 References

Houghton, J. T., Ding, Y., Griggs, D. J., Noguer, M., van der Linden, P. J., Dai, X., Maskell, K. and C. A. Johnson (eds) (2001) *Climate Change 2001: the scientific basis. Contribution of Working Group I to the Third assessment Report of the International Panel on Climate Change*. Cambridge University Press, Cambridge, United Kingdom and New York, USA, pp 881.